University of Reading

Progress Towards the Development of Metal Selective Ligands for Nuclear Waste Reprocessing

A thesis submitted in partial fulfillment of the requirements for the degree of

Doctor of Philosophy

Department of Chemistry

University of Reading

James Westwood

April 2018

Declaration

I confirm that this is my own work and the use of all material from other sources has been properly and fully acknowledged.

James Westwood

April 2018

Acknowledgements

First and foremost, I would like to thank Professor Laurence Harwood for providing me with the opportunity to undertake this PhD, and for all of his valuable advice/suggestions (& poor jokes) along the way. I would also like to thank Professor Michael Hudson, who is sadly no longer with us, for his helpful explanations and enthusiasm (at 9am) during the first part of my PhD.

A special thanks to Dr Ashfaq Afsar for his continuous help and support during my time in Lab 213, all the way from my summer project in 2013 to pretty much the end of my PhD. Without Ash's enthusiasm I would not have contributed towards so many publications. Thanks also to Petr Distler and Jan John in Prague for actually doing the extraction experiments in this thesis and for their great collaboration.

I would also like to thank Dr Andrew Smith and Dr Joe Cowell for their general lab supervision and advice during my PhD. Thanks also to Dr Chris Smith and Dr Philippa Cranwell for their advice and encourgement. It was a pleasure to work alongside all the other members of Lab 213: Andy (Rui) Gu, Diana Monir, Iain Hopkins, Zoe Selfe, Jasraj Singh Babra and Koreans x2 together with the numerous (& laughable) MChems. Thanks also to the office people in G06 during my brief appearance. Thanks to Chad Edwards and Roger Whitehead from Manchester for their synthetic advice. Use of the Chemical Analysis Facility (CAF) and its general maintenance is gratefully acknowledged. Special thanks to Nick Michael for running all my mass spectrometry analysis. Thanks to Yan for her careful introduction to ICP-MS and to Andy Dodson for its subsequent maintenance.

Thanks also go to my favourite housemates: Marina, Niamh and Isobel for the fun and laughs during my time in Reading. Thanks also to Steve and Gary, together with the numerous others for hours of laughter and fun on Battlefield/Fortnite.

Thanks also to my grandparents, Ellen and Pete, for their continuous encouragement; and to my sister, Lauren, for just generally being around during my visits home.

Finally, and most importantly, a special thanks goes to my parents, Richard and Jackie, for their endless support (mostly financially) throughout my PhD; I wouldn't of completed it without them.

Dedicated to my parents Richard and Jackie.

Abstract

Developments in the waste management of radioactive high-level liquid waste produced in the back-end of the nuclear fuel cycle will further develop the public approval of nuclear power as an alternative to the combustion of depleting supplies of fossil fuels. Even though the minor actinides contribute to *ca*. 0.1 % of spent nuclear fuel by mass, they significantly contribute to the relative radiotoxicity of the waste and constitute a thermal burden. In order to transmute the minor actinides into shorter-lived more stable isotopes, they must be isolated from the remaining waste, and especially separated from the very similar trivalent lanthanides. This thesis outlines the synthesis and extraction capability of *N*-donor extractants for the difficult separation of trivalent minor actinides [An(III)] from the chemically similar trivalent lanthanides [Ln(III)] in advanced nuclear fuel cycles. The use of solid-supported extractants including magnetic nanoparticles and macroscopic silica gel for their separation together with recovery of fission/corrosion products present in PUREX streams is also reported.

Abbreviations and Acronyms

An	Actinide
BODO	2,6-*Bis*-(benzoxazol-2-yl)-4-dodecyloxypyridine
BTBP	*Bis*-triazinylbipyridine
BTP	*Bis*-triazinylpyridine
BTPhen	*Bis*-triazinylphenanthroline
$CDCl_3$	Deuterated chloroform
CEA	Commissariat a l'Energie Atomique
CMPO	Carbamoylmethylphosphine oxide
D	Distribution ratio
DIAMEX	Diamide extraction
DMDOHEMA	*N,N'*-dimethyl-*N,N'*-dioctyl[(hexyloxy)ethyl]malonamide
DMSO	Dimethylsulfoxide
dppz	Dipyridophenazine
DTPA	Diethylenetriaminepenta-acetic acid
EDCI	*N*-(3-dimethylaminopropyl)-*N*'-ethylcarbodiimide
EXAFS	Extended X-ray Absorption Fine Structure
GANEX	Group actinide extraction
GDF	Geological disposal facility
GW	Gigawatt
HDEHP	di-(2-ethylhexyl)phosphoric acid
HLLW	High level liquid waste
HOBt	1-hydroxybenzotriazole
IAEA	International Atomic Energy Agency
ICP-MS	Induction-coupled plasma mass spectrometry
KGy	Kilogray
LEU	Low enriched uranium
Ln	Lanthanide
LWR	Light water reactor
m-CPBA	*meta*-chloroperbenzoic acid
MNP	Magnetic nanoparticle
MOX	Mixed oxide fuel
NCS	*N*-chlorosuccinimide
OECD	Organization for Economic Co-operation and Development
OK	Odorless kerosene
PUREX	Plutonium uranium extraction
PPA	Polyphosphoric acid
ppb	Parts per billion
ppm	parts per million
PWR	Pressurised water reactor
SANEX	Selective actinide extraction
SEM	Scanning electron microscopy
SNF	Spent nuclear fuel
SF	Separation factor
TALSPEAK	Trivalent Actinide Lanthanide Separation with Phosphorous-

	Reagent Extraction from Aqueous Komplexes
TBP	Tri-butyl phosphate
TEM	Transmission electron microscopy
TERPY	2,2:6',2"-terpyridine
TODGA	*N,N,N',N'*-tetraoctyldiglycolamide
TPH	Hydrogenated tetrapropene
TPTZ	2,4,6-tri-2-pyridyl-1,3,5-triazine
XANES	X-ray Absorption Near-Edge Structure

Table of Contents

Numbering of the Phenanthroline Core in this Thesis:

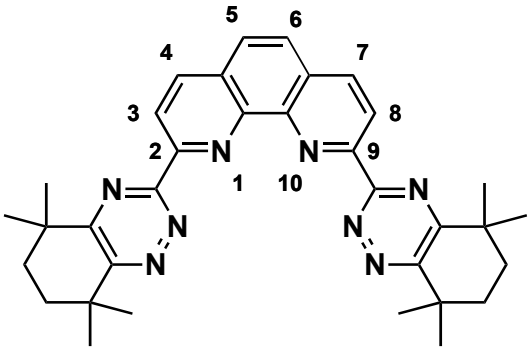

Chapter 1 – A Review of the Development of Ligands for Separation of Minor Actinides from Lanthanides

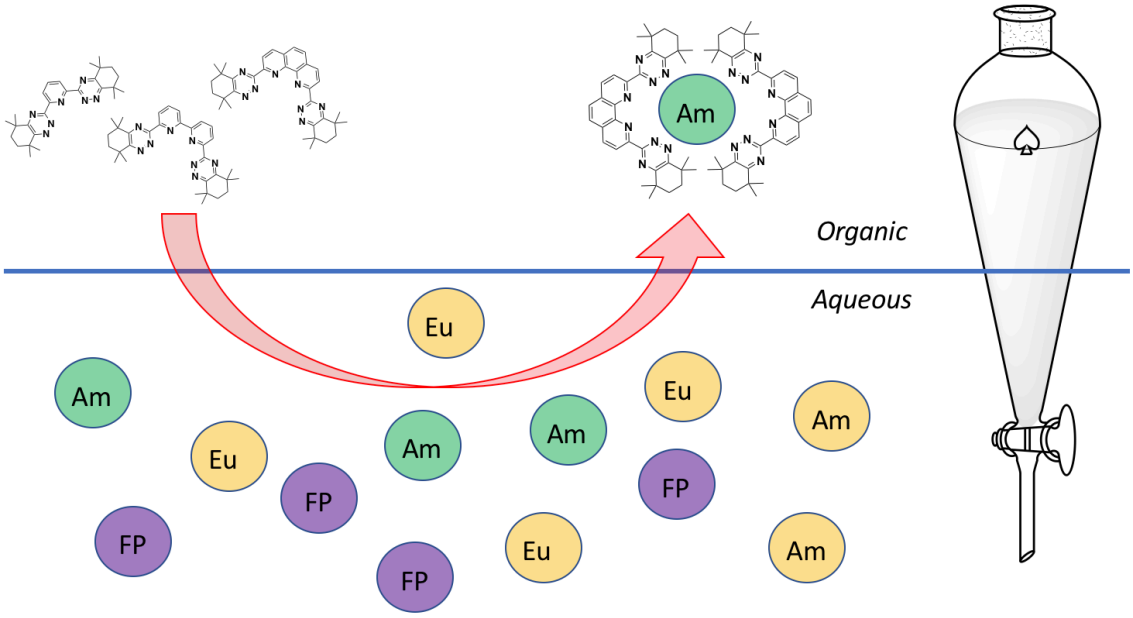

Parts of this chapter will be published as:

J. Westwood and L. M. Harwood, *Controlling Actinide Extraction Chemistry (Separation of Actinides from Lanthanides as part of Nuclear Fuel Recycling)*, in *Encyclopedia of Inorganic and Bioinorganic Chemistry*, John Wiley & Sons Ltd, Online and In Print, 2018, *In press*

1.1 – Introduction:

Actinides exist in small quantities in the geosphere both as a result of natural occurrence and due to human activities. Uranium (^{238}U) is the heaviest atomic mass element generally found in nature, with neptunium (^{237}Np) and plutonium (^{244}Pu) only being found in trace amounts. Human activities, including the development of nuclear weapons, nuclear reactor incidents and particularly the generation of used nuclear fuel (commonly known as *spent nuclear fuel*, SNF) have contributed to the global accumulation of actinides.[1–3]

The separation of actinides from SNF is strongly affected by the presence of a wide range of other elements, including transition metals and lanthanides, which compete for the binding sites in the ligands/compounds used during the extraction. The extraction process is further complicated by the concentration of other metal ions being generally orders of magnitude larger than those of the actinides. Different methods, including solvent extraction, pyro-processing and ion-exchange have previously been used to achieve selective extraction of the minor actinides.[4,5] Ion-exchange techniques are generally non-specific in their binding or separating ability, exploiting differences in the size of the complexes formed or the charge density of the ions in acidic/basic media.[6] The most developed technique at industrial level, which will be focused on in this introductory chapter, is the use of solvent extraction, where ligating molecules are dissolved in an organic phase and used to extract a range of metals from an acidic aqueous phase.

The development of solvent extraction techniques for SNF reprocessing has two especially important roles: the first being for the separation and recovery for re-use of uranium and plutonium (since > 90 % SNF is uranium), as estimates indicate that the world's stocks of uranium will only last for a further 90 years.[7] The second role will be to enable the separation of the minor actinides [neptunium (Np), americium (Am) and curium (Cm)], so that transmutation (inducing fission by high neutron fluxes) would become possible, generating shorter-lived, or stable isotopes, giving waste that will require storage on a time scale about one thousandth that of unprocessed SNF.[2,8,9]

The separation of actinides from within a mix of lanthanides is not as straightforward as, for example, the separation of sodium (227 pm) and caesium (300 pm), which can be achieved based on size of cations, or strontium (+2) and yttrium (+3), where separation can be achieved based on charge.[10] Trivalent lanthanides and actinides have very similar sized ions

and have similar charge densities, so selective extraction of actinides in the presence of lanthanides must be controlled by exploiting the small differences in their bonding and other properties.

1.1.1 – Nuclear Power:

Few authorities question that global warming has been brought about by burning fossil fuels and that to arrest the rate of climate change, it is necessary to develop effective, efficient and sustainable alternative sources of energy. This is coupled with increasing political pressure to reduce air pollution and generation of greenhouse gases as emphasised by the 2016 Paris Agreement.[11]

Nuclear power generation accounted for approximately 11 % of the world's total electricity production during 2013 and was higher among OECD countries (**O**rganisation for **E**conomic **C**o-operation and **D**evelopment), accounting for 18 % overall of these countries' generation capacity in the same year, according to the International Atomic Energy Agency (IAEA).[12]
In comparison with coal power plants, which supplied ~ 40 % of the world's electricity in 2015, the energy liberated from the fission of uranium is about two million times more than that obtained from burning an equal mass of coal.[7,12]
Wind, solar, hydro-electricity and geothermal energy are all clean alternatives to burning coal, oil or gas, but suffer from the drawbacks of being relatively inefficient, expensive, inconsistent or geographically restricted. However, in 2015 the renewables energy sector posted a 15 % year-on-year increase in energy output reaching over 150 Gigawatt (GW) for the first time.[13]

To keep pace with growing electricity demands worldwide, increasing nuclear power output remains a viable option as it maintains a low-carbon emission policy. Many countries are looking to expand their nuclear power generation and in 2015 there were 68 new reactors under construction.[14] The IAEA has estimated that up to 700 GW could be generated by 2030. However, the strategy for a long-term solution for safe disposal of the waste is yet to be clearly established and both the current stockpiling above ground and eventual deep geological deposition of SNF cause great public concern.

1.1.2 – The Nuclear Fuel Cycle (NFC):

During its operation, a typical 1000 MW light water reactor (LWR) produces 20-30 tons of SNF per annum.[8] Therefore, the most important scientific and technological challenge that needs to be addressed for nuclear energy generation to become a viable means of low-carbon energy generation in the long term, is to develop effective strategies to deal with the highly radiotoxic waste. Nearly all nuclear active nations are aiming to use a geological disposal facility (GDF) for the waste as its final destination, whether that be directly as SNF or after some degree of reprocessing.[15]

The nuclear reactions that occur inside a nuclear reactor to generate electricity are essentially the same reactions that occur during the detonation of a nuclear weapon, but proceed at a much slower and more controlled rate. This leads to a slightly different yield of fission products due to the lower neutron energies involved. Uranium is mined from a variety of mineral deposits and is composed of three naturally occurring isotopes, ^{238}U (99.2739 %), ^{235}U (0.7205 %) and ^{234}U (0.0056 %) with the average abundance of uranium in the Earth's crust being about 3 parts per million (ppm).[16] After mining, the ore undergoes milling where the ore is crushed to particle sizes of < 20 mm, wet grounded and leached with sulfuric acid. Separation of the UO_2 liquor and precipitation with ammonia gas gives a powder which is mostly U_3O_8, known as yellowcake.[17]

The ^{235}U is the fissile isotope needed for the production of energy in nuclear reactors and following purification to remove neutron absorbing poisons, enrichment of the fissile ^{235}U isotope is required to increase the isotopic proportion to approximately 3-5 %, which is known as low-enriched uranium (LEU).[7,18] The enriched uranium is fabricated into pellets and packed into fuel rods that are typically constructed using alloys of metals with low neutron absorption cross sections.[19]

The stage from mining the ore to fuel fabrication is known as the *'Front End'* of the nuclear fuel cycle whilst the production of energy and up to storage is known as the '*Back End'*. An overall summary of the nuclear fuel cycle is depicted in **Fig 1.1**.

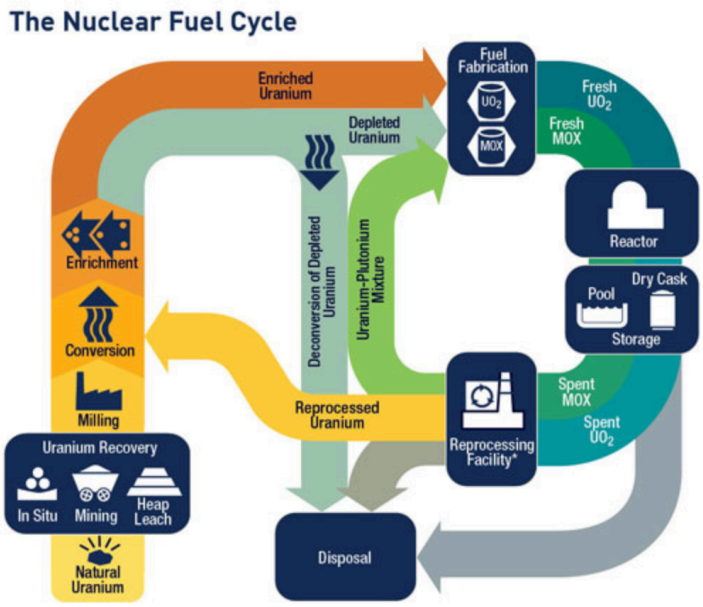

Figure 1.1 – The nuclear fuel cycle (NFC)[20]

To capture energy from uranium, the nuclei are bombarded with neutrons to induce a branched chain reaction. The neutrons ejected after bombardment are so-called 'fast neutrons', where further absorption is unlikely. Thus a moderator is employed, typically D_2O or beryllium, which reduces the kinetic energy of the neutrons.[7] Absorption by ^{235}U repeats the chain reaction; whereas absorption by ^{238}U produces ^{239}U, which can undergo α-decay leading to the production of lighter nuclei (fission products, lanthanides) or undergo ß-decay leading to heavier minor actinides. A range of fission products can be produced from the decay of ^{239}U, ranging from arsenic (As) to terbium (Tb) (atomic mass number 75 through to 160). Only a small proportion of the nuclei produced constitute the heavier minor actinides, neptunium (Np), americium (Am) and curium (Cm).[8,10]

1.2 – Spent Nuclear Fuel:

Irradiated nuclear fuel rods inside a reactor have an approximate life-time of three to five years, after which the rods are removed and submerged in cooling ponds for up to 3 years. This allows the decay of short-lived and intensely radiotoxic elements such as ^{129}I and ^{99}Tc. For reprocessing, the fuel cladding is removed and the rods are then broken up by dissolving in concentrated (7 M) nitric acid to give an aqueous acidic waste stream.[8,17]

The SNF produced by a typical LWR consists mostly of uranium (of which only 0.7 % is ^{235}U), short-lived fission products and lanthanides (> 98 % wt), which do not present significant long-term hazards.[21] From the remainder, the main contributor to the long-term radiotoxicity of the SNF, is plutonium (~ 1 %), together with the minor actinides (Np, Am, Cm, ~ 0.1 %).[22] **Fig 1.2** displays the typical composition of such spent nuclear fuel.[23]

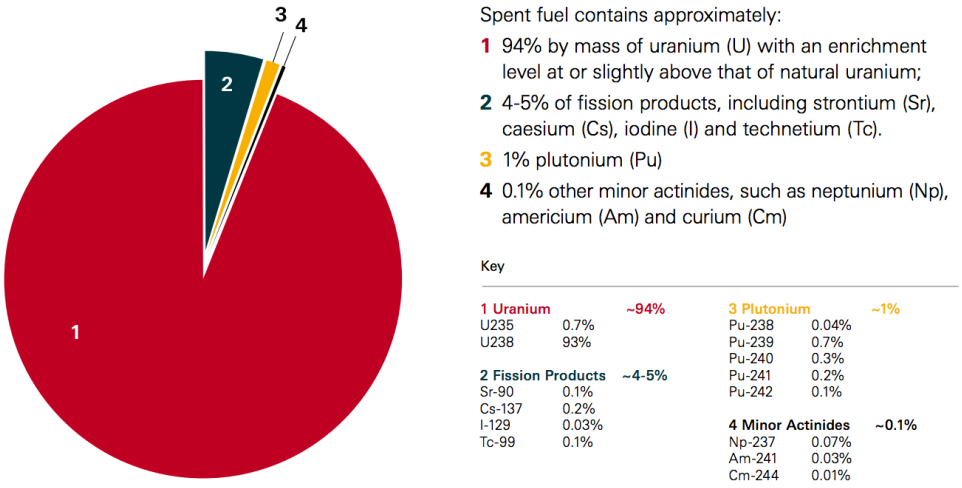

Figure 1.2 – Approximate composition of SNF from irradiated nuclear fuel rods.[23]

The minor actinides are the cause of much of the long-term radiotoxicity of the spent fuel, even though they only account for about 0.1 % by mass of the waste.[22] **Fig 1.3** shows the various scenarios for the time taken for the spent fuel to decay back to the natural radioactivity level of uranium, depending upon the degree of reprocessing carried out. The removal of uranium, plutonium and minor actinides leads to a thousand-fold decrease (yellow line) in the storage time to something that is feasible from a technical and logistical sense. Furthermore, the heat output of such reprocessed waste is far lower, meaning that repositories can be smaller in volume.

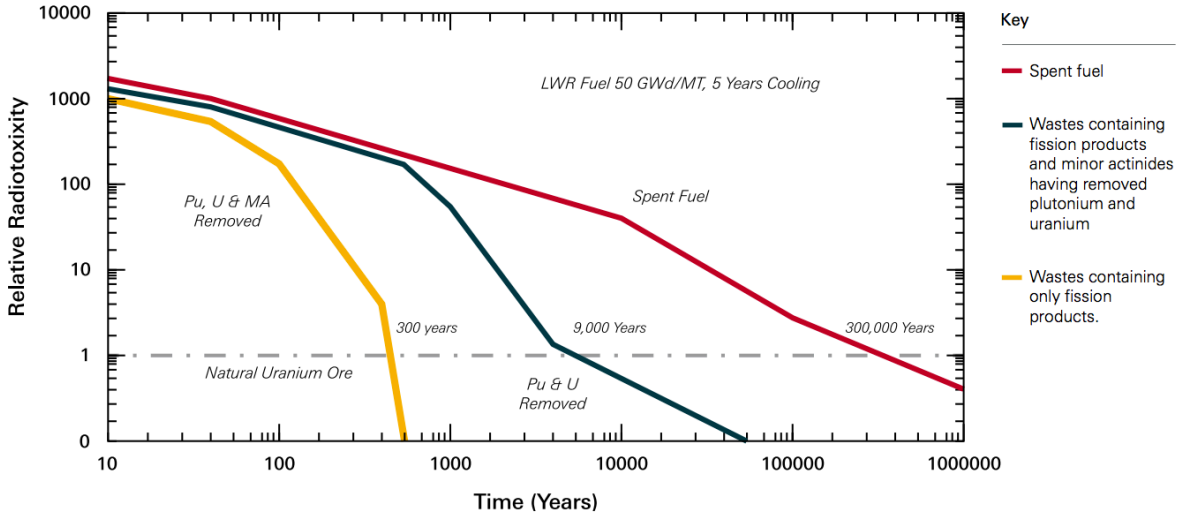

Figure 1.3 – Relative radioactive decay of spent nuclear fuel as a function of degree of reprocessing.[23]

An industrial procedure already applied to spent fuel in France, Russia and (currently) the UK, is the PUREX (**P**lutonium and **UR**anium **EX**traction) process (section **1.4.1**), which removes plutonium and uranium, comprising ~ 95 % of the spent fuel (**Table 1.1**). As shown in **Fig 1.3**, this reduces the radiotoxicity of the spent fuel dramatically, decreasing the time to decay to that of naturally occurring uranium from 300,000 years to around 9000 years (**Fig 1.3**, dark blue line). However, the remaining PUREX raffinate still contains the minor actinides, lanthanides and fission/corrosion products. Further reprocessing is proposed to involve the co-extraction of the minor actinides and lanthanides (TRUEX and DIAMEX, section **1.4.2**), before the extremely difficult selective extraction of the minor actinides from the remaining lanthanides is carried out (SANEX, section **1.4.4**). Removal of all Pu, U and the minor actinides will further decrease the decay time to *ca.* 300 years (**Fig 1.3**, yellow line). This is a significant reduction compared to the lifetime of the initial spent fuel and enhances the potential for storage in a GDF.[23]

Table 1.1 – Approximate mass and $t_{1/2}$ of U and Pu radioisotopes found in SNF per annum.[24]

Radionuclide	$t_{1/2}$ (yrs)	Approx. Mass in SNF (Kg)
^{234}U	2.47×10^5	3
^{235}U	7.10×10^8	215
^{236}U	2.39×10^7	114
^{238}U	4.51×10^9	25700
Total		**26032**
^{238}Pu	86	6
^{239}Pu	2.44×10^4	144
^{240}Pu	6.58×10^3	59
^{241}Pu	13	28
^{242}Pu	3.79×10^5	10
Total		**247**

Table 1.2 – Approximate mass and $t_{1/2}$ of Np, Am and Cm radioisotopes found in SNF per annum.[24]

Radionuclide	$t_{1/2}$ (yrs)	Approx. Mass in SNF (Kg)
^{237}Np	2.14×10^6	20
Total		**20**
^{242}Am	141	0.01
^{243}Am	7950	2.48
Total		**3.81**
^{242}Cm	163 (days)	0.133
^{243}Cm	32	0.002
^{244}Cm	18	0.911
^{245}Cm	9300	0.055
^{246}Cm	5500	0.006
Total		**1.11**

Table 1.2 shows the approximate mass and half-lives ($t_{1/2}$) of neptunium, americium and curium radioisotopes present in SNF from a pressurised water reactor (PWR) per annum, which is very small compared to the isotopes shown in **Table 1.1**, but very significant as the minor actinides are intensely radiotoxic and also constitute a major thermal burden.[8,25]

Fission and corrosion products make up the remainder of the elements present in SNF, where fission products result from decay chains of fissile material and the corrosion products are a result of the degradation of the fuel cladding and of the steel containment. Since the various corrosion and fission products are in a higher abundance in the SNF than actinides, it makes

the selective partitioning of the minor actinides into the organic phase during liquid-liquid extraction much more difficult.[2,9,26]

1.3 – Actinide and Lanthanide Chemistry:

1.3.1 – Actinides:

The actinide elements consist of the elements with atomic numbers from 89 to 103 (Ac-Lr), and the name of the group is derived from the first member of the series, actinium. The actinides form the second series of the '*f*-block elements' whereby f-electrons formally begin with filling the 5f orbital of the 2nd member thorium (Th) and ends with the 15th lawrencium (Lr), leading to a total of 14 f-electrons.[26,27]

Of all the actinides, only thorium, protactinium and uranium are naturally occurring in any significant quantities, with the actinides that follow uranium and up to curium (Cm) being formed by the capture of neutrons by ^{238}U inside nuclear reactors. The elements following curium are generally formed in higher neutron fluxes in specially designed and controlled reactors under laboratory conditions. Discovery of the actinides started in the 18th century where they were initially isolated from minerals and the series was only completed in the late 1960's.[10]

The natural abundance of actinide elements decreases in the series Th > U > Pa and thorium is much more abundant in the Earth's crust than uranium; indeed thorium is even more abundant than lead (Pb).[26] The average abundance of uranium across the Earth's crust is between 2 and 4 ppm. The concentration of uranium in sea water is approximately 3 parts per billion (ppb), which although low, raises the possibility of harvesting in the future and is the focus of on-going research.[28,29] All the actinides are unstable with respect to radioactive decay, but the long half-lives of ^{232}Th (1.4×10^{10} yrs) and ^{235}U (4.5×10^{9} yrs), means they still exist naturally.[10]

Due to the shifting and overlapping energies of the highly complex f-orbitals in actinides, some of the electrons are added to d-orbitals (e.g. in Th and No). The earlier actinides elements (Ac-Pu) show a greater covalency in their bonding with donor molecules compared with the lanthanide series, but their covalency decreases beyond americium due to the shifting of the energy levels of the orbitals involved with bonding.[26]

To extract the actinides effectively from a complex mixture of elements, an understanding of their unique and little-known chemistry is required. Among the earlier actinides, the promotion of electrons from 5f → 6d orbitals occurs much more readily than the corresponding 4f → 5d promotion that occurs in lanthanides.[26] The electron promotion exhibited by the actinides leads to several accessible oxidation states in the earlier actinides, where plutonium can be found in four different oxidation states (III to VI). Orbital contraction, where the 5f orbitals are progressively contracted across the series, and so closer to the core nucleus, explains the restriction of variable oxidation states seen by the actinides that follow Pu; as it becomes progressively harder to remove electrons from the more contracted 5f orbitals.

The preferred oxidation state of the series starts with +3 for actinium and increases up to +6 for uranium before returning to +3 with americium. The most common oxidation state in aqueous media across the series is +3 except for a drop to +2 for nobelium. The most common oxidation states for each actinide together with other known oxidation states are displayed in **Fig 1.4**.[26]

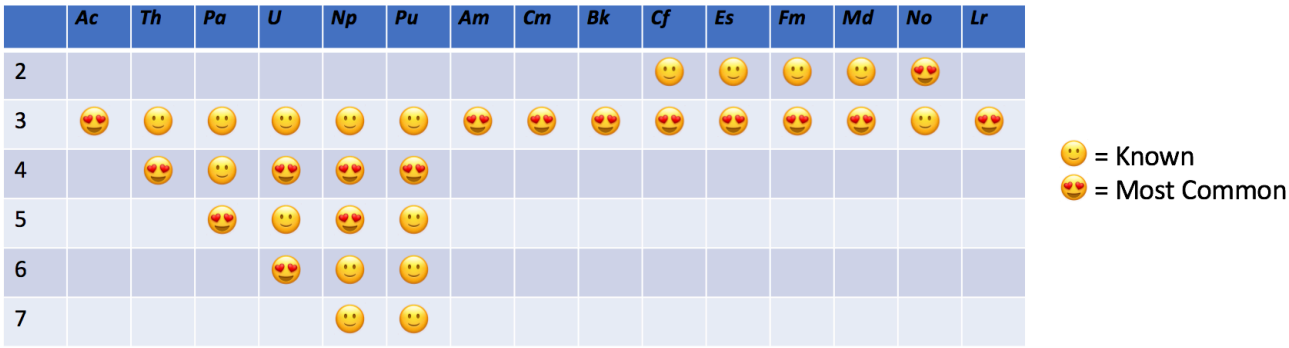

Figure 1.4 – Actinide elements oxidation states

The actinides 5f orbitals have a larger extension into the 6d orbitals showing a greater propensity for valence-orbital mixing compared to the 4f into 5d orbitals in the lanthanides, and so the actinides are considered more likely to be involved in covalent bonding than the lanthanides.[26]

1.3.2 – Lanthanides:

The lanthanide elements consist of the elements with atomic numbers ranging from 57 to 71 (La-Lu), where the name of the group is again derived from the first member of the series, lanthanum (La). Moving across the series, electrons progressively fill the 4f orbital starting with the 2nd member, cerium (Ce), and ending with the 15th, lutetium (Lu). The lanthanide series together with scandium and yttrium make up a group of elements known as "*rare earth elements*', a name derived from their discovery during the 18th and 19th century in Ytterby, Sweden, where the oxides from which they were obtained were considered to be rare minerals at the time.[26,27] Although there are commercially minable deposits in the US and Australia, currently China accounts for greater than 94 % of all lanthanides produced.[30]

The radioactive lanthanide, promethium, is only found in trace amounts as it has no long-lived isotopes. On the other hand, cerium has a global abundance of approximately 65 ppm, which is similar to that of copper and lead. There are 54 lanthanide minerals that are used commercially for extracting the lanthanides, but their extraction, concentration and separation from each other is highly complex.[31]

Due to the higher energy barrier for the promotion of electrons from the 4f → 5d orbitals, a very limited range of oxidation states is observed across the lanthanide series with +3 being the usual oxidation state. The lanthanide elements are considered far less covalent in their bonding to form complexes compared to actinides because the 4f electrons are not as radially extended.[26,32]

Following the neutron absorption by uranium in nuclear fuel, several lanthanide radioisotopes are produced as fission products, where most have half-lives of less than one day. Those with longer half lives include ^{144}Ce, ^{147}Pm, and ^{151}Sm, all of which have half-lives significantly longer (285 days, 2.6 yrs and 90 yrs respectively). These lanthanides produced in SNF are at much higher concentrations than the actinides, but most of them decay into stable isotopes during the initial cooling period of the fuel rod after the end of its use.[33]

1.3.3 – Chemistry of the f-block elements:

The chemistry among the f-block elements is extremely similar. The 'lanthanide contraction' causes a continuous decrease in atomic radius across the lanthanides due to the poor shielding by the 4f electrons. The same phenomenon is observed across the actinides. This is due to the increase in effective nuclear charge across both series having the effect on the core electrons of drawing them closer to the nucleus, resulting in a decrease in atomic radius across both series.[27]

All f-block metals have the trivalent state (M^{III}) as the predominant cation, and the actinides can exhibit variable oxidation states, especially across the earlier (Pa – Am) elements. Variable coordination numbers are observed upon complexation with ligands, but they are usually high (> 6). There is a certain degree of flexibility with the arrangement of the ligands around the metals, as coordination is mainly based on steric factors.

Complex bonding in the f-block elements is essentially ionic, but a key difference between lanthanides and actinides is that there is a slightly more covalent nature to the actinide 5f orbitals when complexing with ligands. Relativistic effects (a combination of relativity and quantum mechanics) play an important role in explaining this key difference between the two series. Since the actinide series have more protons (and therefore electrons), they express a greater orbital extension, and so the 5f electrons are further from the nucleus in actinides than compared to 4f orbitals of the lanthanides and hence are more available for covalent bonding. This effect also causes the actinides to exhibit a greater range of oxidation states. The smaller nuclear charge of the lanthanides means that the relativistic effects that influence actinide bonding are not as evident.[32]

Overall, the extended spatial arrangement of the 5f orbitals of the actinides can lead to some degree of covalency when complexing with ligands and this is the key difference that is targeted by actinide-selective extractants during the separation of fission product lanthanides and minor actinides in SNF.[8,26,34]

1.4 – Extraction Processes:

Scheme 1.1 summarizes a proposed European route for the reprocessing of SNF to produce a closed nuclear fuel cycle:

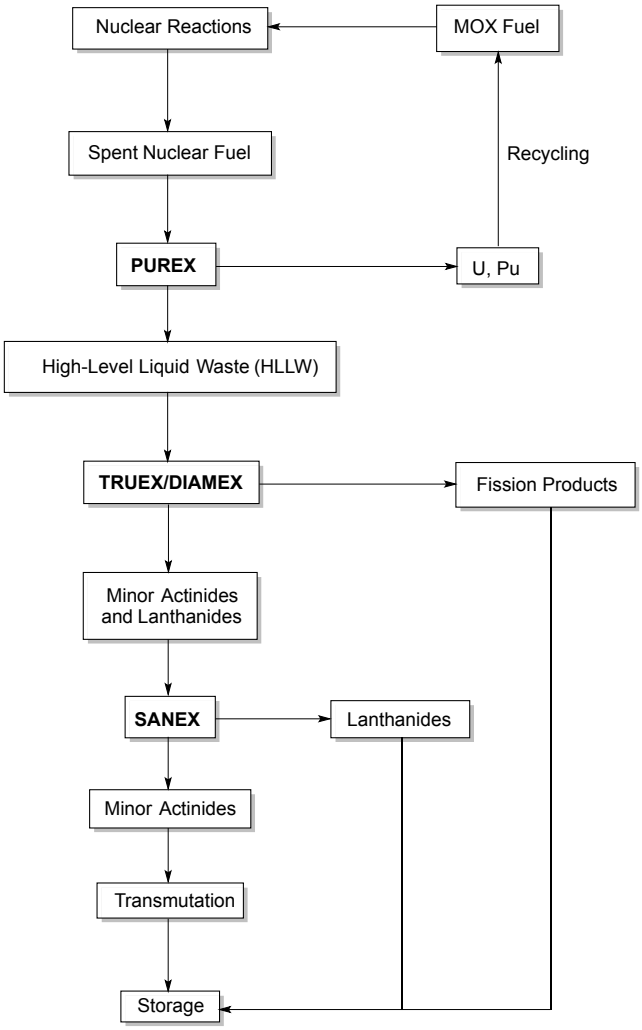

Scheme 1.1 – Summary of a proposed reprocessing plan for spent nuclear fuel in a closed fuel cycle.[8]

1.4.1 – PUREX Process:

The PUREX (**P**lutonium and **UR**anium **EX**traction) process was developed in the USA as a result of nuclear weapon research in the Manhattan Project during World War 2 and is still currently employed by commercial reprocessing plants in France, Russia and the UK, although the UK has announced its intention to stop reprocessing in 2018.[12] Japan has built a reprocessing plant at Rokkasho that was scheduled for operation in 2013 but it is still not operational.[35]

The process involves the separation of uranium and plutonium from the other transuranic elements and fission/corrosion products in the spent fuel using liquid-liquid extraction chemistry, where a concentrated solution (20-30 %) of tributyl phosphate (TBP, **1**) in odourless kerosene (OK) is used as the organic phase extractant.

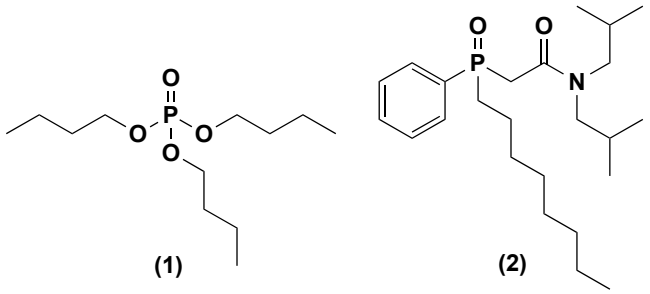

Figure 1.5 – Structure of TBP (**1**) and CMPO (**2**)

The irradiated fuel rods after cooling and dissolution in 7 M HNO_3 produce a mixture of mostly $UO_2(NO_3)_2$ and $Pu(NO_3)_4$ that can be extracted in the +6 and +4 state respectively from a 3 – 6 M HNO_3 feed as $[M(NO_3)_x(\mathbf{1})_2]$ (M = UO_2 or Pu and x = 2 or 4 respectively) into the organic phase. The nature of these complexes depends on the nitric acid concentration, but studies of the complexes by **E**xtended **X**-ray **A**bsorption **F**ine **S**tructure (EXAFS) and **X**-ray **A**bsorption **N**ear **E**dge **S**tructure (XANES) analysis have confirmed that the *bis*-nitrate complexes are exchanged across the organic-aqueous interface.[36]

The remaining fission and corrosion products, lanthanides and minor actinides only form weak complexes with (**1**) and so are retained in the aqueous phase, which can be used as the feed for TRUEX or DIAMEX processes (section **1.4.2**). A drawback to the PUREX process is that some neptunium and technetium are also extracted with the uranium and plutonium and these need to be separated during the fabrication of uranium and plutonium oxides. However, almost all (> 99 %) of the fission products remain in the aqueous raffinate, which is then stored before undergoing a process of vitrification to high level waste (HLW).[37]

The extracted U(VI) and Pu(IV) complexes can be treated with iron and hydrazine, which only reduces Pu(IV) to Pu(III) and leaves U(VI) unaffected. The separated Pu(III) can be treated with HNO_3 to oxidise it back to Pu(IV) and subsequent heating with oxalic acid affords PuO_2.

Similarly, the feed containing (**1**) now loaded with just uranium can be stripped to give an aqueous solution of $UO_2(NO_3)_2$, which on heating and reduction, generates UO_2 (**Scheme 1.2**).[23]

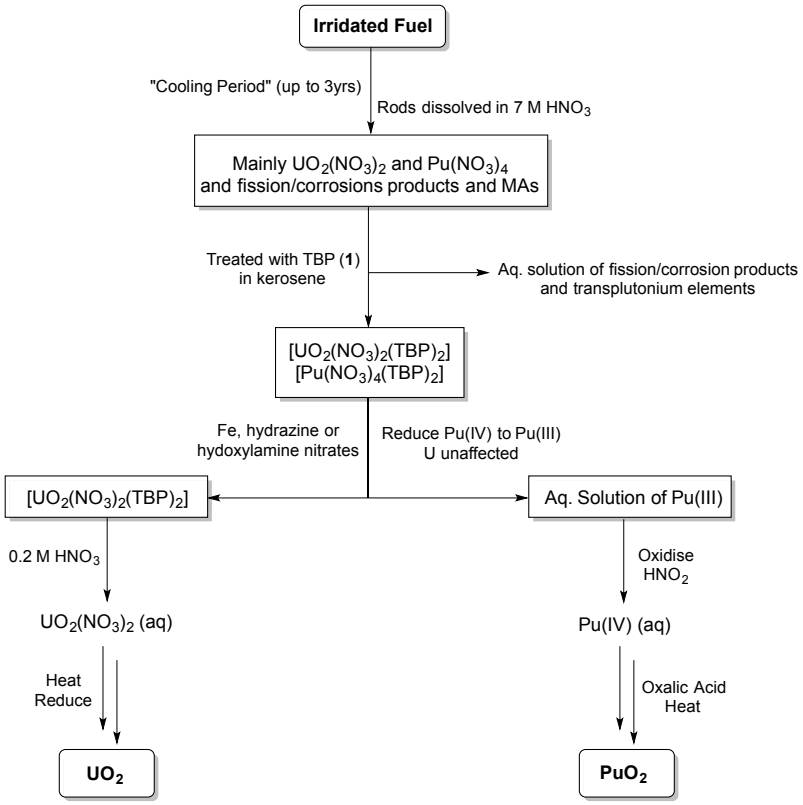

Scheme 1.2 – Summary of the PUREX process.[38]

The recovered uranium and plutonium oxides can be combined and fabricated into pellets to form a mixed oxide (MOX) fuel in order to render the fuel proliferation resistant. Recycled fuel such as MOX can then be re-entered into the nuclear fuel cycle to generate more energy.[34,39,40]

The remaining waste (PUREX raffinate) still contains the minor actinides and lanthanides. As the average ratio of lanthanides to actinides in the spent fuel is *ca*. 40:1, partitioning of the minor actinides from the lanthanides is essential before transmutation in a Generation IV reactor, as the lanthanides have higher neutron cross-capture radii. This means they would shield the actinides from the neutrons in the transmutation process, acting as 'neutron poisons'. If it can be demonstrated on scale, this strategy, known as '*partitioning and transmutation*' (P&T), is a highly promising solution to developing safer geological storage of SNF.[8,22]

1.4.2 – TRUEX and DIAMEX Processes:

Following the removal of uranium and plutonium during the PUREX process, the resultant feedstock containing the minor actinides and lanthanides can be treated with a non-selective ligand, by which all the f-block elements are extracted together from the remaining fission products. Different procedures using different ligands are used either side of the Atlantic. In the United States, the TRUEX process (**TR**ans**U**ranic **EX**traction) process was developed at the Argonne National Laboratory and typically employs bidentate hard *O*-donor ligands, such as carbamoylmethylphosphine oxides (CMPO), to extract the trivalent actinides and lanthanides by coordination to the carbonyl oxygen and phosphonyl oxygen atoms. The extraction ability and phase compatibility of different CMPO compounds varies greatly between the nature of the alkyl substituents on the core. Of all CMPO compounds investigated, [(*N,N*-diisobutylcarbamoyl)methyl](octyl)phenylphosphine oxide (**2**) showed the best combination of extraction properties when applied to a post-PUREX stream (**Fig 1.5**).[41]

CMPO (**2**) is now the principle extractant of trivalent lanthanides and actinides in the TRUEX process wherein a 0.2 M concentration of (**2**) is used in combination with 1.2 M of (**1**) in *n*-dodecane and (**1**) is used to inhibit third phase formation and reduce radiolytic degradation of (**2**). This combination showed good selectivity for the lanthanides and minor actinides over the other fission and corrosion products present in the post-PUREX raffinate and works on HNO_3 solutions of up to 6 M. However, few *O*-donor compounds have shown the ability to extract exclusively the minor actinides in order to separate them from the lanthanides as required for later transmutation.[5,42,43]

In Europe, a different type of ligand is used for the exact same extraction process, comprised of non-selective bidentate malondiamide units (**Scheme 1.3**). The process was developed by the French CEA (**C**ommissariat à l'**E**nergie **A**tomique) and named the DIAMEX process (**DIAM**ide **EX**traction). These malondiamide units can be easily synthesised by reacting malonyl chloride (**3**) with different amines in the presence of base.[34]

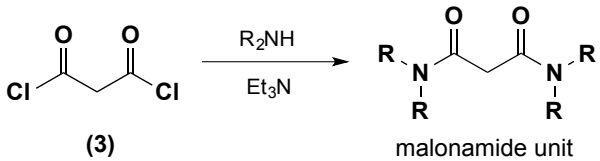

(3) malonamide unit

Scheme 1.3 – Synthesis of malondiamide units.

Current reference molecules for the DIAMEX process include *N, N*'-dimethyl-*N,N'*-dioctyl[(hexyloxy)ethyl]-malonamide (DMDOHEMA, **4**) and *N,N,N',N'*-tetraoctyldigylcolamide (TODGA, **5**). The latter has shown improved performance compared to other malonamide ligands in laboratory demonstration tests on genuine PUREX raffinate solutions, where a typical flow-sheet is shown in **Scheme 1.4**.[44] Addition of oxalic acid prevents the transfer of some problematic fission/corrosion products, such as zirconium and molybdenum, into the organic phase.

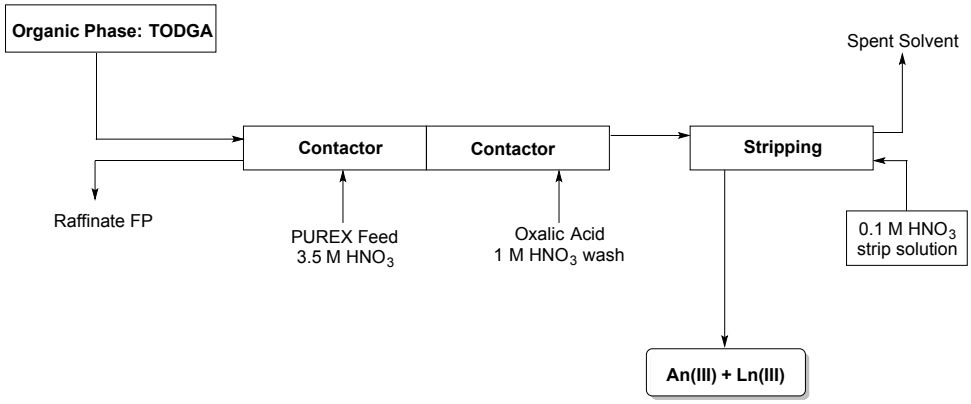

Scheme 1.4 – Flowsheet for a laboratory demonstration DIAMEX process

Substitution of methyl groups α- to the carbonyl in (**5**) has led to improved TODGA homologues, Me-TODGA (**6**) and Me_2-TODGA (**7**), which show improved stability towards the harsh conditions of the extraction processes (high acidity and radiolytic flux).[45]

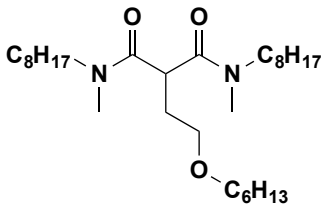

(4)

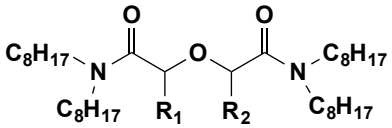

(5) R_1= H, R_2 = H
(6) R_1= Me, R_2 = H
(7) R_1 = Me, R_2 = Me

Figure 1.6 – Malonamide DMDOHEMA (**4**) and diglycolamides (**5-7**)

The nature of the extracted species using malonamide (**4**) has been elucidated by crystal structure analysis of their lanthanide complexes. It was found that the lanthanide ion is 10-

coordinate overall, bound to two bidentate malonamide units and three bidentate nitrate ions.[46]

A key difference between the TRUEX and DIAMEX processes is that the latter process uses compounds that comply with the *CHON principle*. This relates to the fact that, for ligands to be used in the nuclear waste reprocessing industry, they must contain only the elements carbon, hydrogen, oxygen and nitrogen. This minimises the generation of corrosive materials when the ligands are incinerated to give a solid waste form to be stored.[34]

1.4.3 – TALSPEAK Process:

The USA does not currently reprocess any of its SNF from nuclear reactors and currently the TRUEX process is used to clean-up legacy waste from research. Since the late 1960s the TALSPEAK (**T**rivalent **A**ctinide **L**anthanide **S**eparation by **P**hosphorous reagent **E**xtraction from **A**queous **K**omplexes) has been in development for potential process scale partitioning.[47]

The process uses an acidic organophosphorus reagent in the organic phase, a polyaminocarboxylic acid in the aqueous phase and a buffering agent to control pH. The TALSPEAK process differs from the typical solvent extraction processes to be discussed in this chapter, as the actinide elements are retained in the aqueous phase while the lanthanides are extracted. In the 1950s it was reported that the f-block elements could be extracted by di-(2-ethylhexyl)phosphoric acid (HDEHP, **8**) from mineral acid solutions. HDHEP is a liquid cation exchanger that can also act as a complexing agent and was found to form 3:1 complexes with the lanthanide/actinide metal centres, releasing protons into solution as it transferred the metal species into the organic phase. Distribution ratios of approximately 10^5 for La(III) to Lu(III) have been reported and the values overlap significantly with the trivalent actinides.[47] Some separation of individual members is possible with (**8**) alone, but it is not useful for any separation between the groups.

It was reported that, by modifying the aqueous phase with the addition of moderate concentrations of carboxylic acids and lowering the concentration of polyaminocarboxylic acids, a better separation between the lanthanides and actinides could be achieved. Eventually the optimum carboxylic acid was chosen as lactic acid (**9**) and the hold-back reagent employed was DTPA (diethylenetriaminepenta-acetic acid, **10**), which led to a

process that was first disclosed by Oak Ridge National Laboratory in 1968 by B. Weaver and F.A. Kappelmann.[48,49]

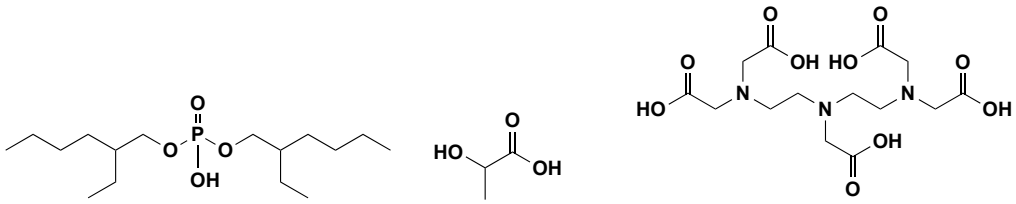

(8) (9) (10)

Figure 1.7 – Structures of HDEHP (**8**), lactic acid (**9**) and DTPA (**10**)

Lactic acid (**9**) was chosen as the most suitable carboxylic acid to be added to the aqueous phase due to the high solubility of its lanthanide salts and DTPA (**10**) was used as the hold-back reagent due to the strong complexes it formed with the actinides. A complete group separation with (**10**) was demonstrated where the three amine nitrogen atoms coordinate to the actinide centre adopting a specific geometry.[50]

Some advances have been made to improve the TALSPEAK process by varying the organic extractants and holdback reagents, especially in order to reduce the acidity of the organophosphorus reagent used.[51] However, the drawbacks include the use of non-CHON reagents and continuous pH buffering of the phases for optimal extraction. DTPA also undergoes radiolysis quite readily, rendering its use in an industrial scale separation technique problematic.

1.4.4 – SANEX Process:

In Europe, the approach adopted to separate the minor actinides from the lanthanides contained in a DIAMEX feed is known as the SANEX (**S**elective **A**cti**N**ide **EX**traction) process. The extraction reagent required for selective actinide binding must exhibit high stability under the harsh conditions of the SANEX process, be sufficiently soluble in the organic solvents used for extraction and show good extraction and stripping kinetics.[50] The most successful ligands derived for potential use in the SANEX process contain several soft donor atoms (e.g. N or S), as these ligands have been found to exploit the slightly more covalent nature of the metal-ligand bonding upon complexation with actinide 5f orbitals. However,

the nature of this covalency is still quite poorly understood, and continues to be the subject of ongoing research.[52–56]

Any compound chosen for use in the SANEX process must fulfil a series of demanding criteria, where the main points are summarised below:[8,57,58]

- The ligand and the extracted metal complex must have good solubility in the organic phase to prevent precipitation occurring;
- The selectivity for the actinides must be sufficiently high (5:1) so that extraction is achieved in the fewest number of steps;
- Extracted complexes formed need not to be so strong that back-extraction (stripping) of the metal species from the complex and recycling is impossible;
- The ligand moiety itself needs to be resistant to radiolysis and acid hydrolysis;
- The ligand must be able to extract from highly acidic conditions, up to 4 M HNO_3;
- The ligand must be cheap and easy to synthesize, in order to be produced economically on a large-scale.

1.4.5 – 1c-SANEX, i-SANEX and GANEX Processes:

Subsequently, other actinide extraction processes have been proposed including 1c-SANEX (1-cycle SANEX) and *i*-SANEX (innovative SANEX). Both processes were born after genuine demonstration tests of the SANEX process. The 1c-SANEX process developed by Wilden *et al*. involves applying a SANEX process directly to PUREX process conditions, to ultimately by-pass the DIAMEX process and reduce the number of stages required to separate actinides from lanthanides. Due to the complex composition of the PUREX raffinate and high acidity, this process is very difficult to design and implement.[59]

The *i*-SANEX process was developed and demonstrated by Geist *et al.* where TODGA (**5-7**) related compounds were used to co-extract all actinide(III) and lanthanide(III) ions into the organic phase (DIAMEX) before a hydrophilic actinide selective stripping agent would complex with the actinides exclusively providing a waste stream of pure actinide species. The extraction by hydrophilic actinide selective compounds is discussed in more detail in section **1.7**, but one of the drawbacks to this process is the use of sulfonated non-CHON ligands and so generation of further waste streams to be disposed of.[60,61]

The GANEX (**G**roup **A**cti**N**ide **EX**traction) concept involves the co-extraction of all the trans-uranic elements (Np, Pu, Am and Cm) by an actinide selective ligand from the dissolved spent fuel. This would take place directly on post-PUREX streams after the bulk removal of uranium. Advantages of this process include the fact that no direct stream of Pu is obtained, and that it would involve the shortest set of stages for any actinide extraction process.[25,62]

1.4.6 – Extraction Methodology:

During the solvent extraction/separation investigations discussed from here onwards in this thesis, the radioisotopes ^{152}Eu and ^{241}Am are used to represent the lanthanide and actinide series respectively, unless otherwise stated. To quantify the effectiveness of the ligand in extracting a metal during liquid-liquid extraction, the amount of the extracted metal present in the organic phase, with respect to the metal remaining in the aqueous phase is known as the *Distribution Ratio* $D_{(M)}$, where values of $D_{(M)} > 1$ are a result of > 50 % extraction of metal into the organic phase. (M = metal)

$$D_{(M)} = \frac{[M]_{org}}{[M]_{aq}} \qquad \textbf{Equation 1.1}$$

When more than one species is present in solution, it is possible to measure the relative removal of one species compared to the other, M_1 to M_2. This is known as the *Separation Factor, SF*. The separation factor for two metal species is the ratio of their *D* values and gives a measure of the selectivity of the ligand for one metal species over another. The larger the separation factor value the more selective the ligand.

$$SF_{(\frac{M_1}{M_2})} = \frac{D_{M_1}}{D_{M_2}} \qquad \textbf{Equation 1.2}$$

For solid phase extraction studies, the weight distribution ratios, D_w, are calculated (**Equation 1.3**), where A_o is the activity of the uncontacted aqueous phase, A_s is the activity of the aqueous phase after contact, *w* is the weight of the solid phase extractant and *V* is the volume in contact with the sample.[63] These values represent the ratio between the radioactivity (α- and γ- emissions) of each isotope in the standard solution and the supernatant. The separation factor is $SF_{Am/Eu} = D_{wAm} / D_{wEu}$ or $SF_{Am/Cm} = D_{wAm} / D_{wCm}$.

$$D_w = \frac{(A_o - A_s)}{A_s} \times \frac{v}{w} \qquad \textbf{Equation 1.3}$$

1.5 – SANEX Process Ligands:

1.5.1 – S-donor Ligands:

Some of the earliest examples of actinide-selective compounds were the *S*-donor dithiophosphinic acids.[64] These commercially available acids were tested for their extraction properties of Am(III) over Eu(III) and Zhu *et al*. showed that Cyanex 301, composed mainly of *bis*(2,4,4-trimethylpentyl)dithiophosphinic acid (**11**) (*ca.* 80 %) efficiently separated actinides with very high selectivities (up to $SF_{Am/Eu}$ > 4000).[65] The impurities present in this commercially available reagent were believed to lower its effectiveness in the extraction of f-block metals. Indeed, once Cyanex 301 was fully purified, and combined with auxiliary *N*-donor units such as 2,2'-bipyridine (**12**) and 1,10-phenanthroline (**13**), the selectivity was enhanced even further with reported separation factors of $SF_{Am/Eu}$ > 30,000 at pH ~ 3.7.[64] However, the shortcomings were that Cyanex 301, and other closely related organophosphinic acids could only extract from low concentration nitric acid streams (< 1 M) and were found to decompose upon exposure to high doses of γ-radiation. Some attempts were made to address these problems by designing aromatic dithiophosphinic acids such as (**14**), but no extraction was observed unless they were combined with TBP (**1**). The aromatic groups of (**14**) enabled the compound to be more stable towards γ-radiation, but complete oxidative degradation of the ligands occurred in highly acidic solutions (> 3 M).[66]

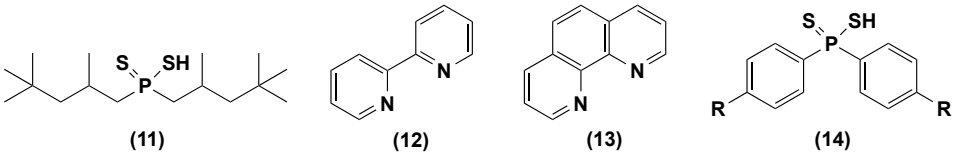

(11) (12) (13) (14)

Figure 1.8 – Cyanex acids (**11**, **14**) and auxillary *N*-donor ligands (**12**, **13**)

1.5.2 – N-donor Ligands:

Since good extraction of Am(III) and Eu(III) was achieved with hydrophobic malondiamides, where the oxygen atoms directed complexation, focus was turned to compounds that contained several softer *N*-donor atoms. Comprehensive reviews of heterocyclic ligands

containing soft nitrogen atoms exhibiting the ability to extract the minor actinides from the lanthanides in HNO_3 streams have appeared.[57,58,67]

One of the first heterocyclic *N*-donor ligands developed was 2,2':6',2''-terpyridine (TERPY, **15**) that, in combination with 2-bromodecanoic acid (**18**) acts as a lipophilic synergist and selectively extracts actinides from weakly acidic solutions. (In this context, the term "synergist" refers to an agent that assists in the extraction of metal complexes into the organic phase by means of ion pairing with the complex cation $[L_nM]^{III}$ to form a more hydrophobic complex).[34]

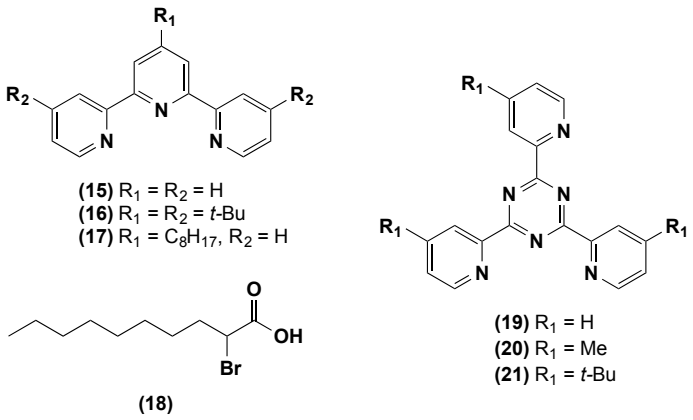

Figure 1.9 – TERPY and TPTZ compounds; 2-bromodecanoic acid (**18**)

Extraction studies revealed that the distribution ratios of the actinide metals greatly decreased upon increasing acidity and the solubility of (**15**) was relatively poor in the organic phase. Attempts at modifying TERPY with bulky alkyl groups (**16**) or a long carbon chain (**17**) to address solubility issues led to an increase in basicity and thus competition between protonation of the donor atoms and metal ligation. As well as competing with metal complexation, protonation of the ligand led to precipitation at the aqueous-organic interface.[8,34]

Inclusion of another pyridine ring and replacement of the central pyridine unit with a less basic triazine ring led to the development of 2,4,6-tri-2-pyridyl-1,3,5-triazine (TPTZ, **19-21**) ligands. Insertion of a triazine ring in TPTZs was rationalized to reduce the basicity of the ligand.[34,57] However, it was found that (**19**) was still protonated in highly acidic media and was quite insoluble in 3 M HNO_3, rendering it inefficient for a SANEX process extraction.

During solvent extraction studies, TPTZ (**19**) performed slightly better than TERPY (**15**), when used in combination with (**18**) and hydrogenated tetrapropene (TPH) as the diluent. TPTZ (**18**) was one of the first *N*-donor ligands to show a $SF_{Am/Eu}$ of > 10. However, these ligands were still unable to extract from solutions more concentrated than 0.1 M HNO_3. It was concluded that protonation of *N*-donor ligands such as (**15**) and (**19**) was competing with metal ion coordination and thus impeding the extraction in solutions of > 0.1 M HNO_3.[57,58,68] A more weakly basic ligand was envisaged to promote complexation with the actinide metals rather than protonation under acidic conditions. This led to the development of benzoxazole containing ligands (**22**); the synthesis of these ligands is shown in **Scheme 1.5** starting from 2,6-pyridine dicarboxylic acid (**23**).

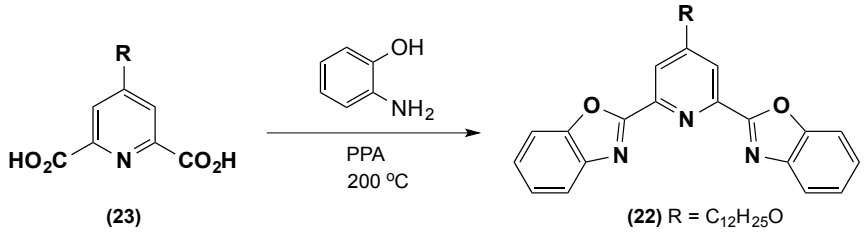

(23) **(22)** R = $C_{12}H_{25}O$

Scheme 1.5 – Synthesis of benzoxazole (**22**) containing ligands.

A feature of this type of ligand can be seen in the synthesis, which proceeded in polyphosphoric acid (PPA) at around 200 °C; thus exhibiting the stability of the benzoxazole system towards strongly acidic conditions.[69] The most promising benzoxazole ligand to be studied was 2,6-bis(benzoxazol-2-yl)-4-dodecyloxypyridine (BODO, **22**). In combination with (**18**) as the synergist, $SF_{Am/Eu} \approx$ 35-80 were observed and for the first time the SF values increased upon increasing acidity (up to 0.1 M HNO_3). However, again there was no significant extraction as the concentration of HNO_3 was increased beyond 0.1 M.

1.5.3 – BTP Ligands:

It was subsequently found that ligands containing the 1,2,4-triazine moiety could extract both Am(III) and Eu(III) from highly concentrated mixtures of HNO_3 (1-4 M), without the need for additional phase transfer agents or synergists. In 1999 it was reported that alkyl substituted 2,6-bis(1,2,4-triazin-3-yl)pyridine (BTP, **24**-**27**) ligands were able to extract Am(III) from Eu(III) with a very high separation factor of $SF_{Am/Eu}$ > 100.[9,70]

Triazine units in *N*-donor ligands such as (**24-27**) were found to exhibit the *α-effect*, wherein if atoms with non-bonding pairs of electrons are adjacent to each other (i.e. nitrogen atoms in this case), there is a decreased affinity of the nitrogens towards protonation due to the inductive effect of the adjacent heteroatom; with a commensurate increased affinity for 'soft' cations. The overlap of the adjacent non-coordinating nitrogen lone pair of the triazine ring with the coordinating lone pair leads to a greater covalent contribution to bonding and a greater orbital overlap with the more diffuse 5f orbitals of the actinides compared with the 4f orbitals of the lanthanides.[34,71]

The first synthesis of tridentate BTP (**24-27**) ligands was reported in 1971 and the generalized synthesis is shown below in **Scheme 1.6**.[72] The BTP ligands were synthesized by reacting hydrazine with a pyridine *bis*-nitrile (**28**) at ambient temperature followed by a condensation reaction of the subsequent pyridine *bis*-aminohydrazide (**29**) with various α-diketones. Variation of the alkyl groups of the BTP family (**24-27**) allowed tuning of the solubility of the ligands and a range of BTP ligands was screened for their ability to separate Am(III) from Eu(III) with very promising results.[57,58,68,73,74]

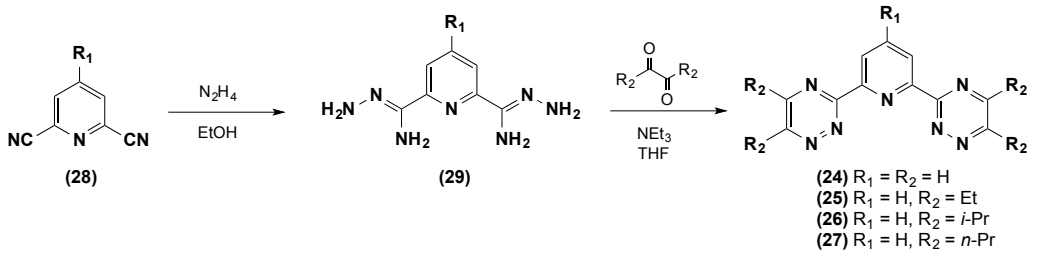

Scheme 1.6 – General synthesis of BTP ligands (**24-27**)

Initial studies on BTP ligand (**24**) showed the ability to separate Am(III) from Eu(III) very efficiently, but more importantly, they performed the extraction without the need for a synergist (e.g. **18**) and they extracted from solutions of much higher acidity than all previous *N*-donor ligands studied. This was a major break-through in the search for a ligand that exhibited potential properties suitable for industrial SANEX use. During developments to increase the solubility of the BTP ligand in industrially viable solvents, two promising BTPs emerged with tetra-*iso*-propyl- and tetra-propyl- side chains, (**26**) and (**27**) respectively.[70]

The extraction of Am(III) (D_{Am}) increased linearly as the concentration of BTP (**26**, **27**) ligand increased, however extraction efficiency decreased upon increasing HNO_3 concentration beyond 1 M. It was rationalized that, as the acid concentration increased, once again

protonation of the ligand was occurring. Nevertheless, a laboratory scale SANEX process was attempted on genuine PUREX raffinate, but during these tests it was shown that both tetra-alkyl substituted BTPs suffered catastrophic radiolytic degradation leading to abandonment of the process.[75]

At this stage, Harwood *et al.* argued that the side chains of BTPs (**26**, **27**) contained benzylic hydrogen atoms that were susceptible to degradation by reacting with hydroxyl radicals generated by radiolysis of water.[8,34] It was proposed to replace these side chains with solubilizing alkyl groups that contained no benzylic hydrogen atoms, and thus the reaction of pivalyl diketone (**30**) with *bis*-aminohydrazide (**29**) in an attempt to prepare tetra(*t*-butyl)-BTP (**31**) was investigated (**Scheme 1.7**). Unfortunately, no reaction occurred and this was rationalized to be due to the fact that diketone (**30**) remained in the *trans*- conformation due to the high-energy barrier to adoption of the *cis*- conformation necessary for condensation to occur.[76]

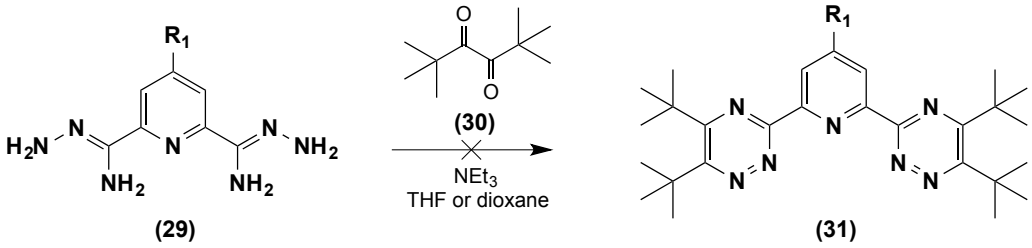

Scheme 1.7 – Attempted reaction of diketone (**30**) with *bis*-aminohydrazide (**29**)

To address the conformational intractability of diketone (**30**), it was suggested to tie the *tert*-butyl groups into a 6-membered ring, locking the diketone into its *cis*-conformer. Thus, $CyMe_4$-diketone (**32**) was synthesised from ethyl isobutyrate (**33**) as depicted in **Scheme 1.8.**[8,77] *In situ*-preparation of LDA and reaction with (**33**) forms an enolate that attacks both sides of ethylene ditosylate to generate di-ester (**34**). Intramolecular acyloin condensation of (**34**) in the presence of sodium and chlorotrimethylsilane affords *bis*-silyl enol ether (**35**) that can then be oxidized with bromine to furnish the $CyMe_4$ diketone (**32**).

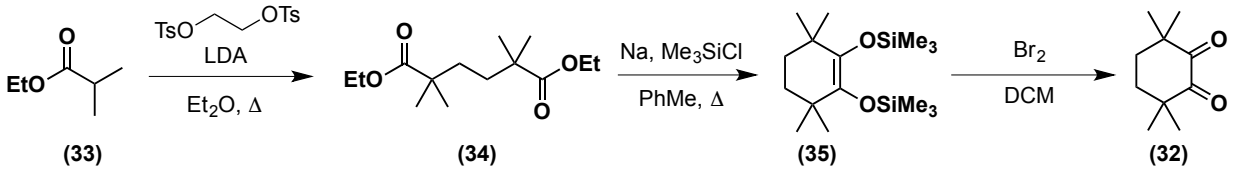

Scheme 1.8 – Synthesis of $CyMe_4$ (**32**) diketone

A benzannelated diketone ($BzCyMe_4$) was also synthesized in an attempt to enhance the solubility and stability of the ligand, and condensation with *bis*-aminohydrazide (**29**) afforded ligands (**36**) and (**37**) respectively, which are shown below in **Fig 1.10**.

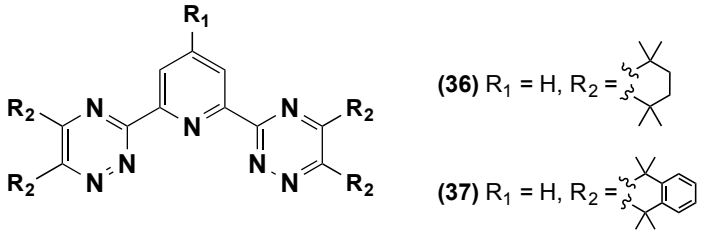

Figure 1.10 – Structure of BTP ligands (**36**, **37**)

Solvent extraction tests of $CyMe_4$-BTP (**36**) surprisingly revealed much higher extraction efficiency (D_{Am} ~ 500) and a far better separation factor ($SF_{Am/Eu}$ > 5000) than any related alkyl BTP ligands (**24-27**). Furthermore, due to (**36**) having no benzylic hydrogen atoms, the ligand demonstrated impressive stability towards acid hydrolysis, surviving boiling 3 M HNO_3 and ligand (**37**) also showed good stability towards doses of γ-radiation up to 100 kGy.[25] Unfortunately, during further extraction studies on BTPs (**26, 27, 36** and **37**) it was revealed that the extent of binding between the ligand and the actinide was so high that back-extraction (stripping) of the actinide from the organic phase could not be achieved. The BTP ligands are believed to associate with the actinide elements in a 3:1 ratio, as shown in a reported X-ray crystal structure of (**36**) with yttrium, shown below in **Fig 1.11**. In such a complex, the metal centre is 9-coordinate and is completely enclosed by three tridentate BTP ligands, with no other directly coordinating species, which provides an insight into the hydrophobic nature of the complex formed and its reluctance to allow the metal to be stripped.[22,78]

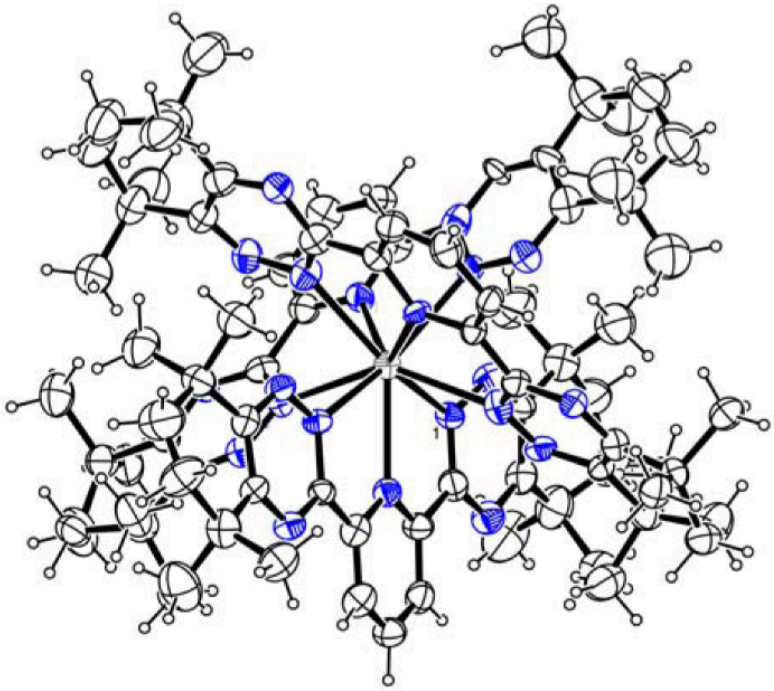

Figure 1.11 – X-ray crystallographic structure of [Y(**36**)$_3$].[Y(NO_3)$_5$].NO_3. Blue = nitrogen. Counter-ions and solvent molecules are omitted for clarity. See Ref. 73 for bond distances and details.

1.6.4 – BTBP Ligands:

Following the break-through and progress made with BTP *N*-donor ligands with good extraction affinity for Am(III) and separation over Eu(III), an additional nitrogen bearing ring was added to increase the number of coordinating nitrogen atoms to four and so the tetra-dentate 6,6'-bis(1,2,4-triazin-3-yl)-2,2'bipyridine ligands (BTBPs, **38**) were born. The reported synthesis of BTBP analogues (**Scheme 1.9**) started with the oxidation of 2,2'-bipyridine (**12**) with hydrogen peroxide in acetic acid to yield *bis*-*N*-oxide (**39**). A Reissert-Henze cyanation reaction with trimethylsilyl cyanide and benzoyl chloride afforded *bis*-nitrile (**40**), which was then reacted with hydrazine in ethanol to form *bis*-aminohydrazide (**41**). Reaction of (**41**) with α-diketones in THF and the presence of base generated the BTBP (**38**) class of ligand.[76]

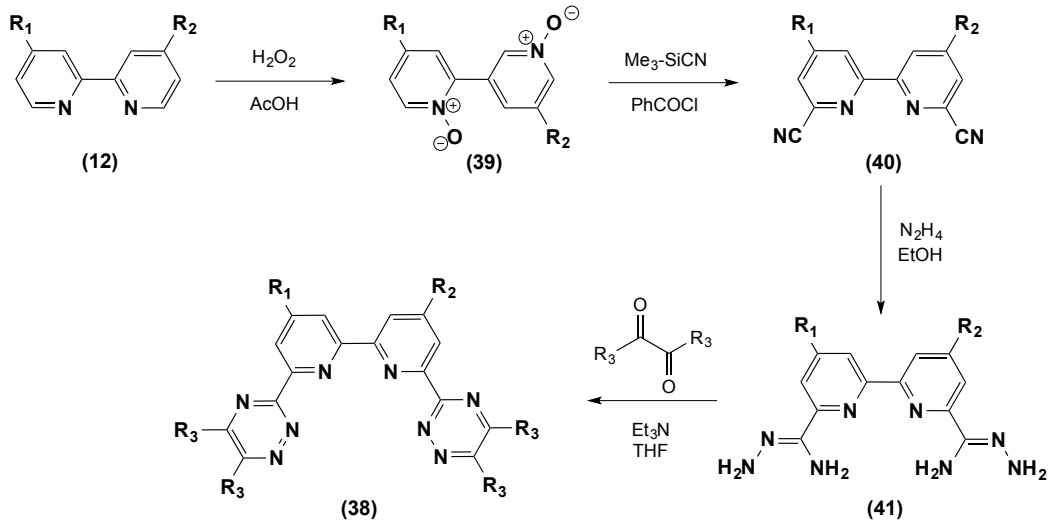

Scheme 1.9 – General synthesis of BTBP (**38**) ligands

Increasing the number of coordinating *N*-donor atoms to four in BTBP and thus introducing a weaker ligand field, brought the possibility of creating a ligand that may form 1:1 or 1:2 as well as 1:3 complexes during extraction, thus leaving sufficient room for other coordinating stripping species. Initial extraction studies of alkylated-BTBPs (**42-45**) showed promising results with both high distribution ratios of Am(III) (D_{Am} ~ 610-685) and high selectivity for Am(III) over Eu(III) ($SF_{Am/Eu}$ ≈ 145-175) from 1 M HNO_3 solutions. Subsequently, $CyMe_4$-BTBP (**46**) was synthesised by reacting *bis*-aminohydrazide (**41**) with diketone (**32**) in triethylamine and 1,4-dioxane and its extraction properties were thoroughly investigated.[22,58,76,78–81]

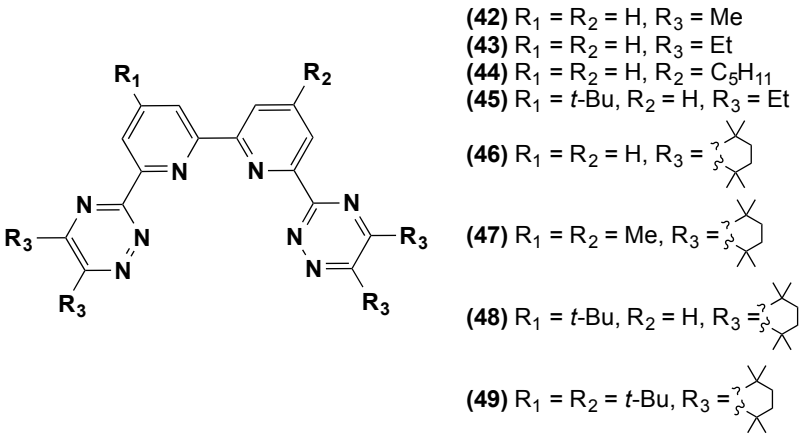

Figure 1.12 – Structure of BTBP analogues (**42-49**)

The studies showed that $CyMe_4$-BTBP (**46**) could extract Am(III) preferentially to Eu(III) in HNO_3 solutions of up to 3 M HNO_3. The ligand remained remarkably resistant to hydrolysis and radiolysis and survived contact with 1 M HNO_3 over 2 months. The complexes that were formed during extraction were not as strong as those seen with BTP's and Am(III) could be successfully back-extracted using glycolic acid. Extremely high selectivities of (**46**) for both Am(III) and Cm(III) over the entire lanthanide series were also reported.[78] However, although the separation factor of Am(III) from Eu(III) in 0.5 M HNO_3 was reported to be $SF_{Am/Eu} \approx 140$, the rate of extraction by (**46**) was much slower than that of the BTP (**36**) and so it was necessary to add DMDOHEMA (**4**) to the organic phase to improve the kinetics; an undesirable necessity. At this point, notwithstanding the previous experience with the tetra-alkyl BTPs (**26, 27**), it was decided to deploy (**46**) in a laboratory scale extraction test using post-PUREX raffinate. The set-up used a 16-stage rig of centrifugal separators (9 for extraction, 3 for scrubbing and 4 for stripping) (**Scheme 1.10**) at the Institute for Trans-Uranium Elements (ITU) in Karlsruhe, Germany in 2008 and produced extremely promising results. Ligand (**46**), together with DMDOHEMA (**4**) in 1-octanol demonstrated > 99.9 % recovery of both Am(III) and Cm(III) from a 2 M HNO_3 DIAMEX solution feed. It was also discovered that a solution of (**46**) and TBP (**1**) in cyclohexanone (PUREX process conditions) selectively extracted Am, Pu, Np and U from a highly acidic feed (4 M HNO_3), pointing to the possible development of a GANEX (**G**roup **A**cti**N**ide **EX**traction) process, which could be applied to a post-PUREX feed to extract only the minor actinides, enabling a complete by-pass of the DIAMEX process. Due to the great success during extraction testing, $CyMe_4$-BTBP (**46**) is widely considered to be the European benchmark ligand for use in the SANEX process.[76,82]

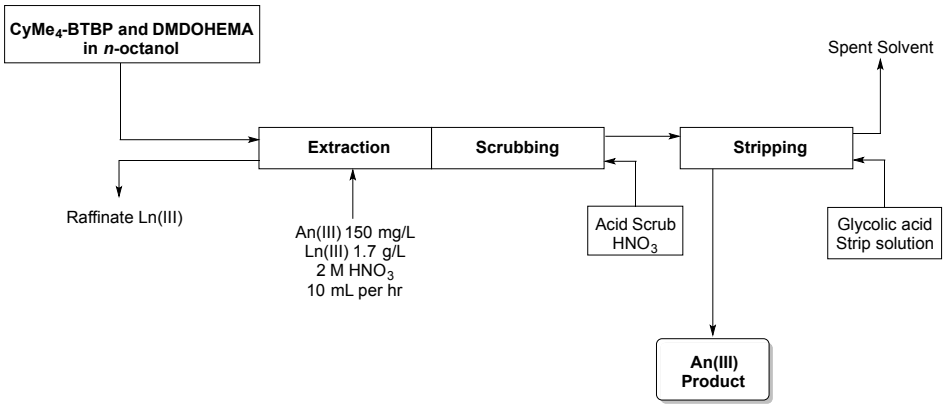

Scheme 1.10 – Process flow sheet of a hot test SANEX process involving ligand (**46**) and DMDOHEMA (**4**) in *n*-octanol.

X-ray crystal structures of BTBP ligand (**46**) with lanthanide metals have been obtained, where an example from Harwood *et al.*, is shown in **Fig 1.13**.[22,83] In this complex with the lanthanide Eu(III), two near orthogonal (**46**) ligands enclose the Eu(III) metal centre. In addition there is a single bi-dentate nitrate ion inside the inner coordination sphere and so the Eu(III) ion is 10-coordinate overall. Although the complex is hydrophobic, the metal centre is not completely enclosed compared with the 3:1 BTP complexes previously investigated (**Fig 1.12**). Complexes of (**44-46**) with Eu(III) in octanol have been studied using **T**ime-**R**esolved **L**aser **F**luorescence **S**pectroscopy (TRLFS) and X-ray diffraction where both 1:2 and 1:1 complexes of BTBP with Eu(III) have been isolated, both of which were 10-coordinate.[83]

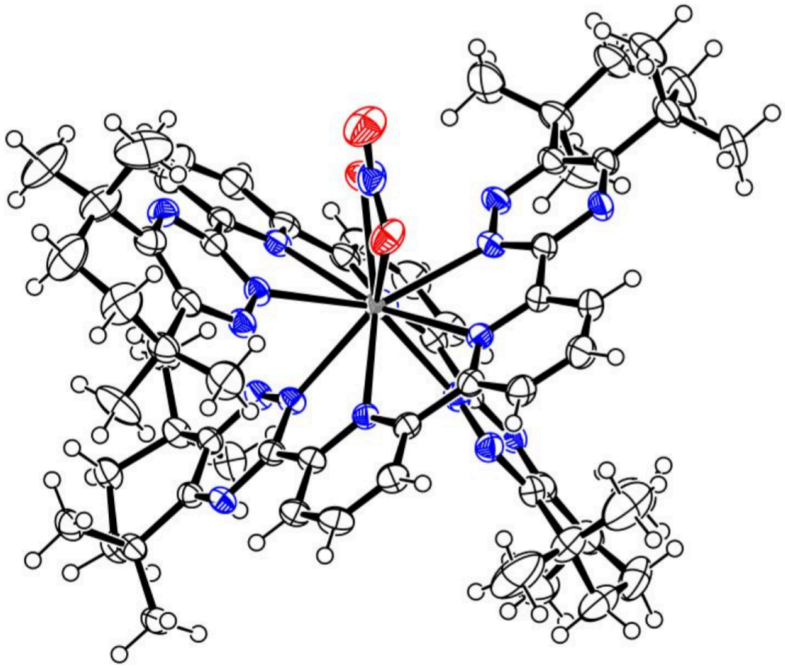

Figure 1.13 – X-ray crystallographic structure of [Eu(**46**)$_2$(NO$_3$)].[Eu(NO$_3$)$_5$]. Blue = nitrogen and red = oxygen. Counter-ions and solvent molecules are omitted for clarity. See Ref. 22 or 83 for bond distances and details.

1.6.5 – BTPhen Ligands:

The rate of extraction by CyMe$_4$-BTBP (**46**) alone was too slow for a laboratory scale SANEX test, necessitating the addition of the DMDOHEMA (**4**) to act as a phase transfer agent. Quantum mechanical calculations of the conformations of (**46**) revealed that the rotation around the central C-C bond of the bi-pyridyl unit showed a high energy barrier towards adopting the ligating conformation; whereas rotation around the C-C bond connecting the

pyridine and triazine units required much less energy.[82] It was argued that the slow rate of extraction could be attributed to this energetically unfavourable rotation of (**46**) from the predominant *trans*-conformation to the sterically less favourable *cis*-conformation in order for metal ligation to occur (**Fig 1.14**).

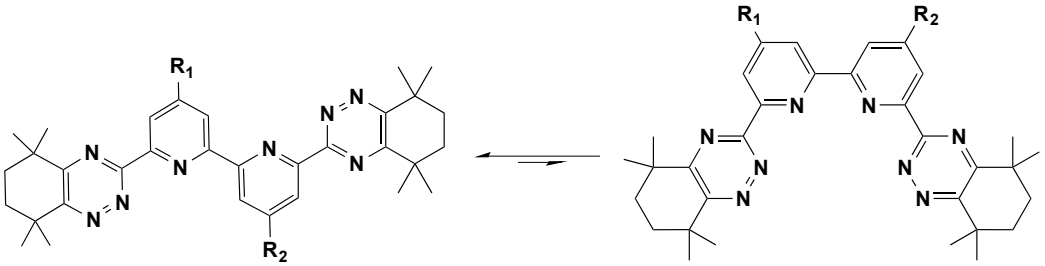

Figure 1.14 – Conformations of $CyMe_4$-BTBP (**46**)

To combat the slow kinetics of extraction by $CyMe_4$-BTBP (**46**), the Harwood group, that had developed the BTBP ligand family, employed the *cis*-locked 1,10-phenanthroline unit as the starting building material instead of 2,2'-bipyridine (**12**), which led to the development of a new class of ligand, the *bis*-triazinyl-phenanthroline (BTPhen) family (**Scheme 1.11**). The synthesis started with commercially available neocuproine (**50**) that was oxidized to *bis*-aldehyde (**51**) using stoichiometric amounts of selenium dioxide followed by a one-pot conversion of (**51**) into the *bis*-nitrile (**52**) via intermediate *bis*-oxime. Stirring nitrile (**52**) in hydrazine and ethanol at ambient temperature generated *bis*-aminohydrazide (**53**) and condensation with diketone (**32**) furnished $CyMe_4$-BTPhen ligand (**54**).[8,22,77]

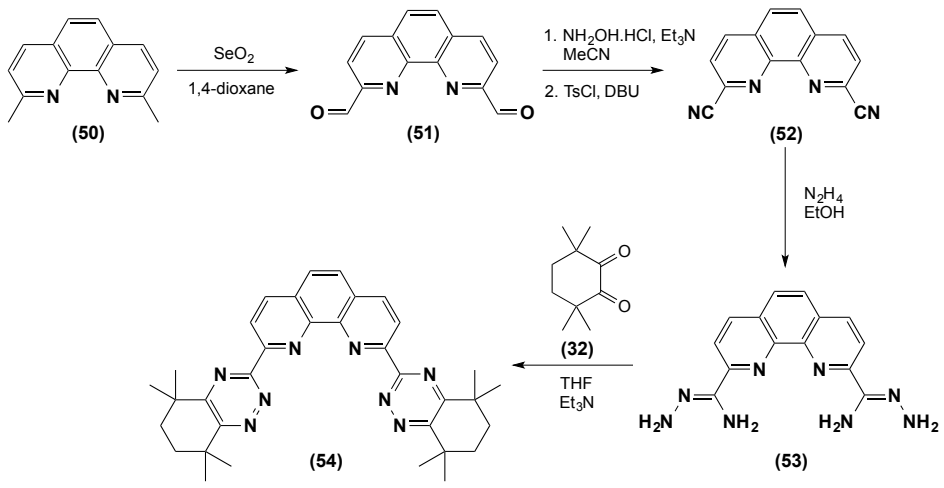

Scheme 1.11 – Synthesis of $CyMe_4$-BTPhen ligand (**54**)

In extraction studies, $CyMe_4$-BTPhen (**54**) in 1-octanol separated Am(III) from Eu(III) remarkably efficiently (D_{Am} > 1000 and D_{Eu} < 10) and was approximately 2 orders of magnitude more efficient than its $CyMe_4$-BTBP (**46**) counterpart. Although separation factors were similar ($SF_{Am/Eu} \approx 200 – 400$, from a range of 1 – 4 M HNO_3) (**Fig 1.15**), BTPhen (**54**) has surfaced as one of the most promising ligands for use in an industrial SANEX process, as faster extraction rates (< 15 min) (**Fig 1.16**) were observed, compared to the slow rates of BTBP (**46**), which were > 60 minutes – and this was in the absence of any phase transfer reagent to aid the extraction.

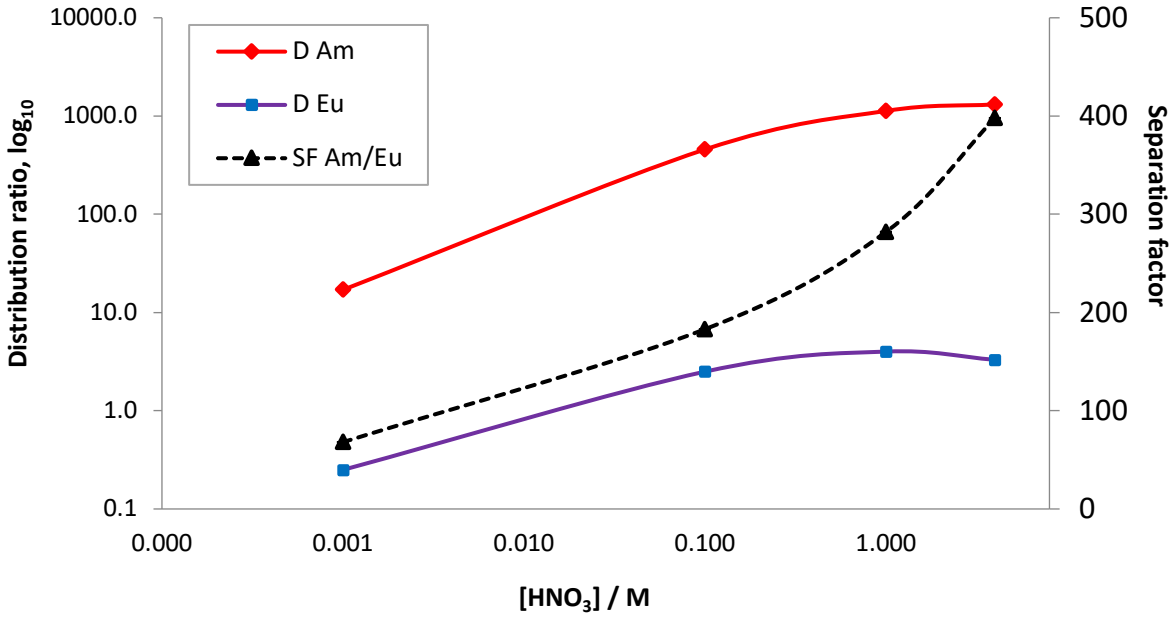

Figure 1.15 – Extraction of Am(III) from Eu(III) by (**54**) as a function of increasing nitric acid concentration. Ligand (0.01 M) in 1-octanol, contact time = 60 mins. Adapted and re-plotted from Ref 77.

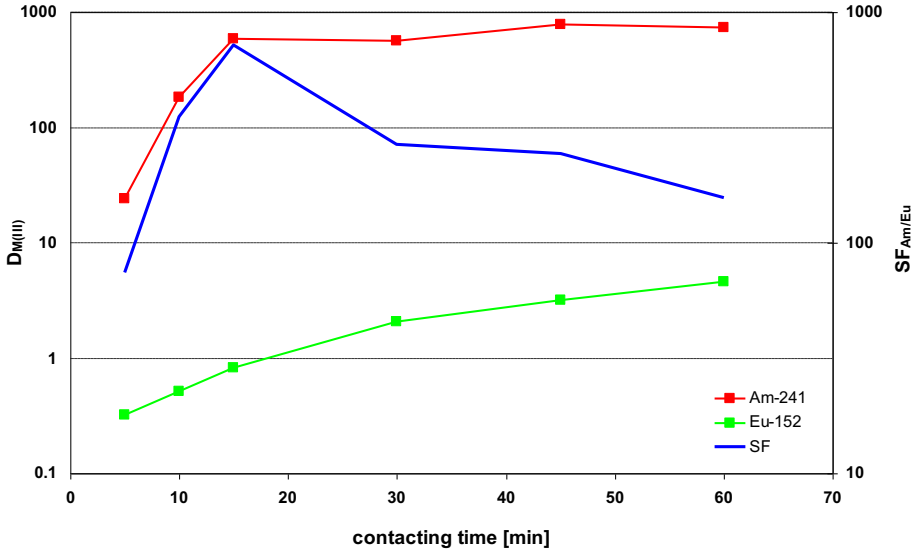

Figure 1.16 – Extraction of Am(III) from Eu(III) by (**54**) from 1 M HNO_3 as a function of time

BTPhen ligand (**54**) showed improved solubility compared to that of BTBP (**46**) and surface tension measurements of both ligands confirmed ligand (**54**) as the more surface active compound in most organic solvents.[77] As the extraction and stripping reactions of actinides in liquid-liquid extraction techniques are occurring at or near to the interface, the greater surface activity of BTPhen (**54**) may, in part, explain its improved extraction properties.

The rigidity of the 1,10-phenathroline unit in (**54**) can mean that complex formation is more kinetically and thermodynamically favourable than the BTBPs. Furthermore, the phenanthroline also possesses a dipole moment; whereas the *trans*-conformer of the 2,2-bipyridine does not. Thus, coordination to water via hydrogen bonding is more likely, leading to improved activity at the organic/water interface; a hypothesis borne out by the greater surface activity measured for BTPhen (**54**) and the fact that (**54**) crystallized with a molecule of water in the binding pocket.[77]

Quantum mechanical studies on both (**46**) and (**54**) have shown that the complexes formed have higher covalency in the N-Am bond over the N-Eu bond, where a greater electron density transfer from the *N*-donor atom of the ligand to the Am(III) over the Eu(III) ion was calculated. This in turn can lead to a larger electron density in the 6d orbital of Am(III) rather than the 5d orbital of Eu(III).[84]

Metal complexes of (**54**) have been crystallized and studied and a Eu(III) complex is shown in **Fig 1.17**.[77] Again, as with BTBP (**46**), the metal centre is 10-coordinate, enclosed by two

almost orthogonal tetra-dentate (**54**) ligands and one bidentate nitrate ion. This contrasts with the 1:3 complexes observed for the BTP ligand (**36**) and it is considered that this allows sufficient room for other displacement ions (water or nitrate) or stripping agents (e.g. glycolic acid) to displace the metal centre once extracted. As well as using X-ray structure determination of crystalline lanthanide complexes, both ligands (**46**) and (**54**) have been shown to form 2:1 lanthanide complexes as the predominant species in solution, studied using ^{1}H NMR spectroscopic titrations.[85]

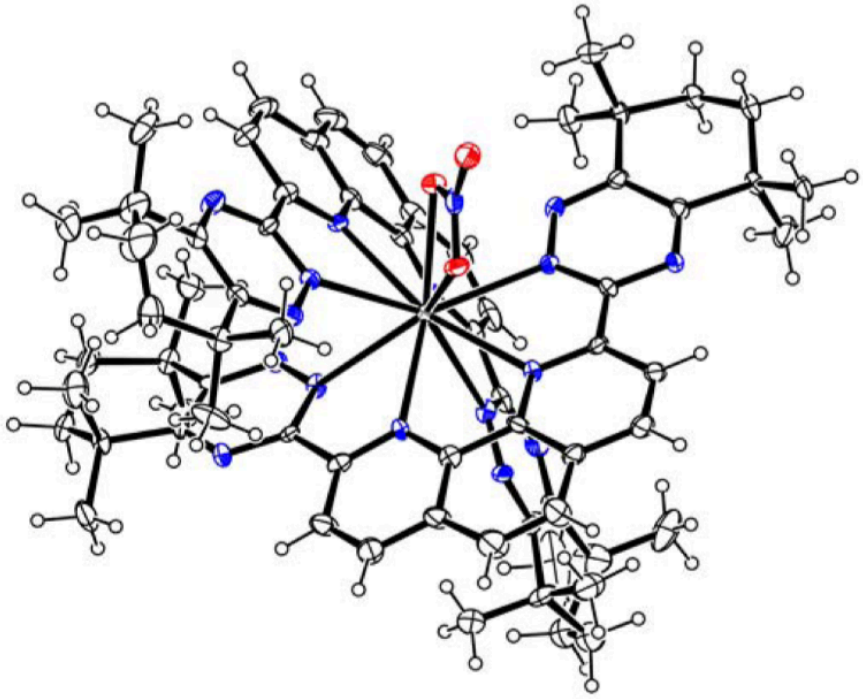

Figure 1.17 – X-ray crystallographic structure of [Eu(**54**)$_2$(NO$_3$)].[Eu(NO$_3$)$_5$]. Blue = nitrogen and red = oxygen. Counter-ions and solvent molecules have been omitted for clarity. See Ref. 77 for bond distances and more details.

However, Lewis *et al.* reported a 1:1 CyMe$_4$-BTPhen (**54**) complex with the transition metal yttrium (although a transition metal, yttrium is more chemically similar to the lanthanides and is considered a 'quasi rare earth element'), (**Fig 1.18**) where the metal centre was surrounded by three bidentate nitrate ions with one MeCN solvent molecule in the outer coordination sphere. The three nitrate ions coordinated directly to yttrium make this complex electronically neutral without any other counter-ions.[82] A 1:1 charge neutral BTPhen complex with europium was also isolated by Whitehead *et al*. in 2017.[86]

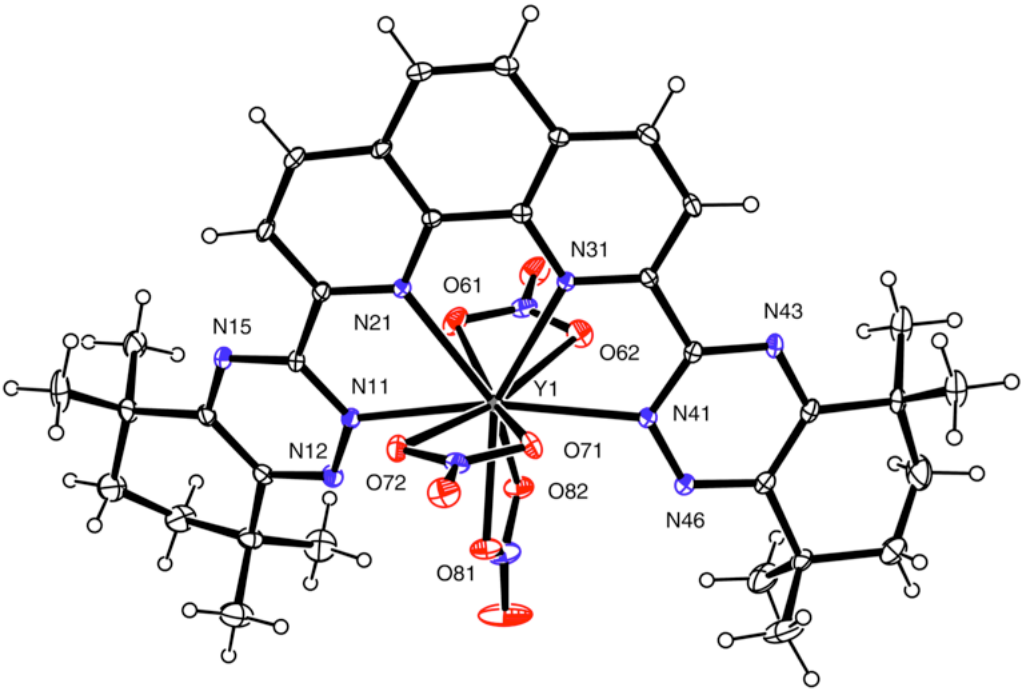

Figure 1.18 – X-ray crystallographic structure of [Y(**54**)$(NO_3)_3$].MeCN; Blue = nitrogen and red = oxygen. Solvent molecules have been omitted for clarity. See Ref. 77 for bond distances and more details

1.6 – Hydrophilic Complexants:

1.6.1 – Tetra-sulfonated Ligands:

Alternative methods of the separation of trivalent actinides from trivalent lanthanides have surfaced (section **1.4.5**), which have built on the TALSPEAK process developed in the US in the 1960s. The concept involves the non-selective co-extraction of both sets of elements using hydrophobic ligands into an organic phase followed by selective back-extraction (stripping) of the minor actinides into an aqueous phase using water-soluble hydrophilic ligands. It has more recently been shown that water soluble derivatives of BTP/BTBP/BTPhen ligands can selectively complex and extract the minor actinides Am(III) and Cm(III) over the corresponding trivalent lanthanides in HNO_3, where a selection of water soluble hydrophilic ligands are shown below in **Fig 1.19**.[60,87,88]

SO_3-Ph-BTP (**55**) exhibited good solubility in water and aqueous HNO_3 and back-extraction studies of (**55**) combined with TODGA (**5**) reported separation factors $SF_{Eu/Am} \approx 250\text{-}1000$.[60,88] However, as with alkyl-BTPs (**24-27**) the efficiency of extraction decreased as the concentration of nitric acid increased.

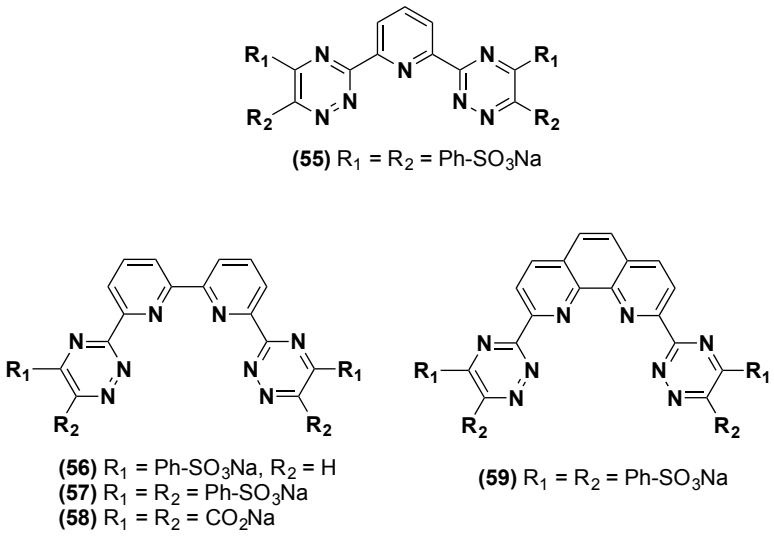

Figure 1.19 – Structures of water soluble hydrophilic BTP/BTBP/BTPhen ligands

Sulfonated BTBPs (**56, 57**) were synthesized and investigated in 2015 by Harwood and Lewis *et al*. and it was found that unsymmetrical BTBP (**56**) exhibited very poor separation of Am(III) over Eu(III) from HNO_3 solutions. It was concluded that the number of sulfonate groups on

the ligand, and the position (C5/C6) was more important than the type of ligand used (e.g. BTP/BTBP/BTPhen). Tetra-sulfonated BTBP (**57**) showed good selectivity for Am(III) and a separation factor $SF_{Eu/Am} \approx 707 \pm 312$ in 0.28 M HNO_3 has been reported.[87] Similar results were obtained for tetra-sulfonated BTPhen (**59**), with $SF_{Eu/Am} \approx 934 \pm 233$ in 0.28 M HNO_3. Both hydrophilic BTBP (**56**) and BTPhen (**59**) systems exhibited similar complexation ability as with their parent un-sulfonated compounds, in combination of TODGA (**5**) in the organic phase.[87]

Since the use of sulfonated BTBP/BTPhen ligands would cause generation of secondary acidic waste upon incineration due to the sulfur content, Harwood *et al.* synthesized water soluble BTBP analogue (**58**) with tetra-sodium carboxylate groups.[89] Extraction studies of ligand (**58**) produced poor selectivity for Am(III) ($SF_{Eu/Am} \approx 19$). Slightly higher separation factors were attained ($SF_{Eu/Am} \approx$ 53-59) when the extraction was performed under alkaline conditions (1-3 M NH_4NO_3) and no stripping of Am(III) from a loaded organic phase by (**58**) was achieved under neutral pH conditions. It was postulated that the mesomeric electron withdrawing nature of the carboxylate group in (**58**) caused lower selectivity for Am(III) when stripping from a loaded organic phase compared to sulfonated ligands (**56, 57** and **59**).

1.6.2 – 1,2,3-Triazole containing Ligands:

More recently in 2016 and 2017, Casnati *et al.* and Whitehead *et al.* have developed a series of CHON compliable water soluble hydrophilic triazole containing ligands (**Fig 1.20**).[90,91] Instead of containing 1,2,4-triazine units, the ligands contain 1,2,3-triazole rings and (**60**) and (**61**) were the first type of these compounds used to investigate Am(III)/Eu(III) separations.[90–92] Extraction experiments revealed that (**60**) could selectively strip Am(III) from 0.25 M HNO_3 with a separation factor of $SF_{Eu/Am} \approx 144$, compared to $SF_{Eu/Am} \approx 7$ as the blank with just TODGA (**5**). Ligand (**61**) boasted $SF_{Eu/Am} \approx 100$ and both ligands (**60, 61**) attained equilibrium after only 5 minutes. The extraction of Am(III)/Cm(III) and Pu(IV) separations was also investigated using ligands (**60, 61**) but no intra-actinide selectivity was observed.[91]

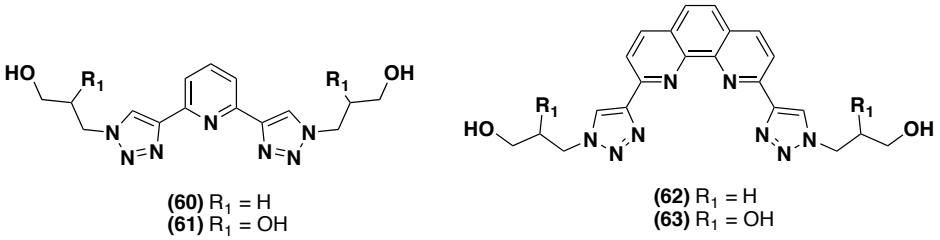

Figure 1.20 – Structure of triazol containing ligands

BTPhen-containing triazoles (**62, 63**) synthesized by Whitehead and Edwards *et al*. were found to be sufficiently soluble in aqueous HNO_3 solutions, with tetraol (**63**) being slightly more soluble (up to 0.01 M HNO_3).[90] Both ligands exhibited similar extraction behaviour to each other, and a clear back-extraction selectivity for Am(III) over Eu(III) from a TODGA (**5**) containing loaded organic phase. Separation factors $SF_{Eu/Am} \approx 36$ and 47 were attained for (**62**) and (**63**) respectively at 0.33 M HNO_3. As with the previously tested BTP/BTBP/BTPhen related ligands, as the concentration of HNO_3 increased, the extraction efficiency decreased due to protonation of the ligand resulting in a lower free ligand concentration.[90] Even though the separation factors achieved with BTPhen triazoles (**62, 63**) are approximately half of those obtained for pyridine triazoles (**60, 61**), the latter extractions required up to 80 mmol L^{-1} for efficient extraction compared to just 10 mmol L^{-1} for BTPhen triazoles (**62, 63**).[90]

The Am(III)/Cm(III) selectivity by BTPhen triazoles (**62, 63**) was also investigated where a separation factor $SF_{Cm/Am} \approx 2.5$ was reported, which is similar to previously reported Cm(III)/Am(III) separations using hydrophilic ligands such as those in **Fig 1.19**. However, this was the first time a fully CHON compliant, hydrophilic 1,10-phenanthroline ligand was used to achieve this difficult intra-actinide separation.[90]

1.7 – Functionalized BTPhen Ligands:

1.7.1 – Solubility and solution phase studies of functionalized BTPhens:

A range of different BTPhen analogues has previously been synthesised by reacting *bis*-aminohydrazide (**53**) with both commercially available diketones and a range of diketones synthesized using different starting esters in the synthesis described in **Scheme 1.8**. Their solubility in diluents used in the nuclear industry has been investigated as well as their solution complexation behaviour. The variety of diketone families investigated involved aliphatic (**64-69**), benzil (**70-73**) and isatin (**74-77**) diketones where a selection is depicted below in **Fig 1.21**.[93,94]

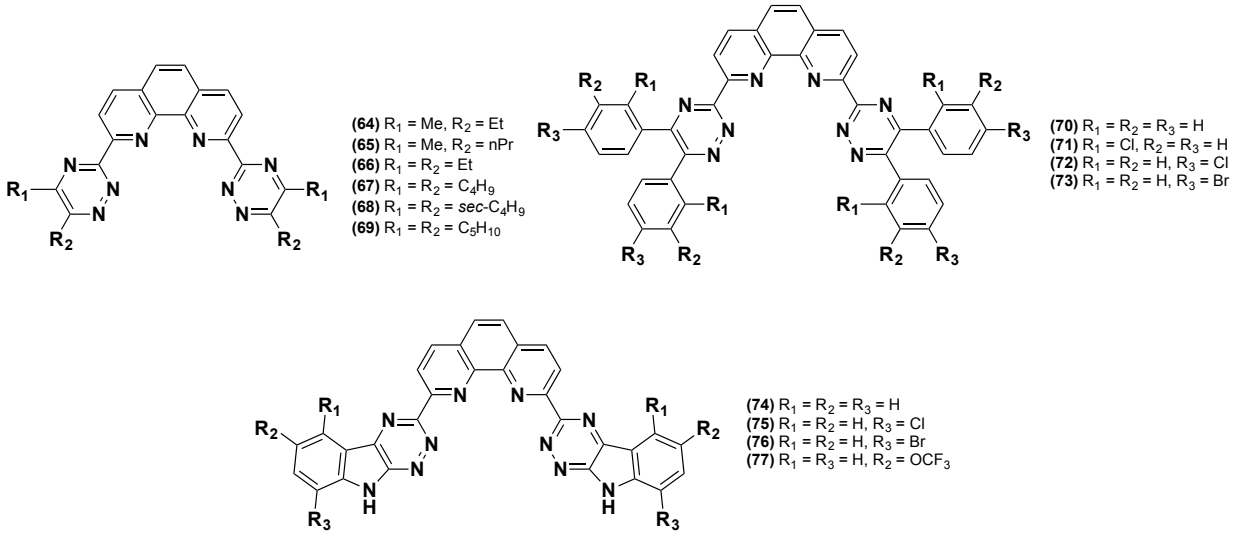

Figure 1.21 – BTPhen analogues: aliphatic (**64-69**), benzil (**70-73**) and isatin (**74-77**).

The solvents in which the ligands were tested were 1-octanol (alcohol), dodecane (aliphatic) and cyclohexanone (cyclic ketone), which broadly represents the different solvent classes used in the nuclear industry. For the aliphatic BTPhens (**64-69**), increasing the length of the side chain increased the solubility of the ligand in both 1-octanol and cyclohexanone at the expense of acid and radiolytic stability. C4-BTPhen (**67**) showed optimal solubility in both 1-octanol (18.8 mM) and cyclohexanone (29.0 mM).[93] All the isatin BTPhens (**74-77**) showed low solubility (< 6 mM) in dodecane and slightly higher solubility in 1-octanol. Cyclohexanone resulted in the highest solubility of isatin BTPhen (**77**, 192 mM) bearing CF_3 functional groups.[94]

The stoichiometry of the complexes formed by ligand (**67**) in solution has also been investigated by lanthanide NMR spectroscopic titrations. The lanthanides used were La(III) (ionic radius = 116 ppm)[27] and Lu(III) (ionic radius = 98 pm)[27] in order to give the greatest difference in the lanthanide(III) radii and thus examine the largest effect of the lanthanide contraction. After 0.5 equivalents of lanthanide salt were added, a 2:1 species was formed as indicated by ^{1}H NMR analysis (**Fig 1.22**). Upon addition of excess lanthanide salt, formation of a new species, proposed to be the 1:1 complex was observed, but the majority of the BTPhen ligand remained as a 2:1 complex, even up to 1.5 equivalents of added lanthanide.[93]

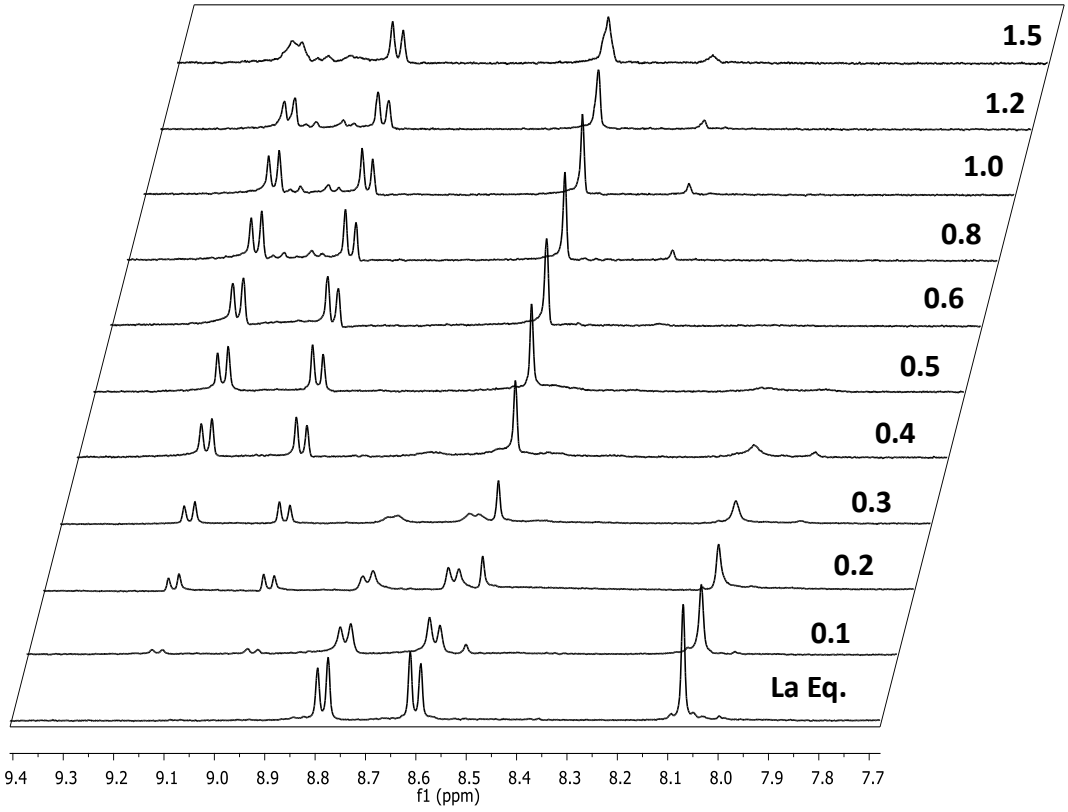

Figure 1.22 – Stacked ^{1}H NMR spectra (7.7-9.4 ppm) of C4-BTPhen (**67**) (0.01 M) titrated with $La(NO_3)_3$ in CD_3CN (See ref. 93 for further details)

1.7.2 – Electronic Modulation at 5,6-positions of BTPhen:

Following the remarkable extraction properties exhibited by $CyMe_4$-BTPhen (**54**), a series of electronically modulated BTPhen ligands bearing substituents at the 5,6-position of the phenanthroline backbone was developed by Afsar and Harwood *et al.*[95] 2,9-dimethyl-1,10-phenanthroline (neocuproine, **50**) was functionalized with bromine atoms across the 5,6-double bond to give both the mono- and di-brominated neocuproine respectively (**78** and **79**) (**Scheme 1.12**).[96]

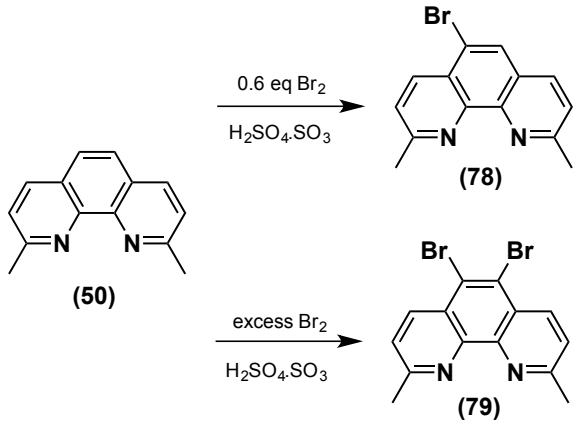

Scheme 1.12 – Functionalization of neocuproine with bromine atoms

Compounds (**78** and **79**) were carried through the synthesis described in **Scheme 1.11** and condensed with dodecane-6,7-dione (**80**) to form modulated C5-BTPhen ligands (**81**) and (**82**). Extraction of Am(III) from Eu(III) across a range of HNO_3 concentrations was investigated and compared to the unmodulated C5-BTPhen ligand (**69**).[95]

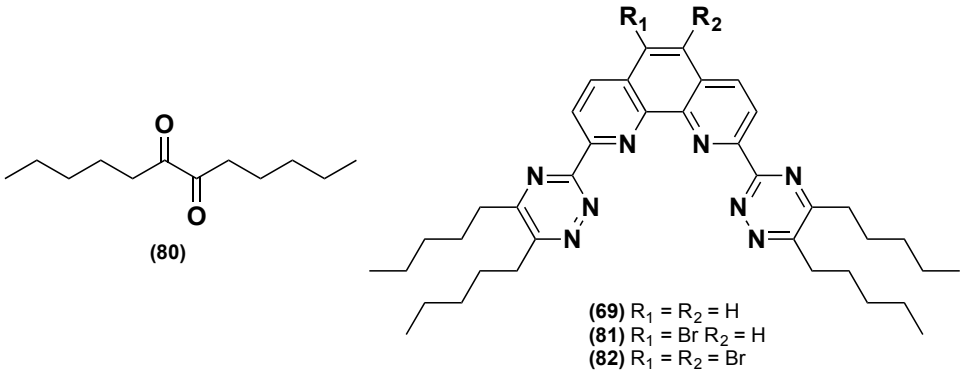

Figure 1.23 – Structure of dodecane-6,7-dione (**80**) and C5-BTPhen ligands (**69, 81-82**)

C5-BTPhen ligand (**69**) exhibited good selectivity with a reported separation factor of $SF_{Am/Eu}$ ≈ 180 at 4 M HNO_3 in 1-octanol and there were no significant decreases in D_{Am} or D_{Eu} values as the HNO_3 concentration was increased from 0.001-4 M. Br-C5-BTPhen (**81**) boasted a similar extraction trend but an overall higher separation factor was observed ($SF_{Am/Eu}$ ≈ 250 at 4 M HNO_3); the D_{Am} values remained at ≈ 100 (as with **69**) but the D_{Eu} values were significantly lower across all HNO_3 concentrations. Br_2-C5-BTPhen ligand (**82**) reported a similar extraction for Am(III) (D_{Am} ~ 100), but now the extraction for Eu(III) was approximately one order of magnitude lower than that of (**69**) with a reported separation factor of $SF_{Am/Eu}$ ≈ 800 at 4 M HNO_3. It has been postulated that the introduction of bromine atoms across the phenanthroline backbone causes inductive withdrawal of electron density from the rings, thus reducing the electron donating capacity of the coordinating nitrogens making the ligand less effective for complexing with lanthanides.[95]

Following these interesting results, Harwood *et al*. carried Br-neocuproine (**78**) through the synthesis in **Scheme 1.11** and condensed the resultant bis(aminohydrazide) with $CyMe_4$-diketone (**32**) to give Br-$CyMe_4$-BTPhen (**83**). Suzuki coupling with 4-hydroxyphenyl boronic acid generated 5-(4-hydroxyphenyl)-$CyMe_4$-BTPhen (**84**), which presented a $CyMe_4$-BTPhen ligand with an electron-donating substituent at the 5-position. The extraction capabilities of these two ligands (**Fig 1.24**) for Am(III), Cm(III) and Eu(III) were thoroughly investigated.[97]

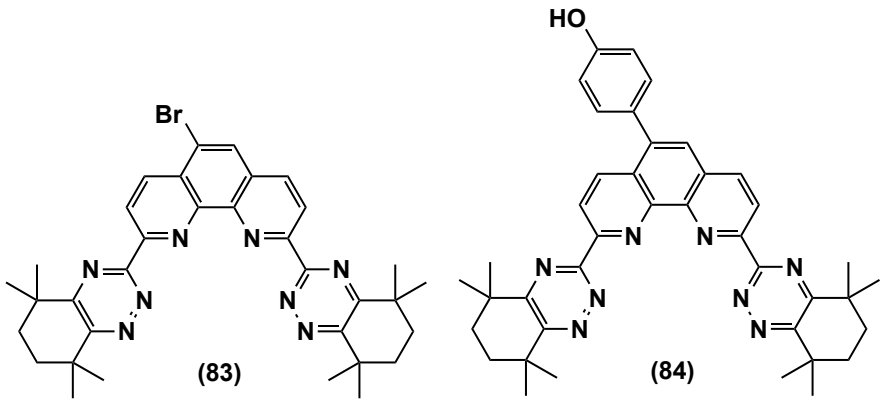

Figure 1.24 – Structure of Br-$CyMe_4$-BTPhen (**83**) and 5-(4-hydroxyphenyl)-$CyMe_4$-BTPhen (**84**)

During the extraction studies of (**83**), it was found that D_{Am} values increased with increasing nitric acid concentration. The *D* values for Eu(III), other trivalent lanthanides and Y(III) were

found to be approximately one order of magnitude lower than those obtained for parent $CyMe_4$-BTPhen (**54**), and the resulting separation factor at 3 M HNO_3 was $SF_{Am/Eu} \approx 680$ appeared to be far superior to that of (**54**). Br-$CyMe_4$-BTPhen (**83**) reported values for *D* to be < 1 for all trivalent lanthanides across most HNO_3 concentrations.[97]

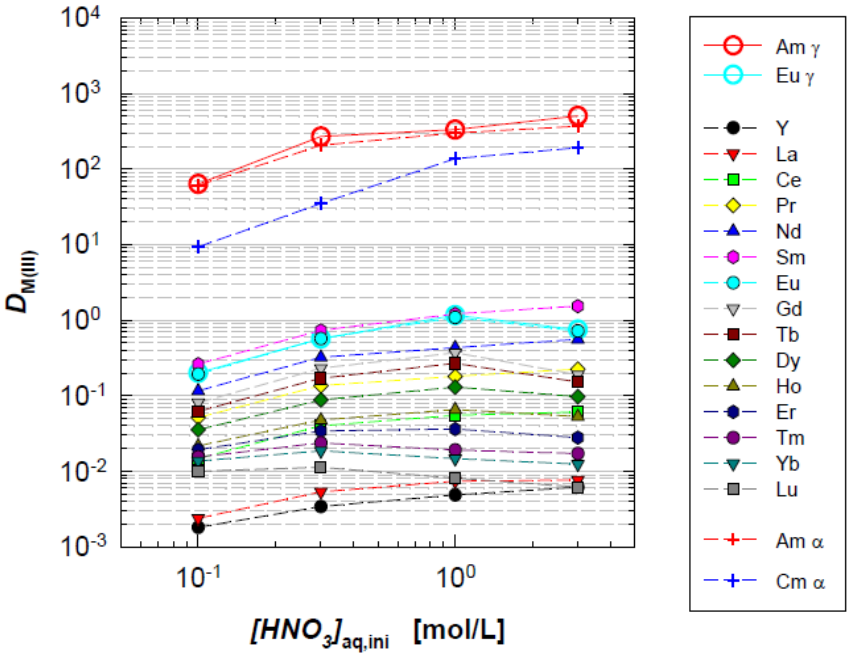

Figure 1.25 – Extraction of Am(III), Ln(III) and Y(III) by 5-Br-$CyMe_4$-BTPhen (**83**) in 1-octanol as a function of nitric acid concentration. See ref. 97 for details.

Investigation of the highly challenging Am/Cm separation by (**83**) (+ markers in **Fig 1.25/1.26**) showed an increase in *D* values as the nitric acid concentration increased, at the expense of selectivity. The highest reported separation factor for Am(III) over Cm(III) was $SF_{Am/Cm}$ ca. 7 at 0.1 M HNO_3, but use of this ligand in the nuclear industry would cause further waste streams as the compound is non-CHON.[97] The effect of the electron donating phenol substituent on the exraction properties of $CyMe_4$-BTPhen is shown below in **Fig 1.26**. Very high *D* values for Am(III) were obtained (D_{Am} > 1000 at 3 M HNO_3), indicating efficient extraction of Am(III). The *D* values obtained for Y(III) and all the trivalent lanthanides fell between those obtained for parent un-modulated $CyMe_4$-BTPhen (**54**) and Br-$CyMe_4$-BTPhen (**83**) leading to a separation factor of $SF_{Am/Eu} \approx 320$ at 3 m HNO_3. Extraction of Am(III) and Cm(III) (+ markers) increased as the nitric acid concentration increased and a maximum separation factor of $SF_{Am/Cm} \approx 5$ was obtained, but this time, with a CHON compliant ligand.

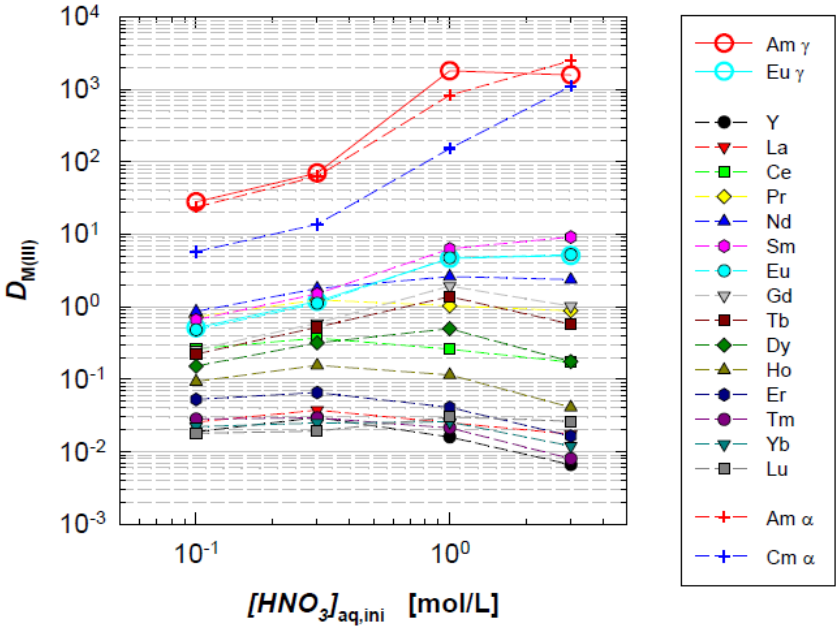

Figure 1.26 – Extraction of Am(III), Ln(III) and Y(III) by 5-(4-hydroxyphenyl)-CyMe$_4$-BTPhen (**84**) in 1-octanol as a function of nitric acid concentration. See ref. 97 for details

1.7.3 – Electronic Modulation at 4,7-positions of BTPhen:

Whitehead and Edwards *et al*., developed a series of 4,7- functionalized BTPhens (**85-87**) in order to investigate the effect of a more direct electronic effect towards the two phenanthroline nitrogen atoms (**Fig 1.27**).[98] The *para*-positioning of the substituents at the 4,7- positions was postulated to lead to an enhanced effect on coordination of minor actinides in the presence of lanthanides. Cl- (**85**) and MeO- (**86**) substituents were investigated due to their strongly electronically modifying nature as well as phenyl- (**87**), which was rationalised to be an intermediate between the two as well as possibly enhancing solubility in the hydrocarbon solvents used in nuclear reprocessing.

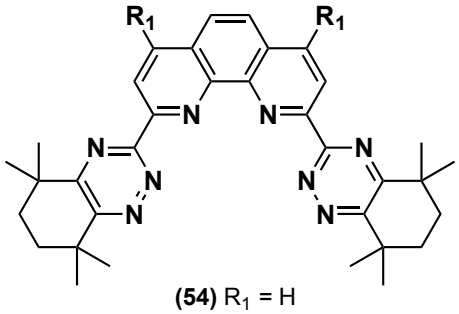

(54) R_1 = H
(85) R_1 = Cl
(86) R_1 = OMe
(87) R_1 = Ph

Figure 1.27 – Structure of 4,7-modified BTPhens (**54**, **85-87**)

The 4,7-dichloro-2,9-dimethyl-1,10-phenanthroline unit was prepared using a protocol described by Ulven *et al*., and then modified by including an electron-donating MeO- substituent by *in situ* reaction with sodium methoxide.[99] The di-phenyl substituents were prepared by a Pd-catalysed Suzuki-Miyaura cross coupling of the di-chloro intermediate with phenylboronic acid.[98]

Extraction and kinetic studies on ligands (**85-87**) revealed that the phenyl system (**87**) attained equilibrium within 1 hour of contact, whilst ligand (**86**) took 2.5 hours. Cl functionalised ligand (**85**) still had not attained equilibrium even after 16 hours of contact time. This was the first report that the extraction kinetics of BTPhen ligands could possibly be due to electronic functionalization of the 1,10-phenanthroline core. The investigation of kinetics of (**85-87**) also revealed that modulation at the 4,7- positions had significant impact on the equilibrium distribution ratios obtained, with orders of magnitude difference observed for Cl-functionalized ligand (**85**) ($D_{Am} \sim 0.4$) and OMe- ligand (**86**) ($D_{Am} \sim 1800$), highlighting the very poor extraction ability of (**85**).[98]

Extraction testing as a function of increasing nitric acid concentration on ligands (**85**-**87**) was also investigated to probe the effect of modulation at 4,7- positions further and revealed that the electron donating methoxy-substituent caused a continuous decrease in distribution ratios for all trivalent actinide/lanthanide species as the HNO_3 concentration increased from 0.1 to 3 M, with an average separation factor $SF_{Am/Eu} \approx 110$. This was attributed to the increased basicity of ligand (**86**) and thus increased protonation as the concentration of HNO_3 increased, decreasing the free ligand concentration.

However, ligand (**85**) demonstrated an increase in the *D* values as HNO_3 concentration increased up to 3 M. Conversely, it was concluded that the 4,7-chloro substituents were

causing a decrease in the basicity of the 1,10-phenanthroline *N*-donor atoms and thus decreasing the competing protonation process. Ligand (**85**) exhibited very little change in selectivity compared to parent $CyMe_4$-BTPhen (**54**) with a recorded separation factor $SF_{Am/Eu} \approx 110$, *cf.* (**54**) $SF_{Am/Eu} \approx 120$, in this study.

Phenyl-functionalized ligand (**87**) was found to have rather limited solubility in the organic solvents for extraction and so analysis was performed at 4.5 mM (compared to 10 mM for (**85, 86**)). The extraction by (**87**) was found to have comparable distribution trends to parent ligand (**54**) with a slight increase for selectivity ($SF_{Am/Eu} \approx 150$). Considering that it is CHON compliant, ligand (**87**) could be a promising development, with its faster extraction kinetics compared to parent BTPhen (**54**).[98]

An X-ray crystallographic structure of ligand (**85**) by slow evaporation in a dichloromethane solution revealed a water molecule present in the cavity of the ligand, consistent with previously reported structures.[77,98] The ligand however was found to be in the *c-c* conformation (triazine rings) compared to the usual *t-t* conformation observed with parent BTPhen (**54**). Additionally, a dichloromethane molecule in the cavity was seen to form non-conventional hydrogen bonds to the triazine nitrogen atoms.[62,98]

1.8 – Immobilization onto Magnetic Nanoparticles (MNPs)

The liquid-liquid extraction processes discussed in this chapter so far come with certain disadvantages, which include the requirement for substantial liquid storage of the generated secondary waste, the need for large volumes of organic solvent and degradation of the solvents over time which result in reduced performance and efficiency.[100] Liquid-liquid extraction processes often require the use of phase modifiers to optimize extraction and third phase formation can be encountered.

The use of magnetic separation technology in the nuclear industry (MACS process – **M**agnetically **A**ssisted **C**hemical **S**eparation) was reported in 1995 by researchers at Argonne National Laboratory.[101] The use of this process was rationalized to reduce the complexity of the reprocessing of used fuel and help facilitate scaling because of its simplicity. Advantages include the ease of separation of the ligand-MNP moiety, since this only requires a small applied magnetic field, and recyclability of the MNPs.[102] More recently, TODGA-coated MNPs (Fe_3O_4@TODGA) captured Am(III) and Pu(IV) from 3-4 M HNO_3 very efficiently where HNO_3 induced pre-organisation of TODGA before nanoparticle coating was important for the sorption of Am(III) and Pu(IV).[103]

As a proof of concept, Harwood *et al*. demonstrated that neocuproine (**50**) could be immobilized onto iodoalkyl-functionalized MNPs by nucleophilic substitution using a phenol linking group at the 5-position of neocuproine. Neocuproine (**50**) is known to coordinate Cu(II) ions, yet extraction studies of Cu(II) with this immobilized ligand system across a range of pH, wherein 2:1 complexation would be impossible, revealed up to 99 % extraction with kinetic studies indicating the extraction was effectively complete after just 5 minutes.[104,105]

Following the development of 5-(4-hydroxyphenyl)-$CyMe_4$-BTPhen (**84**), this ligand was subsequently investigated for its extraction compatibility for Am(III) when covalently bound to silica-coated magnetic nanoparticles (MNPs) (**Fig 1.28**).[85,106] Due to the extreme acidic nature of the post-PUREX streams, un-protected iron-oxide cores cannot be used and so it was rationalized to coat the nanoparticles with silica to provide a chemically resistant layer and furnish a chemical anchor for subsequent functionalization, without effecting the magnetic properties.[107] These functionalized MNPs would then be collected magnetically, instead of using centrifugation, with subsequent recycling of the MNP by stripping the radioactive metals, generating a smaller amount of secondary waste.

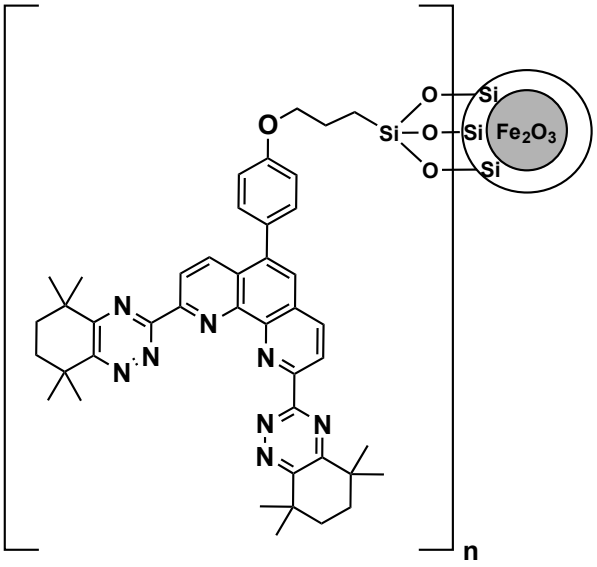

(85)

Figure 1.28 – Structure of $CyMe_4$-functionalized SiO_2-coated MNPs (**85**)

The extraction results of (**85**) for Am(III)/Eu(III) separations are shown in **Fig 1.29**.[106] At low nitric acid concentration (0.001 M), high *D* values (*D* > 700) were obtained for both Am(III) and Eu(III) with no selectivity ($SF_{Am/Eu} \approx 1.7$). However, as the nitric acid concentration increased, Am(III) extraction increased up to 0.1 M before falling, but *D* values for Eu(III) fell substantially to give $SF_{Am/Eu} \approx 65$ at 1 M HNO_3. Remarkably, at 4 M HNO_3 the extraction of Am(III) was recorded as $D_{Am} \sim 55$, but the affinity for Eu(III) was almost completely removed ($D_{Eu} \sim 0.03$), affording a separation factor of $SF_{Am/Eu} > 1300$, which is far superior to the observed separation by parent $CyMe_4$-BTPhen during liquid-liquid extraction experiments ($SF_{Am/Eu} \approx 400$).[77,106]

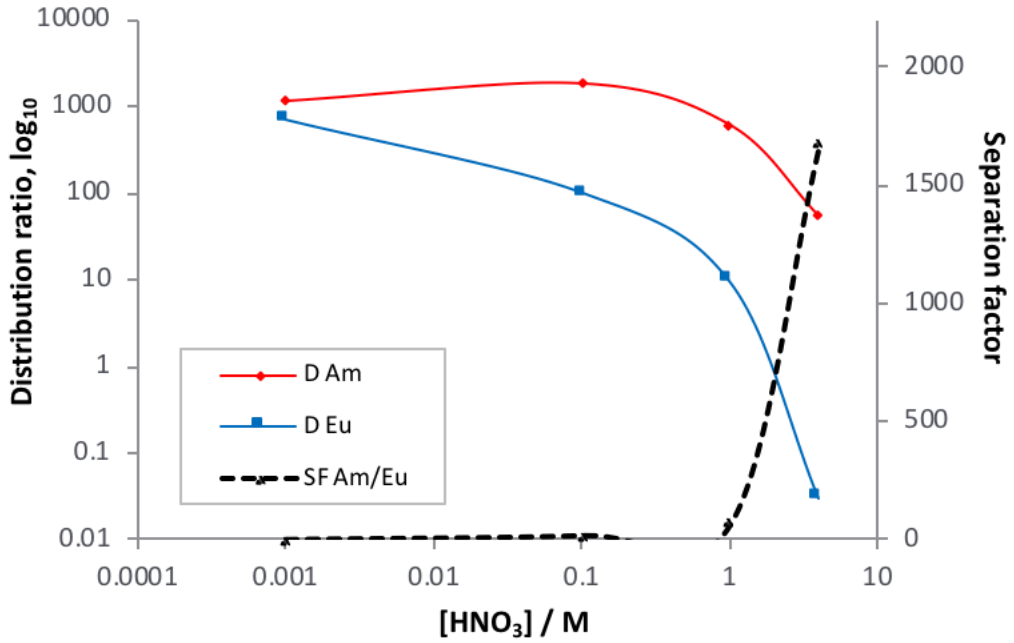

Figure 1.29 – Extraction of Am(III) and Eu(III) by $CyMe_4$-functionalized SiO_2-coated MNPs (**85**) as a function of nitric acid concentration

Separation of Am(III) over Cm(III) was also reported by MNPs (**85**), which afforded a separation factor of $SF_{Am/Cm} \approx 2.2$ at 4 M HNO_3, in agreement with previous results using this ligand when not bound to any support. It was proposed that the shortness of the linking chain attaching the ligand to the MNPs constrained the ligand to form 1:1 complexes when extracting the trivalent actinide metals. Investigations using lanthanide salts have shown the dominant species of BTPhen complexes in solution are 1:2, even at high equivalents of lanthanide.[93] Studying the complex formation in solution using ^1H NMR spectroscopy revealed the appearance of an additional species, which was predicted to be a 1:1 complex. Furthermore, a 1:1 10-coordinate crystal structure has been reported.[82]

During extraction studies on free BTPhen ligand, the formation of a 10-coordinate electronically neutral 1:1 complex may be forming at or near the organic/aqueous interface during the extraction process, where the bidentate nitrate ions are then displaced by another ligand leading to a more stable 1:2 complex in the bulk of the organic solvent. When the ligand is bound to the surface of these MNPs, it is not possible to form 1:2 complexes on the surface of the solid due to sterics, and so it is likely the 1:1 complex remains the dominant species.

Chapter 2 – Results and Discussion

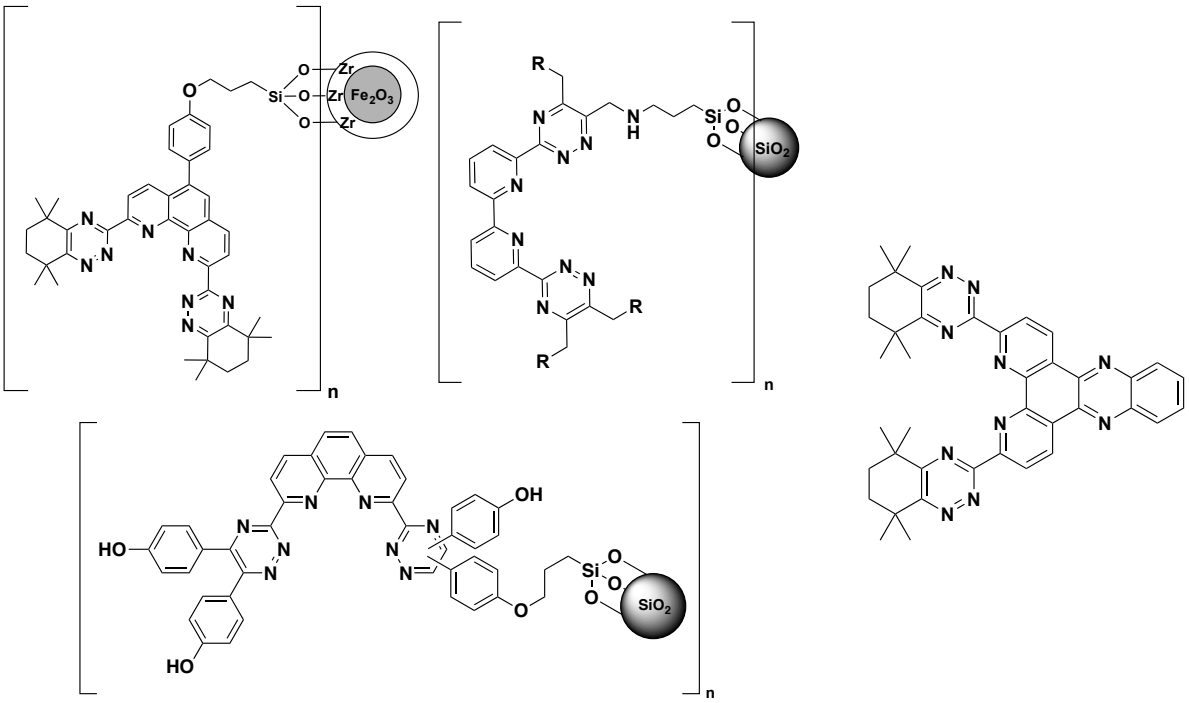

The following work described herein contributed to the following publications:

J. Westwood, A. Afsar, L. M. Harwood, M. J. Hudson, J. John, and P. Distler, *Heterocycles*, 2016, **93**, 453-464

A. Afsar, J. Cowell, P. Distler, L. M. Harwood, J. John and J. Westwood, *Synlett*, 2017, **28**, 2795-2799.

A. Afsar, P. Distler, L. M. Harwood, J. John, J. Cowell and J. Westwood, *Chem. Commun*., 2018, *In press.*

A. Afsar, P. Distler, L. M. Harwood, J. John and J. Westwood, *Chem. Commun*., 2017, **53**, 4010-4013.

J. Westwood, L. M. Harwood, A. Afsar, J. Cowell, P. Distler and J. John, *Lett. Org. Chem.,* 2018, **15**, 340-344

2.1 – Comparison of SiO_2- and ZrO_2-coated MNPs:

This section led to the following publication: J. Westwood, A. Afsar, L. M. Harwood, M. J. Hudson, J. John, and P. Distler, *Heterocycles*, 2016, **93**, 453-464.[108]

Mono-dispersed magnetic nanoparticles (MNPs) with particle sizes of less than 40 nm, offer large surface areas coupled with high surface activity.[109] Their magnetic properties enable them to be easily separated from the supernatant solution by means of an external magnet, making them highly useful for novel separation processes.[110] However, since the iron oxide core of the MNPs is prone to chemical attack under the harsh acidic conditions of nuclear waste streams, a suitable protective coating is essential.[111,112] An effective solution to this problem is to coat the iron oxide centre with zirconia (ZrO_2) or silica (SiO_2), both of which have been shown to provide a chemically resistant surface whilst retaining the ion-exchange properties.[113] Upon coating the MNPs, the free Zr-OH and Si-OH surface groups enable effective attachment of ligands through organic functional groups onto the surface of the coated MNPs. It has been discussed in section **1.8** that $CyMe_4$-BTPhen-functionalized silica-coated MNPs (**85**) show remarkable separation of Am(III) from Eu(III) in a range (0.001 – 4 M) of HNO_3 solutions. In addition, a small but significant selectivity for Am(III) over Cm(III) has been observed at concentrations of 4 M HNO_3.[106]

The synthesis of $CyMe_4$-BTPhen-functionalized zirconia-coated (ZrO_2) maghemite (Fe_2O_3) magnetic nanoparticles (MNPs) (**86**) and their ability to extract Am(III) from Eu(III) and Am(III) from Cm(III) over a range of HNO_3 concentrations (0.001 – 4 M) was investigated and their extraction behaviour was compared to a previously tested model based on silica-coated (SiO_2) $CyMe_4$-BTPhen MNPs (**85**) (**Fig 2.1**).[106]

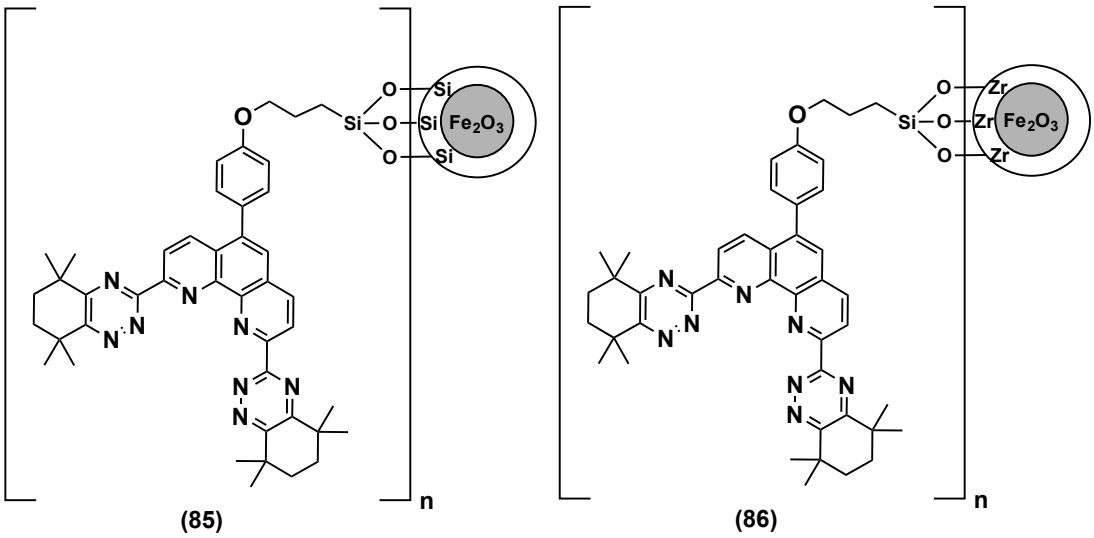

Figure 2.1 – Structures of $CyMe_4$-BTPhen-functionalized SiO_2- (**85**) and ZrO_2- (**86**) MNPs

*2.1.1 – Synthesis and characterization of $CyMe_4$-BTPhen ZrO_2-MNPs (**86**):*

5-(4-hydroxyphenyl)-$CyMe_4$-BTPhen (**84**) was synthesized following previously reported protocols.[77,106] Following mono-bromination of neocuproine (**50**) to give 5-bromo-neocuproine (**78**), oxidation with stoichiometric amounts of selenium dioxide afford Br-*bis*-aldehyde (**87**) in 82 % yield.[96,106] A one-pot reaction of (**87**), firstly forming an intermediate oxime followed by *in situ* elimination afforded Br-*bis*-nitrile (**88**). Stirring *bis*-nitrile (**88**) in hydrazine hydrate and ethanol at ambient temperature gave Br-*bis*-aminohydrazide (**89**) that was condensed with $CyMe_4$ diketone (**32**) to give 5-Br-$CyMe_4$-BTPhen (**83**) (**Scheme 2.1**). $CyMe_4$ diketone (**32**) was prepared in three steps following previously reported procedures (**Scheme 2.2**).[77,114] To enable immobilization onto the surface of ZrO_2-coated MNPs, the final step involved a Suzuki-Miyaura cross-coupling reaction with 4-hydroxyphenyl boronic acid to give 5-(4-hydroxyphenyl)-$CyMe_4$-BTPhen (**84**).[115]

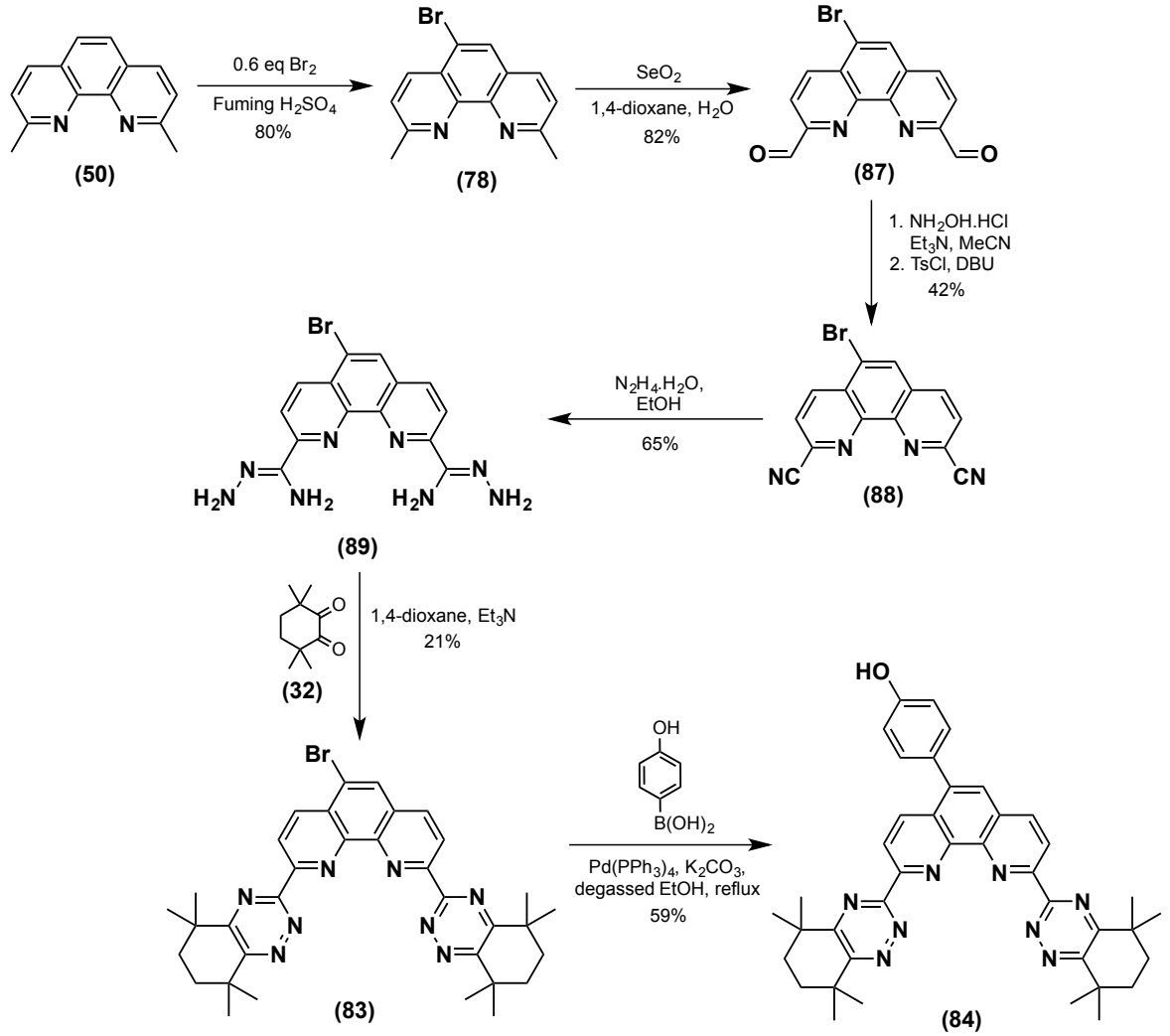

Scheme 2.1 – Synthesis of 5-(4-hydroxyphenyl)-CyMe$_4$-BTPhen (**84**)

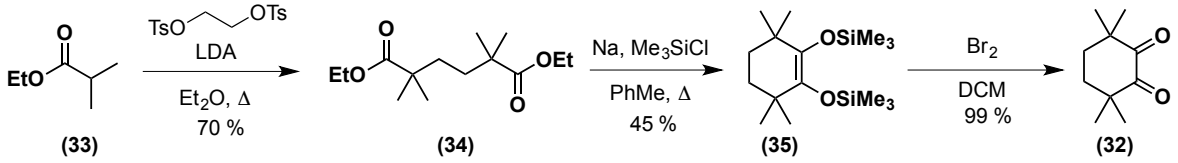

Scheme 2.2 – Synthesis of CyMe$_4$-diketone (**32**)

The synthesis of iodoalkyl-functionalized ZrO_2-coated nanoparticles (**90**) (**Scheme 2.3**) was carried out using previously reported procedures and effectively the same procedure used for the synthesis of SiO_2-coated nanoparticles, except by differing the protective coating.[105–107,116,117] The iron oxide (**91**) magnetic core was prepared using previously reported methods by the co-precipitation of a 2:1 ratio of $FeCl_3$ and $FeCl_2$ in aqueous NaOH solution. The use of sonication instead of traditional mechanical agitation during the synthesis afforded nanoparticles that are smaller and were predicted to have a more

narrow size distribution.[117] The coating of the zirconia surface onto the iron oxide core was achieved using a sol-gel method with Zr(IV) *tert*-butoxide in aqueous ammonia and then reaction of the surface OH groups in (**92**) with 3-(iodopropyl)trimethoxysilane afforded iodoalkyl-functionalized ZrO_2-coated MNPs (**90**).[111,112]

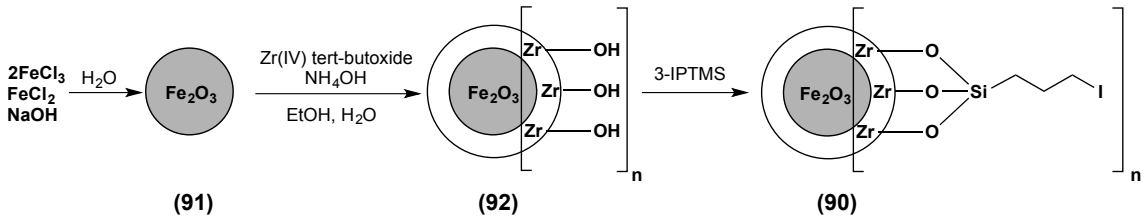

Scheme 2.3 – Synthesis of iodo-functionalized ZrO_2 Fe_2O_3 MNPs (**90**)

Immobilization onto the surface of the ZrO_2-coated MNPs was achieved by nucleophilic substitution of iodine by the 4-hydroxyphenyl functionality of (**84**) by stirring ligand (**84**) in DMF with sodium hydride, as previously reported.[85,106] Separation of the nanoparticles by an external neodymium magnet afforded $CyMe_4$-BTPhen-functionalized ZrO_2-MNPs (**86**) (**Scheme 2.4**).

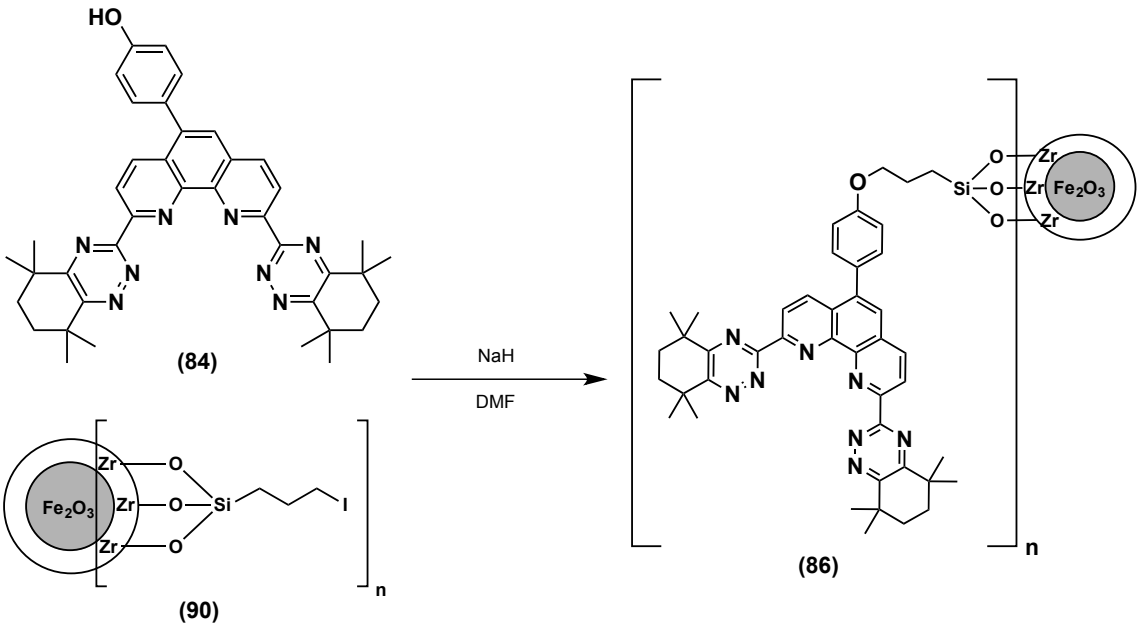

Scheme 2.4 – Immobilization of 5-(4-hydroxyphenyl)-$CyMe_4$-BTPhen (**84**) onto ZrO_2 Fe_2O_3 MNPs (**90**)

Transmission electron microscopy (TEM) images of ZrO_2-coated MNPs (**86**) revealed the thickness of the zirconia coating to be *ca*. 40-45 nm, as also seen with SiO_2 coated MNPs.[85,106] Zirconia has a wide-ranging iso-electric point of pH 4-11 with the result that, in the acidic media used for extraction testing, the particles are protonated and have a net positive charge. Repulsion between the positively charged particles presumably ensures that there is no aggregation, increasing their desired surface activity. The degree of immobilization of the 5(4-hydroxyphenyl)-$CyMe_4$-BTPhen ligand (**84**) onto iodoalkyl-functionalized ZrO_2-MNPs (**90**) was followed by Fourier Transform infra-red spectroscopy (FT-IR) where disappearance of the C-I stretch at 688 cm^{-1} and the presence of C=C aromatic stretches at 1500-1600 cm^{-1} were indicative of covalent attachment, as previously observed with SiO_2-MNPs (**85**).[106] To draw comparisons between both MNPs, the FT-IR spectra of both $CyMe_4$-BTPhen-functionalized ZrO_2-MNPs (**86**) and $CyMe_4$-BTPhen-functionalized SiO_2-MNPs (**85**) are shown in **Fig 2.2**. Both follow the same trend, but a clear difference is the more apparent broad OH absorption at 3400 cm^{-1} for ZrO_2-MNPs (**86**), indicative that there could be some residual OH groups still present after covalent attachment of the ligand, indicating less efficient incorporation of the $CyMe_4$-BTPhen ligand onto the MNPs surface of ZrO_2-coated nanoparticles.

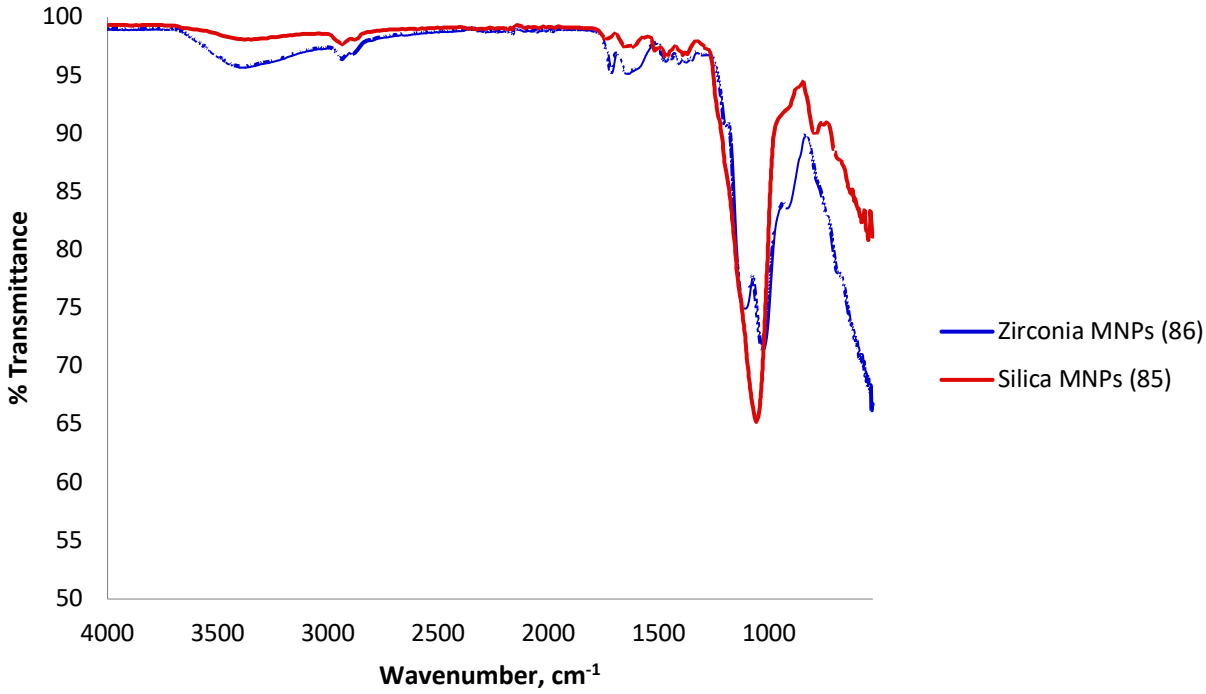

Figure 2.2 – Comparison of the FT-IR spectra of $CyMe_4$-BTPhen-functionalized ZrO_2-MNPs (**86**) and $CyMe_4$-BTPhen-functionalized SiO_2-MNPs (**85**)

Elemental analysis was also used to evaluate surface incorporation of the ligand onto the MNPs surface. Percentage elemental composition of C, H, N and I for $CyMe_4$-BTPhen-functionalized ZrO_2-MNPs (**86**) and the groups previous $CyMe_4$-BTPhen-functionalized SiO_2-MNPs (**85**) are shown in **Table 2.1**. The results clearly indicate that there is a lower incorporation of the ligand onto the MNPs surface in the case for ZrO_2 compared with that of SiO_2. For instance, analysis of ZrO_2-MNPs (**86**) indicates 1.80 % N compared to 3.43 % N for SiO_2-MNPs (**85**).

Table 2.1 – Results of elemental analysis for $CyMe_4$-BTPhen-functionalized ZrO_2-MNPs (**86**) and $CyMe_4$-BTPhen-functionalized SiO_2-coated MNPs (**85**) (*values obtained from ref. 106)

	$CyMe_4$-BTPhen-functionalized ZrO_2-MNPs (86)		***$CyMe_4$-BTPhen-functionalized SiO_2-MNPs* (85)***	
	Experimental	**Theoretical**	***Experimental***	***Theoretical***
C (%)	17.16	22.79	*23.20*	*22.79*
H (%)	3.37	2.14	*3.48*	*2.14*
N (%)	1.80	4.94	*3.43*	*4.94*
I (%)	7.69	0	*8.28*	*0*

The organic content on ZrO_2-MNPs (**86**) was further investigated using thermo-gravimetric analysis (TGA) (appendix **A1**). A similar trend to previously studied SiO_2-MNPs (**85**) was observed; wherein, below 150 ^oC, the mass loss was quite small, presumably due to removal of absorbed water and a near linear mass loss was then observed between *ca*. 250-650 ^oC, which is probably due to the decomposition of the organic content.

*2.1.2 – Extraction Studies of ZrO_2-MNPs (**86**) :*

Extraction experiments of (**86**) were carried out at the Czech Technical University in Prague. The aqueous solutions for the solvent extraction experiments were prepared by spiking nitric acid solutions (0.001 – 4 M) with stock solutions of ^{241}Am, ^{152}Eu and ^{244}Cm and then adding 600 µL of spiked aqueous solution to 18 mg of $CyMe_4$-BTPhen-functionalized ZrO_2-MNPs (**86**). The mixture was sonicated for 10 min and shaken at 1800 rpm for 90 min. After centrifuging for 10 min, aliquots of the aqueous solutions (supernatant) were separated

and taken for measurements. The distribution ratios, *D*, were calculated as the ratio between the radioactivity (α- and γ- emissions) of each isotope in the standard solution and the supernatants after removal of the MNPs. The separation factor is $SF_{Am/Eu} = D_{Am} / D_{Eu}$ or $SF_{Am/Cm} = D_{Am} / D_{Cm}$. Extractions were studied at nitric acid concentrations of 0.001 M, 0.1 M, 1 M and 4 M.

The extraction results obtained for $CyMe_4$-BTPhen-functionalized ZrO_2-coated MNPs (**86**) showed good distribution ratios for both Am(III) ($D_{Am} \sim 142 \pm 4$) and Eu(III) ($D_{Eu} \sim 9.7 \pm 4.2$) at 0.001 M HNO_3 with a separation factor of $SF_{Am/Eu} \approx 14.7 \pm 1.4$ (**Table 2.2**). However, these values were much lower than those results obtained for the same ligand covalently bound in the same manner to SiO_2-MNPs ($D_{Am} \sim 1168.8 \pm 79.1$ and $D_{Eu} \sim 701.4 \pm 32.4$).[106] Increasing HNO_3 concentration to 0.1 M showed a dramatic decrease in Am(III) extraction ($D_{Am} \sim 5.6 \pm 1$) and Eu(III) extraction ($D_{Eu} \sim 0.8 \pm 0.1$) giving a separation factor of $SF_{Am/Eu} \approx 7.4 \pm 7.5$ at 0.1 M HNO_3. In the case for the SiO_2-MNPs (**85**) however, an increase in the extraction of Am(III) at 0.1 M HNO_3 was reported $D_{Am} \sim 1857 \pm 153.5$ whilst Eu(III) extraction decreased to $D_{Eu} \sim 101.1 \pm 2.3$ giving a $SF_{Am/Eu} \approx 18.4 \pm 1.6$.[106] A linear decrease in both Am(III) and Eu(III) extraction was observed for (**86**) upon increasing HNO_3 concentration to both 1 M and 4 M (**Fig 2.3**). Although D_{Am} remained greater than D_{Eu} in both cases, the selectivity was all but lost at 4 M HNO_3 solution with $D_{Am} \sim 0.8 \pm 0.9$ and $D_{Eu} \sim 0.4 \pm 0.9$ resulting in $SF_{Am/Eu} \approx 1.8 \pm 0.4$. This is significantly lower than the results obtained for $CyMe_4$-BTPhen-functionalized SiO_2-coated MNPs (**85**) at 4 M HNO_3 where a $SF_{Am/Eu} \approx 1700 \pm 300$ was obtained.[106]

Table 2.2 – Extraction of Am(III) and Eu(III) by $CyMe_4$-BTPhen-functionalized ZrO_2-MNPs (**86**) as a function of nitric acid concentration.

[HNO_3]	**D_{Am}**	**D_{Eu}**	**$SF_{Am/Eu}$**
0.001	142 ± 4.0	9.7 ± 4.2	14.7 ± 1.4
0.1	5.6 ± 1.0	0.8 ± 1.0	7.4 ± 7.5
1	1.4 ± 0.9	0.7 ± 0.9	2.0 ± 1.7
4	0.8 ± 0.9	0.4 ± 0.9	1.8 ± 0.4

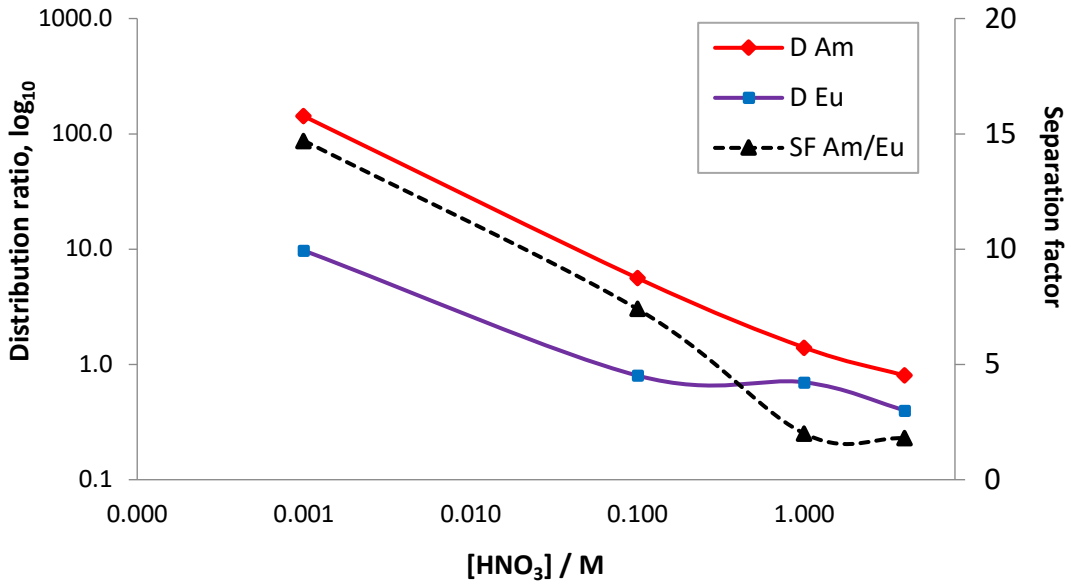

Figure 2.3 – Extraction of Am(III) and Eu(III) by $CyMe_4$-BTPhen-functionalized ZrO_2-MNPs (**86**) as a function of nitric acid concentration.

Distribution ratios for the actinides Am(III) and Cm(III) and the resulting separation factors at 0.001 – 4 M HNO_3 by (**86**) were also examined (**Table 2.3**). The *D* values for both Am(III) and Cm(III) decreased upon increasing HNO_3 concentration, with little or no selectivity observed at 4 M HNO_3 with a $SF_{Am/Cm} \approx 0.7 \pm 0.1$. These values follow the same trend as for SiO_2-MNPs (**85**), but much lower *D* and SF values across all concentrations were attained. SiO_2-MNPs (**85**) produced a $SF_{Am/Cm} \approx 2.2 \pm 0.4$ at 4 M HNO_3, a reasonable separation; whereas ZrO_2-MNPs (**86**) across all concentrations showed a $SF_{Am/Cm}$ that barely rose above 1 (**Fig 2.4**).

Table 2.3 – Extraction of Am(III) and Cm(III) by $CyMe_4$-BTPhen-functionalized ZrO_2-MNPs (**86**) as a function of nitric acid concentration.

[HNO_3]	**D_{Am}**	**D_{Cm}**	**$SF_{Am/Cm}$**
0.001	185 ± 13	145 ± 10	1.3 ± 0.1
0.1	12.7 ± 2.6	10.7 ± 2.6	1.2 ± 0.4
1	4.3 ± 2.3	5.7 ± 2.4	0.8 ± 0.5
4	3.0 ± 2.3	4.4 ± 2.3	0.7 ± 0.1

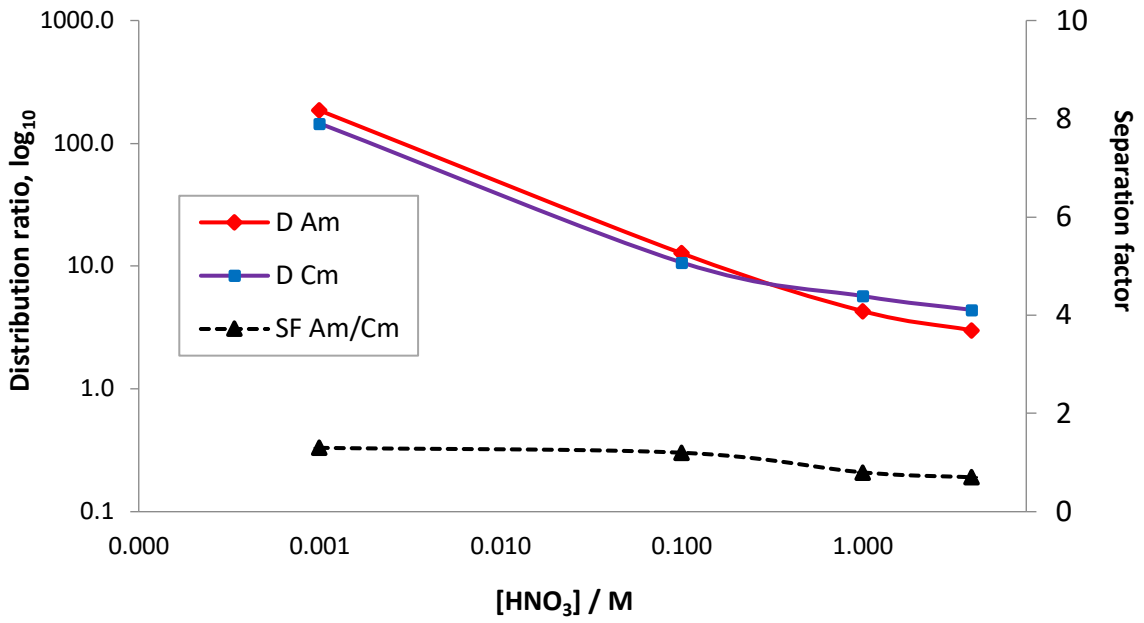

Figure 2.4 – Extraction of Am(III) and Cm(III) by $CyMe_4$-BTPhen-functionalized ZrO_2-MNPs (**86**) as a function of nitric acid concentration.

In summary, the immobilization of a $CyMe_4$-BTPhen ligand via a phenyl ether linker onto the surface of ZrO_2- maghemite (Fe_2O_3) magnetic nanoparticles was carried out and investigated. These MNPs co-extracted both Am(III) and Eu(III) from solutions up to 4 M HNO_3, with low selectivity ($SF_{Am/Eu} \approx 1.8$ at 4 M) compared to that previously reported for SiO_2-coated MNPs (**85**) ($SF_{Am/Eu} > 1300$).[106] Extraction of both actinides Am(III) and Cm(III) was also noted, again without any significant selectivity. Based on FT-IR and elemental analysis data the surface of the ZrO_2-MNPs incure a lower functionalization by the $CyMe_4$-BTPhen ligand than the SiO_2-MNPs counterpart. In the range of acidity in which the extraction studies were performed, the residual surface hydroxyl groups of the zirconia are most likely protonated, giving rise to a positively charged surface which may result in repulsion of the M(III) cations, resulting in less efficient extraction. Both ZrO_2- and SiO_2-coated MNPs equally provide an effective coating to the iron oxide core to enable chemical resistance to the harsh conditions in extraction processes but, since the SiO_2-MNPs can undergo an apparent higher ligand loading, we can conclude that SiO_2-MNPs will be favoured over ZrO_2-MNPs for future investigations to provide an effective solid-based extraction for SANEX-type processes.

2.2 – Improved Synthetic Route for the Preparation of BTPhens and Extraction Studies of Tetra-(4-hydroxyphenyl)BTPhen:

Parts of this section contributed to the following publication: A. Afsar, J. Cowell, P. Distler, L. M. Harwood, J. John and J. Westwood, *Synlett*, 2017, **28**, 2795-2799.[118]

2.2.1 – Selenium free Synthesis of BTPhens:

Previous synthetic protocols for the development of functionalized BTPhen ligands have nearly all proceeded by benzylic oxidation of neocuproine (**50**) using stoichiometric amounts of selenium dioxide, a highly toxic reagent, which resulted in the production of large amounts of precipitated selenium metal.[8,22,34,77] Previous extensive attempts to use sub-stoichiometric amounts of SeO_2 failed to generate the *bis*-aldehyde product in any significant yield. The investigation of electronic effects of substituents (Cl, MeO- and Ph) at the 4,7- positions of the phenanthroline backbone in $CyMe_4$-BTPhen ligands by Whitehead and Edwards *et al.*, (section **1.7.3**) led to the development of an alternative benzylic functionalization by adapting a protocol reported by Ulven in 2011.[99] This proceeded by the per-chlorination of the two methyl groups of 4,7-dichloroneocuproine (**95**) using NCS (*N*-chlorosuccinimide) and a radical initiator dibenzoyl peroxide (**Scheme 2.5**).

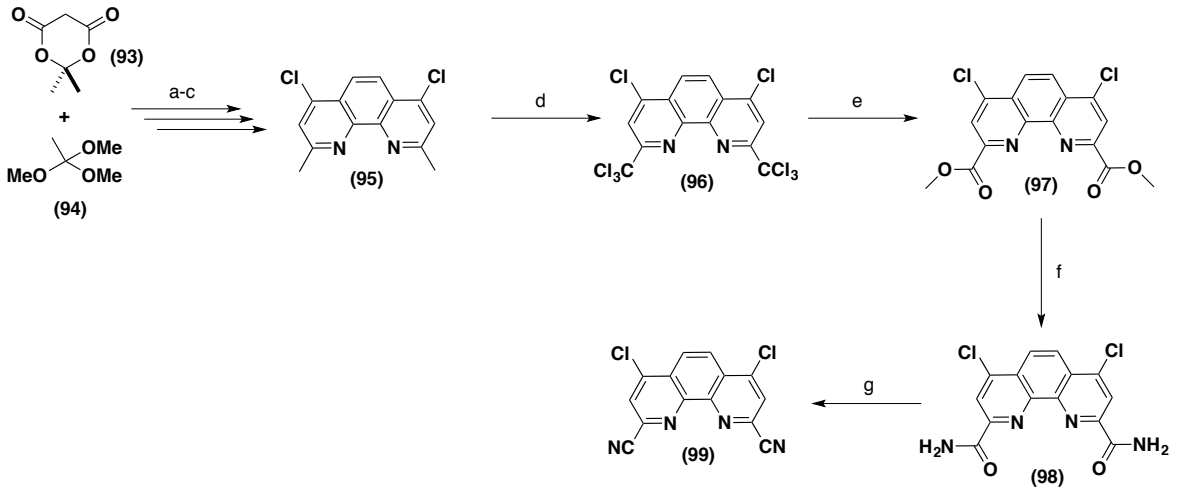

Reagents and conditions: (a) (i) 109 °C, 15 mins; (ii) *o*-phenylenediamine, 109 °C, 2 h; (iii) 25 °C, 16h, 65 %; (b) Ph_2O, 260 °C, 30 mins, 95 %; (c) $POCl_3$, 90 °C, 3.5 h, 98 %; (d) $(PhCOO)_2$, NCS, $CHCl_3$, 62 °C, 16 h, 93 %; (e) (i) H_2SO_4, 95 °C, 1 h; (ii) MeOH, 65 °C, 2 h, 66 %; (f) NH_4OH (29 %), NH_4Cl, 25 °C, 72 h, 85 %; (g) (i) $(COCl)_2$, DMF, 0 °C, 6 h; (ii) pyridine, 25 °C, 1 h, 72 %;

Scheme 2.5 – Synthesis of 4,7-dichloro-1,10-phenathroline-2,9-dicarbonitrile (**99**).[98,99]

This procedure was adapted and applied to neocuproine (**50**) to synthesize the key *bis*-nitrile phenanthroline intermediate (**52**) without the need to use large amounts of toxic selenium dioxide (**Scheme 2.6**). Optimal reaction conditions for the benzylic functionalization involved using a slight excess of recrystallized NCS and 0.05 equivalents of *m*-CPBA (*meta*-chloroperbenzoic acid). The reaction did proceed with both benzoyl peroxide and AIBN as initiators, but in lower overall yield and both required longer reaction times. The role of *m*-CPBA is not fully understood, but the chlorination of the two methyl groups was complete after 18 hours at reflux in high yield (90 %). ^{1}H NMR spectroscopic analysis confirmed complete disappearance of the methyl resonance of neocuproine (**50**) at 2.94 ppm.

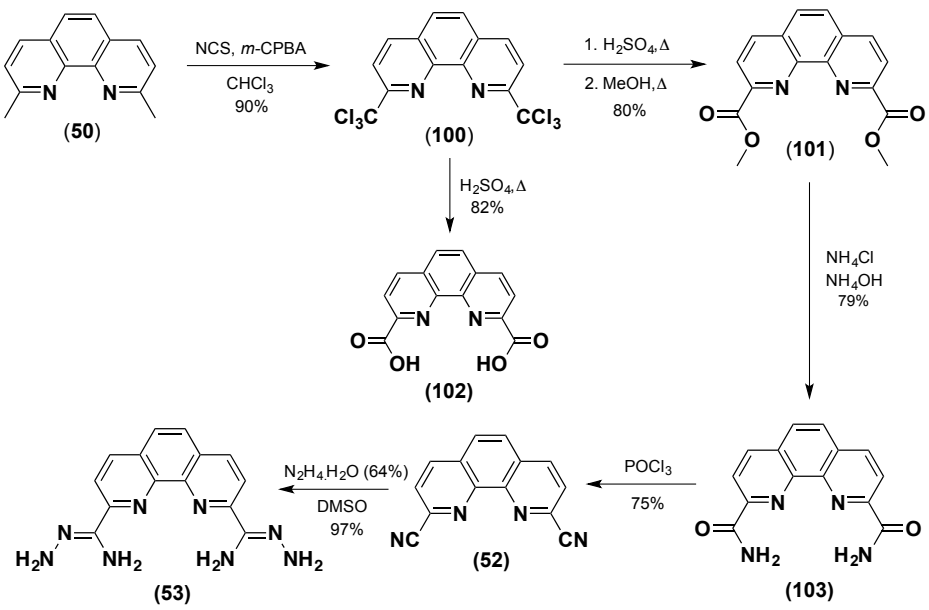

Scheme 2.6 – Synthesis of *bis*-aminohydrazide (**53**) via benzylic functionalization with NCS

2,9-*Bis*-(trichloromethyl)-1,10-phenanthroline (**100**) was subsequently subjected to a one-pot hydrolysis/methanolysis reaction by firstly heating in conc. H_2SO_4 for 4 hrs followed by slow addition of methanol and heating to reflux for 18 hr to furnish *bis*-ester compound (**101**) in 80 % yield.[98] Alternatively, the *bis*-carboxylic acid (**102**) can be isolated in good yield by stirring (**100**) in only conc. H_2SO_4. Stirring *bis*-ester (**101**) in excess ammonium chloride and ammonium hydroxide (35%) afforded *bis*-amide (**103**). Dehydration of the

amide units in (**103**) using the protocol reported by Larsen *et al.* and Whitehead and Edwards *et al.* involving oxalyl chloride and DMF, followed by pyridine produced (**52**) in poor yield.[98,99] Instead dehydration was achieved by heating to reflux in neat phosphorous oxychloride, which generated the key *bis*-nitrile compound (**52**) in 75% yield. Previous reactions of *bis*-nitrile (**52**) with hydrazine hydrate were performed in ethanol and took a number of days to generate *bis*-aminohydrazide (**53**) in good yield.[77,85,95] This was attributed to the poor solubility of nitrile-containing phenanthrolines. Subsequently, it was found that nitrile (**52**) was much more soluble in DMSO or DMF and that reaction with hydrazine in these solvents to form *bis*-aminohydrazide (**53**) occurred much more rapidly and in much higher yield ~ 97 %.

Previous studies of BTPhen-functionalized ligands involved the immobilization onto solid supports using a 4-hydroxyphenyl linking group at the 5-position of the phenanthroline unit by substitution of the corresponding bromine at that position using a Suzuki-Miyaura cross-coupling reaction.[105,106] An alternative route for eventual immobilization was investigated by adding phenol linking groups directly to the 1,2,4-triazine units of BTPhen. This was achieved using 4,4'-dihydroxy benzil (**104**), which was reacted with *bis*-aminohydrazide (**53**) to afford the 4,4',4'',4'''-((1,10-phenanthroline-2,9-diyl)bis(1,2,4-triazine-3,5,6-triyl))tetraphenol [henceforth referred to as tetra-(4-hydroxyphenol)-BTPhen] (**105**) ligand (**Scheme 2.8**). 4,4'-Dihydroxy benzil (**104**) was synthesized in one step from commercially available 4,4'-dimethoxybenzil (**106**) using previously reported procedures (**Scheme 2.7**).[119,120]

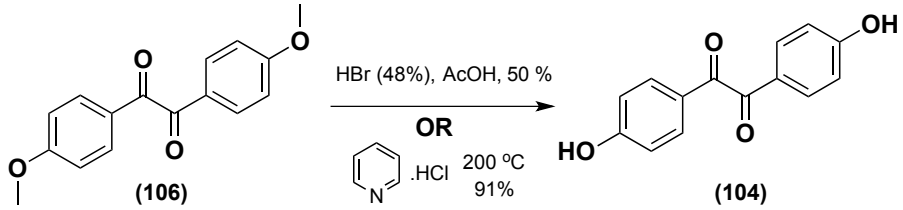

Scheme 2.7 – Synthetic routes to 4,4'-dihydroxy benzil (**104**)

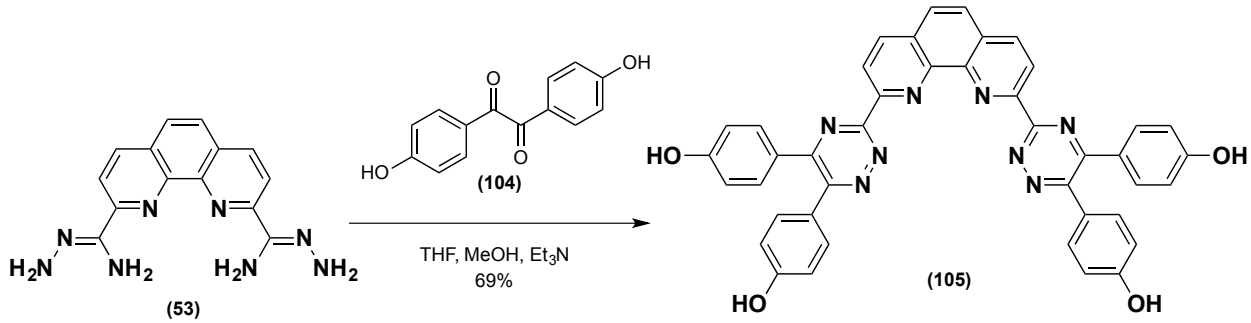

Scheme 2.8 – Synthesis of tetra-(4-hydroxyphenyl)-BTPhen ligand (**105**)

*2.2.2 – Extraction Studies of tetra-(4-hydroxyphenyl)-BTPhen ligand (**105**):*

Novel tetra-(4-hydroxyphenyl) BTPhen ligand (**105**) was evaluated for its solvent-solvent extraction of Am(III) from Eu(III) and Am(III) from Cm(III) as a function of nitric acid concentration at the Czech Technical University in Prague. The aqueous solutions for the solvent extraction experiments were prepared by spiking nitric acid solutions (0.001 – 1 M) with stock solutions of ^{241}Am, ^{152}Eu and ^{244}Cm and then adding 1000 µL of spiked aqueous solution to 10 mM (71 mg) of (**105**) in cyclohexanone. The mixture was sonicated for 10 min and shaken at 1800 rpm for 90 min. After centrifuging for 10 min, aliquots of the aqueous solutions (supernatant) were separated and taken for alpha/gamma measurements.

The extraction data in **Table 2.4** and **Fig 2.6** shows the extraction of Am(III) and Eu(III) by (**105**) as a function of increasing nitric acid concentration. At low HNO_3 concentration (0.001 M) there was no selectivity at all between Am(III) and Eu(III) and relatively poor extraction as $D < 1$. Increasing the concentration to 0.1 M caused a decrease in the extraction of both Am(III) and Eu(III), but more greatly for Eu(III), which was diminished to ~ 0.09, giving a slightly higher separation factor than at 0.001 M of $SF_{Am/Eu} \approx 3.3$. At 0.5 M HNO_3 there was an increase in the extraction of Am(III) to $D_{Am} \sim 1.4$ and a further decrease in Eu(III) extraction, resulting in a higher separation factor of $SF_{Am/Eu} \approx 25.3$. A similar extraction of both Am(III) and Eu(III) was observed at 1 M HNO_3 giving a separation factor of $SF_{Am/Eu} \approx 26$. It was not possible to evaluate this ligand at higher acid concentrations as cyclohexanone is miscible with higher HNO_3 concentrations.

Table 2.4 – Extraction of Am(III) and Eu(III) by tetra(4-hydroxyphenyl)-BTPhen ligand (**105**) as a function of nitric acid concentration.

$[HNO_3]$	D_{Am}	D_{Eu}	$SF_{Am/Eu}$
0.001	0.48 ± 0.02	0.44 ± 0.02	1.1 ± 0.1
0.1	0.29 ± 0.01	0.09 ± 0.01	3.3 ± 0.2
0.5	1.4 ± 0.01	0.06 ± 0.01	25.3 ± 1.5
1	1.7 ± 0.10	0.06 ± 0.01	26.0 ± 1.5

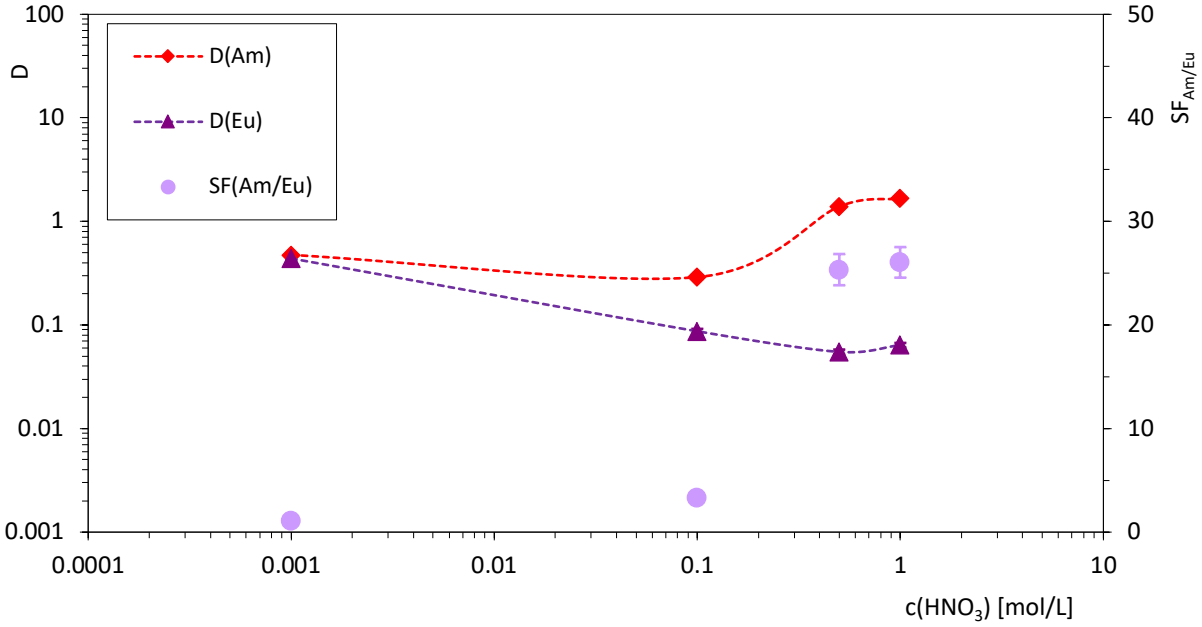

Figure 2.6 – Extraction of Am(III) and Eu(III) by tetra(4-hydroxyphenyl)-BTPhen ligand (**105**) as a function of nitric acid concentration.

The extraction ability of ligand (**105**) for Am(III) and Cm(III) as a function of increasing nitric acid is shown below in **Table 2.5** and **Fig 2.7**. At low HNO_3 concentration (0.001-0.1 M), the extraction in D values for both metals was quite low $D < 1$, with no distinction between the two. Increasing the concentration to 0.5 and 1 M HNO_3 resulted in increases for both metals, but with the extraction more apparent for Am(III) affording separation factors of $SF_{Am/Cm} \approx 2$ and 2.1 respectively.

Table 2.5 – Extraction of Am(III) and Cm(III) by tetra(4-hydroxyphenyl)-BTPhen ligand (**105**) as a function of nitric acid concentration.

$[HNO_3]$	D_{Am}	D_{Cm}	$SF_{Am/Cm}$
0.001	0.36 ± 0.04	0.40 ± 0.07	0.9 ± 0.2
0.1	0.26 ± 0.03	0.26 ± 0.02	1.0 ± 0.1
0.5	1.4 ± 0.10	0.72 ± 0.05	2.0 ± 0.2
1	1.6 ± 0.10	0.74 ± 0.05	2.1 ± 0.2

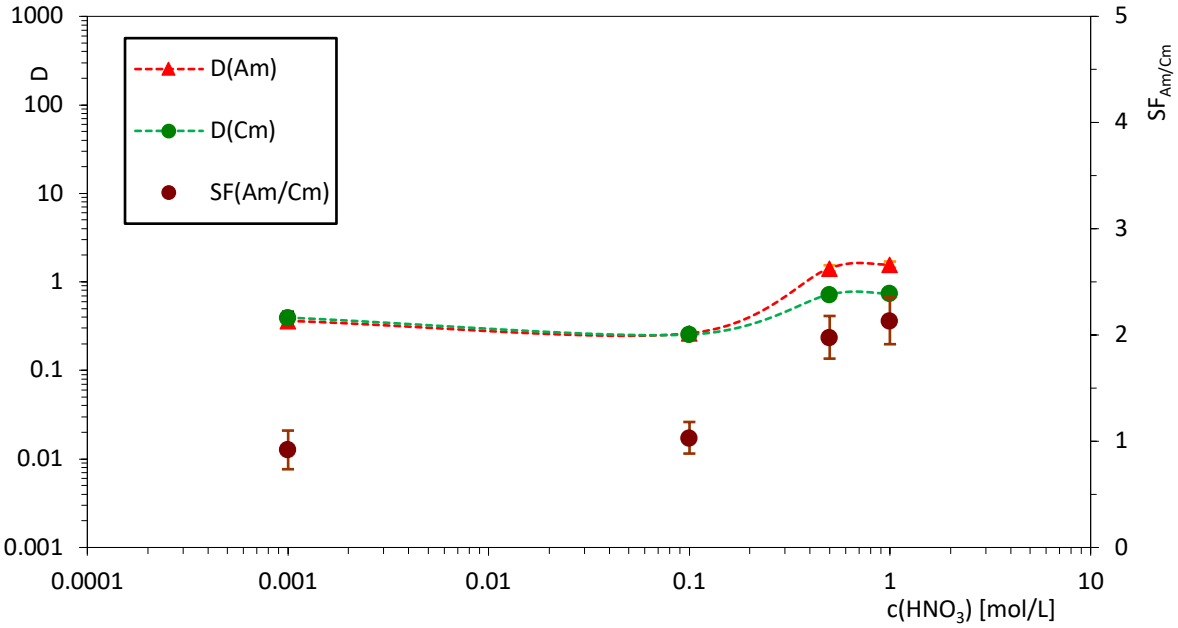

Figure 2.7 – Extraction of Am(III) and Cm(III) by tetra(4-hydroxyphenyl) BTPhen ligand (**105**) as a function of nitric acid concentration.

Overall, this tetra(4-hydroxyphenyl)-BTPhen (**105**) ligand shows generally poor extraction of Am(III) from Eu(III) across HNO_3 concentrations up to 1 M. Even though the values of *D* remained < 2 during this investigation, the trend of increasing extraction of Am(III) as the HNO_3 concentration increases is still shown, indicating that the extraction process is dependent on the concentration of nitrate ions in solution.

*2.2.3 – Immobilization of tetra-(4-hydroxyphenyl)-BTPhen (**105**) onto SiO_2-coated MNPs (**107**):*

The ability of previously studied $CyMe_4$-BTPhen immobilized MNPs (e.g. **85** and **86**) to extract minor actinides from lanthanides shows promise for the development of an efficient solid-liquid extraction technique for waste reprocessing. Previously, attachment of the organic ligand onto the surface of iodoalkyl-functionalized MNPs was achieved by using one 4-hydroxyphenyl linking group at the 5-position of the phenanthroline unit of the ligand.[106,121] Following the synthesis of novel tetra-(4-hydroxyphenyl) BTPhen ligand (**105**) and thus a new mode of immobilization via the phenol linking groups attached to the triazine unit, we investigated the extraction ability of this ligand covalently bound to silica-coated MNPs (**107**).

The synthesis of SiO_2-coated nanoparticles (**107**) (**Scheme 2.9**) was carried out using the groups previously reported procedure.[106,117] Immobilization of ligand (**105**) onto the surface of SiO_2-MNPs (**107**) was achieved by stirring ligand (**105**) in DMF with sodium hydride. Separation of the nanoparticles by an external neodymium magnet afforded BTPhen functionalized-MNPs (**110**) (**Scheme 2.10**).

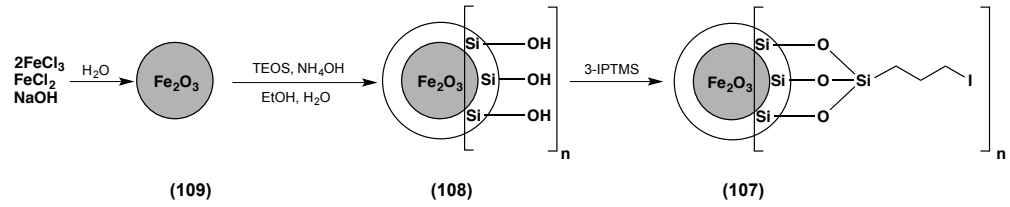

Scheme 2.9 – Synthesis of iodoalkyl-functionalized SiO_2-coated Fe_2O_3 MNPs (**107**)

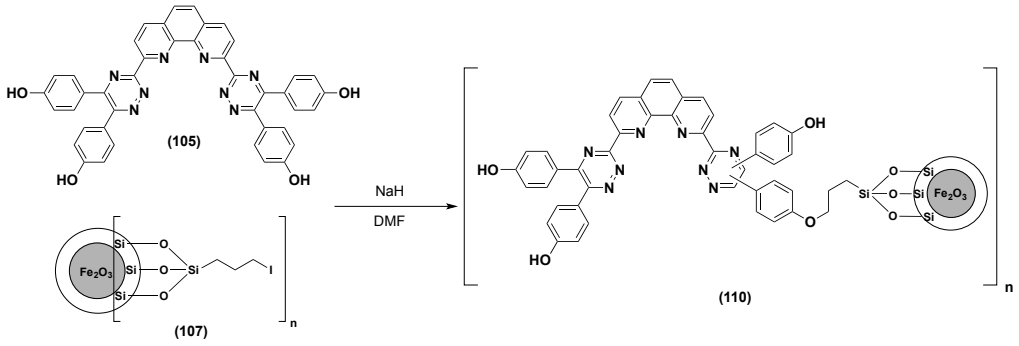

Scheme 2.10 – Immobilization of tetra-(4-hydroxyphenyl) BTPhen (**105**) onto iodo-functionalized SiO_2-coated MNPs (**107**)

Several characterisation techniques were employed to assess the degree of surface immobilization of tetra-(4-hydroxyphenyl)-BTPhen (**105**) onto the surface of SiO_2-MNPs (**107**). Comparison of the FT-IR spectra of iodoalkyl-functionalized SiO_2-coated MNPs (**107**) and BTPhen functionalized-MNPs (**110**) in **Fig 2.7** showed strong absorption bands centred at 1050 cm^{-1} owing to the Si-O-Si stretching, which was apparent for both samples. Absorptions at 1500-1600 cm^{-1} for the C=C aromatic vibrations could only be seen for the BTPhen functionalized-MNPs (**110**), indicating incorporation of the ligand onto the MNP surface. Comparison of the thermogravimetric analysis (TGA) of both iodoalkyl-functionalized SiO_2-coated MNPs (**107**) and BTPhen functionalized-MNPs (**110**) revealed that the amount of tetra-phenol BTPhen ligand (**105**) bound onto the surface of the MNPs was approximately 31 % (appendix **A2**).

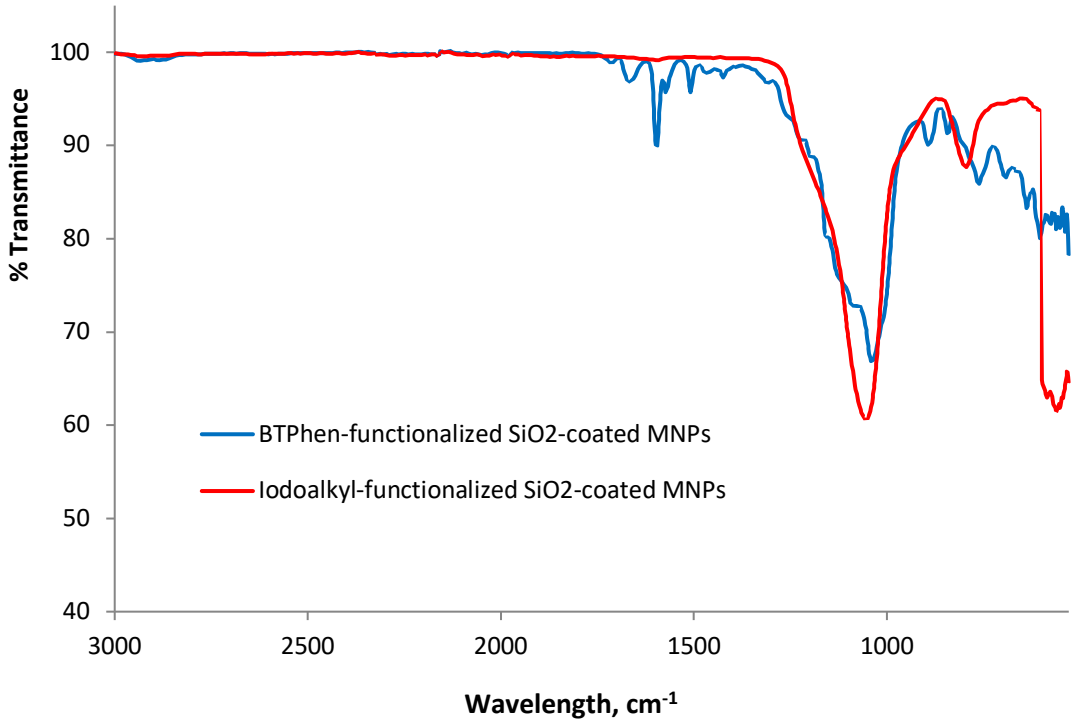

Figure 2.7 – Comparison of the FT-IR spectra of iodoalkyl-functionalized SiO_2-coated MNPs (**107**) and BTPhen functionalized-MNPs (**110**)

The surface morphology and structural features of the BTPhen functionalized-MNPs (**110**) were also examined by transmission electron microscopy (TEM) and scanning electron microscopy (SEM) (**Fig 2.8**). The spherical core structure of the MNPs could be observed, together with the addition of a more disordered organic moiety layer.

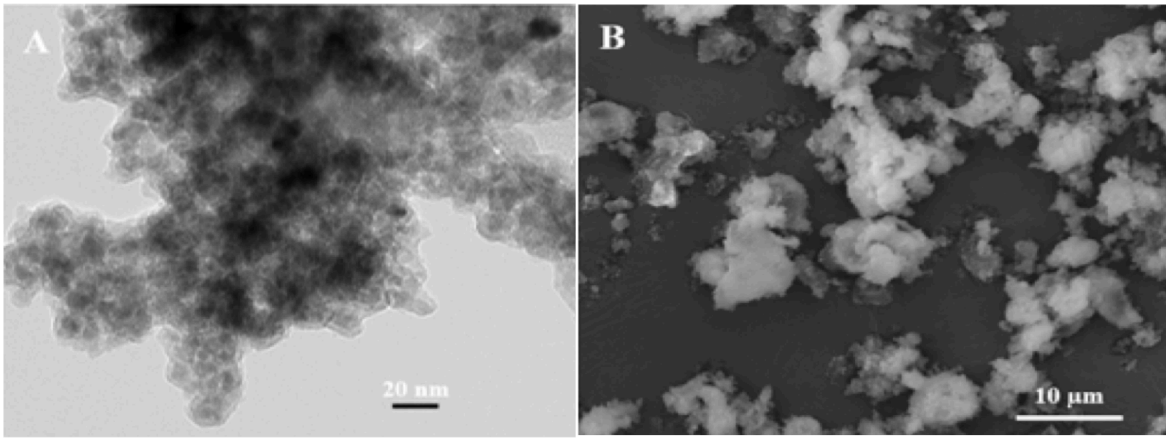

Figure 2.8 – TEM (A) and SEM (B) analysis of BTPhen functionalized-MNPs (**110**)

Furthermore, elemental analysis (**Table 2.6**) found a decrease in the iodine content from 38.9 % in (**107**) to 1.4 % in (**110**) and the presence of ca. 0.9 % nitrogen confirming the modification of MNPs with the tetra-(4-hydroxyphenyl) BTPhen ligand (**105**).

Table 2.6 – Results of elemental analysis for iodoalkyl-functionalized SiO_2-coated MNPs (**107**) and BTPhen functionalized SiO_2-coated MNPs (**110**)

	Iodoalkyl-functionalized SiO_2-coated MNPs (107)	**BTPhen-functionalized SiO_2-coated MNPs (110)**
C (%)	11.59	29.62
H (%)	2.50	3.27
N (%)	-	0.93
I (%)	38.92	1.39

*2.2.4 – Extraction Studies of BTPhen functionalized SiO_2-coated MNPs (**110**):*

The BTPhen functionalized SiO_2-coated MNPs (**110**) were evaluated for their ability to extract Am(III) from Eu(III) and Am(III) from Cm(III) at the Czech Technical University in Prague. The aqueous solutions for the solid phase extraction experiments were prepared by spiking nitric acid solutions (0.001 – 4 M) with stock solutions of ^{241}Am, ^{152}Eu and ^{244}Cm and then adding 1 mL of spiked aqueous solution to 22.7 mg of BTPhen-functionalized SiO_2-coated MNPs (**110**). The suspension was sonicated for 10 min and shaken at 1800 rpm for 90 min. After centrifuging for 10 min, aliquots of the supernatant were separated and taken for alpha and gamma measurements.

The results in **Table 2.7** show the weight distribution ratios for Am(III) and Eu(III) (D_{wAm} and D_{wEu}) and the separation factors for Am(III) over Eu(III) ($SF_{Am/Eu}$) for BTPhen-functionalized SiO_2-coated MNPs (**110**) as a function of increasing nitric acid concentration (0.001–4 M). The MNPs (**110**) exhibited high extraction ability for both Am(III) and Eu(III) ($D_w > 600$) at 0.001 M HNO_3 solution with no selectivity ($SF_{Am/Eu} \approx 0.73 \pm 0.04$) for Am(III) over Eu(III). At 0.1 M HNO_3, the D_w for Am(III) was larger than 450 and the D_w for Eu(III) decreased from ~ 858 to ~15 indicating that an effective selective extraction can still be achieved in 0.1 M HNO_3 solution ($SF_{Am/Eu} \approx 30$).

Table 2.7 – Extraction of Am(III) and Eu(III) by BTPhen functionalized SiO_2-coated MNPs (**110**) as a function of nitric acid concentration.

[HNO_3]	D_{wAm}	D_{wEu}	$SF_{Am/Eu}$
0.001	625 ± 30	858 ± 24	0.73 ± 0.04
0.1	456 ± 19	15 ± 1	30 ± 2
1	25 ± 1	< 3	> 8
4	10 ± 1	< 3	> 3

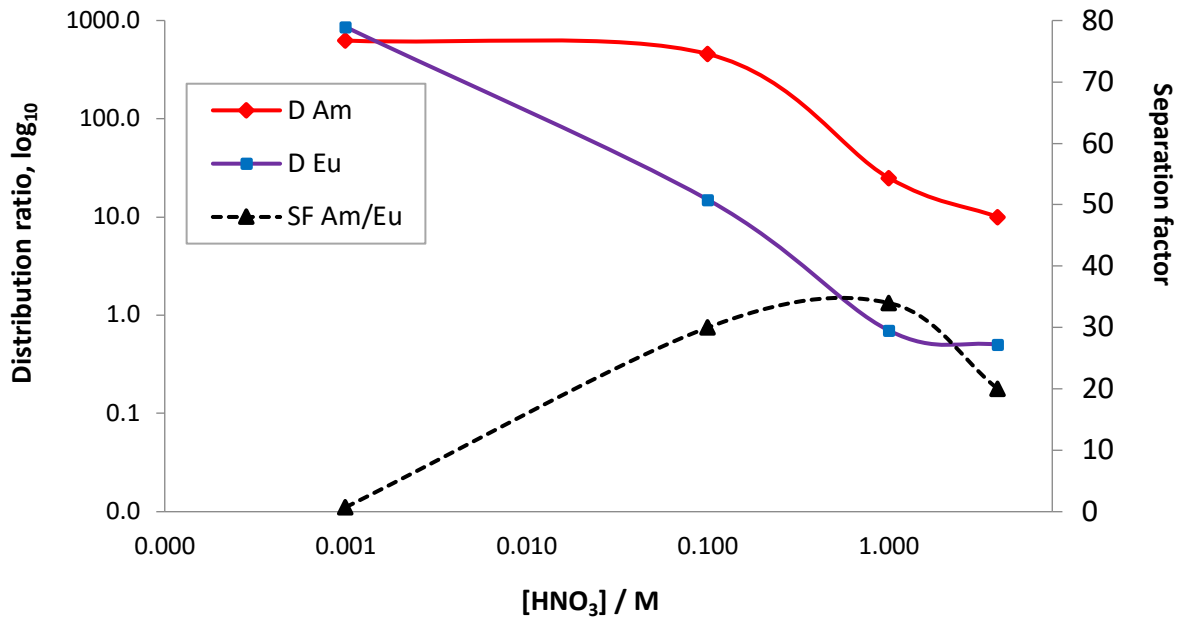

Figure 2.9 – Extraction of Am(III) and Eu(III) by BTPhen functionalized SiO_2-coated MNPs (**110**) as a function of nitric acid concentration.

As the concentration of HNO_3 increased up to 1 M, decreases in the D_w for both Am(III) and Eu(III) were observed ($D_{wAm} \sim 25 \pm 1$; and D_w observed for Eu(III) was under the detection limit, i.e., $D_{wEu} < 3.0$) which resulted in a separation factor of $SF_{Am/Eu} > 8$. At 4 M HNO_3 a further decrease in the D_w value for Am(III) gave $D_{wAm} \sim 10$ and the observed value for Eu(III) was again $D_{wEu} < 3.0$) with a resulting separation factor of $SF_{Am/Eu} > 3$.

Weight distribution ratios for Am(III) and Cm(III), and the separation factors at different nitric acid concentrations were also examined (**Table 2.8** and **Fig 2.10**). The D_w values for both Am(III) and Cm(III) decreased with increasing nitric acid concentration, in agreement with the above results for Am(III)/Eu(III), resulting in a small but significant $SF_{Am/Cm} \approx 3.0 \pm 0.5$ at 0.1 M HNO_3.

Table 2.8 – Extraction of Am(III) and Cm(III) by BTPhen functionalized SiO_2-coated MNPs (**110**) as a function of nitric acid concentration.

$[HNO_3]$	D_{wAm}	D_{wCm}	$SF_{Am/Cm}$
0.001	613 ± 92	512 ± 68	1.2 ± 0.2
0.1	500 ± 61	163 ± 14	3.0 ± 0.5
1	21 ± 3	10 ± 3	2.1 ± 0.6
4	13 ± 3	7 ± 2	1.8 ± 0.4

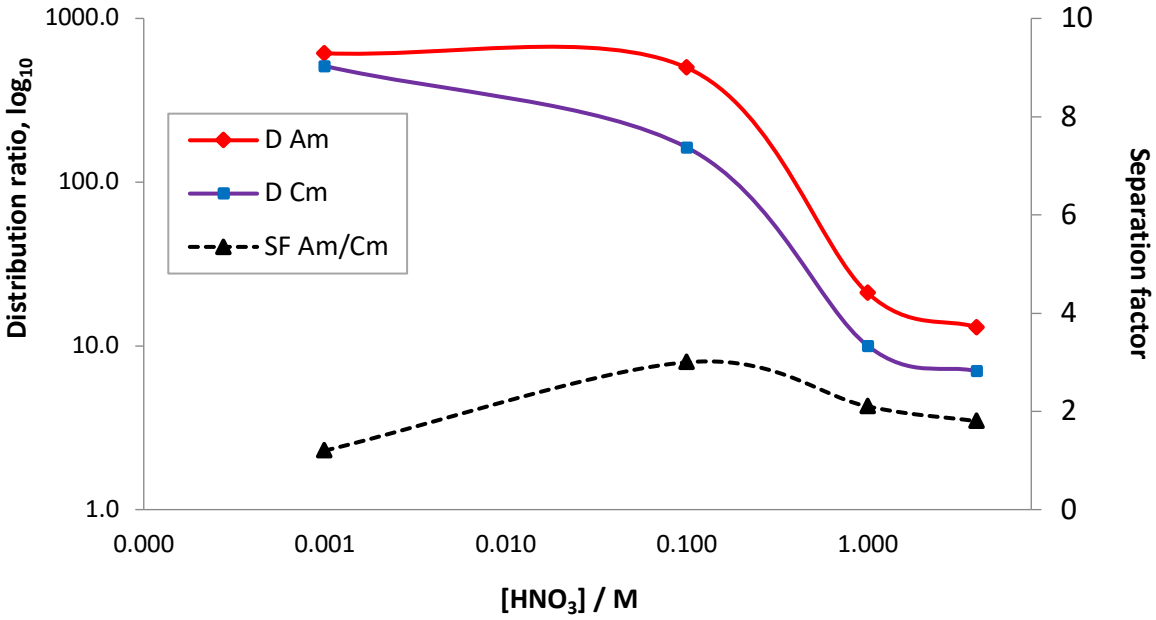

Figure 2.10 – Extraction of Am(III) and Cm(III) by BTPhen functionalized SiO_2-coated MNPs (**110**) as a function of nitric acid concentration.

Overall, these BTPhen functionalized MNPs (**110**) exhibited good selectivity for Am(III) over Eu(III) at 0.1 M HNO_3 (with a separation factor of $SF_{Am/Eu} \approx 30$) and showed a small but significant selectivity for Am(III) over Cm(III) with a nominal separation factor of around 3 in 0.1 M HNO_3. Furthermore, both Am(III) and Eu(III) could be co-extracted at low concentrations of HNO_3 (0.001 M) if required. The uptake behaviour of Am(III) and Eu(III) by MNPs (**110**) at different molarities of HNO_3 demonstrates that the extraction process is highly dependent on HNO_3 concentration and these results represent a development towards the possible use of solid-phase materials for the important and challenging minor actinide–lanthanide separation.

*2.2.5 – Immobilization of tetra-(4-hydroxyphenyl) BTPhen (**105**) on chloropropyl-functionalised SiO_2 gel (**111**):*

The following section contributed to the publication: A. Afsar, P. Distler, L. M. Harwood, J. John and J. Westwood, *Chem. Commun*., 2017, **53**, 4010-4013.[122]

Considering that the minor actinide content in post-PUREX raffinate is smaller than that of U and Pu in the spent fuel, immobilization of actinide-selective ligands onto solid supports could provide an alternative method for carrying out separation and pre-concentration of minor actinides from PUREX raffinates.[123,124] Further benefits of a system based on a solid-phase extractant include – no requirement for mixing or phase separation and possible use of pressure or vacuum to increase flow rate; or as recently discussed the use of simple magnetic separation.[125] Tetra-(4-hydroxyphenyl) BTPhen (**105**) was subsequently immobilized onto commercially available macroscopic chloropropyl-functionalized silica gel (**111**). The reaction proceeded by stirring tetra-(4-hydroxyphenyl) BTPhen (**105**) in DMF with sodium hydride (**Scheme 2.11**). Chloropropyl-functionalized silica gel (**111**) was purchased from Sigma Aldrich (particle size 230-400 mesh and a pore size of 60 Å) and used as supplied. The extent of labelling was ~ 2.5 % loading and the matrix active group was ~ 8 % functionalized.[126]

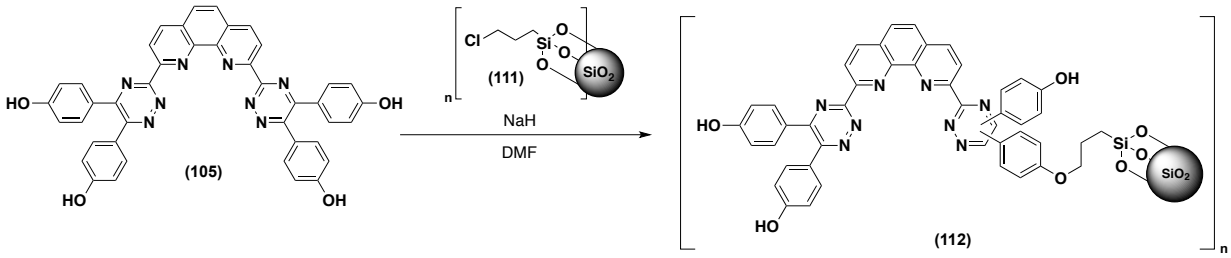

Scheme 2.11 – Immobilization of tetra-(4-hydroxyphenyl) BTPhen (**105**) onto chloropropyl-functionalized SiO_2 gel (**111**)

To assess the degree of functionalization of ligand (**105**) onto the surface of SiO_2 gel (**111**), several techniques were employed. Comparison of the FT-IR spectra of both the chloropropyl-functionalized SiO_2 gel (**111**) and BTPhen-functionalized SiO_2 gel (**112**) (**Fig 2.11**) showed the strong Si-O-Si stretching bond at 1050 cm^{-1} for both and small C=C aromatic vibrations between 1500-1600 cm^{-1} only for BTPhen-functionalized SiO_2 gel (**112**).

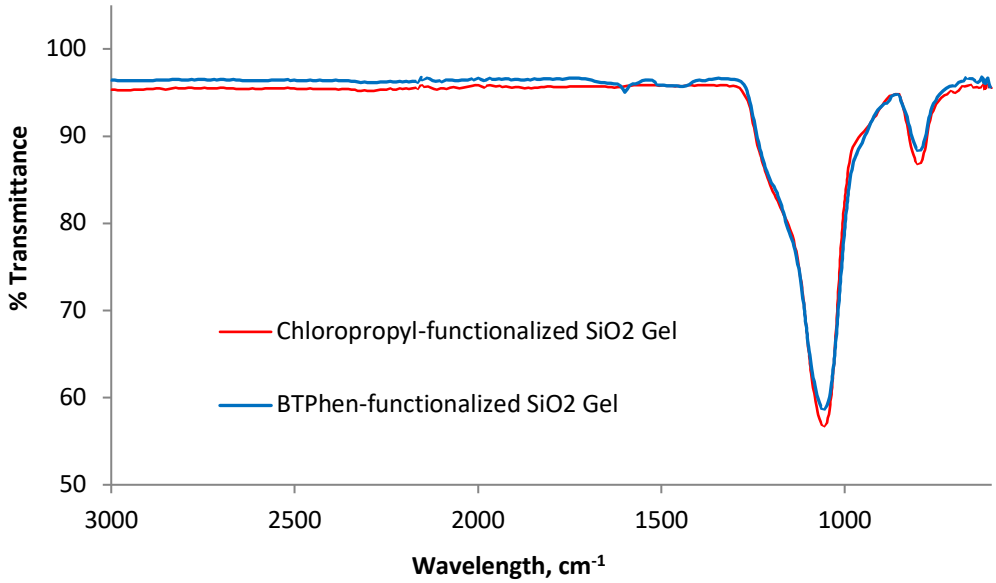

Figure 2.11 – FR-IR spectra of chloropropyl-functionalized SiO_2 gel (**111**) and BTPhen-functionalized SiO_2 gel (**112**)

Elemental analysis of both chloropropyl-functionalized SiO_2 gel (**111**) and BTPhen-functionalized SiO_2 gel (**112**) show an increased C, H and N content for the BTPhen-functionalized SiO_2 gel (**112**) and a large decrease in the % of Cl, indicative of effective incorporation (**Table 2.9**). TGA analysis of (**112**) (appendix **A3**) revealed a usual pattern where, up to 150 ^oC the mass loss was quite small – presumably due to removal of absorbed water and, after that, there was a more-or-less linear mass loss from 250-700 ^oC, which is probably due to decomposition of the organic content. Comparison of the TGA analyses between (**111**) and (**112**) revealed the content of BTPhen ligand (**105**) in the BTPhen-functionalized SiO_2 gel (**112**) to be *ca*. 10 %.

Table 2.9 – Results of elemental analysis for chloropropyl-functionalized SiO_2 gel (**111**) and BTPhen-functionalized SiO_2 gel (**112**)

	Chloropropyl-functionalized SiO_2 Gel (111)	**BTPhen-functionalized SiO_2 Gel (112)**
C (%)	5.05	8.10
H (%)	1.22	1.28
N (%)	-	1.08
Cl (%)	3.61	0.49

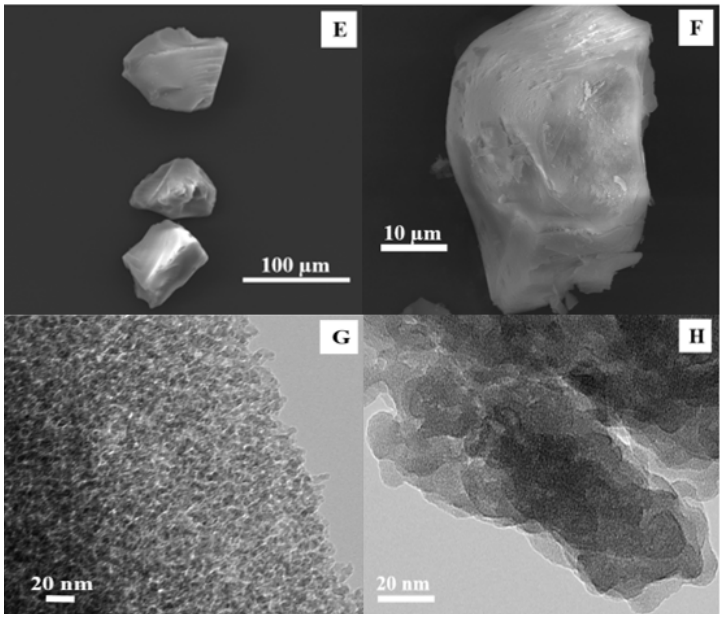

Figure 2.12 – SEM images (E, F) and TEM images (G, H) of chloropropyl-functionalized SiO_2 gel (**111**) (E, G) and BTPhen-functionalized SiO_2 gel (**112**) (F, H)

The surface morphology of chloropropyl-functionalized SiO_2 gel (**111** – E, G) and BTPhen-functionalized SiO_2 gel (**112** – F, H) shown in **Fig 2.12** were examined using SEM and TEM. Comparison of the SEM images of E and F indicates an increase in surface roughness as the ligand becomes incorporated onto the surface of the silica. The TEM micrograph of BTPhen-functionalized SiO_2 gel (**112**) (H) showed an increase in the average size of the silica gel particles compared to the un-functionalized silica gel in image G.

*2.2.6 – Extraction Studies of BTPhen-functionalized SiO_2 Gel (**112**):*

BTPhen functionalized SiO_2 gel (**112**) was investigated for its ability to extract Am(III) from Eu(III) at the Czech Technical University in Prague. Aqueous solutions for the solid phase extraction experiments were prepared by spiking nitric acid solutions (0.001–4 M) with stock solutions of ^{241}Am and ^{152}Eu and then adding 1 mL of spiked aqueous solution to 17 mg of BTPhen-functionalized SiO_2 gel (**112**) (~ 10 mM). The suspension was sonicated for 10 min and shaken at 1800 rpm for 90 min. After centrifuging for 10 min, aliquots of the supernatant were separated and taken for alpha and gamma measurements.

Table 2.10 and **Fig 2.13** shows the weight distribution ratios for Am(III) and Eu(III) (D_{wAm} and D_{wEu}) and the separation factors for Am(III) over Eu(III) ($SF_{Am/Eu}$) for BTPhen-functionalized SiO_2 gel (**112**) as a function of nitric acid concentration (0.001–4 M). High distribution ratios of ($D_w > 90$) were observed for both Am(III) and Eu(III) at 0.001 M HNO_3 solution with very little selectivity ($SF_{Am/Eu} \approx 0.7 \pm 0.04$) for Am(III) over Eu(III).

Table 2.10 – Extraction of Am(III) and Eu(III) by BTPhen functionalized SiO_2 gel (**112**) as a function of nitric acid concentration.

[HNO_3]	**D_{wAm}**	**D_{wEu}**	**$SF_{Am/Eu}$**
0.001	94 ± 3	136 ± 68	0.7 ± 0.04
0.1	4883 ± 974	630 ± 14	7.7 ± 1.7
1	250 ± 12	4.2 ± 0.4	60 ± 6
4	28 ± 1	≈ 0.2	≈ 140

Increasing the HNO_3 concentration to 0.1 M led to a more significant increase in the D_w for Am(III) ($D_{wAm} \sim 4883 \pm 974$) compared to that for Eu(III) ($D_{wEu} \sim 640 \pm 974$), which resulted in an improved $SF_{Am/Eu} \approx 7.7 \pm 1.7$. At 1M HNO_3, decreases in D_w for both Am(III) and Eu(III) were observed ($D_{wAm} \sim 250 \pm 12$, $D_{wEu} \sim 4.2 \pm 0.4$), but the reduction in D_{wEu} was far greater, leading to an even higher separation factor ($SF_{Am/Eu} \approx 60 \pm 6$). More interestingly at 4 M HNO_3 a further decrease in the D_w value for Am(III) afforded $D_{wAm} \sim 28 \pm 1$, but in the case for Eu(III), extraction was almost completely removed, resulting in $D_{wEu} \sim 0.2$, giving a resulting separation factor of $SF_{Am/Eu} \approx 140$, meaning that only Am(III) was retained on the

BTPhen-functionalized SiO_2 gel (**112**). The effect of increasing HNO_3 concentration on the extraction of Am(III) and Eu(III) follows the same trend as reported for the previous system involving $CyMe_4$-BTPhen functionalized SiO_2-coated MNPs (**85**). During that study, it was proposed the shortness of the linking chain of the ligand to the MNPs constrained the BTPhen ligand to form 1:1 complexes with the M(III) cations, with 3 bidentate nitrate ions also ligating to the metal centre making the complex 10-coordinate and so electronically neutral.[106] To verify that this was a ligand effect, extraction capabilities of chloropropyl-functionalized SiO_2 gel (**111**) were also investigated but no extraction was observed for Am(III) or Eu(III) over the full range of concentrations of HNO_3.

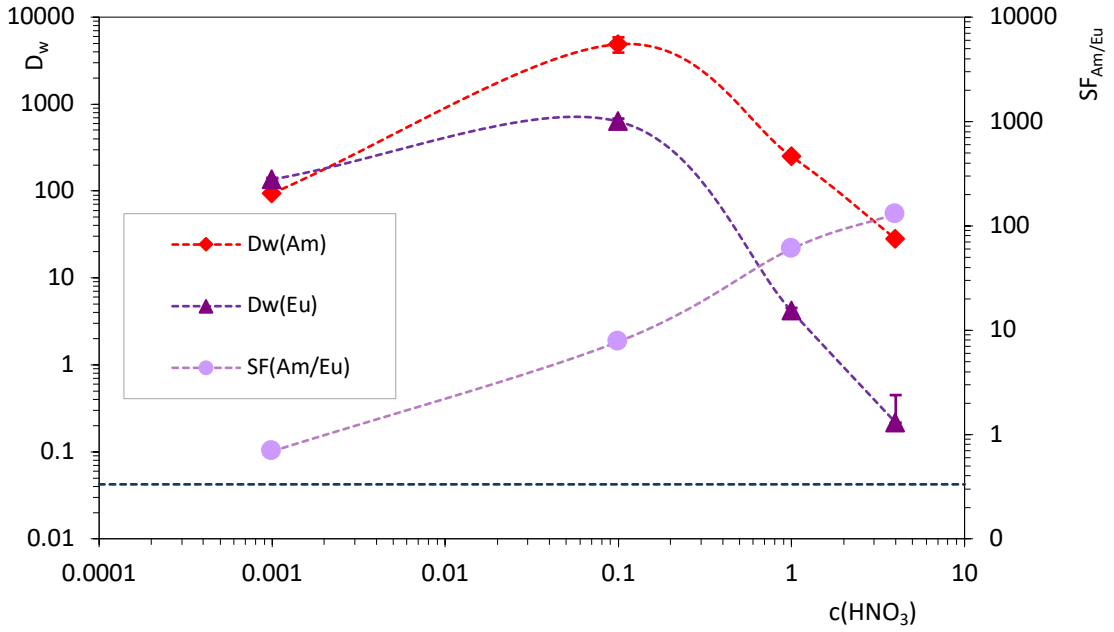

Figure 2.13 – Extraction of Am(III) and Eu(III) by BTPhen-functionalized SiO_2 gel (**112**) as a function of nitric acid concentration.

In summary, the BTPhen-functionalized SiO_2 gel (**112**) extracts both minor actinides and lanthanides at low concentrations of HNO_3 yet exhibits very high selectivity for minor actinides over lanthanides at 4 M HNO_3 ($SF_{Am/Eu} \approx 140$).

2.3 – Selenium Free Synthesis of CyMe$_4$-BTPhen ligands and Immobilization onto SiO$_2$ gels

The following section contributed to the publication: A. Afsar, P. Distler, L. M. Harwood, J. John, J. Cowell and J. Westwood, *Chem. Commun*., 2018, *In press*

2.3.1 – Synthesis and characterization:

After the development of improved synthetic routes to BTPhen containing ligands using selenium free methods, we applied this route to 5-bromo-1,10-phenanthroline (**78**) to develop Br-*bis*-nitrile (**88**) in higher overall yield (**Scheme 2.12**). Our previous route using stoichiometric amounts of selenium dioxide and a one-pot conversion of the corresponding di-aldehyde (**87**) to *bis*-nitrile (**88**) proceeded at ~ 34 % overall yield. The newly developed route, avoiding the use of toxic selenium dioxide, even though it resulted in more steps to synthesize target *bis*-nitrile (**88**), gave a higher overall yield of ~ 58 %.

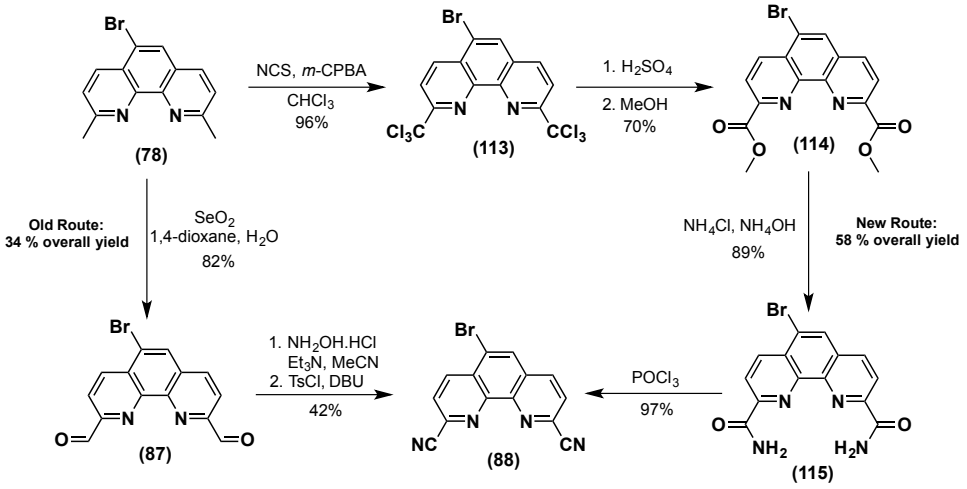

Scheme 2.12 – Improved synthetic protocol for Br-*bis*-nitrile (**88**).

Conversion of the Br-*bis*-nitrile (**88**) to Br-*bis*-aminohydrazide (**89**) occurred efficiently in DMSO as the solvent, as seen previously with 1,10-phenanthroline nitrile (**52**). Condensation with commercially available 2,3-butanedione in THF and Et$_3$N afforded ligand (**116**) in 71 % yield. Previously, the condensation of (**89**) with CyMe$_4$-diketone (**32**) proceeded under similar conditions, taking up to 3 days to attain an efficient yield. It was found that the reaction occurred more efficiently by heating to reflux in acetic acid, with consumption of the diketone (**32**) complete after only 3 hours, affording ligand (**83**) in 80 % yield.

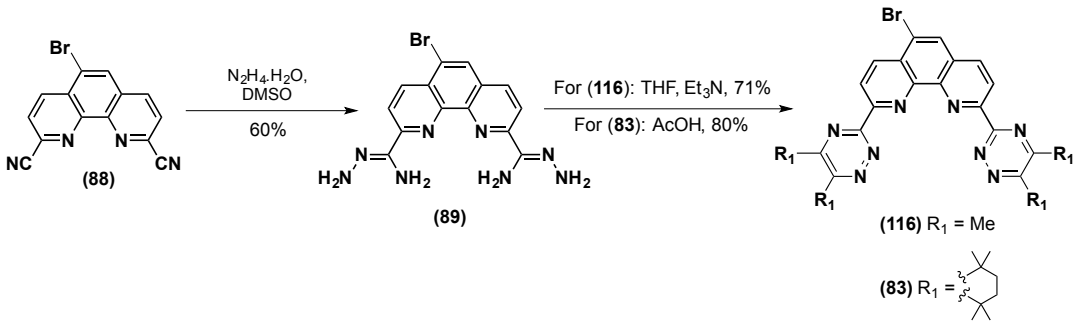

Scheme 2.13 – Synthesis of Br-*bis*-aminohydrazide (**89**) and ligands (**83** and **116**)

During the investigations with ZrO_2-MNPs (**86**), Suzuki coupling of (**83**) with 4-hydroxyphenyl boronic acid produced target 5-(4-hydroxyphenyl)-$CyMe_4$-BTPhen (**84**) in 59 % yield after applying the same conditions as previously reported to complete the transformation of neocuproine (**50**) to 4-(2,9-dimethyl-1,10-phenanthrolin-5-yl)phenol (**117**) as shown in **Scheme 2.14**.[106,115]

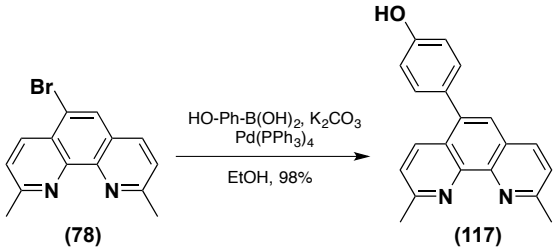

Scheme 2.14 – Suzuki coupling conditions to produce (**117**)

Repeating these conditions from batch to batch of Br-$CyMe_4$-BTPhen (**83**) failed to generate clean 5-(4-hydroxyphenyl)-$CyMe_4$-BTPhen (**84**) in any significant yield (> 5%) for further extraction investigations. Simultaneously, Suzuki coupling of any functional phenyl groups to Br-C1-BTPhen (**116**) failed to generate any 5-coupled-C1-BTPhen ligand for preliminary investigations. After extensive and, at times, frustrating optimization studies, applying a 5:1:1 ratio of toluene:ethanol:water to the repeatedly triturated Br-$CyMe_4$-BTPhen (**83**) afforded target 5-(4-hydroxyphenyl)-$CyMe_4$-BTPhen (**84**) in 75 % yield. Condensation of the diketone (**32**) also occurred efficiently in neat AcOH (80 % yield), albeit only on small scale (500 mg). Immobilization of (**84**) onto chloropropyl-functionalized SiO_2 gel (**111**) generated $CyMe_4$-BTPhen functionalized SiO_2 gel (**118**) (**Scheme 2.15**).

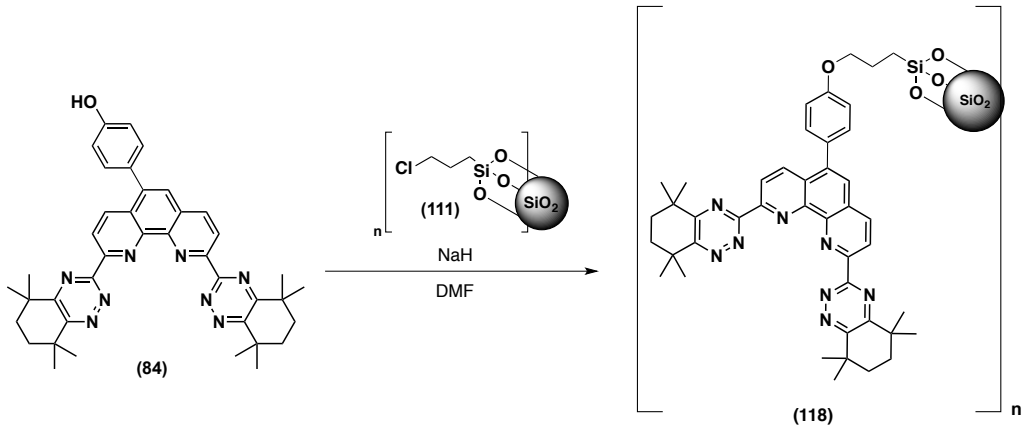

Scheme 2.15 – Immobilization of 5-(4-hydroxyphenyl)-CyMe$_4$-BTPhen (**84**) onto chloropropyl-functionalized SiO_2 gel (**111**)

As with previous solid-supported ligands, a range of techniques was used to assess the content of ligand (**84**) bound to the surface of (**111**). Comparative FT-IR (**Fig 2.14**) showed the presence of absorption bands at 1500-1600 cm^{-1} assigned to the C=C aromatic vibration of (**84**), indicating the attachment of organic content. Elemental analysis (**Table 2.11**) showed an increase in the C, H and N content for CyMe$_4$-BTPhen functionalized SiO_2 gel (**118**) compared to chloropropyl-functionalized SiO_2 gel (**111**), and reduction in Cl % to 0.10. TGA analysis (appendix **A4**) allowed the determination of the degree of surface modification through comparison of the relative mass loss in CyMe$_4$-BTPhen functionalized SiO_2 gel (**118**) compared to chloropropyl-functionalized SiO_2 gel (**111**) and the extent of loading was determined to be *ca*. ~ 25 %.

Table 2.11 – Results of elemental analysis for chloropropyl-functionalized SiO_2 gel (**111**) and CyMe$_4$-BTPhen-functionalized SiO_2 gel (**118**).

	Chloropropyl-functionalized SiO_2 Gel (111)	**CyMe$_4$-BTPhen-functionalized SiO_2 Gel (118)**
C (%)	5.05	11.60
H (%)	1.22	2.01
N (%)	-	1.40
Cl (%)	3.61	0.10

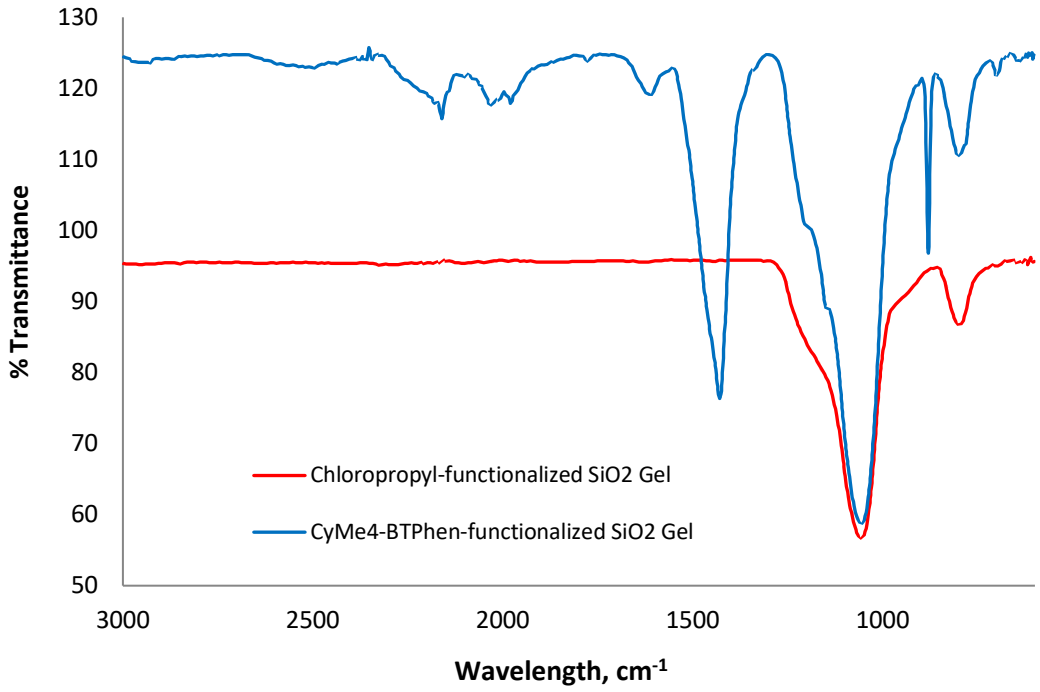

Figure 2.14 – FR-IR spectra of chloropropyl-functionalized SiO_2 gel (**111**) and $CyMe_4$-BTPhen-functionalized SiO_2 gel (**118**)

*2.3.2 – Extraction Studies of $CyMe_4$-BTPhen-functionalized SiO_2 gel (**118**):*

Solid phase extraction investigations of $CyMe_4$-BTPhen-functionalized SiO_2 gel (**118**) were carried out at the Czech Technical University in Prague. Previous solid-supported ligands included MNPs were believed to form 1:1 complexes when extracting the metals Am(III) and Eu(III) due to the shortness of the linking chain between the ligand and the solid support. To investigate whether the extraction is effected by anions surrounding these 1:1 complexes and whether or not this plays an important role in the separation of Am(III) from Eu(III), the extraction experiments of (**118**) were conducted in both nitric and perchloric acid, where the latter contains no coordinating counter-ions.

The aqueous solutions for the solid phase extraction experiments were prepared by spiking nitric acid (HNO_3) and perchloric acid ($HClO_4$) solutions (0.001 – 4 M) with stock solutions of ^{241}Am and ^{152}Eu and then adding 1 mL of spiked aqueous solution to accurately weighed (16.7 mg) of $CyMe_4$-BTPhen-functionalized SiO_2 gel (**118**). The suspensions were sonicated for 10 min and shaken at 1800 rpm for 90 min. After centrifuging for 10 min, aliquots of the supernatant were separated and taken for gamma measurements.

The extraction experiments were studied at HNO_3 and $HClO_4$ concentrations of 0.001 M, 0.1 M, 1 M and particularly 4 M. The weight distribution ratios (D_{wAm} and D_{wEu}) and separation factors for Am(III) over Eu(III) ($SF_{Am/Eu}$) for $CyMe_4$-BTPhen-functionalized SiO_2 gel (**118**) as a function of increasing HNO_3 concentration are shown in **Table 2.12** and **Fig 2.15**.

High distribution ratios (D_w > 160) were observed for both Am(III) and Eu(III) at 0.001 M HNO_3 solution with no significant selectivity ($SF_{Am/Eu} \approx 1.1 \pm 0.1$) for Am(III) over Eu(III). At 0.1 M HNO_3, there was a significant increase in D_w values for both Am(III) ($D_{wAm} \sim 11630 \pm 2033$) and Eu(III) ($D_{wEu} \sim 5618 \pm 720$) resulting in a slightly higher separation of $SF_{Am/Eu} \approx 2.1 \pm 0.4$. Decreases in the D_w values for both Am(III) and Eu(III) were observed ($D_{wAm} \sim 3813 \pm 384$, $D_{wEu} \sim 63.9 \pm 2.3$) at 1 M HNO_3 solution, but a higher separation factor ($SF_{Am/Eu} \approx 60 \pm 6$) resulted. Finally, at 4 M HNO_3 a further decrease in the D_w value for Am (III) afforded $D_{wAm} \sim 354 \pm 12$; the D_w value observed for Eu(III) was reduced to < 2.3 and the resulting separation factor was an impressive $SF_{Am/Eu} \approx 154$.

Table 2.12 – Extraction of Am(III) and Eu(III) by $CyMe_4$-BTPhen-functionalized SiO_2 gel (**118**) as a function of nitric acid concentration.

[HNO_3]	**D_{wAm}**	**D_{wEu}**	**$SF_{Am/Eu}$**
0.001	183 ± 6	165 ± 6	1.11 ± 0.05
0.1	11630 ± 2033	5618 ± 720	2.1 ± 0.4
1	3813 ± 384	64 ± 2	60 ± 6
4	354 ± 12	< 2.3	≈ 154

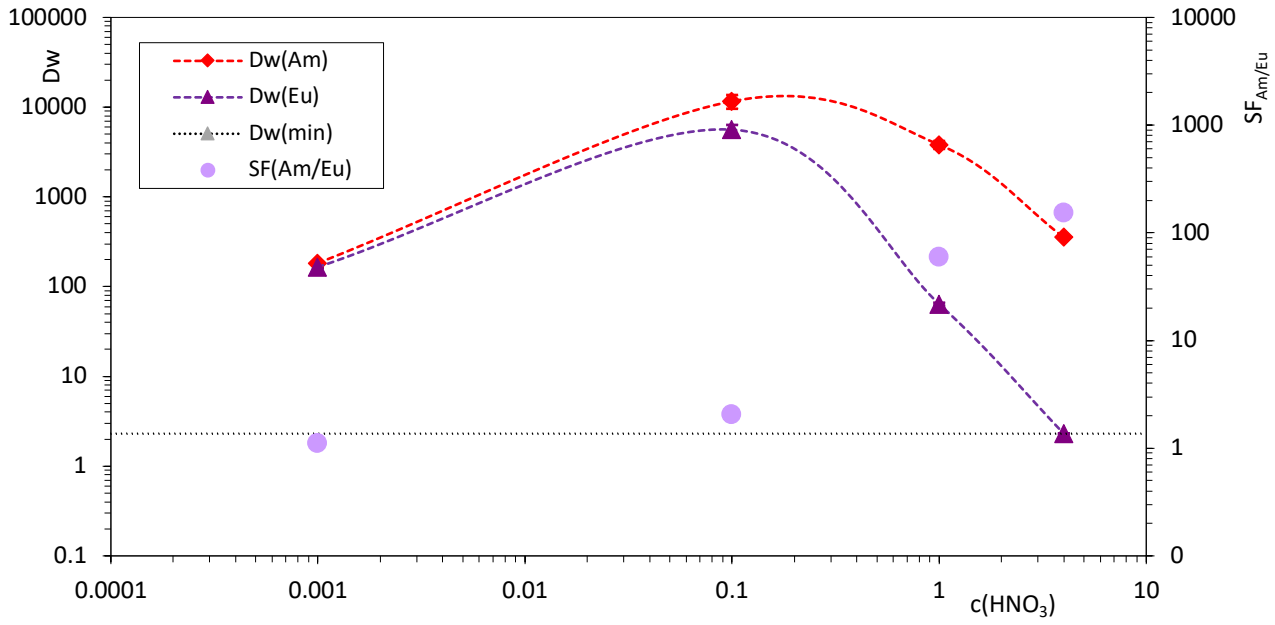

Figure 2.15 – Extraction of Am(III) and Eu(III) by $CyMe_4$-BTPhen-functionalized SiO_2 gel (**118**) as a function of nitric acid concentration. Mass of sorbent: approximately 16 mg, phase volume: 1 mL, V/m ratio: ~ 60 mL/g.

The observed decrease in D_w values for (**118**) with increasing [HNO_3] concentration was previously seen with other solid-supported BTPhen ligands ($CyMe_4$-BTPhen-functionalized SiO_2-MNPs (**85**) and BTPhen-functionalized SiO_2 gel (**112**)) and, once again, can probably be attributed to the increased degree of ligand protonation and thus decreased free ligand concentration.

Table 2.13 and **Fig 2.16** show weight distribution ratios for Am(III) and Eu(III) (D_{wAm} and D_{wEu}) and separation factors for Am(III) over Eu(III) ($SF_{Am/Eu}$) for $CyMe_4$-BTPhen-functionalized SiO_2 gel (**118**) as a function of increasing $HClO_4$ concentration (0.001 M – 4 M), respectively. As seen during the extraction in HNO_3, the D_w values for both Am(III) and Eu(III) firstly increase, achieving maximum values at 0.1 M $HClO_4$, and then decrease with subsequent increasing $HClO_4$ concentration, in agreement with the earlier results. Even though high D_w values were obtained for both Am(III) (D_{wAm} ~ 221 ± 9 and D_{wAm} ~ 6864 ± 1298) and Eu(III) (D_{wEu} ~ 145 ± 5 and D_{wEu} ~ 312 ± 14) at 0.001 M and 0.1 M $HClO_4$ concentrations respectively, all the values (except for that at 0.001 $HClO_4$) are significantly lower than those measured in HNO_3. The separation factors were calculated as $SF_{Am/Eu} \approx$ 1.5 ± 0.1, 22.0 ± 2.6, 119 ± 27 and ≈ 1 at 0.001, 0.1, 1 and 4 M $HClO_4$, respectively. When comparing (**118**) in HNO_3 and $HClO_4$, it can be seen that the absence of $[NO_3]^-$ decreases

the values of D_w, especially at higher acid concentrations. These results indicate that the bidentate properties of the nitrate ion probably play an important role in these Am(III) and Eu(III) separations. The separation factors $SF_{Am/Eu}$ are similar in nitric and perchloric acids except for the case of 4 mol/L concentration where the substitution of HNO_3 with $HClO_4$ results in a dramatic drop of $SF_{Am/Eu}$ from > 154 down to ≈ 1.

Table 2.13 – Extraction of Am(III) and Eu(III) by $CyMe_4$-BTPhen-functionalized SiO_2 gel (**118**) as a function of perchloric acid concentration.

[$HClO_4$]	**D_{wAm}**	**D_{wEu}**	**$SF_{Am/Eu}$**
0.001	221 ± 9	145 ± 5	1.5 ± 0.1
0.1	6864 ± 1298	312 ± 14	22 ± 2.6
1	285 ± 13	2.4 ± 0.9	119 ± 27
4	< 2	< 2	≈ 1

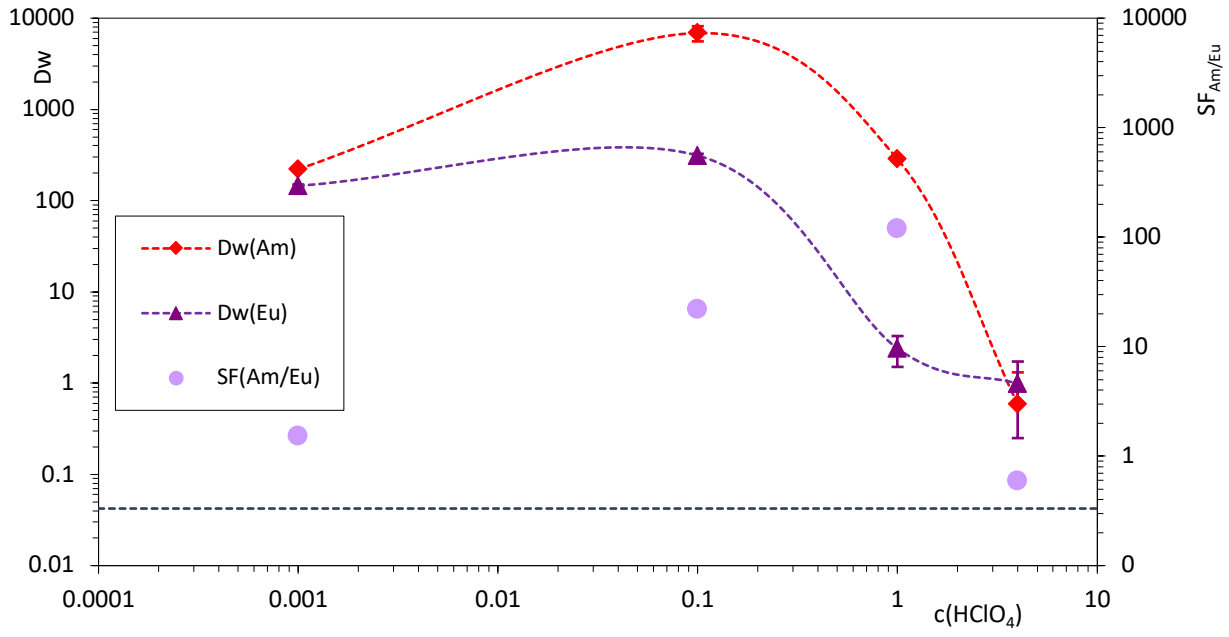

Figure 2.16 – Extraction of Am(III) and Eu(III) by $CyMe_4$-BTPhen-functionalized SiO_2 gel (**118**) as a function of perchloric acid concentration. Mass of sorbent: approximately 16 mg, phase volume: 1 mL, V/m ratio: ~ 60 mL/g

Overall, the remarkable capacity of $CyMe_4$-BTPhen-functionalized SiO_2 gel (**118**), which achieves efficient extraction of both Am(III) and Eu(III) at low nitric acid concentration (0.001 M HNO_3), yet exhibits high selectivity ($SF_{Am/Eu} \approx 154$) for Am(III) over Eu(III) at 4 M HNO_3 has been observed. This silica-based solid extractant is currently the most efficient immobilized minor actinide selective extractant, exceeding the previously discussed tetra(4-hydroxyphenyl)-BTPhen-functionalized SiO_2 gel (**112**) ($SF_{Am/Eu} \approx 140$). Since the extraction experiments were also carried out in $HClO_4$ medium, we can conclude that the three bidentate nitrate ions surrounding the 1:1 complex of (**118**) giving rise to charge neutrality provide a vital role in the selective separation of minor actinides from lanthanides at high nitric acid concentrations. Although this interesting finding helps deduce the possible mode of complexation adopted by the ligand for extraction, further more detailed examination of (**118**) and related MNPs (**85**) are required to probe their different extraction properties. Both systems are identical from a chemical point of view, where $CyMe_4$-BTPhen is grafted onto SiO_2 via 4-hydroxyphenyl and a propyl linker, but their extraction behaviour is somewhat different.

2.4 – Synthesis and Screening of BTBP-functionalized SiO_2 gel:

The following section contributed to the publication: A. Afsar, P. Distler, L. M. Harwood, J. John and J. Westwood, *Chem. Commun*., 2017, **53**, 4010-4013.[122]

2.4.1 – Synthesis and Characterization:

Following previously reported protocols, the synthesis of ligand (**120**) was proceeded via the double *N*-oxidation of 2,2'-bipyridine (**12**) using hydrogen peroxide in acetic acid.[81,127] A modified Reissert-Henze reaction of *bis*-*N*-oxide (**39**) using trimethylsilyl cyanide and benzoyl chloride afforded *bis*-nitrile (**40**) in 68 % yield. Conversion of the *bis*-nitrile (**40**) into *bis*(aminohydrazide) (**41**) was achieved by stirring in excess hydrazine hydrate in ethanol at ambient temperature.[81,127] Condensation of *bis*(aminohydrazide) (**41**) with commerical 1,4-dibromo-2,3-butanedione (**119**) in THF afforded the 6,6′-bis(5,6-bis(bromomethyl)-1,2,4-triazin-3-yl)-2,2′-bipyridine (**120**) ligand in 82 % yield (**Scheme 2.16**).

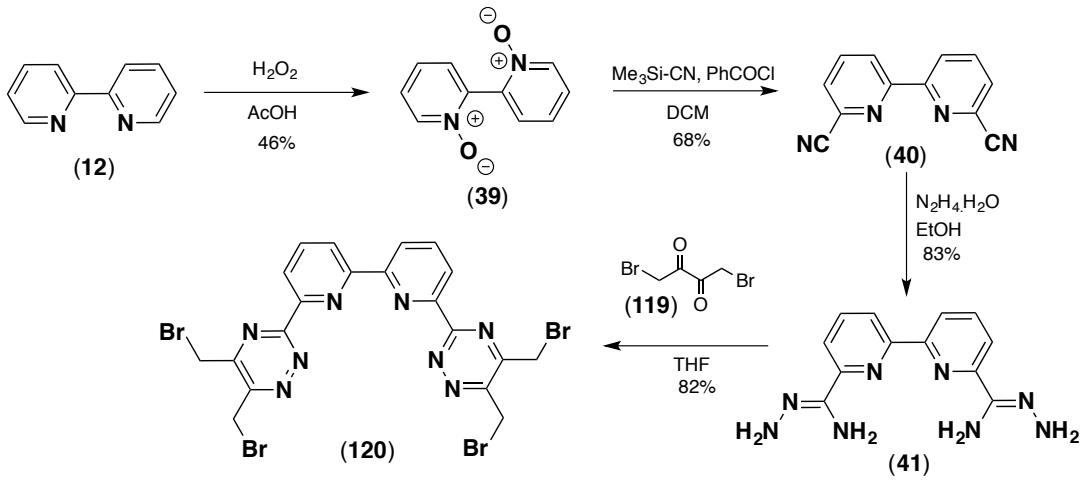

Scheme 2.16 – Synthesis of 6,6'-bis(5,6-bis(bromomethyl)-1,2,4-triazin-3-yl)-2,2'-bipyridine (**120**)

As seen previously with tetra-(4-hydroxyphenyl)-BTPhen (**105**), the incorporation of bromomethyl substituents onto the triazine units of this BTBP ligand (**120**) enables a direct route of immobilization onto solid supported materials. BTBP ligand (**120**) was subsequently immobilized onto commercially available macroscopic aminopropyl-functionalized silica gel (**121**). The reaction proceeded by stirring ligand (**120**) and silica gel (**121**) in DMF with triethylamine (**Scheme 2.17**). Aminopropyl-functionalized silica gel (**121**) was purchased directly from Sigma Aldrich and used as supplied. The extent of aminopropyl functionalization of the initial silica gel substrate was ~ 1 mmol g^{-1} NH_2 loading and the

silica gel was approximately ~ 9 % functionalized by weight. The particle size of the original functionalized silica gel was 40-63 μm with 60 Å pore size.[128]

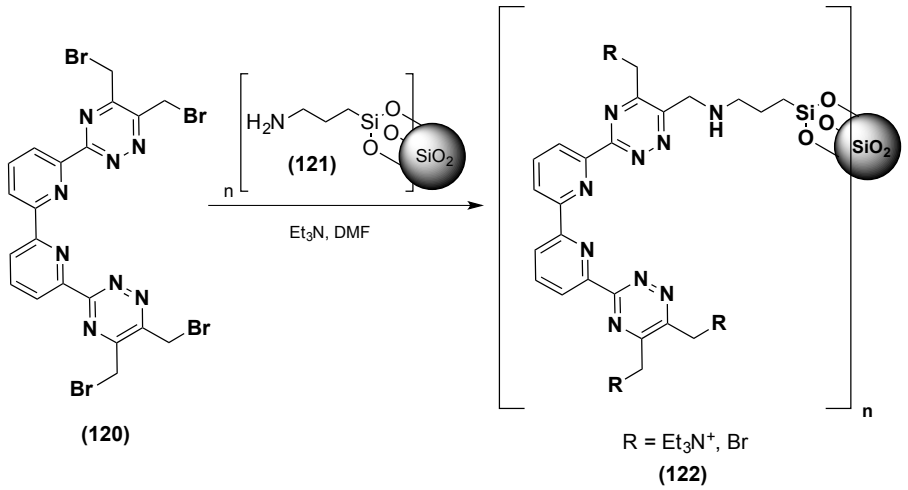

Scheme 2.17 – Immobilization of BTBP ligand (**120**) onto aminopropyl-functionalized silica gel (**121**)

Several characterization techniques were employed to assess the degree of immobilization of BTBP ligand (**120**) onto the aminopropyl-functionalized SiO_2 gel (**121**) surface. The FT-IR spectra (**Fig 2.17**) showed the Si-O-Si stretching at 1100 cm^{-1} for both (**121**) and (**122**), but the presence of bands at 1500-1600 cm^{-1} in (**122**) owing to the C=C aromatic vibrations confirmed the incorporation of ligand (**120**) on to the SiO_2 surface. Elemental analysis showed an increase in the content of C, H and N for the ligand functionalized silica gel (**122**) (**Table 2.14**). Since the results from elemental analysis showed some residual Br remaining on BTBP-functionalised SiO_2 gel (**122**), the nature of the R groups on (**122**) was undetermined and could either be Br or Et_3N^+, from the use of triethylamine in the immobilization step. Thermogravimetric analysis (appendix **A5**) was used to determine the degree of surface modification of (**120**) onto the silica surface to be *ca*. 14 %.

Table 2.14 – Results of elemental analysis for aminopropyl-functionalized SiO_2 gel (**121**) and BTBP functionalized SiO_2 gel (**122**)

	Aminopropyl functionalized SiO_2 Gel (121)	**BTBP functionalized SiO_2 Gel (122)**
C (%)	5.04	14.43
H (%)	1.50	1.92
N (%)	1.63	5.48
Br (%)	-	2.68

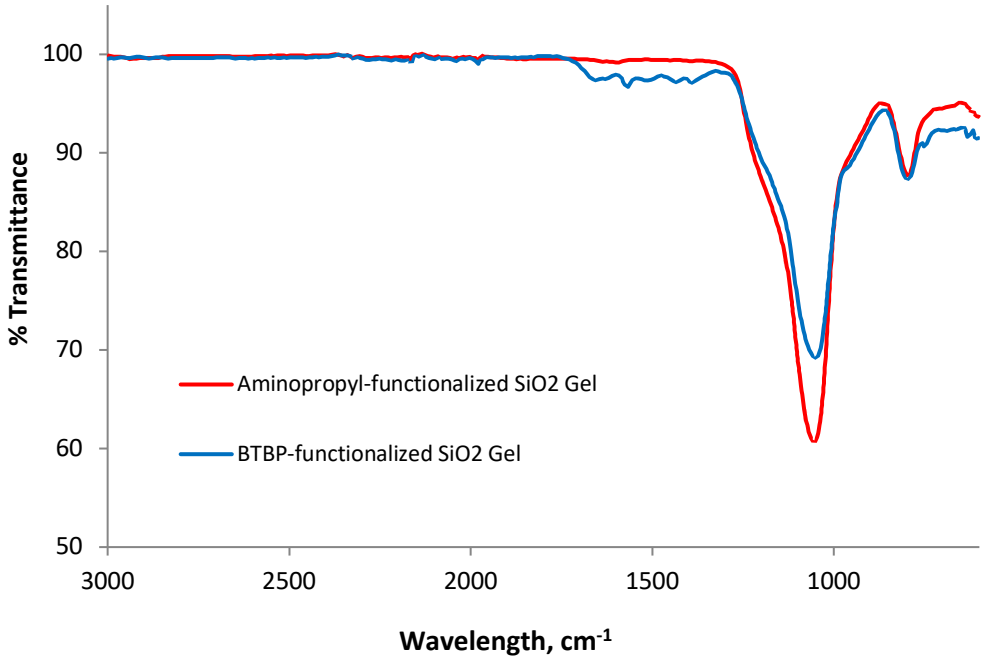

Figure 2.17 – Comparison of the FT-IR spectra of aminopropyl-functionalized SiO_2 gel (**121**) and BTBP functionalized SiO_2 gel (**122**)

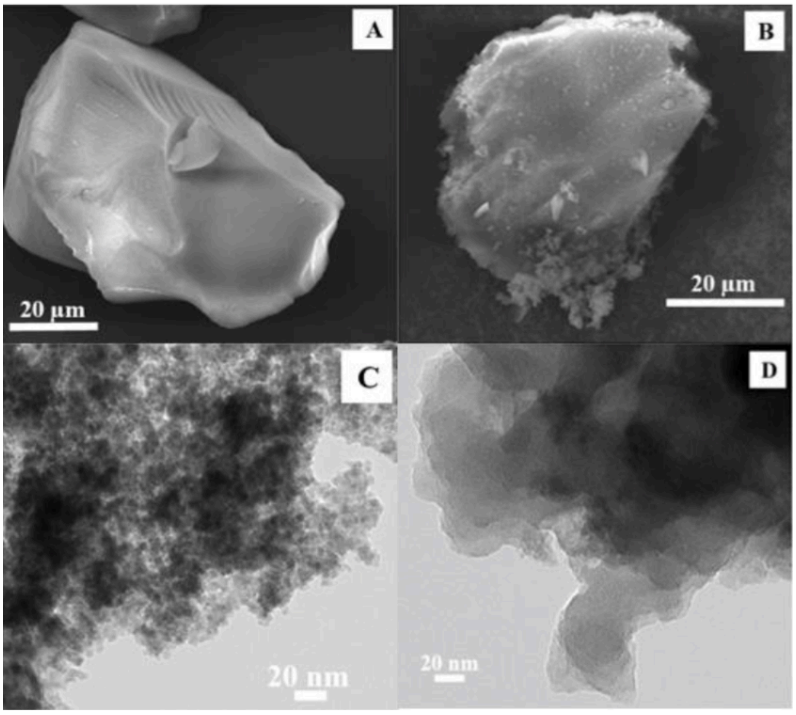

Figure 2.18 – SEM images (A, B) and TEM images (C, D) of aminopropyl-functionalized silica gel (**121** – A, C) and BTBP functionalized SiO_2 gel (**122 –** B, D)

The SEM images (A, B) in **Fig 2.18** show the smooth surface of the aminopropyl-functionalized silica gel (**121**) before surface modification and the increased surface roughness as a result of incorporation of the BTBP ligand onto the surface can be seen in image B. The TEM micrographs (C and D) show the increased size and coverage of the silica gel surface with the organic ligand (image D) compared to the unfunctionalized silica gel in image C.

*2.4.2 – Extraction Studies of BTBP-functionalized SiO_2 Gel (**122**):*

BTBP functionalized silica gel (**122**) was investigated for its ability to extract Am(III) from Eu(III) at the Czech Technical University in Prague. The aqueous solutions for the solid phase extraction experiments were prepared by spiking nitric acid solutions (0.001–4 M) with stock solutions of ^{241}Am and ^{152}Eu and then adding 1 mL of spiked aqueous solution to 14 mg of BTBP-functionalized SiO_2 gel (**122**) (~ 10 mM). The suspension was sonicated for 10 min and shaken at 1800 rpm for 90 min. After centrifuging for 10 min, aliquots of the supernatant were separated and taken for alpha and gamma measurements.

Table 2.15 and **Fig 2.19** show the weight distribution ratios for Am(III) and Eu(III) (D_{wAm} and D_{wEu}) and the separation factors for Am(III) over Eu(III) ($SF_{Am/Eu}$) for BTBP-functionalized SiO_2 gel (**122**) as a function of nitric acid concentration (0.001–4 M). The distribution values for both D_{wAm} and D_{wEu} remained < 1 for the majority of the extractions indicating poor extraction of both Am(III) and Eu(III). The separation factors were calculated as $SF_{Am/Eu} \approx 32 \pm 17$, 193 ± 171, 46 ± 45 and 8 ± 7 at 0.001, 0.1, 1 and 4 M HNO_3, respectively. The low separation factor values indicate that BTBP ligand (**120**) immobilized on SiO_2 gel did not significantly differentiate in the extraction of Am(III) or Eu(III) from HNO_3 solutions, especially since D_w values remained < 1 in most cases, indicating poor extraction of both metals into the immobilized phase.

Table 2.15 – Extraction of Am(III) from Eu(III) by BTBP functionalized silica gel (**122**) as a function of nitric acid concentration.

$[HNO_3]$	D_{wAm}	D_{wEu}	$SF_{Am/Eu}$
0.001	0.361 ± 0.015	0.011 ± 0.011	32 ± 17
0.1	1.301 ± 0.028	0.007 ± 0.007	193 ± 171
1	0.259 ± 0.014	0.006 ± 0.006	46 ± 45
4	0.049 ± 0.012	0.007 ± 0.007	8 ± 7

Extraction capabilities of aminopropyl-functionalized SiO_2 gel (**121**) were also investigated as a comparison; however no extraction was observed for Am(III) or Eu(III), over the full range of concentrations of HNO_3. Studies of the extraction of Am(III) and Cm(III) produced similar results to those shown in **Fig 2.19**, where D_w values remained < 1 across most HNO_3 concentrations and no selectivity for Am(III) over Cm(III) was observed using BTBP-functionalized SiO_2 gel (**122**).

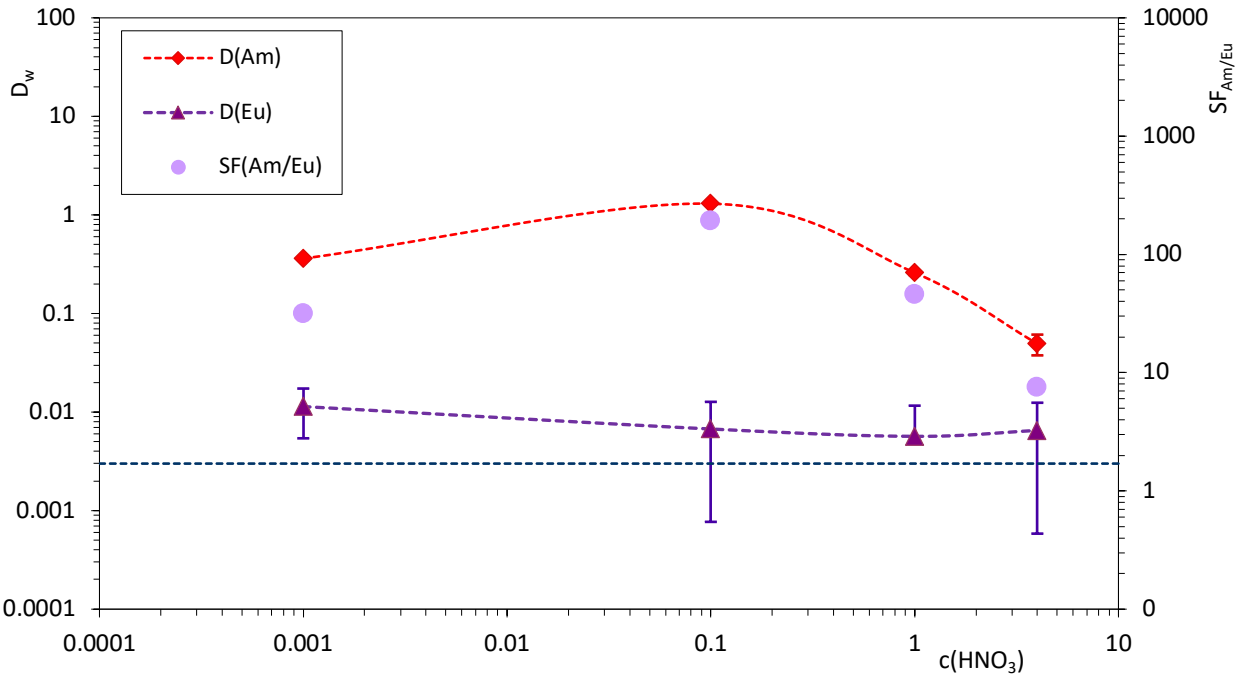

Figure 2.19 – Extraction of Am(III) and Eu(III) by BTBP functionalized silica gel (**122**) as a function of nitric acid concentration.

To investigate whether the BTBP-functionalized SiO_2 gel (**122**) had any potential application in the removal of fission and corrosion products such as Ni(II), Pd(II), Ag(I) and Cd(II), extraction experiments were performed to extract metal ions from 2 % HNO_3 solution (pH = 0.5) using a column technique. BTBP-functionalized SiO_2 gel (**122**) (10 g, ~ 1.4 g BTBP (**120**) loading), packed into a glass column (diameter 3.8 cm, bed volume ~ 35 mL) was first washed with 2 % HNO_3 solution (100 mL). Standard solutions at pH 0.5 containing a range of metals, each at 100 ppb concentration (100 mL) were then passed through the column at a rate of 10 mL min^{-1} and the filtrate was collected and analysed by ICP-MS. The uptake of various metal ions – Sc(III), Mn(II), Fe(III), Co(II), Ni(II), Cu(II), Zn(II), Mo(IV), Ag(I), Cd(II), Sb(V), Pb(II), Pd(II), Os(IV), Ir(III), Pt(IV), Au(III), Zr(IV), Nb(V), Hf(IV), Ta(V), W(VI) and Re(IV) at pH 0.5, by BTBP-functionalized SiO_2 gel (**122**) showed > 80 % uptake efficiency in one-cycle for all the metals except Sb(V) in **Fig 2.20**.

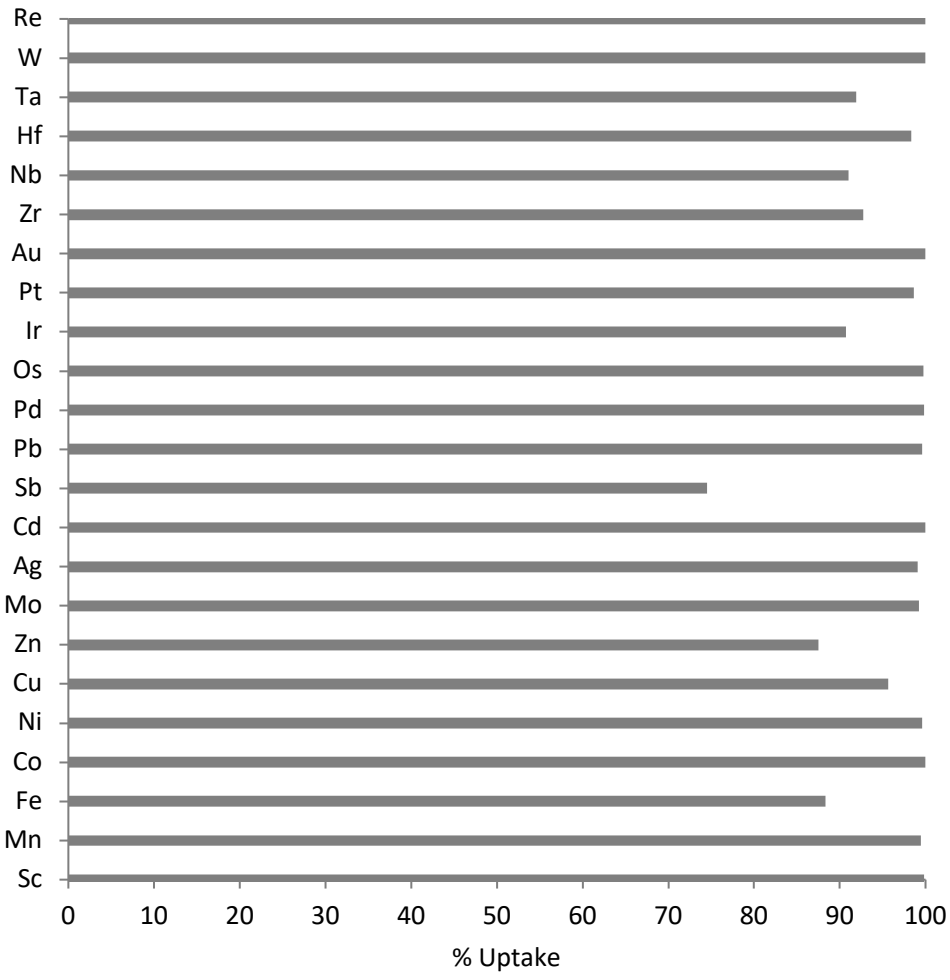

Figure 2.20 – Percentage uptake of metal ions (100 ppb) from aqueous solution at pH 0.5 by BTBP-functionalized SiO_2 gel (**122**)

Importantly, near quantitative extraction of certain problematic corrosion and fission products [Ni(II), Pd(II), Ag(I) and Cd(II)] that are found in the nitric acid solutions of PUREX raffinates was observed. Significantly, the BTBP-functionalized SiO_2 gel (**122**) did not show any affinity towards alkali metals or alkaline earth metals such as Na^+ , K^+, Mg^{2+} and Ca^{2+} or Al^{3+}.

2.5 – Synthesis of Nitro-phenanthroline derivatives and Screening of (dppz)-BTPhen ligand:

The following section led to the publication: J. Westwood, L. M. Harwood, A. Afsar, J. Cowell, P. Distler and J. John, *Lett. Org. Chem.,* 2018, **15**, 340-344.

*2.5.1 – Synthesis of Nitro-phenanthroline derivatives and (dppz)-BTPhen ligand (**135**):*

Following the successful immobilization of BTBP and BTPhen related ligands onto solid supported materials including MNPs and silica gel, an alternative route of immobilization was investigated as a way to by-pass the need for Suzuki coupling at the 5-position of bromine-bearing phenanthrolines. Introduction of a nitro- group (**123**) at that position was proposed, as not only would the nitro- group possibly provide a further insight into the interesting electronic effects towards the two coordinating nitrogen donor atoms in the phenanthroline unit during extraction, but the nitro- group could also be reduced using well reported protocols to an amine (**124**) and thus provide a more direct mode of immobilization onto, for example, chloropropyl functionalized silica gel (**111**) or related (**125**) solid materials (**Scheme 2.18**).[129]

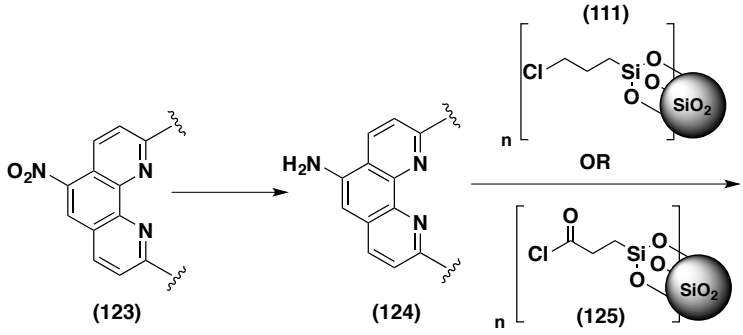

Scheme 2.18 – Nitro group reduction and possible immobilization routes

Attempts at nitration at the 5-position of neocuproine (**50**) using previously reported procedures produced the 5-nitro-1,10-phenanthroline (**123**) in low yield (< 5 %).[130–132] It was found that using a mixture of fuming sulfuric acid (20 % SO_3) and conc. HNO_3 increased the yield of desired product (**123**), but also led to the isolation of considerable amounts of a by-product that was revealed to be 5,6-dioxo-phenanthroline dicarboxylic acid (**126**) (**Scheme 2.19**).

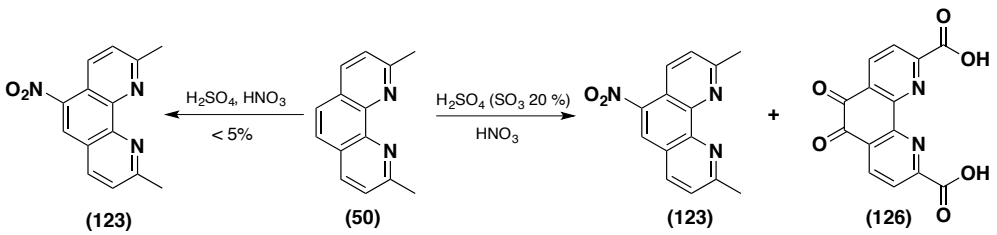

Scheme 2.19 – Formation of 5-nitro-1,10-phenanthroline (**123**) and 5,6-dioxo-phenanthroline dicarboxylic acid (**126**) [longer reaction times lead to increased yields of (**126**)]

Following the isolation of 5-nitro-1,10-phenanthroline (**123**), the improved selenium-free synthetic protocol developed for the preparation of BTPhen units was applied (**Scheme 2.20**). Conversion of (**123**) into the *bis*-(trichloromethyl) (**127**) analogue occurred in 72 % yield and conversion to dimethyl 5-nitro-1,10-phenanthroline-2,9-dicarboylate (**128**) proceeded at 65 % isolated yield.[130] Using our previous method of treating *bis*-ester (**128**) with concentrated ammonium hydroxide in the presence of ammonium chloride failed to generate *bis*-amide (**130**) at all. Therefore, alternative amide formation conversions were investigated and it was found that formation of *bis*-amide (**130**) could be achieved using amide coupling conditions.[133] Thus, hydrolysis of the methyl-ester in (**128**) using HCl (1 M) generated *bis*-carboxylic acid derivative (**129**) required for amide coupling. Reaction of *bis*-carboxylic acid (**129**) with EDCI.HCl (*N*-(3-dimethylaminopropyl)-*N*′-ethylcarbodiimide hydrochloride), HOBt (1-hydroxybenzotriazole), ammonium chloride and di*iso*propylethylamine then produced the desired *bis*-amide (**130**) very efficiently in 91 % yield.

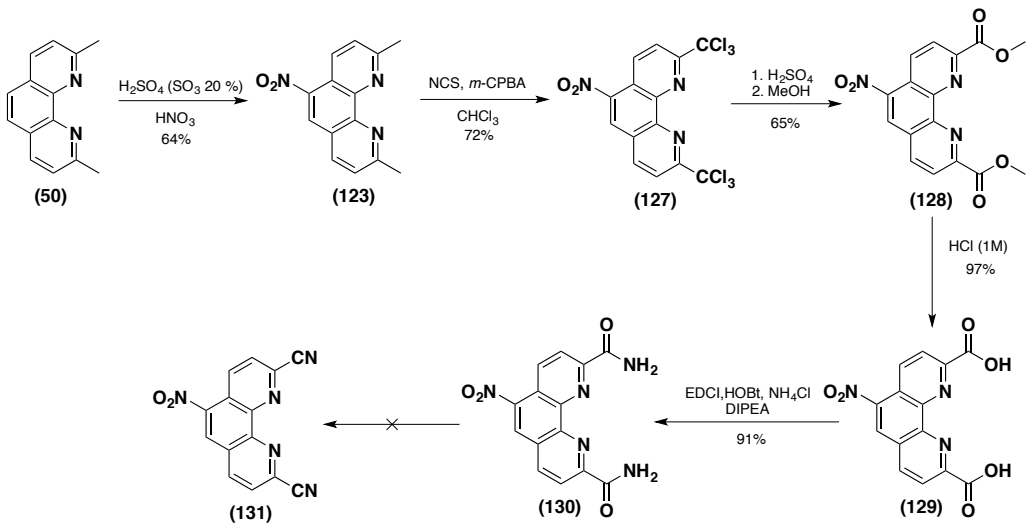

Scheme 2.20 – Synthesis towards 5-nitro-1,10-phenanthroline-2,9-dicarbonitrile (**131**)

However, attempts to dehydrate the amide groups in (**130**) using oxalyl chloride, DMF and base, or phosphorous oxychloride failed to produce the desired novel 5-nitro-1,10-phenanthroline-2,9-dicarbonitrile (**131**).

Our attention then returned to the (unintentional) formation and isolation of 5,6-dioxo-phenanthroline dicarboxylic acid (**126**). The 5,6 double bond across the phenanthroline unit in neocuproine (**50**) has previously been oxidised to the dione using potassium bromide in a mixture of concentrated HNO_3 and H_2SO_4 acids.[134] These same reaction conditions have also affected the complete oxidation of both methyl groups to carboxylates, as well as the 5,6-double bond to the dione.[135] Increasing the reaction time of the acidic reaction conditions in **Scheme 2.19** led to increased yields of (**126**) up to 78 % and without the need for KBr. With the generation of product (**126**), possessing di-carboxylic acid groups required in the newly developed route for the preparation of BTPhens, we explored the addition of extra functionality by extending the aromatic system of the phenanthroline unit by condensation with aromatic di-amines. This new (dppz) (**di**pyrido**p**hena**z**ine) moiety inside the BTPhen structure was incorporated as a possible future alternative to immobilization of related ligands onto solid supports. The extended aromatic system may also enhance the solubility of these ligands in solvents used in the nuclear reprocessing industry, especially un-symmetrical (dppz) units. *Ortho*-phenylenediamine units bearing amine/hydroxyl groups could be used to effect the immobilization onto solid supports rather than performing the Suzuki coupling on halogen bearing phenanthroline units (**Scheme 2.21**).

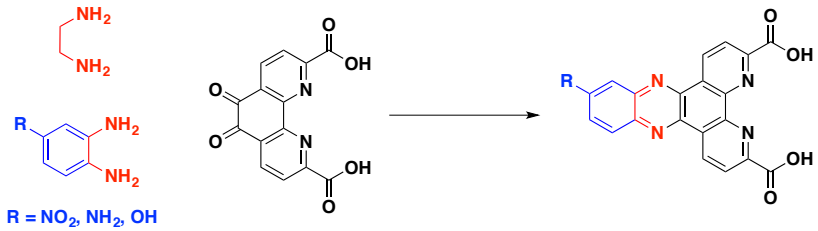

Scheme 2.21 – Possible scope of (dppz) moieties

Subsequent condensation of (**126**) with commercially available *o*-phenylenediamine in ethanol, as reported in the literature, furnished the (dppz)-diacid unit (**132**) in 49 % yield (**Scheme 2.22**).[136] Our previously discussed improved synthetic route towards BTPhen

ligands involved conversion of di-acid units into methyl esters and subsequent amination using excess ammonium chloride and concentrated ammonium hydroxide. The formation of the (dppz)-*bis*-amide unit (**133**) in efficient yield was proving difficult again using this method and so an alternative, faster one-pot method of di-amide formation was envisaged. It was found that (dppz)-*bis*-acid (**132**) could undergo a one-pot reaction firstly with $SOCl_2$ to form the intermediate diacyl chloride, followed by the addition of concentrated ammonium hydroxide to form *bis*-amide (**133**) in 96 % overall yield. Previous synthetic routes towards BTPhen analogues involved the dehydration of *bis*-amides with either oxalyl chloride in DMF followed by base or heating to reflux in neat phosphorous oxychloride and then reaction of the subsequent *bis*-nitrile with hydrazine hydrate in either ethanol or DMSO.[98,118] However, it proved difficult again to dehydrate *bis*-amide (**133**) and isolate the (dppz)-*bis*-nitrile compound using either of these methods. As an alternative, we developed an improved one-pot procedure for the isolation of *bis*-aminohydrazide (**134**) that firstly involved the dehydration of *bis*-amide (**133**) with TFAA and pyridine in DMF followed by the addition of hydrazine hydrate to form *bis*-aminohydrazide (**134**) in 90 % overall yield. These reaction conditions were also applied to our Br-*bis*-amide (**115**), which successfully generated Br-*bis*-aminohydrazide (**89**) in an efficient 82 % yield (**Scheme 2.23**). Condensation of (**134**) with 3,3,6,6-tetramethylcyclohexane-1,2-dione ($CyMe_4$-diketone) (**32**) in acetic acid at reflux afforded the (dppz)-BTPhen ligand (**135**) in 75 % yield after 3 hrs.

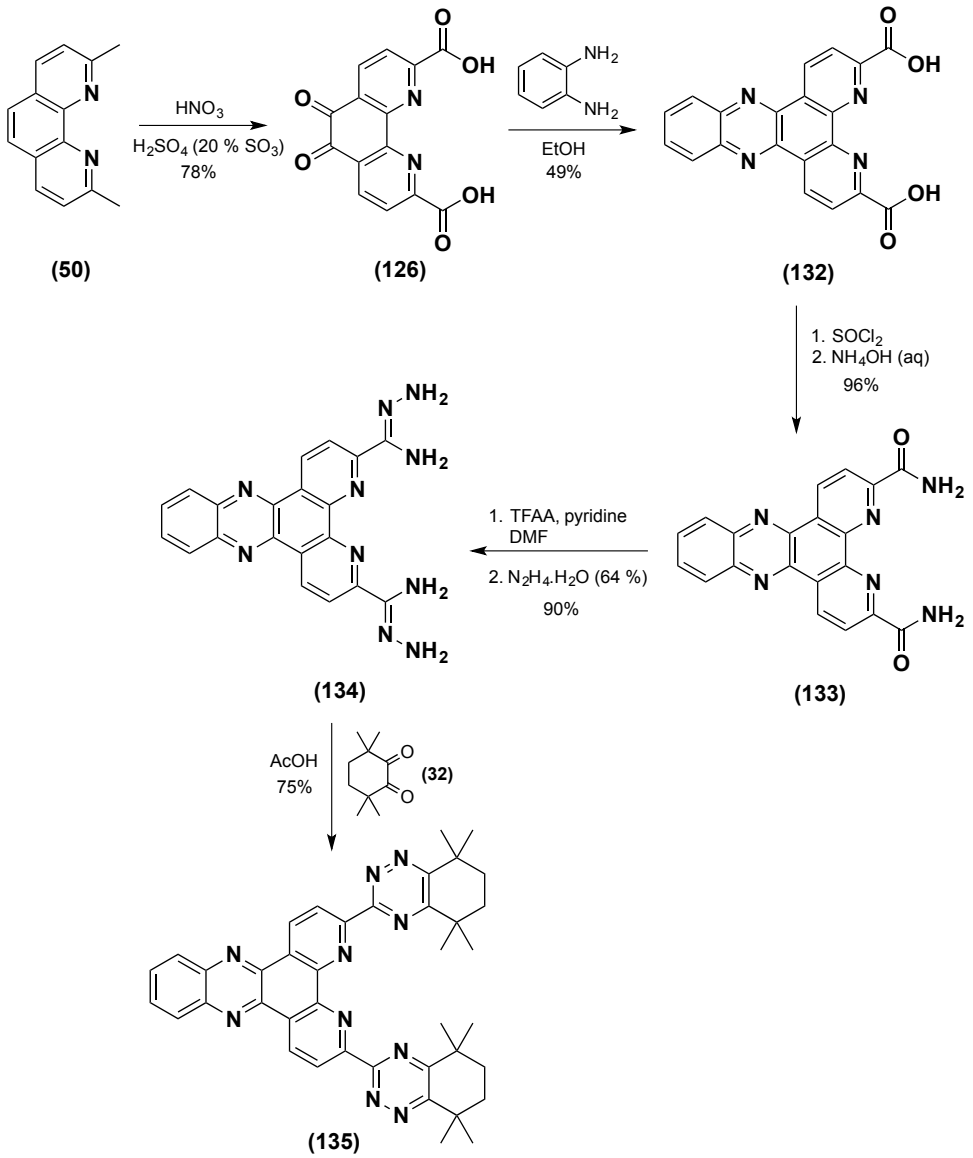

Scheme 2.22 – Synthesis of (dppz)-BTPhen ligand (**135**)

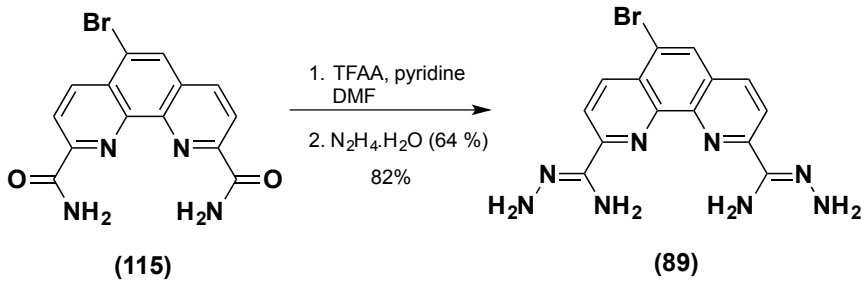

Scheme 2.23 – One-pot synthesis of Br-*bis*-aminohydrazide (**89**)

*2.5.2 – Extraction Studies of (dppz)-BTPhen (**135**):*

Solvent extraction experiments of (dppz)-BTPhen ligand (**135**) were carried out at the Czech Technical University in Prague. The aqueous solutions were prepared by spiking HNO_3 solutions (0.001-2 M) with ^{241}Am and ^{152}Eu radiotracers. Organic solutions of ligand (**135**) (5 mM) were prepared in cyclohexanone with gentle heating. Each organic phase (1 mL) was shaken separately with each of the aqueous phases (1 mL) for 90 mins at 22 ^{o}C (non-thermostatted) using a Heidolph Multi Reax Shaker (1800 rpm). After phase separation by centrifugation, two parallel 200 µL aliquots of each phase were withdrawn for gamma measurement. For gamma measurements, the aliquots were pipetted into plastic ampules and their walls were washed with 1 mL of distilled water or cyclohexanone. Gamma activity measurements of ^{241}Am and ^{152}Eu were performed with a γ-ray spectrometer EG&G Ortec (USA) with a PGT (USA) HPGe detector. The γ-lines at 59.5 keV and 121.8 keV were examined for ^{241}Am and ^{152}Eu respectively. The errors given in the **Table 2.16 and 2.17** are 1σ errors based on counting statistics.

The extraction data summarised in **Table 2.16** and **Fig 2.21** show the distribution ratios for Am(III) and Eu(III) (D_{Am} and D_{Eu}) and the separation factors for Am(III) over Eu(III) ($SF_{Am/Eu}$) as a function of nitric acid concentration (0.001-2 M). At low HNO_3 concentration (0.001 M) the ligand extracted both Am(III) and Eu(III) with a low separation factor of $SF_{Am/Eu} \approx 1.9$. Increasing the HNO_3 concentration to 0.1 M caused a significant drop for both D_{Am} and D_{Eu} to < 1, and the extraction of Eu(III) was diminished almost completely to $D_{Eu} \sim 0.017$. Upon further increase in nitric acid concentration to 0.5 M, the D_{Am} values increased slightly; whereas the D_{Eu} values decreased. A similar $SF_{Am/Eu}$ value was observed at 1 M HNO_3 due to both D_{Am} and D_{Eu} values increasing, but now the americium was being extracted back into the organic phase again as $D_{Am} > 1$.

Table 2.16 – Extraction of Am(III) from Eu(III) by (dppz)-BTPhen ligand (**135**) as a function of nitric acid concentration.

[HNO_3]	D_{Am}	D_{Eu}	$SF_{Am/Eu}$
0.001	16.4 ± 1.4	8.5 ± 0.4	1.9 ± 0.2
0.1	0.58 ± 0.02	0.017 ± 0.002	34 ± 4.0
0.5	0.77 ± 0.03	0.007 ± 0.002	110 ± 39
1	2.04 ± 0.07	0.018 ± 0.002	113 ± 14
2	9.40 ± 0.60	0.042 ± 0.003	225 ± 22

At 2 M HNO_3, the extraction of Am(III) increased to $D_{Am} \sim 9.4 \pm 0.6$ whilst D_{Eu} remained < 0.05 giving a separation factor of $SF_{Am/Eu} \approx 225$. The trend of increasing separation factor with increasing nitric acid concentration can be seen in **Fig 2.21**. There are similarities with the results obtained for this new (dppz)-ligand (**135**) compared to the extraction results previously reported for $CyMe_4$-BTBP (**46**) and $CyMe_4$-BTPhen (**54**), where increasing the HNO_3 concentration caused an increase in the separation factor. For example, comparing BTPhen (**54**) to (**135**), higher $SF_{Am/Eu}$ values were obtained across some of the HNO_3 concentrations examined for (**135**). For instance, the extraction of Am(III) and Eu(III) by 5 mM of $CyMe_4$-BTPhen (**54**) at 1 M HNO_3 reported a separation factor $SF_{Am/Eu} \approx 44$, almost three times lower than that of (dppz)-ligand (**135**).[74]

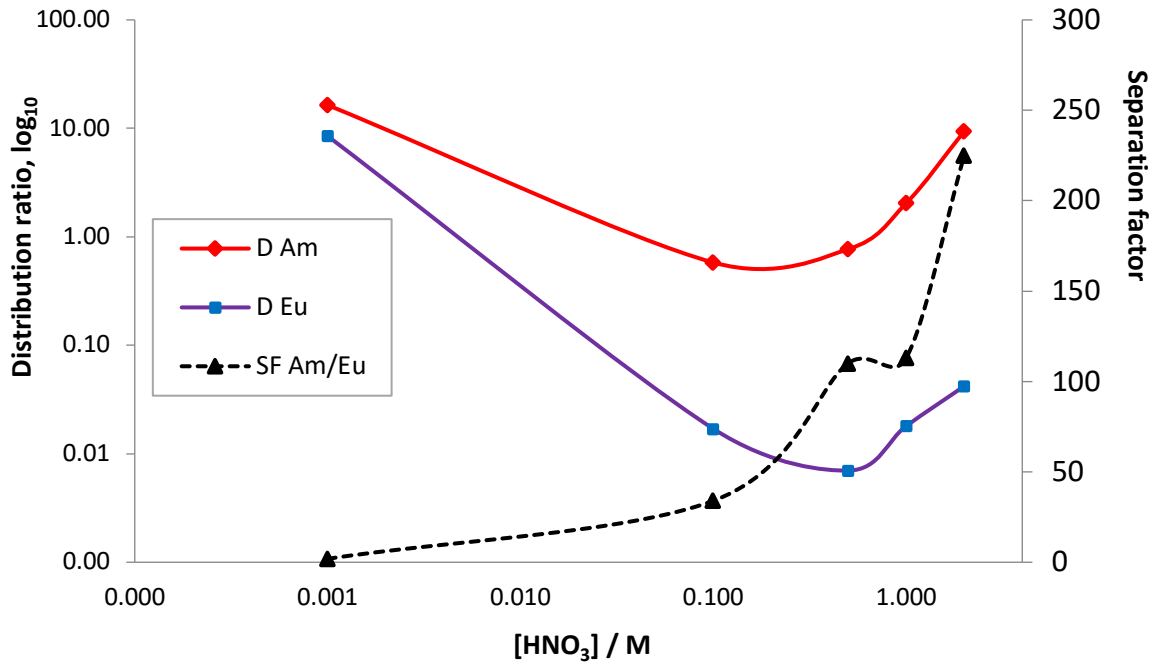

Figure 2.21 – Extraction of Am(III) from Eu(III) by (dppz)-BTPhen (**135**) as a function of nitric acid concentration.

The extraction of Am(III) from Eu(III) as a function of increasing perchloric acid concentration (0.001 – 2 M) was also investigated and is shown below in **Table 2.17** and **Fig 2.22**. The change of acidic medium from nitric acid to perchloric acid was once again carried out to investigate the role of any coordinating nitrate ions in the extraction process. At low $HClO_4$ concentration (0.001 M), the ligand extracted both Am(III) and Eu(III) in almost a 4:1 ratio ($SF_{Am/Eu} \approx 3.8$). Increasing the $HClO_4$ concentration to both 0.1 and 0.5 M, afforded increases in D_{Am} values to ~ 40 and ~ 53 respectively. However, the values of D_{Eu} decreased to ~ 1.15 and ~ 0.4 respectively giving good separation factors of $SF_{Am/Eu} \approx 35$ and 119. Similar extraction results were obtained at 1 M $HClO_4$, but at 2 M, the extraction of Am(III) was D_{Am} ~ 139 and values for D_{Eu} remained < 1 giving a separation factor of $SF_{Am/Eu} \approx 167$.

Table 2.17 – Extraction of Am(III) from Eu(III) by (dppz)-BTPhen (**135**) as a function of perchloric acid concentration.

$[HClO_4]$	D_{Am}	D_{Eu}	$SF_{Am/Eu}$
0.001	23.82 ± 2.1	6.29 ± 0.29	3.8 ± 0.4
0.1	40.19 ± 6.2	1.15 ± 0.03	35 ± 6
0.5	53.36 ± 11.3	0.41 ± 0.01	119 ± 27
1	61.68 ± 15.3	0.56 ± 0.02	111 ± 28
2	138.53 ± 59.5	0.83 ± 0.03	167 ± 72

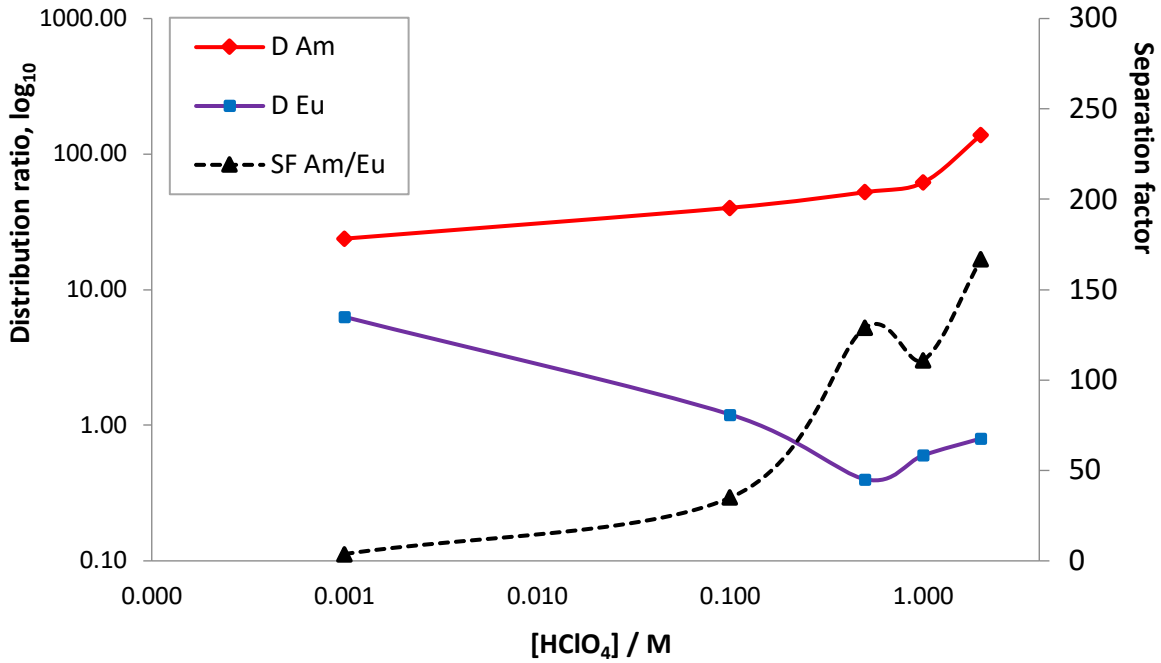

Figure 2.22 – Extraction of Am(III) from Eu(III) by (dppz)-BTPhen (**135**) as a function of perchloric acid concentration.

Since these solvent extraction experiments were carried out on free (dppz)-BTPhen ligand (**135**), where the ligand was not constrained to the surface of any solid support, the extraction occurring at the organic:aqueous interface may ultimately involve forming 1:2 complexes of metal:ligand and hence could explain the observation of no real difference in extraction results on changing from nitric to perchloric acid compared to the reduced efficiency of extraction when using related ligands bound to MNPs or SiO_2 gels in perchloric acid.

Chapter 3 – Conclusions and Future Work

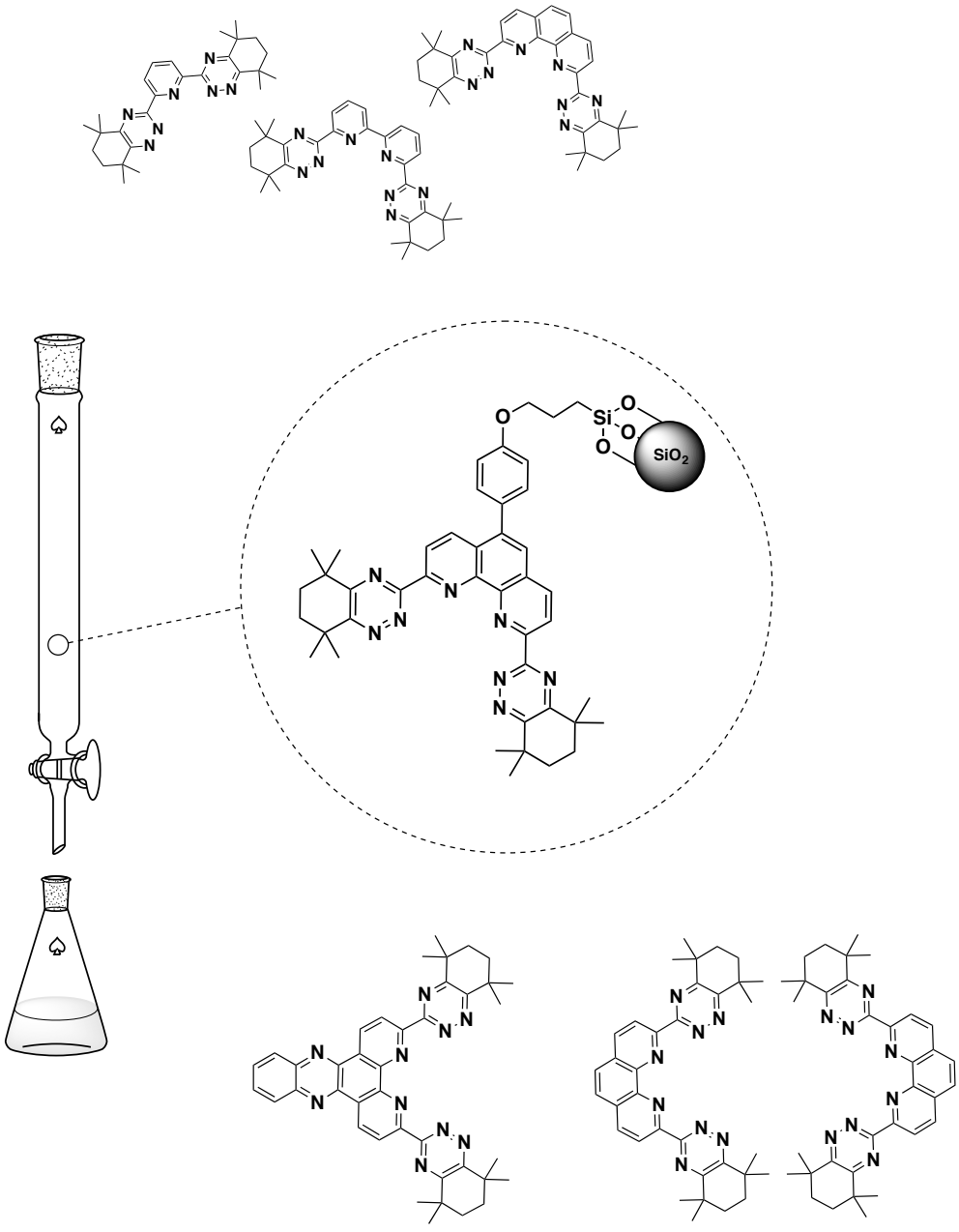

3.1 – Conclusions

The opening chapter of this thesis outlines a review into the development of ligands which can afford the separation of trivalent minor actinides from trivalent lanthanides under harsh process conditions of high HNO_3 concentration (~ 4 M). The use of both hydrophobic and hydrophilic extracting agents are discussed and recent advances in the immobilization of *N*-donor ligands onto the surface of solid materials, notably, magnetic nanoparticles is covered.

Following the synthesis and comparison of $CyMe_4$-BTPhen functionalized ZrO_2-coated MNPs (**86**) with our previously investigated model using SiO_2-coated MNPs (**85**), it was concluded using FT-IR and elemental analysis that the surface of the zirconia coated nanoparticles was less functionalized with the $CyMe_4$-BTPhen ligand. As a result, the ZrO_2-MNPs (**86**) co-extracted both Am(III) and Eu(III) from solutions up to 4 M HNO_3, with low selectivity ($SF_{Am/Eu} \approx 1.8$ at 4 M) compared to that of previously reported for SiO_2-coated MNPs (**85**) ($SF_{Am/Eu} > 1300$).[106] With residual OH groups present on the surface of the MNPs and subsequent protonation during the acidic media of the extraction studies, much lower *D* and SF values were obtained during the separation of Am(III) from Eu(III). This could be due to repulsion of the metals from the charged surface of the MNPs. Since both ZrO_2- and SiO_2- can effectively coat the MNPs to provide chemical resistance to the harsh conditions, it was concluded that SiO_2 coatings would be preferred in future investigation due to its apparent higher ligand loading.

Developments in the synthesis of BTPhen ligands using selenium free synthetic protocols proceeded by benzylic functionalization with NCS to afford *bis*-(trichloromethyl) units which could be readily converted to *bis*-carboxylic acid and *bis*-methyl-ester compounds. Using this improved synthetic route, tetra-(4-hydroxyphenyl)-BTPhen (**105**) was investigated for its extraction of Am(III) from Eu(III) as a ligands itself, covalently bound to silica-coated MNPs (**110**) and incorporated onto the surface of macroscopic silica gel (**112**). MNPs (**110**) exhibited good selectivity for Am(III) over Eu(III) at low nitric acid concentration and indicated that the extraction process is highly dependent on the [HNO_3] concentration.

BTPhen functionalized SiO_2 gel (**112**) also revealed efficient extraction of Am(III) from Eu(III) at low nitric acid concentration, but also repeated the trend of increasing separation factor ($SF_{Am/Eu}$) as the nitric acid concentration increased up to 4 M, as previously reported in the remarkable extraction properties of $CyMe_4$-functionlized SiO_2-coated MNPs (**85**).

Applying the selenium free synthetic protocol to functionalized phenanthroline units was also carried out, where the synthesis of Br-$CyMe_4$-BTPhen (**83**) occurred in more efficient overall yield. After some extensive optimization studies, Suzuki coupling with 4-hydroxyphenyl boronic acid in order to provide an anchor onto solid supports enabled the immobilization of $CyMe_4$-BTPhen onto chloro functionalized silica gel. Our previous solid-based model of SiO_2-MNPs (**85**) was hypothesized that the ligands were forming 1:1 complexes when extracting the metals Am(III) and Eu(III) due to the shortness of the linking chain between the ligand and the solid support. In order to probe the effect of anions surrounding these proposed 1:1 complexes for charge neutrality and whether they play an important role in the separation of Am(III) from Eu(III), the extraction experiments of $CyMe_4$-BTPhen functionalized SiO_2 gel (**118**) were conducted in both nitric and perchloric acid, where the latter contains no coordinating counter-ions. Interestingly, at 4 M HNO_3 acid, the system selectively extracted Am(III) from Eu(III) with a separation of $SF_{Am/Eu} \approx 154$, whilst the same system in 4 M perchloric acid afforded $SF_{Am/Eu} \approx 1$. This strongly indicates that the extraction process is highly dependent on the concentration of HNO_3 and thus the coordination of three bidenate nitrate ions in the 1:1 ligand complex for charge neutrality.

Following the development of solid based extractants using SiO_2 gels, a BTBP analogue (**120**) was synthesized and efficiently immobilized onto amino-functionalized SiO_2 gel. Even though the extraction of Am(III) from Eu(III) by this BTBP system proved inefficient, the use of a column technique revealed very efficient uptake (> 80 %) of certain problematic corrosion and fission products present in nuclear waste streams. As a proof of concept, this simple laboratory solid-based column technique could ultimately provide a route to pre-concentrate the stream to contain only minor actinides and lanthanides before the extremely challenging selective extraction of actinides is conducted.

Since repeating the Suzuki coupling of bromine-bearing phenanthrolines proved challenging at times, synthetic approaches to nitro-phenanthrolines were investigated. Using a mixture of fuming sulfuric and concentrated nitric acids generated the desired 5-nitro-1,10-phenanthroline unit (**123**) in reasonable yield and these harsh acidic conditions also led to the isolation of 5,6-dioxo-phenanthroline dicarboxylic acid (**126**). Applying the improved synthetic route towards the preparation of BTPhens failed to generate the target 5-nitro-1,10-phenanthroline-2,9-dicarbonitrile (**131**), where isolation of the *bis*-amide unit (**130**) proved problematic and alternative procedures were applied.

Isolation of (**126**) enabled us to explore the addition of aromatic functionality to the phenanthroline system by condensation with *ortho*-phenylenediamine. After employing two one-pot reactions, a novel (dppz)-*bis*-aminohydrazide scaffold (**134**) was isolated and subsequently condensed with $CyMe_4$-diketone (**32**) to furnish (dppz)-BTPhen ligand (**135**). The ligand revealed preferential extraction of Am(III) over Eu(III) in both HNO_3 and $HClO_4$ media where separation factors of $SF_{Am/Eu} \approx 225$ and ≈ 167 respectively were attained. Since these extraction investigations were carried out on free ligand, where it was not constrained to the surface of a solid support, the extracted complex may be forming 1:2 metal:ligand complexes and thus explaining the minor effect upon changing acid media on these extraction results.

3.2 – Future Work

The use of ligands immobilized onto magnetic particles for use in the nuclear industry is subject to further, more detailed examination. The simplistic ease of magnetic separation needs to be thoroughly investigated within the steel containers and pipework used in the nuclear industry. The use of solid based extractants rather than solvent-solvent extraction may ultimately reduce the amount of used solvent waste to be incinerated, however the current use of ion-exchange resins in the nuclear industry requires substantial treatment prior to their disposal.

Functionalizing silica gels with BTBP/BTPhen ligands led to some interesting and promising results with regard to the extraction and separation of Am(III) from Eu(III), but also the

recovery of some problematic fission and corrosion products present in post-PUREX streams. Currently the preferred option for the treatment of high-level radioactive waste in the UK is vitrification within a borosilicate matrix and long-term storage (1000s of years) of the glass waste in a GDF. Systems based on silica are advantageous in this respect as it may be possible to directly convert these silica containing materials into borosilicate-based waste ready for storage.[137]

Further investigations using these functionalised silica systems would involve performing the extraction and recovery of fission/corrosion products from 4 M HNO_3 streams, akin to the conditions of the PUREX stream. The results presented here were conducted using 2 % HNO_3, which is ≈ 0.3 M (pH = 0.5). More promising results have been reported by using hydrophilic masking agents which retain the fission products in the aqueous phase enabling extraction of minor actinides Am(III) and Cm(III).[138]

The absorption of Am(III) by BTPhen-functionalized SiO_2 gel (**112**) during the extraction experiments was efficient (high D_{wAm} values) across all HNO_3 concentrations studied, even at 4 M, and so further studies are required in order to investigate the eventual stripping of the metal from the solid sorbent. When using SiO_2 gel as the sorbent, it may become important to have efficient removal of all fission/corrosion products from the acidic streams prior to passing through a column of SiO_2 gel as it is reported to be known for absorption of numerous fission products, in particular zirconium, which may complicate the vitrification process and storage.[139]

Repeated cycle tests would also need to be carried out as no one-stage solid extraction set up would result in complete removal of all Am(III) from the aqueous solution; therefore small amounts of radiotoxic long-lived isotopes of Am(III) will contaminate the aqueous waste, probably leading to larger volumes of secondary waste. As discussed in Chapter 1, a multistage counter-current solvent-solvent extraction by $CyMe_4$-BTBP (**46**) revealed a > 99.99 % recovery of Am(III) and Cm(III); the relatively large volume of secondary organic 'CHON' waste produced in this process can, however, be completely incinerated.

The extraction investigations of $CyMe_4$-BTPhen functionalized SiO_2-gel (**118**) would require further studies in order to confirm the nature of the complex formed during the extraction. Though this may prove difficult when the extraction experiments are performed using radiotracer isotopes, but lanthanide X-ray crystal structures of 1:1 complexes forming on the surface of the silica gel would be conclusive. *In situ*- analytical techniques using FT-IR and Raman may also support the formation of the complex with three bidentate nitrate ions.

It may also be important to consider the differing acid strengths of the two acids examined in this thesis for any further extraction testing. Nitric and perchloric acid differ by almost 9 orders of magnitude on acid scale, and it may be due to differing protonation rates of the ligand in the acid media used that effects the extraction, and not the increasing concentration of nitrate ions. Further studies would also employ the use of other acids, for example HI, which has a similar acid strength to $HClO_4$, but I^- is more suited to coordination to metal ions compared to ClO_4^-.

Other solid support options may also be explored with regards to immobilization of BTBP/BTPhen related ligands. Recently, Suzuki coupling with 4-vinylphenyl boronic acid onto bromine bearing BTPhen ligands produced a ligand bearing a vinyl group which can be polymerized with, for example, styrene to produce a hydrophobic polymer loaded with an actinide selective ligand. The use of this material in the nuclear industry would require thorough investigation, from ligand loading to resistance to the harsh 4 M HNO_3 conditions.

Chapter 4 – Experimental

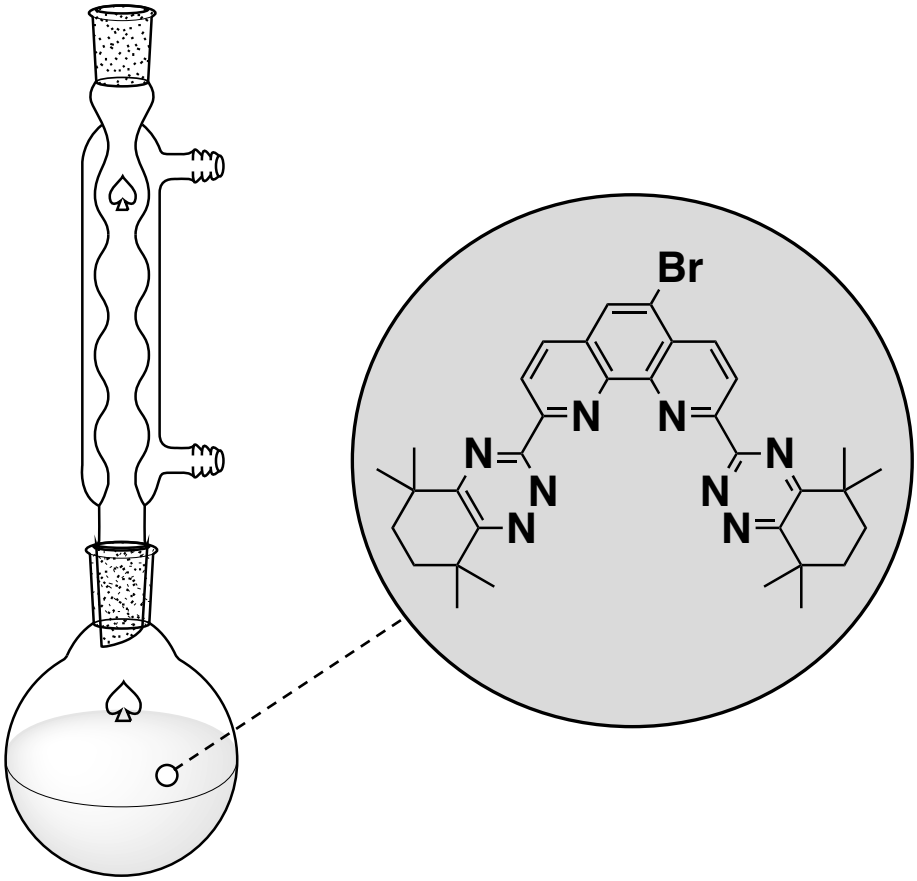

4.1 – General Procedures:

All reagents were either supplied by Acros, Aldrich, Fisher or Fluorochem chemical suppliers, and were used as supplied unless otherwise stated.

NMR spectra were recorded using either a Bruker AMX400 or an Avance DFX400 instrument. Deuterated chloroform ($CDCl_3$), deuterated DMSO (dimethyl sulfoxide-d_6) and deuterium oxide (D_2O) were used as solvents. Chemical shifts (δ) are reported in parts per million (ppm) with the abbreviations s, d, t, q, quin, sext, dd, and br denoting singlet, doublet, triplet, quartet, quintet, sextet, double doublet and broad resonances respectively. Coupling constants (*J*) are quoted in Hertz (Hz).

IR spectra were recorded on a Perkin Elmer RX1 FT-IR (ATR) instrument with peak intensities indicated by the abbreviations: w, weak; m, medium; s, strong; br, broad.

All melting points were determined on a Stuart SMP10 melting point apparatus and are uncorrected.

Mass spectra were recorded under conditions of electrospray ionisation (ESI) on a Thermo Scientific LTQ-Orbitrap XL with an Thermo Scientific Accela HPLC. Elemental analyses presented in this thesis were carried out by Medac Ltd., Chertsey Road, Chobham, Surrey, UK.

4.2 – Synthesis of Ligands:

*4.2.1 – Synthesis of 5-bromo-2,9-dimethyl-1,10-phenanthroline (**78**):*[96]

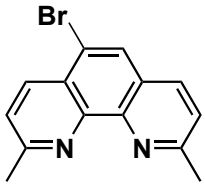

(78)

2,9-Dimethyl-1,10-phenanthroline (**50**) (15.0 g, 72.8 mmol) was dissolved in fuming sulfuric acid (75 mL, 20 % SO_3) and bromine (2.25 mL, 43.6 mmol, 0.6 eq) was added slowly and the mixture was heated at 170 °C for 18 h. The flask was allowed to cool to room temperature, the solution was quenched with water (250 mL, CARE!) with external cooling and then the mixture was neutralized with 30 % NaOH solution to pH 6-7. The resulting mixture was extracted with chloroform (3 x 200 mL) and the combined organic extracts were dried over $MgSO_4$. The extracts were filtered, the solvent removed *in vacuo* and the remaining solid was triturated with Et_2O (100 mL) and dried in a vacuum oven (60 °C) to afford the title compound (**78**) as a pale yellow solid (14.1 g, 80 %) m.p. 175-178 °C. Lit. 174-176 °C.[96] FT-IR (ATR) ν_{max} / cm^{-1} 3385w, 3048w, 2916w, 2163w, 1603m, 1589m, 1546w, 1491w, 1435w, 1400w, 546m, 545m.

δ_H (400 MHz, $CDCl_3$) 8.55 (d, *J* = 8.2 Hz, 1H, Ar*H*), 8.06 (d, *J* = 8.2 Hz, 1H, Ar*H*), 8.04 (s, 1H, Ar*H*), 7.60 (d, *J* = 8.2 Hz, 1H, Ar*H*), 7.51 (d, *J* = 8.2 Hz, 1H, Ar*H*), 2.98 (s, 3H, CH_3), 2.95 (s, 3H, CH_3); δ_C (101 MHz, $CDCl_3$) 159.6, 158.9, 145.2, 144.2, 136.2, 135.2, 128.7, 126.8, 126.5, 124.9, 124.3, 118.5, 25.0 (*C*H_3), 24.7 (*C*H_3); (FTMS + p ESI) cald. $C_{14}H_{12}N_2Br$ $[M+H]^+$: 287.0106; observed 287.0140; $C_{14}H_{12}N_2{}^{81}Br$ $[M+H]^+$: 289.0085; observed 289.0101;

*4.2.2 – Synthesis of 5-bromo-1,10-phenanthroline-2,9-dicarbaldehyde (**87**):*[106]

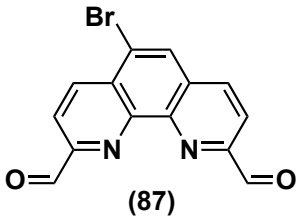

(87)

Selenium dioxide (11.54 g, 104 mmol, 2.1 eq) was dissolved in 1,4-dioxane (150 mL) and water (12 mL) and the mixture heated to reflux. To this, a solution of 5-bromo-2,9-dimethyl-1,10-phenanthroline (**78**) (14.06 g, 49.5 mmol) in 1,4-dioxane (150 mL) was added dropwise over 30 minutes and then the solution was heated to reflux for 3 h. While still hot, the mixture was filtered to remove precipitated selenium metal and then the filtrate was left to cool to room temperature. The filtrate was concentrated *in vacuo* and the residual solid was triturated with Et_2O (100 mL). The insoluble product was filtered and washed with Et_2O (50 mL) and allowed to dry in a vacuum oven (60 ^oC) to afford the title compound (**87**) as a brown solid (12.43 g, 82 %) m.p. 207-210 ^oC. Lit. 206-208 ^oC.[106] FT-IR (ATR) ν_{max} / cm^{-1} 3068w, 2856w, 2191w, 1973w, 1697s (C=O), 1598w, 1548w, 1351w, 1237w.

δ_H (400 MHz, DMSO) 10.32 (s, 1H, C*H*O), 10.22 (s, 1H, C*H*O), 8.90 (d, *J* = 8.5 Hz, 1H, Ar*H*), 8.75 (s, 1H, Ar*H*), 8.70 (d, *J* = 8.3, 1H, Ar*H*), 8.40 (d, *J* = 8.5 Hz, 1H, Ar*H*), 8.30 (d, *J* = 8.3 Hz, 1H, Ar*H*); δ_C (101 MHz, DMSO) 193.7 (*C*HO),193.1 (*C*HO), 152.4, 145.5, 144.5, 138.1 137.7, 134.5, 132.3, 131.7, 129.9, 122.4, 121.1, 120.7; (FTMS + p ESI) cald. $C_{14}H_8N_2O_2Br$ $[M+H]^+$: 314.9763; observed 314.9964; $C_{14}H_8N_2O_2{}^{81}Br$ $[M+H]^+$: 316.9743; observed 316.9733;

*4.2.3 – Synthesis of 5-bromo-1,10-phenanthroline-2,9-dicarbonitrile (**88**):*[106]

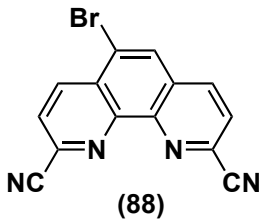

(88)

To a suspension of 5-bromo-1,10-phenanthroline-2,9-dicarbaldehyde (**87**) (12.34 g, 39.6 mmol) in MeCN (350 mL) were added hydroxylamine hydrochloride (6.05 g, 87 mmol, 2.2 eq) and triethylamine (36.6 mL, 261 mmol, 6.6 eq). The mixture was heated to reflux for 4 h and then, after cooling the mixture to room temperature, *p*-toluenesulfonyl chloride (24.9 g, 130.5 mmol, 3.3 eq) and DBU (17.7 mL, 118.7 mmol, 3 eq) were added and the mixture was heated under reflux for 18 h. While still hot the mixture was filtered and the residual solid was washed with hot MeCN (25 mL). The filtrate was concentrated *in vacuo* to afford a brown semi-solid that was triturated with MeOH (100 mL) and then filtered and washed with MeOH (100 mL), followed by Et_2O (100 mL) to afford the title compound (**88**) as a brown solid (4.59 g, 42 %) m.p. 151-154 ^oC. Lit. 152-154 ^oC.[106] FT-IR (ATR) ν_{max} / cm^{-1} 3082w, 2984w, 2238w (C≡N), 1616w, 1497w, 1366w.

δ_H (400 MHz, DMSO) 8.81 (d, *J* = 8.4 Hz, 1H, Ar*H*), 8.71 (d, *J* = 8.4 Hz, 1H, Ar*H*), 8.68 (s, 1H, Ar*H*), 8.48 (d, *J* = 8.4 Hz, 1H, Ar*H*), 8.38 (d, *J* = 8.4 Hz, 1H, Ar*H*); δ_C (101 MHz, DMSO) 145.5, 144.9, 142.9, 137.8, 133.4, 133.1, 132.3, 130.4, 129.1, 126.8, 122.3, 117.4 (*C*N),117.0 (*C*N); (FTMS + p ESI) cald. $C_{14}H_5N_4Br$ $[M+H]^+$: 308.9770; observed 308.9764; $C_{14}H_5N_4{}^{81}Br$ $[M+H]^+$: 310.9750; observed 310.9751

*4.2.4 – Synthesis of 5-bromo-1,10-phenanthroline-2,9-bis-aminohydrazide (**89**):*[106]

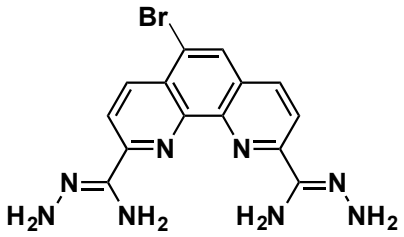

(89)

To a suspension of 5-bromo-1,10-phenanthroline-2,9-dicarbonitrile (**88**) (4.59 g, 15.0 mmol) in EtOH (150 mL) was added hydrazine hydrate (100 mL, 64 %) and the mixture was stirred at room temperature for 6 d. The mixture was then concentrated *in vacuo* to give a brown semi-solid that was triturated with MeOH (100 mL) and Et_2O (100 mL). The solid residue was filtered off, washed with Et_2O (50 mL) and dried in a vacuum oven (60 ^oC) to afford the title compound (**89**) as a brown solid (3.55 g, 65 %) m.p. > 300 ^oC. Lit. > 300^oC.[106] FT-IR (ATR) ν_{max} / cm^{-1} 3450w (NH), 3339br (NH), 3188w (NH), 2922w, 2853w, 1634w, 1601w, 1581m, 1544w, 1490w, 1448w, 1403w.

δ_H (400 MHz, DMSO) 8.54 (d, *J* = 8.8 Hz, 1H, Ar*H*), 8.42 (m, 2H, Ar*H*), 8.37 (d, *J* = 8.6, 1H, Ar*H*), 8.31 (d, *J* = 8.6 Hz, 1H, Ar*H*), 6.14 (br s, 4H, NH_2), 5.76 (s, 4H, NH_2); δ_C (101 MHz, DMSO) 151.9, 151.7, 144.2, 143.1, 143.0, 142.7, 135.3, 135.1, 129.2, 128.4, 126.7, 120.1, 119.7, 119.1; (FTMS + p ESI) cald. $C_{14}H_{13}N_8Br$ $[M+H]^+$: 379.0519; observed: 373.0524; $C_{14}H_{13}N_8{}^{81}Br$ $[M+H]^+$: 375.0499; observed 375.0503;

*4.2.5 – Synthesis of diethyl-2,2,5,5-tetramethylhexanedioate (**34**):*[77,114]

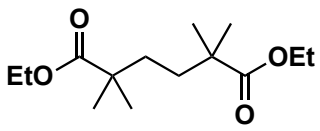

(34)

Anhydrous diethyl ether (500 mL) was placed under nitrogen, di*iso*propylamine (41.0 mL, 288 mmol, 1.1 eq) was added via syringe through a septum and the solution was cooled to –20 °C by means of a dry ice-acetone bath. *n*-Butyllithium (182.0 mL, 1.6 M in hexane, 261 mmol, 1 eq) was added dropwise via syringe and the solution was maintained at –20 °C for 1 h. Ethyl isobutyrate (35.0 mL, 261 mmol, 1 eq) was slowly added dropwise over 30 min and the solution was then allowed to warm to room temperature before stirring for an additional 1 h. Ethylene di(*p*-toluenesulfonate) (50.0 g, 135 mmol, 0.5 eq) was added in small additions and the mixture was heated under reflux for 18 h. The flask was allowed to cool to room temperature and the residual insoluble solid was filtered off and washed with ether (2 x 50 mL) and DCM (2 x 100 mL). The combined filtrates were washed with sat. aq. ammonium chloride (200 mL) and the aqueous layer was extracted with ether (100 mL). The combined organic extracts were washed with water (150 mL), dried over $MgSO_4$, filtered and concentrated *in vacuo* to afford the crude product as a yellow oil (24.1 g). The crude product was purified by vacuum distillation using a 10 inch Vigreux column to afford the title compound (**34**) as a colourless oil (19.6 g, 62 %) b.p = 72-76 °C at 0.1 mm Hg; FT-IR (ATR) ν_{max} / cm^{-1} 2963w, 2939w, 2879w, 1717s (C=O), 1678m.

δ_H (400 MHz, $CDCl_3$) 4.10 (q, *J* = 7.1 Hz, 4H), 1.45 (s, 4H), 1.26 (t, *J* = 7.1 Hz, 6H), 1.15 (s, 12H); δ_C (101 MHz, $CDCl_3$) 177.6 (C=O), 60.2, 41.8, 35.5, 25.0, 14.2;(FTMS + pESI) cald $C_{14}H_{26}O_4$ $[M+Na]^+$: 281.1723; observed: 281.1722;

*4.2.6 – Synthesis of 1,2-bis(trimethylsilyloxy)-3,3,6,6-tetramethylcyclohex-1-ene (**35**):*[77,114]

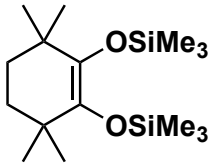

(35)

Sodium metal (8.69 g, 378 mmol, 5 eq) was added to dry toluene (300 mL) and the mixture was heated to reflux until the sodium melted. Diethyl-2,2,5,5-tetramethylhexanedioate (**34**) (19.4 g, 75.6 mmol) was added, followed by chlorotrimethylsilane (47.5 mL, 378.1 mmol, 5 eq) and the mixture was heated under reflux for 18 h. The mixture was then left to cool to room temperature and was filtered under nitrogen through a Schlenk tube. The solid residue was washed sequentially with toluene (100 mL) and THF (50 mL) and the filtrate was concentrated *in vacuo* to afford a pale yellow liquid (11.70 g). The crude product was purified by vacuum distillation to afford the title compound (**35**) as a colourless liquid (8.07 g, 35 %), b.p. 68-72 ^{o}C at 0.1 mm Hg. The excess sodium metal from the reaction was quenched carefully with *i*Pr-OH (100 mL); FT-IR (ATR) ν_{max} / cm^{-1} 2962w, 2933w, 2875w, 2255w, 1656m, 1462m, 1377w.

δ_H (400 MHz, $CDCl_3$) 1.25 (s, 4H, C*H*$_2$), 0.83 (s, 12H, C*H*$_3$), 0.00 (s, 18H, Si(C*H*$_3$)$_3$); δ_C (101 MHz, $CDCl_3$) 137.3, 34.4, 34.1, 26.0, 0.00; (FTMS + pESI) cald $C_{16}H_{34}O_2Si_2$ [M+Na]$^+$: 337.1990; observed: 337.1994;

*4.2.7 – Synthesis of 3,3,6,6-tetramethylcyclohexane-1,2-dione (**32**):*[77,114]

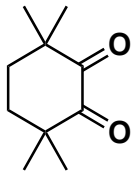

(32)

1,2-Bis(trimethylsilyloxy)-3,3,6,6-tetramethylcyclohex-1-ene (**35**) (8.07 g, 25.66 mmol) was dissolved in DCM (200 mL) and bromine (1.50 mL, 28.23 mmol, 1.1 eq) was added dropwise over 5 minutes and the solution was stirred at room temperature for 2 h. The solution was then diluted with DCM (100 mL), washed with water (50 mL) and sat. aq. sodium thiosulfate (100 mL), dried over $MgSO_4$, filtered and concentrated *in vacuo* to afford the title compound (**32**) as a pale yellow solid (4.30 g, 99 %) m. p. 113-115 ^oC; FT-IR (ATR) ν_{max} / cm^{-1} 2971w, 2937w, 2879w, 2255w, 1707s (C=O), 1460w, 1383w;

δ_H (400 MHz, $CDCl_3$) 1.81 (s, 4H, C*H*$_2$), 1.09 (s, 12H, C*H*$_3$); δ_C (101 MHz, $CDCl_3$) 207.3 (C=O), 48.6, 34.6, 22.9; (FTMS + pESI) cald $C_{10}H_{16}O_2Na$ $[M+Na]^+$: 191.1043; observed: 191.1044;

*4.2.8 – Synthesis of 5-bromo-2,9-bis(5,5,8,8-tetramethyl-5,6,7,8-tetrahydro-1,2,4-benzotriazin-3-yl)-1,10-phenanthroline (**83**):*[106]

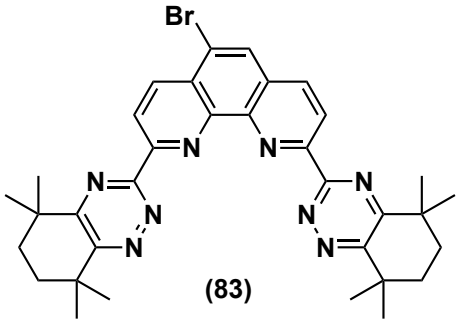

(83)

To a suspension of 5-bromo-1,10-phenanthroline-2,9-bis-aminohydrazide (**89**) (1.0 g, 2.70 mmol) in 1,4-dioxane (150 mL) were added 3,3,6,6-tetramethylcyclohexane-1,2-dione (**32**) (1.01 g, 5.94 mmol, 2.2 eq) and triethylamine (4 mL) and the suspension was heated under reflux for 3 d. The solution was allowed to cool to room temperature, filtered and washed with DCM (50 mL). The filtrate was concentrated *in vacuo* and triturated with ether (50 mL). The solution was allowed to cool in the freezer for 30 mins and then filtered to afford the title compound (**83**) as a yellow solid. The process of triturating with ether and cooling in the freezer was repeated further to increase the yield of product (0.36 g, 21 %) m.p. 197-200°C. Lit. 198-200 °C.[106] FT-IR (ATR) ν_{max} / cm^{-1} 3531br, 3486br, 2959w, 2927w, 2865w, 1644w, 1609m, 1510m, 1475w.

δ_H (400 MHz, $CDCl_3$) 8.95 (d, *J* = 8.6 Hz, 1H, Ar*H*), 8.89 (d, *J* = 8.6 Hz, 1H, Ar*H*), 8.87 (d, *J* = 6.4 Hz, 1H, Ar*H*), 8.39 (d, *J* = 8.4 Hz, 1H, Ar*H*), 8.29 (s, 1H, Ar*H*), 1.91 (s, 8H, CH_2), 1.56 (s, 12H, CH_3), 1.54 (s, 12H, CH_3); δ_C (101 MHz, $CDCl_3$) 165.1, 165.0, 163.4, 163.3, 161.3, 161.1, 154.7, 154.4, 146.9, 146.0, 137.3, 136.3, 130.6, 129.8, 128.9, 124.1, 124.0, 122.0, 37.5, 36.7, 33.8, 33.6, 29.8, 29.3; (FTMS + pESI) cald $C_{34}H_{38}N_8Br$ $[M+H]^+$: 637.2397; observed: 637.2392; $C_{34}H_{38}N_8{}^{81}Br$ $[M+H]^+$: 639.2377; observed: 639.2371;

*4.2.9 – Synthesis of 5-bromo-2,9-bis(5,6-dimethyl-1,2,4-triazin-3-yl)-1,10-phenanthroline (**116**):*[121]

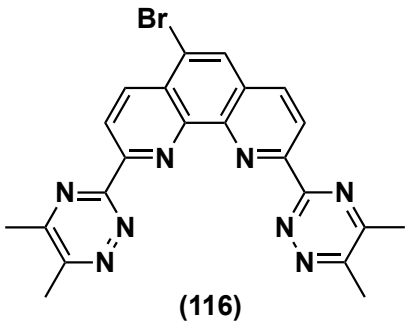

(116)

To a suspension of 5-bromo-1,10-phenanthroline-2,9-bis-aminohydrazide (**89**) (0.50 g, 1.71 mmol) in 1,4-dioxane (100 mL) were added 2,3-butandione (0.31 mL, 3.59 mmol, 2.1 eq) and triethylamine (10 mL). The mixture was heated under reflux for 3 d, then allowed to cool to room temperature. The filtrate was evaporated and the residual solid was triturated with ether (50 mL) and allowed to dry in air to afford the title compound (**116**) as a pale brown solid (0.48 g, 71 %) m.p. 218-221 °C. Lit. 216-218 °C.[121] FT-IR (ATR) ν_{max} / cm^{-1} 3516w, 3407w, 3174w, 2985w, 1626m, 1528w.

δ_H (400 MHz, DMSO) 8.91 (d, *J* = 8.4 Hz, 1H, Ar*H*), 8.87 (d, *J* = 8.4 Hz, 1H, Ar*H*), 8.81 (d, *J* = 8.4 Hz, 1H, Ar*H*), 8.75 (d, *J* = 8.4 Hz, 1H, Ar*H*), 8.71 (s, 1H, Ar*H*), 2.76 (s, 6H, CH_3), 2.71 (s, 6H, CH_3); δ_C (101 MHz, DMSO) 161.1, 160.8, 160.1, 160.0, 157.7, 157.6, 153.6, 153.5, 146.1, 145.1, 137.1, 136.8, 131.1, 129.6, 128.1, 123.8, 123.5, 120.9, 21.7 (*C*H_3), 19.3 (*C*H_3); (FTMS + pESI) cald $C_{22}H_{18}N_8Br$ $[M+H]^+$: 473.0832; observed: 473.0831; $C_{22}H_{18}N_8{}^{81}Br$ $[M+H]^+$: 475.0812; observed: 475.0801;

*4.2.10 – Synthesis of 4-(2,9-bis(5,5,8,8-tetramethyl-5,6,7,8-tetrahydrobenzo-1,2,4-triazin-3-yl)-1,10-phenanthrolin-5-yl)phenol (**84**):*[106]

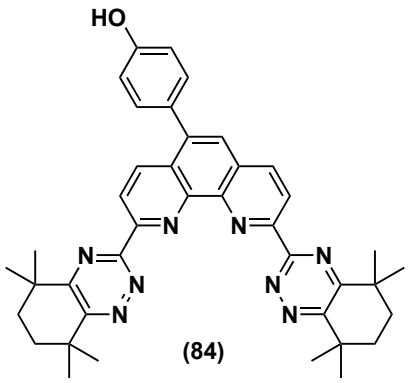

(84)

A suspension of 5-bromo-2,9-bis(5,5,8,8-tetramethyl-5,6,7,8-tetrahydro-1,2,4-benzotriazin-3-yl)-1,10-phenanthroline (**83**) (0.50 g, 0.78 mmol), tetrakis(triphenylphosphine)palladium(0) (0.03 g, 0.03 mmol, 0.03 eq), 4-hydroxyphenylboronic acid (0.13 g, 0.87 mmol, 1.1 eq) and potassium carbonate (0.13 g, 0.94 mmol, 1.2 eq) in degassed EtOH (75 mL) was heated to reflux for 18 h under nitrogen. The solution was allowed to cool to room temperature, filtered and the solid reside washed with EtOH (25 mL). The filtrate was concentrated *in vacuo* and the remaining residue was dissolved in DCM (100 mL) and washed with brine (100 mL). The aqueous layer was extracted with DCM (2 x 50 mL), the combined organic extracts dried over magnesium sulfate, filtered and concentrated *in vacuo*. The solid was triturated with ether (100 mL), filtered and washed with ether (100 mL) to afford the title compound (**84**) as a yellow solid (0.31 g, 59 %). m.p. 250-252 ^{o}C. Lit. 251-253 ^{o}C.[106] FT-IR (ATR) ν_{max} / cm^{-1} 3399br, 2962br, 2931w, 2865w, 1611w, 1587m, 1514w, 1471w, 1456m, 1389w, 1365w, 1344w, 1274w.

δ_H (400 MHz, $CDCl_3$) 8.88 (d, *J* = 8.4 Hz, 1H, Ar*H*), 8.77 (d, *J* = 8.4 Hz, 1H, Ar*H*), 8.42 (d, *J* = 8.4 Hz, 1H, Ar*H*), 8.34 (d, *J* = 8.3 Hz, 1H, Ar*H*), 7.70 (s, 1H, Ar*H*), 6.81 (d, *J* = 7.9 Hz, 2H, Ar*H*), 6.59 (d, *J* = 8.2 Hz, 2H, Ar*H*), 1.92 (s, 8H, CH_2), 1.61 (s, 12H, CH_3), 1.57 (s, 12H, CH_3); δ_C (101 MHz, $CDCl_3$) 165.3, 165.2, 163.6, 163.5, 161.3, 161.0, 157.7, 153.3, 153.2, 146.5, 145.3, 140.2, 137.3, 136.3, 130.1, 129.5, 129.4, 128.2, 127.1, 123.7, 122.9, 115.6, 37.6, 36.7, 33.8, 29.9, 29.3; (FTMS + pESI) cald $C_{40}H_{43}N_8O$ $[M+H]^+$: 651.3554; observed: 651.3553;

*4.2.11 – Synthesis of 4-(2,9-dimethyl-1,10-phenanthrolin-5-yl)phenol (**117**):*[105,115]

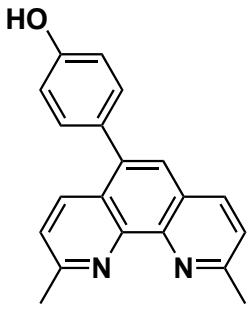

(117)

A suspension of 5-bromo-2,9-dimethyl-1,10-phenanthroline (**78**) (0.50 g, 1.74 mmol), tetrakis(triphenylphosphine)palladium(0) (0.06 g, 0.05 mmol, 0.03 eq), 4-hydroxyphenylboronic acid (0.27 g, 1.92 mmol, 1.1 eq) and potassium carbonate (0.29 g, 2.09 mmol, 1.2 eq) in degassed EtOH (80 mL) was heated to reflux for 18 h under nitrogen. The solution was then cooled to room temperature, filtered and the solid residue washed with EtOH (25 mL). The filtrate was evaporated and the solid was triturated with ether (25 mL). The insoluble solid was filtered and washed with ether (25 mL) and chloroform (25 mL) and allowed to dry in a vacuum oven (60 ^{o}C) to afford the title compound (**117**) as a pale yellow solid (0.51 g, 98 %) m.p. > 300 ^{o}C. Lit. > 300 ^{o}C.[115] FT-IR (ATR) ν_{max} / cm^{-1} 3214br (OH), 1608m, 1591w, 1490w, 1373w, 1277w.

δ_H (400 MHz, DMSO) 8.37 (d, *J* = 8.5 Hz, 1H, Ar*H*), 8.29 (d, *J* = 8.2 Hz, 1H, Ar*H*), 7.65 (s, 1H, Ar*H*), 7.56 (dd, *J* = 8.4 Hz, 2.6 Hz, 2H, Ar*H*), 7.11 (d, *J* = 8.4 Hz, 2H, Ar*H*), 6.57 (d, *J* = 8.3 Hz, 2H, Ar*H*), 2.77 (s, 6H, C*H*$_3$); δ_C (101 MHz, DMSO) 162.7, 157.6, 157.5, 145.1, 143.4, 138.0, 136.1, 134.6, 131.6, 130.7, 126.3, 125.8, 124.9, 124.4, 123.4, 122.3, 116.7, 25.0 (C*H*$_3$), 24.8 (C*H*$_3$); (FTMS + pESI) cald $C_{20}H_{17}N_2O$ $[M+H]^+$: 301.1335; observed: 301.1337

*4.2.12 – Synthesis of 5-bromo-2,9-bis(trichloromethyl)-1,10-phenanthroline (**113**):*

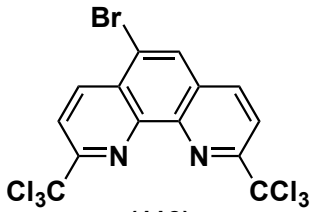

(113)

5-Bromo-2,9,dimethyl-1,10-phenanthroline (**78**) (15.0 g, 52.2 mmol), *N*-chlorosuccinimide (48.90 g, 365.7 mmol, 7 eq) and *m*-CPBA (450 mg, 2.61 mmol, 0.05 eq) were dissolved in $CHCl_3$ (120 mL) and heated to reflux for 3 d. The solution was allowed to cool to room temperature and the precipitated succinimide was filtered off and washed with $CHCl_3$ (50 mL). The filtrate was washed with 2M NaOH solution and extracted with $CHCl_3$ (4 x 100 mL). The combined organic extracts were dried over $MgSO_4$, filtered and concentrated *in vacuo*. The yellow semi-solid was then triturated with MeOH:petrol ether (40-60 ^oC), 50:50 (100 mL) and the solid was collected by filtration and dried in a vacuum oven (40 ^oC) to afford the title compound (**113**) as a yellow solid (24.47 g, 96 %) m.p. 72-75 ^oC; FT-IR (ATR) ν_{max} / cm^{-1} 2928w, 1600w, 1586w, 1551w.

δ_H (400 MHz, $CDCl_3$) 8.86 (d, *J* = 8.8 Hz, 1H, Ar*H*), 8.41 (d, *J* = 8.8 Hz, 1H, Ar*H*), 8.38 (d, *J* = 8.6 Hz, 1H, Ar*H*), 8.34 (d, *J* = 8.6 Hz, 1H, Ar*H*), 8.30 (s, 1H, Ar*H*); δ_C (101 MHz, $CDCl_3$) 157.3, 157.0, 143.3, 142.1, 138.9, 138.8, 131.4, 129.7, 128.3, 121.3, 121.0, 120.7, 97.9 (*C*Cl_3), 97.4 (*C*Cl_3); (FTMS + pESI) cald $C_{14}H_6N_2BrCl_6$ $[M+H]^+$: 490.7840; observed: 490.7840; $C_{14}H_6N_2BrCl_5{}^{37}Cl$ $[M+H]^+$: 492.7811; observed: 492.7812; $C_{14}H_6N_2BrCl_4{}^{37}Cl_2$ $[M+H]^+$: 494.7781; observed: 494.7784; $C_{14}H_6N_2BrCl_3{}^{37}Cl_3$ $[M+H]^+$: 496.7752; observed: 496.7755; $C_{14}H_6N_2BrCl_2{}^{37}Cl_4$ $[M+H]^+$: 498.7722; observed: 498.7725;

*4.2.13 – Synthesis of dimethyl-5-bromo-1,10-phenanthroline-2,9-dicarboxylate (**114**):*

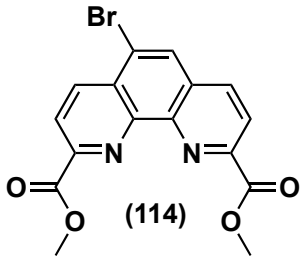

(**114**)

5-Bromo-2,9-bis(trichloromethyl)-1,10-phenanthroline (**113**) (4.48 g, 9.15 mmol) was dissolved in conc. H_2SO_4 (20 mL) and heated to reflux for 6 h. The solution was allowed to cool to room temperature and MeOH (15 mL) was slowly added and then the mixture was heated to reflux for 18 h. The solution was allowed to cool and the excess MeOH was removed *in vacuo*. The acidic residue was poured into ice-water (200 mL) and the precipitated solid was filtered, washed with water (2 x 100 mL) and Et_2O (2 x 100 mL) and dried in a vacuum oven (60 ^oC) to afford the title compound (**114**) as a pale grey solid (2.41 g, 70 %) m.p. 195-198 ^{o} C; FT-IR (ATR) ν_{max} / cm^{-1} 3061w, 2957w, 1716s (C=O), 1598m, 1552w.

δ_H (400 MHz, DMSO) 8.85 (d, *J* = 8.6 Hz, 1H, Ar*H*), 8.71 – 8.69 (m, 2H, Ar*H*), 8.51 (d, *J* = 8.6 Hz, 1H, Ar*H*), 8.42 (d, *J* = 8.6 Hz, 1H, Ar*H*), 4.05 (s, 3H, CH_3), 4.03 (s, 3H, CH_3); δ_C (101 MHz, DMSO) 165.2 (*C*=O), 165.0 (*C*=O), 148.2, 148.0, 145.5, 144.4, 137.4, 137.4, 131.9, 130.6, 129.3, 124.6, 124.3, 121.8, 52.9 (*C*H_3), 52.8 (*C*H_3); (FTMS + pESI) cald $C_{16}H_{11}O_4N_2BrNa$ $[M+Na]^+$: 396.9794, observed: 396.9794; $C_{16}H_{11}O_4N_2{}^{81}BrNa$ $[M+Na]^+$: 398.9774; observed: 398.9772;

*4.2.14 – Synthesis of 5-bromo-1,10-phenanthroline-2,9-dicarboxamide (**115**):*

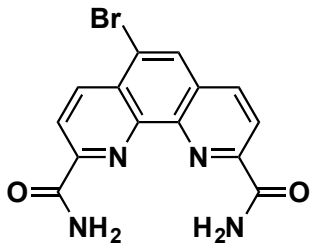

(115)

Dimethyl-5-bromo-1,10-phenanthroline-dicarboxylate (**114**) (4.50 g, 11.99 mmol) was suspended in a solution of ammonium chloride (2.56 g, 47.86 mmol, 4 eq) in aqueous ammonium hydroxide (100 mL, 35 %) and the mixture stirred at room temperature for 3 d. The mixture was poured into water (200 mL) and the precipitated solid was filtered off, washed with water (3 x 100 mL), Et_2O (2 x 100 mL) and dried in a vacuum oven (60 ^oC) to afford the title compound (**115**) as a grey solid (3.71 g, 89 %) m.p. > 300 ^{o} C; FT-IR (ATR) ν_{max} / cm^{-1} 3051w, 2955w, 1714s (C=O), 1597w, 1551w.

δ_H (400 MHz, DMSO) 8.98 (s, 1H, NH_2), 8.97 (s, 1H, NH_2), 8.83 (d, *J* = 8.6 Hz, 1H, Ar*H*), 8.67 (d, *J* = 8.3 Hz, 1H, Ar*H*), 8.65 (s, 1H, Ar*H*), 8.57 (d, *J* = 8.6 Hz, 1H, Ar*H*), 8.47 (d, *J* = 8.3 Hz, 1H, Ar*H*), 7.97 (s, 1H, NH_2), 7.91 (s, 1H, NH_2); δ_C (101 MHz, DMSO) 165.9 (*C*=O), 165.6 (*C*=O), 150.6, 150.5, 144.5, 143.4, 137.4, 131.3, 130.3, 129.1, 128.9, 122.2, 121.8, 121.2; (FTMS + pESI) cald $C_{14}H_9O_2N_4BrNa$ $[M+Na]^+$: 366.9801, observed: 366.9802; $C_{14}H_9O_2N_4{}^{81}BrNa$ $[M+Na]^+$: 368.9781; observed: 368.9781;

*4.2.15 – Synthesis of 5-bromo-1,10-phenanthroline-2,9-dicarbonitrile (**88**):*

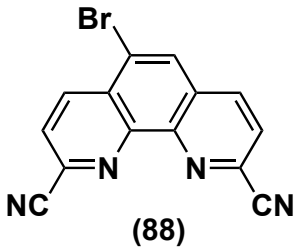

(88)

5-Bromo-1,10-phenanthroline-2,9-dicarboxamide (**115**) (3.70 g, 10.7 mmol) was suspended in phosphorous oxychloride (15 mL, 160 mmol, 15 eq) and the mixture heated to reflux for 18 h. The solution was allowed to cool to room temperature and then slowly poured into ice-water (100 mL) with external cooling. The slurry was diluted with water (100 mL) and the precipitated solid was filtered off and washed with water (2 x 100 mL), Et_2O (2 x 100 mL) and dried in a vacuum oven (60 ^oC) to afford the title compound (**88**) as a brown solid (3.07 g, 97 %) m.p. 152-154 ^oC. Lit. 151-153 ^oC.[106] FT-IR (ATR) ν_{max} / cm^{-1} = 3082w, 2984w, 2238w (CN), 1616m, 1497w, 1366w.

δ_H (400 MHz, DMSO) 8.92 (d, *J* = 8.5 Hz, 1H, Ar*H*), 8.81 – 8.79 (m, 2H, Ar*H*), 8.53 (d, *J* = 8.5 Hz, 1H, Ar*H*), 8.45 (d, *J* = 8.3 Hz, 1H, Ar*H*); δ_C (101 MHz, DMSO) 151.9, 151.7, 144.2, 143.1, 143.0, 142.7, 135.3, 135.0, 129.2, 128.4, 126.7, 120.1, 119.7 (*C*N), 119.0 (*C*N); (FTMS + pESI) cald $C_{14}H_6N_4Br$ $[M+H]^+$: 308.9770; observed: 308.9773; $C_{14}H_6N_4{}^{81}Br$ $[M+H]^+$: 310.9750; observed: 310.9751;

*4.2.16 – Synthesis of 5-bromo-1,10-phenanthroline-2,9-bis(carbohydrazonamide) (**89**):*

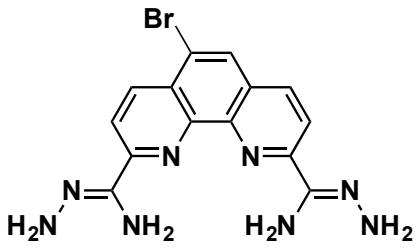

(89)

5-Bromo-1,10-phenanthroline-2,9-dicarbonitrile (**88**) (1.07 g, 3.46 mmol) was dissolved in DMSO (10 mL), hydrazine hydrate (10 mL, 50-60 %) was added slowly over 5 minutes and then the mixture was stirred at room temperature for 18 h. The solution was then poured into water (200 mL) and the resulting precipitate was filtered off, washed with water (2 x 100 mL) and Et_2O (2 x 100 mL), then dried in a vacuum oven (60 ^oC) to afford the title compound (**89**) as a brown solid (0.78 g, 60 %) m.p. > 300 ^oC. Lit. > 300 ^oC.[106] FT-IR (ATR) ν_{max} / cm^{-1} 3450br (NH), 3339br (NH), 3188w, 2922w, 2853w, 1634w, 1601m, 1581w, 1544w.

δ_H (400 MHz, DMSO) 8.54 (d, *J* = 8.8 Hz, 1H, Ar*H*), 8.43 (s, 1H, Ar*H*), 8.41 (d, *J* = 8.8 Hz, 1H, Ar*H*), 8.37 (d, *J* = 8.6 Hz, 1H, Ar*H*), 8.30 (d, *J* = 8.6 Hz, 1H, Ar*H*), 6.13 (br s, 4H, NH_2), 5.82 (s, 4H, NH_2); δ_C (101 MHz, DMSO) 151.9, 151.8, 144.2, 143.2, 142.9, 142.8, 135.3, 135.0, 129.2, 128.4, 126.7, 120.0, 119.7, 119.1; (FTMS + pESI) cald $C_{14}H_{14}N_8Br$ $[M+H]^+$: 373.0519; observed: 373.0524; $C_{14}H_{14}N_8{}^{81}Br$ $[M+H]^+$: 375.0499; observed: 375.0503;

*4.2.17 – Synthesis of 5-bromo-1,10-phenanthroline-2,9-bis(carbohydrazonamide) (**89**):*

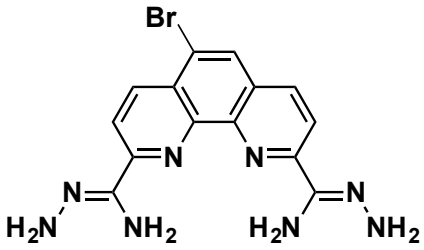

(89)

5-Bromo-1,10-phenanthroline-2,9-dicarboxamide (**115**) (0.25 g, 0.67 mmol) was suspended in DMF (8 mL) and pyridine (0.45 mL, 5.36 mmol, 8 eq) and then trifluoroacetic acid (0.40 mL, 2.68 mmol, 4 eq) was added. The mixture was stirred at room temperature for 5 h, hydrazine hydrate (3 mL, 64 %) was added slowly and the mixture was stirred for a further 18 h at room temperature. Water (100 mL) was added and the precipitated brown solid was filtered off, washed with water (50 mL), Et_2O (100 mL) and dried in a vacuum oven (60 ^oC) to afford the title compound (**89**) as a yellow solid (0.21 g, 82 %) m.p. > 300 ^oC. Lit. > 300 ^oC.[106] FT-IR (ATR) ν_{max} / cm^{-1} 3450br (NH), 3339br (NH), 3188w, 2922w, 2853w, 1634w, 1601m, 1581w, 1544w.

δ_H (400 MHz, DMSO) 8.54 (d, *J* = 8.8 Hz, 1H, Ar*H*), 8.43 (s, 1H, Ar*H*), 8.41 (d, *J* = 8.8 Hz, 1H, Ar*H*), 8.37 (d, *J* = 8.6 Hz, 1H, Ar*H*), 8.30 (d, *J* = 8.6 Hz, 1H, Ar*H*), 6.13 (br s, 4H, NH_2), 5.82 (s, 4H, NH_2); δ_C (101 MHz, DMSO) 151.9, 151.8, 144.2, 143.2, 142.9, 142.8, 135.3, 135.0, 129.2, 128.4, 126.7, 120.0, 119.7, 119.1; (FTMS + pESI) cald $C_{14}H_{14}N_8Br$ $[M+H]^+$: 373.0519; observed: 373.0524; $C_{14}H_{14}N_8{}^{81}Br$ $[M+H]^+$: 375.0499; observed: 375.0503;

*4.2.18 – Synthesis of 5-bromo-2,9-bis(5,5,8,8-tetramethyl-5,6,7,8-tetrahydro-1,2,4-benzotriazin-3-yl)-1,10-phenanthroline (**83**):*

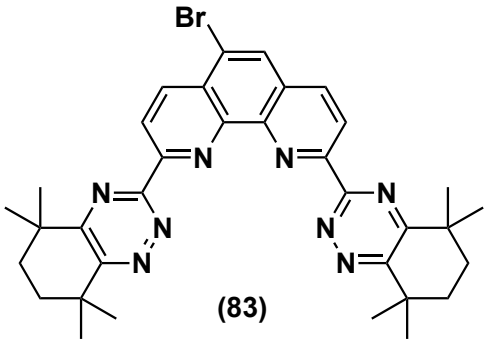

(83)

To a suspension of 5-bromo-1,10-phenanthroline-2,9-bis-aminohydrazide (**89**) (0.5 g, 1.35 mmol) in AcOH (50 mL) were added 3,3,6,6-tetramethylcyclohexane-1,2-dione (**32**) (0.51 g, 2.97 mmol, 2.2 eq). The solution was heated under reflux for 3 hrs and then allowed to cool to room temperature and poured into water (100 mL). The resulting precipitate was collected by filtration and the crude powder was triurated with Et_2O (100 mL) to afford the title compound (**83**) as a yellow solid (0.69 g, 80 %) m.p. 197-200°C; FT-IR (ATR) ν_{max} / cm^{-1} 3531br, 3486br, 2959w, 2927w, 2865w, 1644w, 1609m, 1510m, 1475w.

δ_H (400 MHz, $CDCl_3$) 8.95 (d, *J* = 8.6 Hz, 1H, Ar*H*), 8.89 (d, *J* = 8.6 Hz, 1H, Ar*H*), 8.87 (d, *J* = 6.4 Hz, 1H, Ar*H*), 8.39 (d, *J* = 8.4 Hz, 1H, Ar*H*), 8.29 (s, 1H, Ar*H*), 1.91 (s, 8H, CH_2), 1.56 (s, 12H, CH_3), 1.54 (s, 12H, CH_3); δ_C (101 MHz, $CDCl_3$) 165.1, 165.0, 163.4, 163.3, 161.3, 161.1, 154.7, 154.4, 146.9, 146.0, 137.3, 136.3, 130.6, 129.8, 128.9, 124.1, 124.0, 122.0, 37.5, 36.7, 33.8, 33.6, 29.8, 29.3; (FTMS + pESI) cald $C_{34}H_{38}N_8Br$ $[M+H]^+$: 637.2397; observed: 637.2392; $C_{34}H_{38}N_8{}^{81}Br$ $[M+H]^+$: 639.2377; observed: 639.2371;

*4.2.19 – Synthesis of 2,9-bis(trichloromethyl)-1,10-phenanthroline (**100**):*

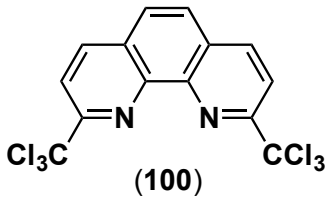

(**100**)

2,9-Dimethyl-1,10-phenanthroline (**50**) (5.0 g, 24.0 mmol), *N*-chlorosuccinimide (22.40 g, 168 mmol, 7 eq) and *m*-CPBA (0.207 g, 1.20 mmol, 0.05 eq) were dissolved in $CHCl_3$ (100 mL) and the mixture heated to reflux for 18 h. The solution was allowed to cool and the precipitated succinimide was filtered off and washed with $CHCl_3$ (50 mL). The filtrate was washed with 2M NaOH (3 x 100 mL) and extracted with $CHCl_3$ (2 x 100 mL). The organic extracts were collected and dried over $MgSO_4$, filtered and concentrated *in vacuo*. The residue was then triturated with MeOH:petrol ether (40-60 ^oC), 50:50 (100 mL) and the solid was collected by filtration to give the title compound (**100**) as a pale yellow solid (9.07 g, 90 %) m.p. 194-197 ^{o} C; FT-IR (ATR) ν_{max} / cm^{-1} 3008w, 1941w, 1810w, 1620w, 1580m, 1491m, 1363m.

δ_H (400 MHz, $CDCl_3$) 8.44 (d, *J* = 8.6 Hz, 2H, Ar*H*), 8.32 (d, *J* = 8.6 Hz, 2H, Ar*H*), 7.96 (s, 2H, Ar*H*); δ_C (101 MHz, $CDCl_3$) 158.0, 143.3, 138.2, 129.2, 127.6, 120.5, 98.21 (*C*-Cl_3); (FTMS + pESI) cald $C_{14}H_6N_2Cl_6$ $[M+Na]^+$: 434.8554; observed: 434.8553; $C_{14}H_6N_2Cl_5{}^{37}Cl$ $[M+Na]^+$: 436.8525; observed 436.8523; $C_{14}H_6N_2Cl_4{}^{37}Cl_2$ $[M+Na]^+$: 438.8495; observed 438.8492; $C_{14}H_6N_2Cl_3{}^{37}Cl_3$ $[M+Na]^+$: 440.8466; observed 440.8463; $C_{14}H_6N_2Cl_2{}^{37}Cl_4$ $[M+Na]^+$: 442.8436; observed 442.8433;

*4.2.20 – Synthesis of 1,10-phenanthroline-2,9-dicarboxylic acid (**102**):*

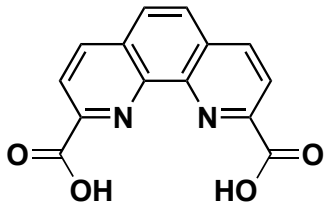

(**102**)

2,9-Bis(trichloromethyl)-1,10-phenanthroline (**100**) (4.25 g, 10.2 mmol) was dissolved in conc. H_2SO_4 (20 mL) and heated to 110 °C for 18 h. The solution was allowed to cool to room temperature and poured into ice-water (200 mL, CARE!). The precipitated solid was filtered and washed successively with water (2 x 100 mL) and Et_2O (2 x 100 mL) and then dried in a vacuum oven (60 °C) to afford the title compound (**102**) as a tan solid (2.27 g, 82 %) m.p. 234-236 °C; FT- IR (ATR) ν_{max} / cm^{-1} 3333br (OH), 3062br, 1701s, (C=O), 1621m, 1601w, 1555w, 1447w, 1369w.

δ_H (400 MHz, DMSO) 8.72 (d, *J* = 8.4 Hz, 2H, Ar*H*), 8.41 (d, *J* = 8.4 Hz, 2H, Ar*H*), 8.18 (s, 2H, Ar*H*); δ_C (101 MHz, DMSO) 166.2 (*C*=O), 148.2, 144.6, 138.1, 130.4, 128.3, 123.4; (FTMS + pESI) cald $C_{14}H_7N_2O_4$ $[M+H]^+$: 267.0411; observed: 267.0409;

*4.2.21 – Synthesis of dimethyl 1,10-phenanthroline-2,9-dicarboxylate (**101**):*

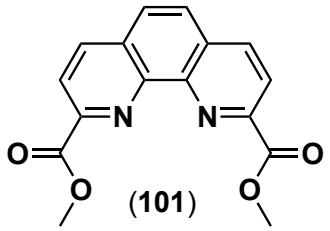

(**101**)

2,9-Bis(trichloromethyl)-1,10-phenanthroline (**100**) (1.2 g, 4.6 mmol) was dissolved in conc. H_2SO_4 (10 mL) and heated to 110 °C for 4 h. The solution was allowed to cool to room temperature and MeOH (25 mL) was added slowly and then the mixture heated to reflux for 18 h. The solution was allowed to cool and the excess MeOH was removed *in vacuo*. The acidic residue was poured onto ice-water (200 mL) and the precipitated solid was filtered off, washed with H_2O (2 x 100 mL), Et_2O (2 x 100 mL) and dried in a vacuum oven (60 °C) to afford the title compound (**101**) as a tan solid (1.32 g, 97 %) m.p. 195-198 °C; FT-IR (ATR) ν_{max} / cm^{-1} 3026w, 2954w, 1719s (C=O), 1638m, 1556w, 1439w.

δ_H (400 MHz, DMSO) 8.71 (d, *J* = 8.3 Hz, 2H, Ar*H*), 8.39 (d, *J* = 8.3 Hz, 2H, Ar*H*), 8.20 (s, 2H, Ar*H*), 4.03 (s, 6H, CH_3); δ_C (101 MHz, DMSO) 165.5 (*C*=O), 147.6, 145.0, 138.0, 130.5, 128.5, 123.6, 52.7 (*C*H_3); (FTMS + pESI) cald $C_{16}H_{13}O_4N_2$ $[M+H]^+$: 297.0870; observed: 297.0867; $C_{16}H_{12}O_4N_2$ $[M+Na]^+$: 319.0689; observed: 319.0683;

*4.2.22 – Synthesis of 1,10-phenanthroline-2,9-dicarboxamide (**103**):*

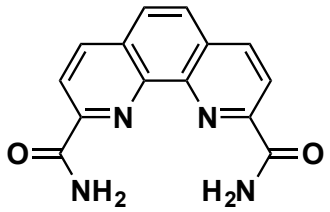

(103)

Dimethyl 1,10-phenanthroline-2,9-dicarboxylate (**101**) (5.01 g, 16.91 mmol) was suspended in a solution of ammonium chloride (2.0 g, 37.39 mmol, 2.2 eq) in aqueous ammonium hydroxide (100 mL, 35 %) and the mixture stirred at room temperature for 18 h. The mixture was diluted with H_2O (200 mL) and the precipitate was collected by filtration and washed with H_2O (2 x 100 mL), Et_2O (2 x 100 mL) and dried in a vacuum oven (60 ^oC) to afford the title compound (**103**) as a grey solid (3.55 g, 79 %) m.p. > 300 ^oC; FT-IR (ATR) ν_{max} / cm^{-1} 3023br (NH), 2952w (NH), 1720s (C=O), 1619m, 1556w.

δ_H (400 MHz, DMSO) 8.98 (s, 2H, N*H*$_2$), 8.70 (d, *J* = 8.3 Hz, 2H, Ar*H*), 8.46 (d, *J* = 8.3 Hz, 2H, Ar*H*), 8.15 (s, 2H, Ar*H*), 7.88 (s, 2H, N*H*$_2$); δ_C (101 MHz, DMSO) 166.1 (*C*=O), 150.0, 143.9, 138.0, 130.1, 127.9, 121.1; (FTMS + pESI) cald $C_{14}H_{10}O_2N_4Na$ $[M+Na]^+$: 289.0696; observed: 289.0694;

*4.2.23 – Synthesis of 1,10-phenanthroline-2,9-dicarboxamide (**103**):*

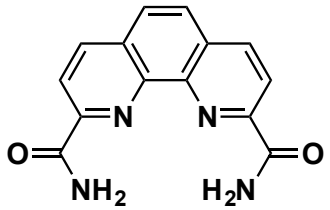

(103)

1,10-Phenanthroline-2,9-dicarboxylic acid (**102**) (0.90 g, 3.36 mmol), 1-hydroxybenzotriazole hydrate (0.91 g, 6.72 mmol, 2 eq), *N*-(3-Dimethylaminopropyl)-*N*'-ethylcarbodiimide hydrochloride (1.29 g, 6.72 mmol, 2 eq) and ammonium chloride (0.36 g, 6.72 mmol, 2 eq) were dissolved in DMF (10 mL). *N*,*N*-Di*iso*propylethylamine (1.2 mL, 6.72 mmol, 2 eq) was added and the mixture was stirred at room temperature for 18 h. The solution was diluted with H_2O (100 mL) and the precipitated solid was filtered, washed with H_2O (2 x 50 mL), Et_2O (2 x 50 mL) and dried in a vacuum oven to give the title compound (**103**) as a grey solid (0.49 g, 55 %) m.p. > 300 ^oC; FT-IR (ATR) ν_{max} / cm^{-1} 3023br (NH), 2952w (NH), 1720s (C=O), 1619m, 1556w.

δ_H (400 MHz, DMSO) 8.96 (s, 2H, N*H*$_2$), 8.71 (d, *J* = 8.3 Hz, 2H, Ar*H*), 8.46 (d, *J* = 8.3 Hz, 2H, Ar*H*), 8.17 (s, 2H, Ar*H*), 7.88 (s, 2H, N*H*$_2$); δ_C (101 MHz, DMSO) 166.1 (*C*=O), 150.0, 143.9, 138.0, 130.1, 127.9, 121.1; (FTMS + pESI) cald $C_{14}H_{10}O_2N_4Na$ $[M+Na]^+$: 289.0696; observed: 289.0694;

*4.2.24 – Synthesis of 1,10-phenanthroline-2,9-dicarbonitrile (**52**):*

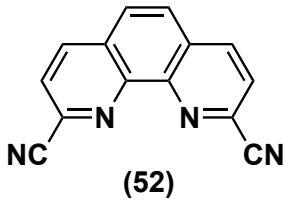

(52)

1,10-Phenanthroline-2,9-dicarboxamide (**103**) (2.00 g, 8.84 mmol) was dissolved in phosphorous oxychloride (10 mL, 106.96 mmol, 12 eq) and the mixture heated to reflux for 18 h. The solution was allowed to cool to room temperature and poured onto ice-water (100 mL) with external cooling. The slurry was diluted with water (100 mL) and the resultant precipitate was filtered off and washed with water (2 x 100 mL), Et_2O (2 x 100 mL) and dried in a vacuum oven (60 ^oC) to afford the title compound (**52**) as a brown solid (1.52 g, 75 %) m.p. 280-283 ^oC; FT-IR (ATR) ν_{max} / cm^{-1} 3086w, 3063w, 2238w (CN), 1621m, 1500w, 1368w.

δ_H (400 MHz, DMSO) 8.83 (d, *J* = 8.2 Hz, 2H, Ar*H*), 8.41 (d, *J* = 8.2 Hz, 2H, Ar*H*), 8.26 (s, 2H, Ar*H*); δ_C (101 MHz, DMSO) 144.8, 138.6, 132.9, 130.5, 129.2, 127.5, 117.6 (*C*N); (FTMS + pESI) cald $C_{14}H_6N_4Na$ $[M+Na]^+$: 253.0485; observed: 253.0483;

*4.2.25 – Synthesis of 1,10-Phenanthroline-2,9-bis(carbohydrazonamide) (**53**):*

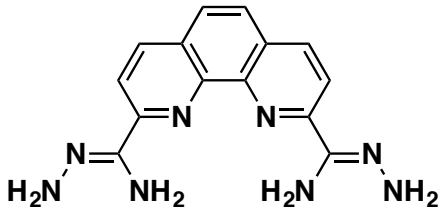

(53)

1,10-Phenanthroline-2,9-dicarbonitrile (**52**) (1.60 g, 6.95 mmol) was dissolved in DMSO (20 mL), and hydrazine hydrate (20 mL, 50-60 %) was added slowly over 5 minutes. The resulting mixture was stirred for 18 h at room temperature, then was poured into H_2O (250 mL) and the resulting precipitate was isolated by filtration, washed with H_2O (100 mL), Et_2O (2 x 100 mL) and dried in a vacuum oven (60 ^oC) to give the title compound (**53**) as a pale brown solid (1.98 g, 97 %) m. p > 300 ^oC; FT-IR (ATR) ν_{max} / cm^{-1} 3326w (NH), 3174br (NH), 3043w (NH), 1619m, 1497w, 1128w.

δ_H (400 MHz, DMSO) 8.39 (d, *J* = 8.6 Hz, 2H, Ar*H*), 8.29 (d, *J* = 8.6 Hz, 2H, Ar*H*), 7.95 (s, 2H, Ar*H*), 6.15 (s, 4H, NH_2), 5.62 (s, 4H, NH_2); δ_C (101 MHz, DMSO) 151.2, 143.6, 143.4, 136.1, 128.2, 126.1, 119.0; (FTMS + pESI) cald $C_{14}H_{14}N_8Na$ $[M+Na]^+$: 317.1234; observed: 317.1233;

*4.2.26 – Synthesis of 4,4'-dihydroxy benzil (**104**):*

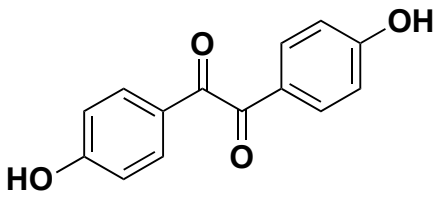

(104)

Method 1:[120]

To 4,4'-dimethoxybenzil (1.50 g, 5.55 mmol) were added aqueous HBr (15 mL, 48 %) and AcOH (20 mL) and the mixture was heated to reflux for 18 h. The solution was allowed to cool to room temperature and poured into water (200 mL). The precipitated solid was filtered and washed with water (100 mL) and dried in a vacuum oven (60 °C) to afford the title compound as a pale grey solid (0.69 g, 50 %) m.p. 239-242 °C.

Method 2:[119]

4,4'-Dimethoxybenzil (2.0 g, 7.40 mmol) and pyridinium hydrochloride (5.13 g, 44.40 mmol, 6 eq) were heated up to 200 °C until the solids melted. Heating was maintained for 2 h, then the solution was cooled to 80 °C and water (100 mL) was added. The precipitated solid was allowed to cool to room temperature, filtered off, washed with water (4 x 100 mL) and dried in a vacuum oven (60 °C) to afford the title compound as a pale tan solid (1.63 g, 91 %) m.p. 239-242 °C.

δ_H (400 MHz, DMSO) 10.84 (s, 2H, O*H*), 7.75 (d, *J* = 8.8 Hz, 4H, Ar*H*), 6.93 (d, *J* = 8.8 Hz, 4H, Ar*H*); δ_C (101 MHz, DMSO) 193.7 (*C*=O), 163.9, 132.2, 124.2, 116.1; (FTMS + pESI) cald $C_{14}H_{10}O_4Na$ [M+Na^+]: 265.0471; observed: 265.0476; FT-IR (ATR) ν_{max} / cm^{-1} 3393br, 1632m, 1590w, 1555m, 1510w, 1332w, 1290w, 1215w, 1165w;

*4.2.27 – Synthesis of 4,4',4'',4'''-((1,10-phenanthroline-2,9-diyl)bis(1,2,4-triazine-3,5,6-triyl))tetraphenol (**105**):*

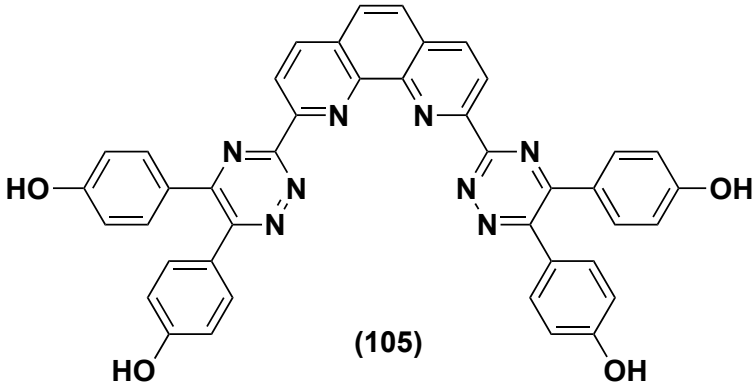

(105)

1,10-Phenanthroline-2,9-bis(carbohydrazonamide) (**53**) (0.60 g, 2.0 mmol) and 4,4'-dihydroxy benzil (**104**) (1.10 g, 4.6 mmol, 2.3 eq) were suspended in a mixture of THF (100 mL) and MeOH (100 mL). Triethylamine (50 mL, 356.2 mmol) was added and the mixture was heated to reflux for 3 d then allowed to cool to room temperature. The mixture was filtered and the solid residue was washed with DCM (25 mL). The filtrate was concentrated *in vacuo*, then triturated with MeOH (50 mL) and the solid was isolated by filtration, washed with MeOH (25 mL) and Et_2O (50 mL) and then dried in air to afford the title compound (**105**) as a yellow solid (0.99 g, 69 %) m.p. 280-282 ^oC; FT-IR (ATR) ν_{max} / cm^{-1} 3206br, 1608m, 1590w, 1483w, 1442w, 1377w, 1276w.

δ_H (400 MHz, DMSO) 8.61 (d, *J* = 8.0 Hz, 2H, Ar*H*), 8.58 (d, *J* = 8.0 Hz, 2H, Ar*H*), 8.11 (s, 2H, Ar*H*), 7.71 – 7.51 (m, 8H, Ar*H*), 6.93 – 6.78 (m, 8H, Ar*H*); δ_C (101 MHz, DMSO) 160.5, 159.6, 159.0, 155.3, 154.6, 152.6, 145.5, 137.7, 131.6, 130.7, 129.5, 127.7, 126.1, 125.5, 122.9, 115.4; (FTMS + pESI) cald $C_{42}H_{27}N_8O_4$ $[M+H]^+$: 707.2150; observed: 707.2153;

*4.2.28 – Synthesis of 2,2'-bipyridine-1,1'-dioxide (**39**):*[81,127]

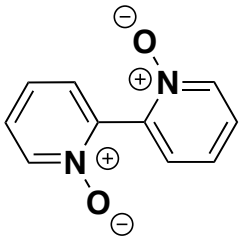

(**39**)

2,2'-Bipyridine (**12**) (24.00 g, 153.78 mmol) was dissolved in acetic acid (150 mL) and hydrogen peroxide (60 mL, 30 %, 767.42 mmol, 5 eq) was added dropwise. The solution was stirred at 75°C for 8 h, allowed to cool to room temperature and then stirred overnight. The mixture was diluted with acetone (500 mL) and then concentrated *in vacuo* to reduce the volume until precipitation occurred. The slurry was then cooled in a freezer for 30 minutes and then the precipitate was filtered and dried in air to afford the title compound (**39**) as a colourless solid (13.16 g, 46 %) m.p 268-270 °C (decomposed); FT-IR (ATR) ν_{max} / cm^{-1} 3037br, 1472w, 1425w, 1279w, 1251m, 1145w, 1117w, 1097w.

δ_H (400 MHz, D_2O) 8.41 – 8.43 (m, 2H, Ar*H*), 7.78 – 7.81 (m, 2H, Ar*H*), 7.69 – 7.23 (m, 4H, Ar*H*); δ_C (100 MHz, D_2O) 141.8, 139.6, 131.4, 128.8, 128.4; (FTMS + pESI) cald $C_{10}H_9O_2N_2$ $[M+H]^+$: 189.0654; observed 189.0659; $C_{10}H_8O_2N_2Na$ $[M+Na]^+$: 211.0473; observed: 211.0478;

*4.2.29 – Synthesis of 2,2'-bipyridine-6,6'-dicarbonitrile (**40**):*[81,127]

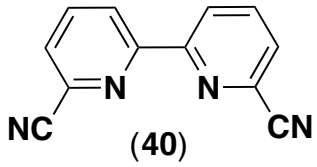

(**40**)

2,2'-Bipyridine-1,1'-dioxide (**39**) (5.15 g, 27.4 mmol) was dissolved in DCM (100 mL) and trimethylsilyl cyanide (10.5 mL, 83.61 mmol, 3.1 eq) was added. Benzoyl chloride (10 mL, 86.90 mmol, 3.2 eq) was added dropwise, the solution was stirred at room temperature for 3 d and then heated to reflux for 24 h. The solution was left to cool to room temperature and 10 % aq. potassium carbonate solution (100 mL) was added and the heterogeneous mixture stirred vigorously for 10 minutes. The insoluble solid was filtered off and washed with water (100 mL) and Et_2O (50 mL) to afford the title compound as a tan solid. The biphasic filtrate was separated and the aqueous phase was extracted with DCM (2 x 100 mL). The combined organic phases were dried over $MgSO_4$, filtered and concentrated *in vacuo*. The solid residue was triturated with MeOH (50 mL), filtered off and washed with Et_2O (100 mL) to afford additional product. The combined solids were allowed to dry to afford the title compound (**40**) as a tan solid (3.86 g, 68 %) m.p 248-251 ^oC; FT-IR (ATR) ν_{max} / cm^{-1} 3018br, 2236w (CN), 1784m, 1723m, 1575w, 1556w, 1433w, 1376w, 1218m.

δ_H 400 MHz, $CDCl_3$) 8.72 (dd, *J* = 8.0, *J*' = 1.3 Hz, 2H, Ar*H*), 8.02 (dd, *J* = 7.9, *J*' = 7.8 Hz, 2H, Ar*H*), 7.78 (dd, *J* = 7.6, *J*' = 0.4 Hz, 2H, Ar*H*); δ_C (100 MHz, $CDCl_3$) 155.5, 138.4, 133.4, 129.1, 124.7, 117.0; (FTMS + pESI) cald $C_{12}H_7N_4$ $[M+H]^+$: 207.0661; observed: 207.0655;

*4.2.30 – Synthesis of 2,2'-bipyridine-6,6'-bis(carbohydrazonamide) (**41**):*[81]

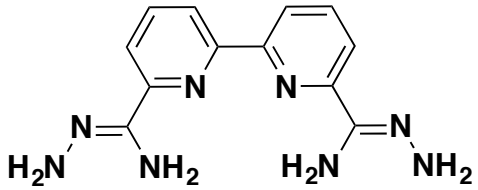

(**41**)

2,2'-Bipyridine-6,6'-dicarbonitrile (**40**) (3.85 g, 18.67 mmol) was suspended in EtOH (100 mL) and then hydrazine hydrate (60 mL, 64 %) was added. The reaction was left to stir for 3 d and then the insoluble solid was filtered off, washed with water (400 mL) and Et_2O (200 mL), then left to dry in air to afford the title compound (**41**) as a pale-yellow solid (4.20 g, 83 %) m.p > 300 °C. FT-IR (ATR) /cm^{-1} 3448br, 3304br, 3195br, 1660m, 1619w, 1576w, 1451m, 1389w, 1369w;

δ_H (400 MHz, DMSO) 8.61 (dd, *J* = 7.7, *J*' = 1.0 Hz, 2H, Ar*H*), 7.97 (dd, *J* = 7.7, *J*' = 1.0 Hz, 2H, Ar*H*), 7.89 (t, *J* = 7.7 Hz, 2H, Ar*H*), 5.95 (br s, 4H, NH_2), 5.42 (br s, 4H, NH_2); δ_C (100 MHz, DMSO) 153.2, 150.9, 114.0, 137.3, 120.2, 119.6; (FTMS + pESI) cald $C_{12}H_{15}N_8$ $[M+H]^+$: 271.1412; observed 271.1414; cald $C_{12}H_{14}N_8Na$ $[M+Na]^+$: 293.1230; observed: 293.1234;

*4.2.31 – Synthesis of 6,6'-bis(5,6-bis(bromomethyl)-1,2,4-triazin-3-yl)-2,2'-bipyridine (**120**):*

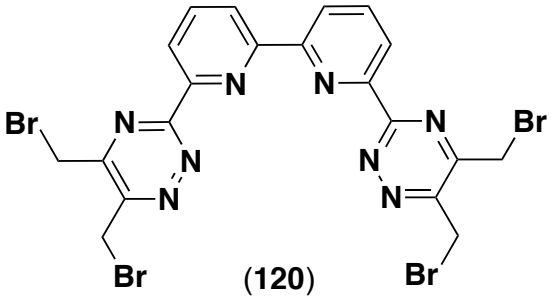

(**120**)

2,2'-Bipyridine-6,6'-dicarbohydrazonamide (**41**) (10.86 g, 40.20 mmol) was suspended in THF (500 mL) and 1,4-dibromobutane-2,3-dione (**119**) (22.01 g, 90.20 mmol, 2.2 eq) was added. The suspension was stirred at room temperature for 3 d. The insoluble solid was filtered off and washed successively with methanol (300 mL), acetone (300 mL) and diethyl ether (300 mL). The solid was allowed to dry in air to afford the title compound (**120**) as a yellow solid (22.59 g, 82 %) m.p. 202–204 °C (decomposed); FT-IR (ATR) ν_{max} / cm^{-1} 3087br, 3037br, 3014w, 1576m, 1557w, 1517w, 1442m, 1425w, 1406w.

δ_H (400 MHz, $CDCl_3$) 8.93 (d, *J* = 7.8 Hz, 2H, Ar*H*), 8.67 (d, *J* = 7.8 Hz, 2H, Ar*H*), 8.13 (t, *J* = 7.8, 2H, Ar*H*), 5.03 (s, 4H, CH_2), 4.82 (s, 4H, CH_2); δ_C (100 MHz, $CDCl_3$) 161.6, 156.1, 155.3, 154.7, 150.4, 137.3, 124.0, 123.0, 27.0 (*C*H_2), 25.7 (*C*H_2); (FTMS + pESI) cald $C_{20}H_{15}N_8Br_4$ $[M+H]^+$: 682.8148; observed: 682.8124; $C_{20}H_{15}N_8Br_2{}^{81}Br_2$ $[M+H]^+$: 686.8107; observed: 686.8080; $C_{20}H_{15}N_8{}^{81}Br_4$ $[M+H]^+$: 690.8066; observed: 690.8040;

*4.2.32 – Synthesis of 5-nitro-2,9-dimethyl-1,10-phenanthroline (**123**):*

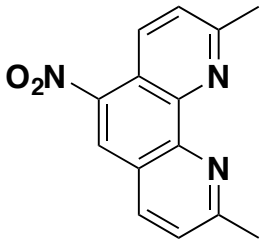

(123)

2,9-Dimethyl-1,10-phenanthroline (**50**) (2.50 g, 12.0 mmol) was dissolved in fuming H_2SO_4 (12 mL, 20 % SO_3) and HNO_3 (8 mL) was added slowly. The mixture was heated to 150 ^oC for 18 h, cooled to room temperature and then poured into ice-water (200 mL, CARE!) with external cooling. The precipitated solid was filtered off, washed with water (100 mL) and the pH of the filtrate was adjusted to 7 with 2 M NaOH. The filtrate was then extracted with $CHCl_3$ (4 x 100 mL) and the organic extracts were collected, dried over $MgSO_4$, filtered and concentrated *in vacuo* to afford the title compound (**123**) as a yellow solid (1.96 g, 64 %) m.p. 196-198 ^oC; FT-IR (ATR) ν_{max} / cm^{-1} 3464w, 1607w, 1514m, 1486m, 1341m, 1198w.

δ_H (400 MHz, $CDCl_3$) 8.93 (s, 1H, Ar*H*), 8.78 (d, *J* = 8.8 Hz, 1H, Ar*H*), 8.63 (d, *J* = 8.4 Hz, 1H, Ar*H*), 7.84 – 7.79 (m, 2H, Ar*H*), 2.86 (s, 3H, CH_3), 2.85 (s, 3H, CH_3); δ_C (101 MHz, $CDCl_3$) 162.3, 159.7, 146.0, 144.6, 142.9, 138.3, 131.8, 124.8, 124.6, 124.5, 123.5, 118.4, 25.3 (*C*H_3), 24.8 (*C*H_3); (FTMS + pESI) cald $C_{14}H_{12}O_2N_3$ $[M+H]^+$: 254.0924; observed: 254.0925;

*4.2.33 – Synthesis of 5-nitro-2,9-bis(trichloromethyl)-1,10-phenanthroline (**127**):*

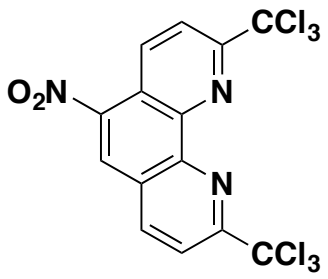

(127)

5-Nitro-2,9-dimethyl-1,10-phenanthroline (**123**) (2.75 g, 10.90 mmol), *N*-chlorosuccinimide (10.15 g, 76 mmol, 7 eq) and *m*-CPBA (177 mg, 0.54 mmol, 0.05 eq) were dissolved in $CHCl_3$ (80 mL) and heated to reflux for 18 h. The solution was allowed to cool to room temperature and the precipitated succinimide was filtered off and washed with $CHCl_3$ (50 mL). The filtrate was washed with 2M NaOH (2 x 100 mL) and extracted with $CHCl_3$ (2 x 100 mL). The combined organic extracts were dried over $MgSO_4$, filtered and concentrated *in vacuo*. The yellow semi-solid was then triturated with MeOH:petrol ether (40-60 ^oC), 50:50 (100 mL) and the residue was collected by filtration and dried in a vacuum oven (60 ^oC) to afford the title compound (**127**) as a yellow solid (3.60 g, 72%) m.p. 226-228 ^oC; FT-IR (ATR) ν_{max} / cm^{-1} 1510w, 1330w, 820m, 779w, 743m.

δ_H (400 MHz, $CDCl_3$) 9.24 (d, *J* = 9.2 Hz, 1H, Ar*H*), 8.85 (s, 1H, Ar*H*), 8.64 (d, *J* = 8.8 Hz, 1H, Ar*H*), 8.51 – 8.45 (m, 2H, Ar*H*); δ_C (101 MHz, $CDCl_3$) 160.9, 159.1, 145.1, 144.8, 143.8, 140.0, 135.2, 126.2, 126.1, 121.9, 121.8, 121.6, 97.5 (*C*-Cl_3), 97.4 (*C*-Cl_3); (FTMS + pESI) cald $C_{14}H_6O_2N_3Cl_6$ $[M+H]^+$: 457.8586; observed: 457.8585; $C_{14}H_6O_2N_3Cl_5{}^{37}Cl$ $[M+H]^+$: 459.8556; observed: 459.8555; $C_{14}H_6O_2N_3Cl_3{}^{37}Cl_3$ $[M+H]^+$: 463.8497; observed: 463.8495;

*4.2.34 – Synthesis of dimethyl 5-nitro-1,10-phenanthroline-2,9-dicarboxylate (**128**):*

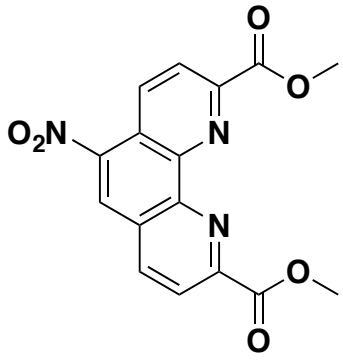

(128)

5-Nitro-2,9-bis(trichloromethyl)-1,10-phenanthroline (**127**) (3.2 g, 6.96 mmol) was dissolved in conc. H_2SO_4 (20 mL) and heated to reflux for 5 h. The solution was allowed to cool to room temperature, MeOH (40 mL) was added slowly and the mixture was heated to reflux for a further 18 h. After cooling the solution, the excess MeOH was removed *in vacuo* and the acidic residue was poured into water (200 mL). The resulting precipitated solid was filtered off, washed with water (2 x 100 mL), Et_2O (2 x 100 mL) and dried in a vacuum oven (60 °C) to afford the title compound (**128**) as a pale tan solid (1.54 g, 65 %) m.p. 259-261 °C; FT-IR (ATR) ν_{max} / cm^{-1} 2922w, 1701s, 1534w, 1443w, 1406w, 1240w, 1165w.

δ_H (400 MHz, DMSO) 9.22 (s, 1H, Ar*H*), 9.10 (d, *J* = 8.8 Hz, 1H, Ar*H*), 9.01 (d, *J* = 8.4 Hz, 1H, Ar*H*), 8.57 – 8.52 (m, 2H, Ar*H*), 4.06 (s, 6H, CH_3); δ_C (101 MHz, DMSO) 165.0 (*C*=O), 164.8 (*C*=O), 150.3, 148.3, 146.2, 145.1, 144.9, 140.7, 134.5, 127.8, 127.4, 124.6, 122.5, 53.1 (*C*H_3); (FTMS + p ESI) cald $C_{16}H_{12}N_3O_6$ [M+H^+]: 342.0721; observed: 342.0725; $C_{16}H_{11}N_3O_6Na$ [M+Na]$^+$: 364.0540; observed: 364.0542;

*4.2.35 – Synthesis of 5-nitro-1,10-phenanthroline-2,9-dicarboxylic acid (**129**):*

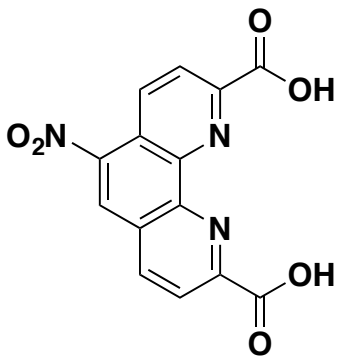

(129)

Dimethyl 5-nitro-1,10-phenanthroline-2,9-dicarboxylate (**128**) (0.5 g, 1.47 mmol) was dissolved in HCl (10 mL, 1 M) and the mixture heated to reflux for 18 h. The solution was allowed to cool to room temperature and diluted with water (100 mL). The precipitated solid was filtered and washed with water (50 mL) and Et_2O (25 mL) to afford the title compound (**129**) as a yellow solid (0.45 g, 97 %) m.p. 220-222 ^oC; FT-IR (ATR) ν_{max} / cm^{-1} 2925br, 1700s (C=O), 1545m, 1406w, 1236w, 1165w.

δ_H (400 MHz, DMSO) 9.22 (s, 1H, Ar*H*), 9.09 (d, *J* = 8.8 Hz, 1H, Ar*H*), 9.00 (d, *J* = 8.0 Hz, Ar*H*), 8.57 – 8.51 (m, 2H, Ar*H*); δ_C (101 MHz, DMSO) 165.9 (*C*=O), 165.7 (*C*=O), 151.2, 149.2, 146.1, 144.9, 144.8, 140.6, 134.4, 127.7, 127.2, 124.5, 122.4; (FTMS + p ESI) cald $C_{14}H_8N_3O_6$ $[M+H]^+$: 314.0408; observed: 314.0409; $C_{14}H_7N_3O_6Na$ $[M+Na]^+$: 336.0227; observed: 336.0227;

*4.2.36 – Synthesis of 5-nitro-1,10-phenanthroline-2,9-dicarboxamide (**130**):*

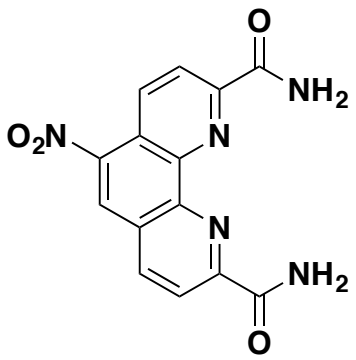

(130)

5-Nitro-1,10-phenanthroline-2,9-dicarboxylic acid (**129**) (1.0 g, 3.19 mmol), 1-hydroxybenzotriazole hydrate (0.86 g, 6.38 mmol, 2 eq), *N*-(3-dimethylaminopropyl)-*N*'-ethylcarbodiimide hydrochloride (1.22 g, 6.38 mmol, 2 eq) and ammonium chloride (0.34 g, 6.38 mmol, 2 eq) were dissolved in DMF (10 mL). *N*,*N*-Di*iso*propylethylamine (1.11 mL, 6.38 mmol, 2 eq) was added and the mixture was stirred at room temperature for 18 h. The solution was diluted with H_2O (100 mL) and the precipitated solid was filtered, washed with H_2O (2 x 50 mL), Et_2O (2 x 50 mL) and then dried in a vacuum oven (60 ^oC) to afford the title compound (**130**) as a pale green solid (0.90 g, 91 %) m. p. > 300 ^oC; FT-IR (ATR) ν_{max} / cm^{-1} 3077br, 1651s, 1530m, 1493w, 1455w, 1372w, 1337w, 1200w;

δ_H (400 MHz, DMSO) 9.16 (s, 1H, Ar*H*), 9.07 (d, 1H, *J* = 8.8 Hz, Ar*H*), 9.02 (s, 1H, NH_2), 8.99 (s, 1H, NH_2), 8.96 (d, 1H, *J* = 8.4 Hz, Ar*H*), 8.60 – 8.55 (m, 2H), 8.00 (s, 1H, NH_2), 7.96 (s, 1H, NH_2); δ_C (101 MHz, DMSO) 165.5 (*C*=O), 165.4 (*C*=O), 152.8, 150.8, 145.4, 144.6, 144.2, 140.4, 134.2, 127.4, 126.9, 122.4, 121.9; (FTMS + p ESI) cald $C_{14}H_9N_5O_4Na$ $[M+Na]^+$: 334.0547; observed: 334.0549;

*4.2.37 – Synthesis of 5,6-dioxo-5,6-dihydro-1,10-phenanthroline-2,9-dicarboxylic acid (**126**):*

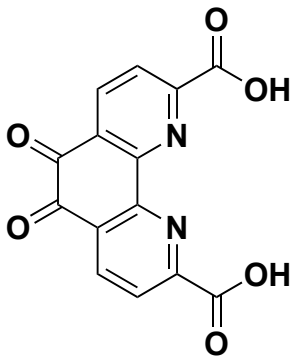

(126)

2,9-Dimethyl-1,10-phenanthroline (**50**) (4.0 g, 19.2 mmol) was dissolved in fuming H_2SO_4 (15 mL, 20 % SO_3) and then HNO_3 (20 mL) was slowly added. The mixture was heated to 150 ^oC for 18 h, then cooled to room temperature and poured into ice-water (200 mL, CARE!) with external cooling. The precipitated solid was filtered and washed with H_2O (100 mL), Et_2O (50 mL), and then dried in a vacuum oven (60 ^oC) to afford the title compound (**126**) as a bright yellow solid (4.49 g, 78 %) m.p. 178-180 ^oC; FT-IR (ATR) ν_{max} / cm^{-1} 3501br (OH), 3092w, 1937w, 1705s (C=O), 1568m, 1424w, 1383m, 1289w;

δ_H (400 MHz, DMSO) 8.60 (d, *J* = 8.0 Hz, 2H, Ar*H*), 8.27 (d, *J* = 8.0 Hz, 2H, Ar*H*); δ_C (101 MHz, DMSO) 176.6 (*C*=O), 165.5 (HO-*C*=O), 151.9, 151.5, 137.1, 131.3, 125.7; (FTMS + pESI) cald $C_{14}H_7N_2O_6$ $[M+H]^+$: 299.0299; observed: 299.0299; $C_{14}H_6N_2O_6Na$ $[M+Na]^+$: 321.0118; observed: 321.0116;

*3.2.38 – Synthesis of dipyrido[3,2-a:2',3'-c]phenazine-3,6-dicarboxylic acid (**132**):*

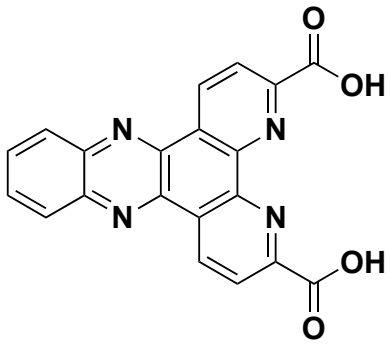

(132)

5,6-Dioxo-5,6-dihydro-1,10-phenanthroline-2,9-dicarboxylic acid (**126**) (1.5 g, 5.03 mmol) and *o*-phenylenediamine (0.54 g, 5.03 mmol, 1 eq) were suspended in EtOH (60 mL) and AcOH (1 mL) and the mixture heated to reflux for 18 h. The solution was allowed to cool to room temperature, diluted with H_2O (25 mL) and the precipitated solid was filtered, washed with H_2O (100 mL), Et_2O (50 mL) and then dried in a vacuum oven (60 ^oC) to afford the title compound (**132**) as a pale brown solid (0.91 g, 49 %) m.p 215-218 ^oC; FT-IR (ATR) ν_{max} / cm^{-1} 3411br (OH), 2909br, 1725s (C=O), 1678m, 1567w, 1481w.

δ_H (400 MHz, DMSO) 9.70 (d, *J* = 8.4 Hz, 2H, Ar*H*), 8.56 (d, *J* = 8.4 Hz, 2H, Ar*H*), 8.45 – 8.42 (m, 2H, Ar*H*), 8.14 – 8.11 (m, 2H, Ar*H*); δ_C (101 MHz, DMSO) Insufficiently soluble to obtain a meaningful spectrum. (FTMS + pESI) cald $C_{20}H_{11}N_4O_4$ $[M+H]^+$: 371.0780; observed: 371.0774; $C_{20}H_{10}N_4O_4Na$ $[M+Na]^+$: 393.0600; observed: 393.0594

*4.2.39 – Synthesis of dipyrido[3,2-*a*:2',3'-*c*]phenazine-3,6-dicarboxamide (**133**):*

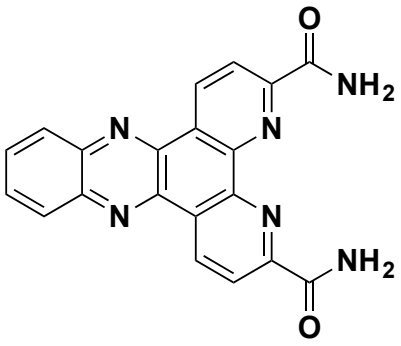

(133)

Dipyrido[3,2-*a*:2',3'-*c*]phenazine-3,6-dicarboxylic acid (**132**) (0.86 g, 2.32 mmol) was suspended in $SOCl_2$ (5 mL) and the mixture heated to reflux for 4 h. The solution was allowed to cool and extracted with DCM (10 mL) and the organic extract concentrated *in vacuo* to give a pale brown solid. Aqueous ammonium hydroxide (10 mL, 35 %) was slowly added with external cooling and the mixture was stirred at room temperature for 18 h. Water (100 mL) was added and the solid residue was filtered, washed with water (100 mL), Et_2O (50 mL) and dried in a vacuum oven (60 ^oC) to afford the title compound (**133**) as a pale brown solid (0.82 g, 96 %) m.p. > 300 ^oC (decomp); FT-IR (ATR) ν_{max} / cm^{-1} 3447br (NH), 3172br (NH), 1693s (C=O), 1566m, 1481w, 1349w.

δ_H (400 MHz, DMSO) 9.71 (d, *J* = 8.4 Hz, 2H, Ar*H*), 8.99 (s, 2H, NH_2), 8.57 (d, *J* = 8.4 Hz, 2H, Ar*H*), 8.46 – 8.43 (m, 2H, Ar*H*), 8.17 – 8.15 (m, 2H, Ar*H*), 7.99 (s, 2H, NH_2); δ_C (101 MHz, DMSO) Insufficiently soluble to obtain a meaningful spectrum. (FTMS + pESI) cald $C_{20}H_{13}N_6O_2$ $[M+H]^+$: 369.1095; observed: 369.1097; $C_{20}H_{12}N_6O_2Na$ $[M+Na]^+$: 391.0914; observed 391.0915;

*4.2.40 – Synthesis of (3Z,6Z)-dipyrido[3,2-a:2',3'-c]phenazine-3,6-bis(carbohydrazonamide) (**134**):*

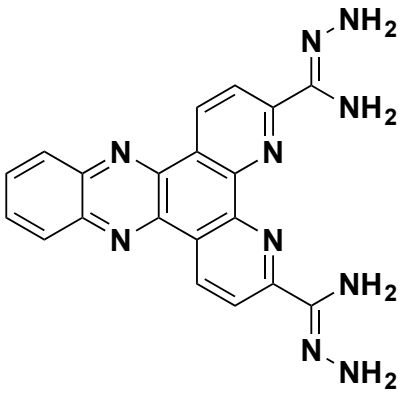

(134)

Dipyrido[3,2-*a*:2',3'-*c*]phenazine-3,6-dicarboxamide (**133**) (0.50 g, 1.36 mmol) was suspended in DMF (8 mL) and pyridine (0.87 mL, 10.86 mmol, 8 eq), then trifluoroacetic acid (0.77 mL, 5.43 mmol, 4 eq) was added. The mixture was stirred at room temperature for 5 h, then hydrazine hydrate (3 mL, 64 %) was added slowly and the mixture was stirred for 18 h at room temperature. Water (100 mL) was added and the precipitated brown solid was filtered off, washed with water (50 mL), Et_2O (100 mL) and dried in a vacuum oven (60 ^oC) to afford the title compound (**134**) as a pale brown solid (0.49 g, 90 %) m.p. 295-300 ^oC (decomp); IR (ATR) ν_{max} / cm^{-1} 3448br (NH), 3185br (NH), 1694m, 1567m, 1480w, 1349w;

δ_H (400 MHz, DMSO) 9.46 (d, *J* = 8.8 Hz, 2H, Ar*H*), 8.47 (d, *J* = 8.4 Hz, 2H, Ar*H*), 8.40 – 8.38 (m, 2H, Ar*H*), 8.07 – 8.04 (m, 2H, Ar*H*), 6.38 (s, 4H, NH_2), 6.18 (s, 4H, NH_2); δ_C (101 MHz, DMSO) Insufficiently soluble to obtain a meaningful spectrum. (FTMS + pESI) cald $C_{20}H_{17}N_{10}$ $[M+H]^+$: 397.1632; observed: 397.1632; $C_{20}H_{16}N_{10}Na$ $[M+Na]^+$: 419.1452; observed 419.1451;

*4.2.41 – Synthesis of 3,6-bis(5,5,8,8-tetramethyl-5,6,7,8-tetrahydrobenzo[*e*][1,2,4]triazin-3-yl)dipyrido[3,2-*a*:2',3'-*c*]phenazine (**135**):*

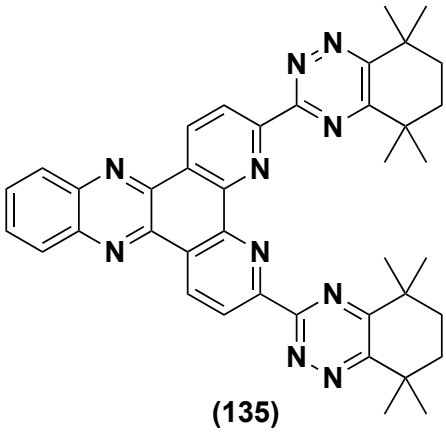

(135)

(3*Z*,6*Z*)-Dipyrido[3,2-*a*:2',3'-*c*]phenazine-3,6-bis(carbohydrazonamide) (**134**) (0.28 g, 0.71 mmol) and 3,3,6,6-tetramethylcyclohexane-1,2-dione (**32**) (0.25 g, 1.48 mmol, 2.1 eq) were dissolved in AcOH (25 mL) and heated to reflux for 3 h. The solution was cooled to room temperature and then poured into H_2O (100 mL), filtered and washed with H_2O (50 mL), Et_2O (50 mL) and dried in a vacuum oven (60 ^oC) to afford the title compound (**135**) as a yellow powder (0.35 g, 75 %) m.p. 240-243 ^oC; FT-IR (ATR) ν_{max} / cm^{-1} 2963m, 2926m, 2861m, 1621w, 1512w, 1456w, 1385w, 1340m, 1248m;

δ_H (400 MHz, $CDCl_3$) 9.76 (d, *J* = 8.4 Hz, 2H), 8.92 (d, *J* = 8.4 Hz, 2H), 8.33 – 8.31 (m, 2H), 7.93 – 7.90 (m, 2H), 1.92 (s, 8H), 1.59 (s, 12H), 1.57 (s, 12H); δ_C (101 MHz, $CDCl_3$) 159.1, 163.5, 161.1, 155.9, 142.7, 140.9, 134.9, 131.1, 129.6, 128.8, 124.4, 37.6, 36.7, 33.8, 33.6, 29.9, 29.3; (FTMS + pESI) cald $C_{40}H_{41}N_{10}$ $[M+H]^+$: 661.3510; observed 661.3522; $C_{40}H_{40}N_{10}Na$ $[M+Na]^+$: 683.3330; observed 683.3333;

4.3 – Synthesis of Magnetic Nanoparticles (MNPs):

4.3.1 – General Procedures:

Following literature procedures, the complete precipitation of the core Fe_2O_3 was achieved under alkaline conditions whilst maintaining a molar ratio of Fe(II):Fe(III) of 1:2 under nitrogen. The resulting magnetic core was either coated with SiO_2 or ZrO_2 using Sol-gel method. Incorporation of the Zr-OH or Si-OH surface groups enabled reaction with (3-iodopropyl)trimethoxysilane where the iodo-functional group allowed immobilization of the ligands by substation of iodine by the hydroxyphenyl substituent.[105,117,121,123]

*4.3.2 – Synthesis of iodoalkyl-functionalized ZrO_2-Coated Fe_2O_3 MNPs (**90**):*

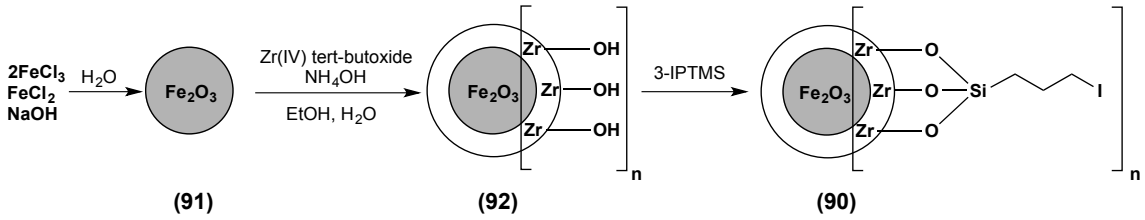

(91) (92) (90)

$FeCl_2.4H_2O$ (0.80 g, 4 mmol) and $FeCl_3$ (1.30 g, 8 mmol) was dissolved in degassed deionized water (50 mL) and were added dropwise into 2 M NaOH solution (200 mL) with vigorous stirring. After 1 h, the resulting Fe_2O_3 MNPs (**91**) were separated by putting the vessel on a neodymium magnet and decanting the supernatant. The MNPs (**91**) were washed with degassed deionized water (200 mL) and 0.01 M HCl (100 mL) to remove unreacted iron salts. Fe_2O_3 MNPs (**91**) were dispersed in a mixed solution of degassed EtOH (300 mL) and degassed deionized water (75 mL) by sonication for 10 min. Ammonium hydroxide (35 %, 36 mL) and zirconium (IV) tert-butoxide (5.1 mL) were consecutively added to the reaction mixture and the reaction was allowed to proceed at room temperature for 2 h under continuous sonication. (3-Iodopropyl)trimethoxysilane (6 mL) was then added and the reaction was allowed to proceed for further 3 h. The resultant functionalized particles (**90**) were obtained by magnetic separation and thoroughly washed with degassed EtOH (4 x 250 mL). Finally, the resultant MNPs (**90**) (2.30 g) were dried at 120 °C.

*4.3.3 – Synthesis of iodoalkyl-functionalized SiO_2-Coated Fe_2O_3 MNPs (**107**):*

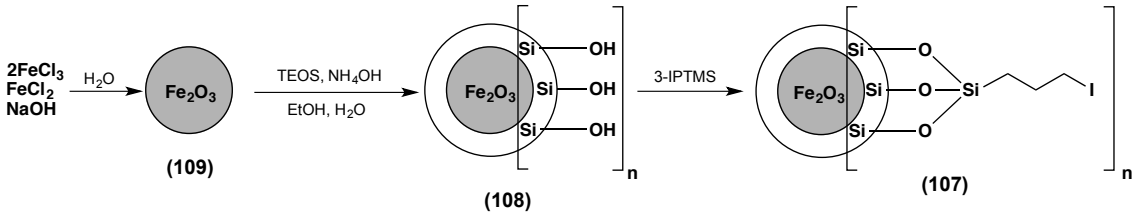

$FeCl_2.4H_2O$ (0.80 g, 4 mmol) and $FeCl_3$ (1.30 g, 8 mmol) dissolved in degassed deionized water 40 mL were added dropwise into 2M NaOH solution (200 mL) with vigorous stirring. After 1 hour, the resulting Fe_2O_3 MNPs (**109**) were separated by putting the vessel on a neodymium magnet and decanting the supernatant. The MNPs (**109**) were washed with degassed deionized water (200 mL) and 0.01 M HCl (17 %, 100 mL) to remove unreacted iron salts. Fe_2O_3 MNPs (**109**) were then dispersed in a mixed solution of degassed EtOH (400 mL) and degassed deionized water (100 mL) by sonication for 10 min. Ammonium hydroxide (35 %, 36 mL) and tetraethyl orthosilicate (3.6 mL, 16 mmol) were consecutively added to reaction mixture and the reaction was allowed to proceed at room temperature for 2 h under continuous sonication. (3-Iodopropyl)trimethoxysilane (6.2 mL, 32 mmol) was then added and the reaction was allowed to proceed for further 3 h. The resultant functionalized particles (**107**) were obtained by magnetic separation and thoroughly washed with degassed EtOH (200 mL). Finally, the resultant MNPs (**107**) (2.74 g) were dried at 120 °C.

4.4 – Immobilization of ligands onto MNPs:

*4.4.1 – Immobilization of 5-(4-hydroxyphenyl)-CyMe$_4$-BTPhen (**84**) onto ZrO$_2$-MNPs (**90**):*

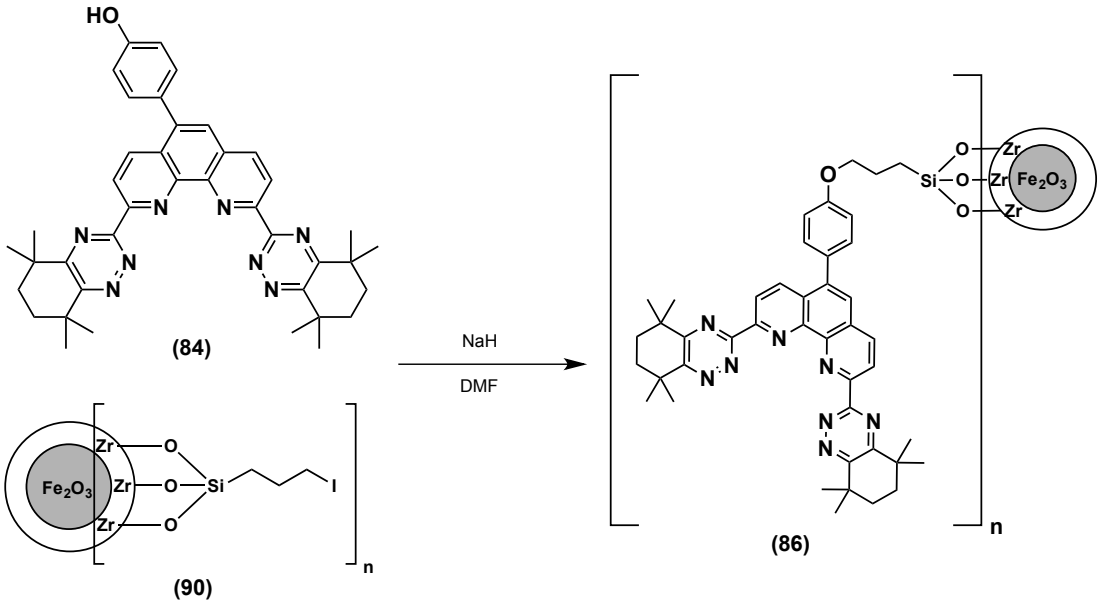

Sodium hydride (60% dispersion in mineral oil, 0.03 g, 0.9 mmol, 1.3 eq) was added to a solution of 5(4-hydroxyphenyl)-CyMe$_4$-BTPhen (**84**) (0.46 g, 0.7 mmol) in DMF (100 mL) at 120 °C and stirred for 30 min. Iodoalkyl-functionalized ZrO$_2$-coated MNPs (**90**) (0.72 g) were slowly added and the reaction mixture was stirred at 120 °C overnight. CyMe$_4$-BTPhen-functionalized MNPs (**86**) were separated by an external magnet and were thoroughly washed with degassed EtOH (200 mL). Finally, the MNPs (**86**) (0.24 g) were allowed to dry at 120 °C. Found % C: 17.16, % H: 3.37, % N: 1.80, % I: 7.69. FT-IR (ATR) ν_{max} / cm^{-1} 3500br, 3000 br, 1600w, 1550w, 1050s (Si-O-Si).

*4.4.2 – Immobilization of tetra(4-hydroxyphenyl)BTPhen (**105**) on SiO_2-coated MNPs (**107**):*

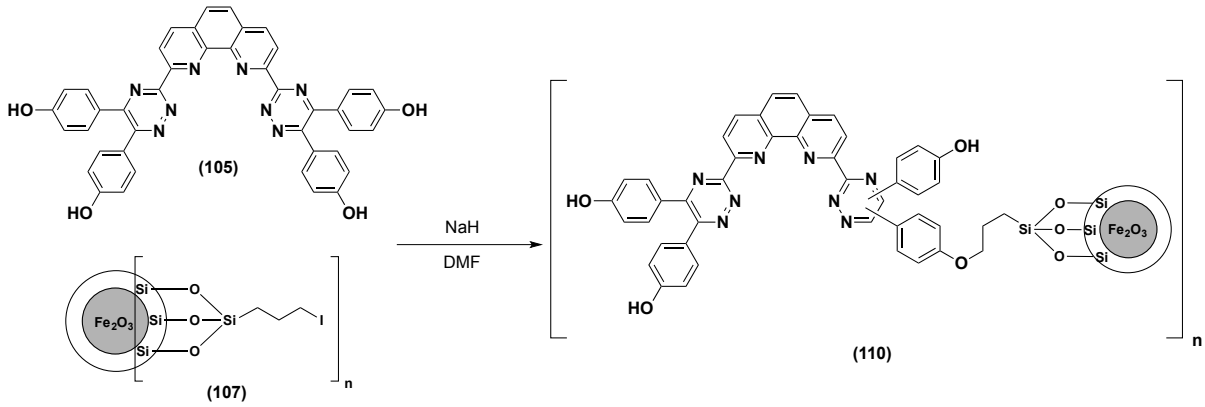

Sodium hydride (60 % dispersion in mineral oil, 0.25 g, 6.3 mmol, 1.1 eq) was added to a solution of tetra(4-hydroxyphenyl)BTPhen (**105**) (1.01 g, 1.4 mmol) in DMF (150 mL) at 120 °C and stirred for 30 min. Iodoalkyl-functionalized SiO_2-coated MNPs (**107**) (1.64 g) were slowly added and the reaction mixture was stirred at 120 °C for 18 hrs. BTPhen-functionalized MNPs (**110**) were separated by an external neodymium magnet and were thoroughly washed with degassed ethanol (200 mL). Finally, the MNPs (**110**) (0.98 g) were allowed to dry at 120 °C. Found % C: 29.62, % H: 3.27, % N: 0.93, % I: 1.39. FT-IR (ATR) ν_{max} / cm^{-1} 1600w, 1570w, 1550w, 1050s (Si-O-Si).

4.5 – Immobilization of Ligands onto Silica Gels:

4.5.1 – General Procedures:

Aminopropyl functionalized silica gel (**121**) was purchased directly from Sigma Aldrich and used as supplied. The extent of labelling was ~ 1 mmol/g NH_2 loading and approximately ~ 9 % functionalized by weight. Particle size of the silica gel is 40-63 μm and 60 (Angstrom) pore size. Chloropropyl functionalized silica gel (**111**) was purchased from Sigma Aldrich and used as supplied. The extent of labelling was ~ 2.5 % loading and the matrix active group was ~ 8 % functionalised. Particle size 230-400 mesh and a pore size of 60 Å.[126,128]

*4.5.2 – Immobilization of 6,6'-bis(5,6-bis(bromomethyl)-1,2,4-triazin-3-yl)-2,2'-bipyridine (**120**) onto aminopropyl-functionalized silica gel (**121**):*

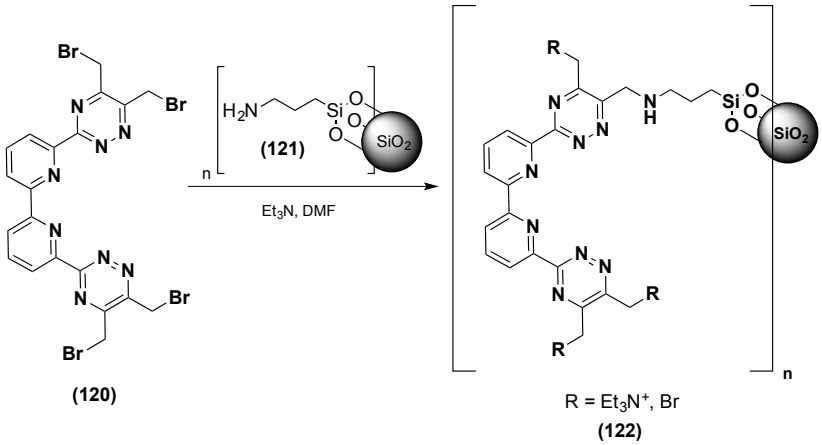

Triethylamine (11 mL, 78.36 mmol, 6 eq) was added to a suspension of aminopropyl-functionalized SiO_2 gel (**121**) (25 g, ~ 1 mmol/g NH_2 loading) in DMF (200 mL) at 120 °C and stirred for 30 min. 6,6'-bis(5,6-bis(bromomethyl)-1,2,4-triazin-3-yl)-2,2'-bipyridine (**120**) (8.95 g, 13.06 mmol) was slowly added and the reaction mixture was stirred at 120 °C overnight. BTBP-functionalized SiO_2 gel (**122**) was collected by filtration and was thoroughly washed with water (300 mL) and ethanol (300 mL). Finally, the functionalized SiO_2 gel (**122**) (28.24 g) was allowed to dry at 120 °C.

*4.5.3 – Immobilization of tetra-(4-hydroxyphenyl)-BTPhen (**105**) on chloropropyl-functionalized silica gel (**112**):*

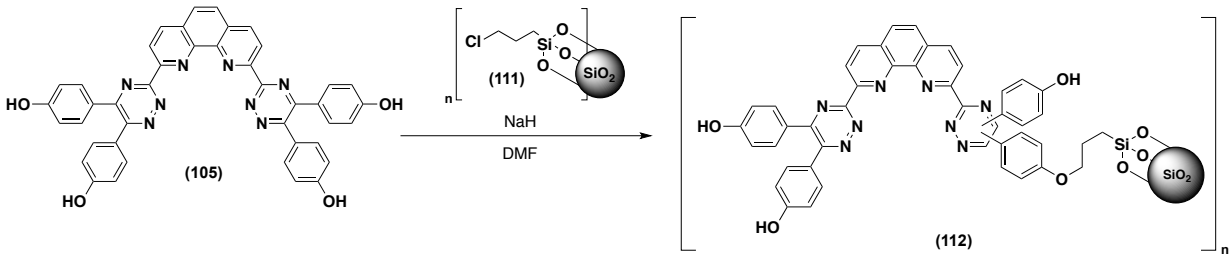

Sodium hydride (60 % dispersion in mineral oil, 0.24 g, 6 mmol, 2 eq) was added to a solution of tetra(4-hydroxyphenyl)-BTPhen (**105**) (2.11 g, 3 mmol) in DMF (100 mL) at 120 °C and stirred for 30 min. Chloropropyl-functionalized SiO_2 gel (**111**) (4.04 g, ~ 2.5 mmol/g loading) was slowly added and the reaction mixture was stirred at 120 °C overnight. BTPhen-functionalized SiO_2 gel (**112**) was collected by filtration and was thoroughly washed with water (100 mL) and ethanol (100 mL). Finally, (**112**) (3.95 g) was allowed to dry at 120 °C. Found % C: 8.10, % H: 1.28, % N: 1.08, % Cl: 0.49. FT-IR (ATR) ν_{max} / cm^{-1} 1600w, 1050s (Si-O-Si), 700w.

*4.5.4 – Immobilization of 5-(4-hydroxyphenyl)-CyMe$_4$-BTPhen (**84**) onto chloropropyl-functionalized SiO$_2$ gel (**111**)*

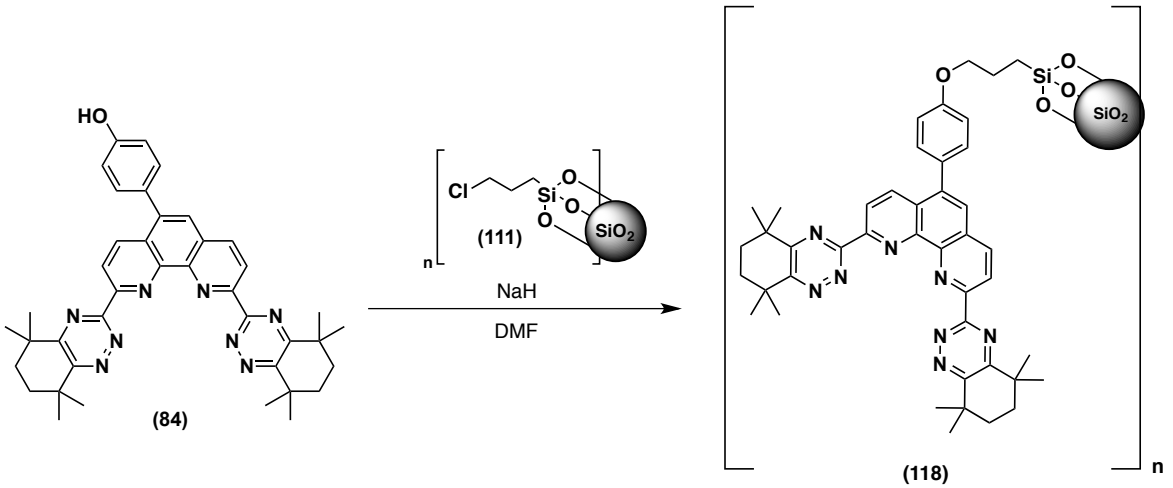

Sodium hydride (60 % dispersion in mineral oil, 0.03 g, 1.54 mmol, 2 eq) was added to a solution of 5-(4-hydroxyphenyl)-CyMe$_4$-BTPhen (**84**) (0.50 g, 0.77 mmol) in DMF (25 mL) at 120 °C and stirred for 30 min. Chloropropyl-functionalized SiO$_2$ gel (**111**) (0.32 g, ~ 2.5 mmol/g loading) was slowly added and the reaction mixture was stirred at 120 °C overnight. BTPhen-functionalized SiO$_2$ gel (**118**) was collected by filtration and was thoroughly washed with water (50 mL) and ethanol (50 mL). Finally, the silica gel (**118**) (0.38 g) was allowed to dry at 120 °C. Found % C: 11.60, % H: 2.01, % N: 1.40, % Cl: 0.10. FT-IR (ATR) ν_{max} / cm^{-1} 2100w, 2000w, 1600w, 1500s, 1050s (Si-O-Si), 700w.

4.6 – Extraction Experiment Details

4.6.1 – General Procedures:

Extraction experiments by the BTBP and BTPhen ligands discussed in the thesis were carried out at Czech Technical University in Prague by Dr Petr Distler. Activity measurements of ^{241}Am, ^{152}Eu and ^{244}Cm were performed with a γ-ray spectrometer EG&G Ortec (USA) with a PGT (USA) HPGe detector and α-ray spectrometer Octete plus Ortec (Germany) with ion-implanted-silicon ultra α-detector (USA). The distribution ratios, *D*, were calculated as the ratio between the radioactivity (α- and γ-emissions) of each isotope in the standard solution and the supernatants. The γ-lines at 59.5 keV and 121.8 keV were examined for ^{241}Am and ^{152}Eu respectively. The errors given in the extraction data **Tables** are 1σ errors based on counting statistics.

*4.6.2 – Extraction Studies of $CyMe_4$-BTPhen functionalized ZrO_2-MNPs (**86**):*

The aqueous solutions for the solvent extraction experiments were prepared by spiking nitric acid solutions (0.745 mL) (0.001 – 4 M) with stock solutions of 5 µL of ^{241}Am (≈ 400 Bq/µL), 3 µL of ^{152}Eu (≈ 1.000 Bq/µL), and 7 µL of ^{244}Cm (≈ 300 Bq/µL) and then adding 600 µL of spiked aqueous solution to 18 mg of (**86**). 150 µL of each labelled solution was taken as a standard (to allow mass balance calculations) for γ- measurements and 10 µL was taken as a standard for α- measurements. The suspension was sonicated for 10 min and shaken on a Heidolph Reax shaker at 1800 rpm for 90 min. After centrifuging for 10 min, aliquots of the aqueous solutions (supernatant) were separated and taken for alpha/gamma measurements after removal of the MNPs (**86**).

*4.6.3 – Extraction Studies of Tetra-(4-hydroxyphenyl)-BTPhen ligand (**105**):*

The aqueous solutions for the solvent extraction experiments were prepared by spiking nitric acid solutions (0.001 – 1 M) with stock solutions of ^{241}Am, ^{152}Eu and ^{244}Cm and then adding 1000 µL of spiked aqueous solution to 10 mM of (**105**) in cyclohexanone. The mixture was sonicated for 10 min and shaken at 1800 rpm for 90 min. After centrifuging

for 10 min, aliquots of the aqueous solutions (supernatant) were separated and taken for alpha/gamma measurements.

*4.6.4 – Extraction Studies of BTPhen-functionalized SiO_2-coated MNPs (**110**):*

The aqueous solutions for the solid phase extraction experiments were prepared by spiking nitric acid solutions (0.001 – 4 M) with stock solutions of ^{241}Am, ^{152}Eu and ^{244}Cm and then adding 1 mL of spiked aqueous solution to 22.7 mg of BTPhen-functionalized SiO_2-coated MNPs (**110**). The suspension was sonicated for 10 min and shaken at 1800 rpm for 90 min. After centrifuging for 10 min, aliquots of the supernatant were separated and taken for alpha/gamma measurements.

*4.6.5 – Extraction Studies of BTPhen-functionalized SiO_2 Gel (**112**):*

Aqueous solutions for the solid phase extraction experiments were prepared by spiking nitric acid solutions (0.001–4 M) with stock solutions of ^{241}Am and ^{152}Eu radiotracers and then adding 1 mL of spiked aqueous solution to 17 mg of BTPhen-functionalized SiO_2 gel (**112**) (~ 10 mM). The suspension was sonicated for 10 min and shaken at 1800 rpm for 90 min. After centrifuging for 10 min, aliquots of the supernatant were separated and taken for alpha/gamma measurements.

*4.6.6 – Extraction Studies of $CyMe_4$-BTPhen-functionalized SiO_2 gel (**118**):*

The aqueous solutions for the solid phase extraction experiments were prepared by spiking nitric acid (HNO_3) and perchloric acid ($HClO_4$) solutions (0.001 – 4 M) with stock solutions of ^{241}Am and ^{152}Eu and then adding 1 mL of spiked aqueous solution to 16.7 mg of $CyMe_4$-BTPhen-functionalized SiO_2 gel (**118**). The suspensions were sonicated for 10 min and shaken at 1800 rpm for 90 min. After centrifuging for 10 min, aliquots of the supernatant were separated and taken for alpha/gamma measurements.

*4.6.7 – Extraction Studies of BTBP-functionalized SiO_2 Gel (**122**):*

The aqueous solutions for the solid phase extraction experiments were prepared by spiking nitric acid solutions (0.001–4 M) with stock solutions of ^{241}Am and ^{152}Eu radiotracers and

then adding 1 mL of spiked aqueous solution to 14 mg of BTBP-functionalized SiO_2 gel (**122**) (~ 10 mM). The suspension was sonicated for 10 min and shaken at 1800 rpm for 90 min. After centrifuging for 10 min, aliquots of the supernatant were separated and taken for alpha/gamma measurements.

*4.6.8 – Extraction Studies of (dppz)-BTPhen ligand (**135**):*

The aqueous solutions were prepared by spiking HNO_3 solutions (0.001-2 M) with ^{241}Am and ^{152}Eu radiotracers. Organic solutions of ligand (**135**) (5 mM) were prepared in cyclohexanone with gentle heating. The aqueous phases were pre-equilibrated with neat cyclohexanone by shaking them for 30 min at 1800 rpm and volume ratio of 4:1 (aq:org). The organic phases were pre-equilibrated with the respective aqueous phases by shaking them for 30 min at 1800 rpm and a volume ratio of 1:1. Of 1.2 mL of labelled aqueous phases, 200 µL standard was taken (to allow for mass balance calculations) prior to contacting the aqueous phase with the organic phase. Each organic phase (1 mL) was shaken separately with each of the aqueous phases (1 mL) for 90 min at 22 ^oC (non-thermostatted) using a Heidolph Multi Reax Shaker (1800 rpm). After phase separation by centrifugation for 10 min, two parallel 200 µL aliquots of each phase were withdrawn for gamma measurement. For gamma measurements, the aliquots were pipetted into plastic ampules and their walls were washed with 1 mL of distilled water or cyclohexanone.

4.7 – ICP-MS Experiments

ICP-MS analysis was run on a Thermo-Fisher iCAP Q ICP-MS with Rh as the internal standard. Standard solutions were prepared using a stock solution of 2 % HNO_3 spiked with 5 ppb Rh. Standards were made using various metal mixes purchased from Sigma-Aldrich as TraceCERT (Traceable Certified Reference Materials). Standards used to calibrate the ICP-MS were 10, 25, 50 and 100 ppb. A 3.8 cm diameter glass column was loaded with 10 g of BTBP-functionalized SiO_2 gel (**122**) and rinsed with 100 mL 2 % HNO_3 blank solution. A solution of 100 mL of 100 ppb metal mix solution was eluted through the column at a rate of 10 mL per minute and fractions of 10 mL were collected and 2 mL aliquots were taken from each fraction for measurement using the ICP-MS. An average of three readings was taken.

Appendices

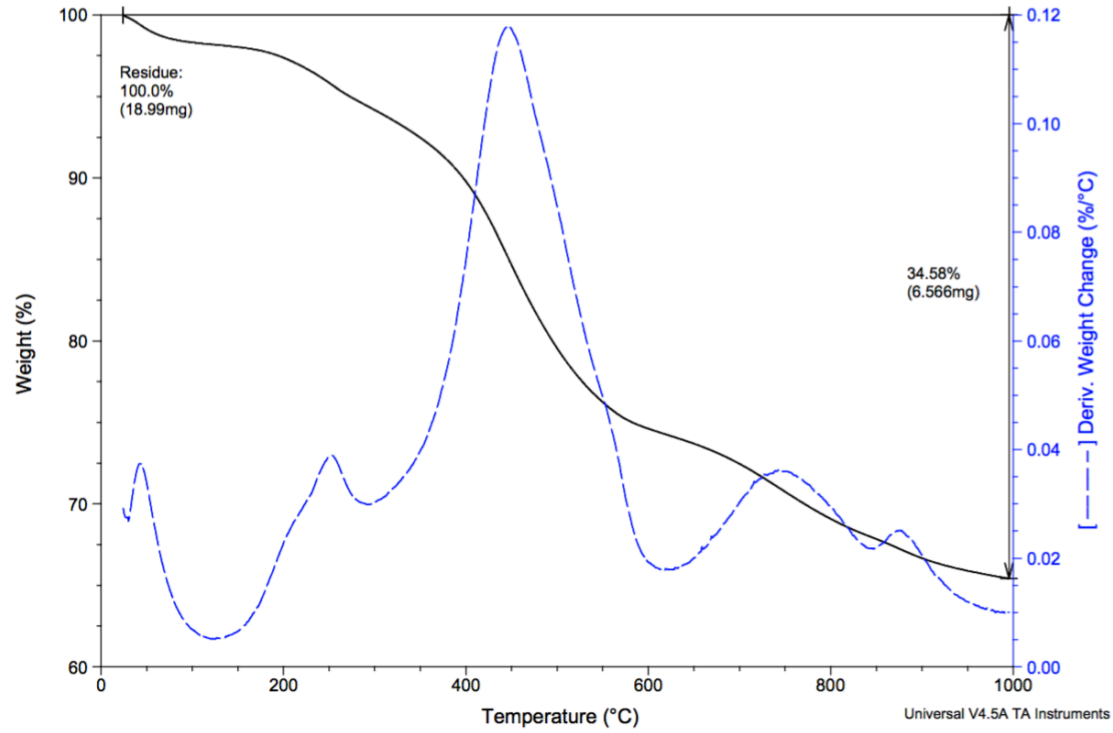

Appendix A1 – TGA for ZrO_2-MNPs (**90**)

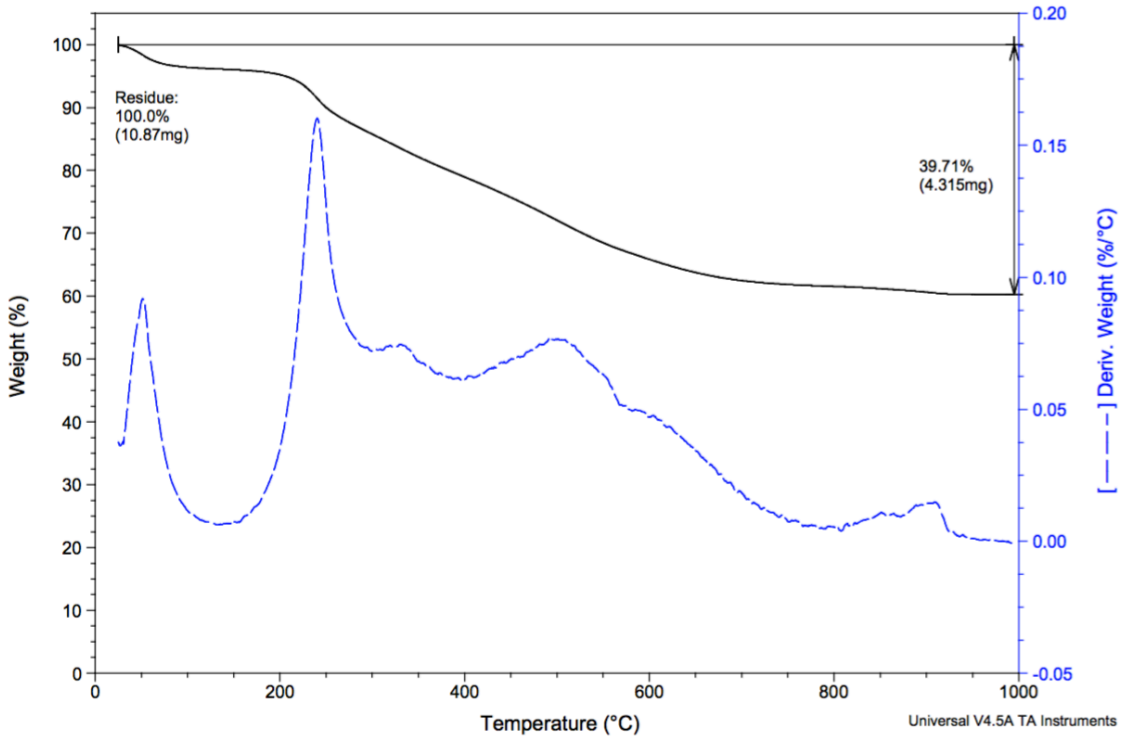

Appendix A1 – TGA for $CyMe_4$-functionalized ZrO_2-MNPs (**86**)

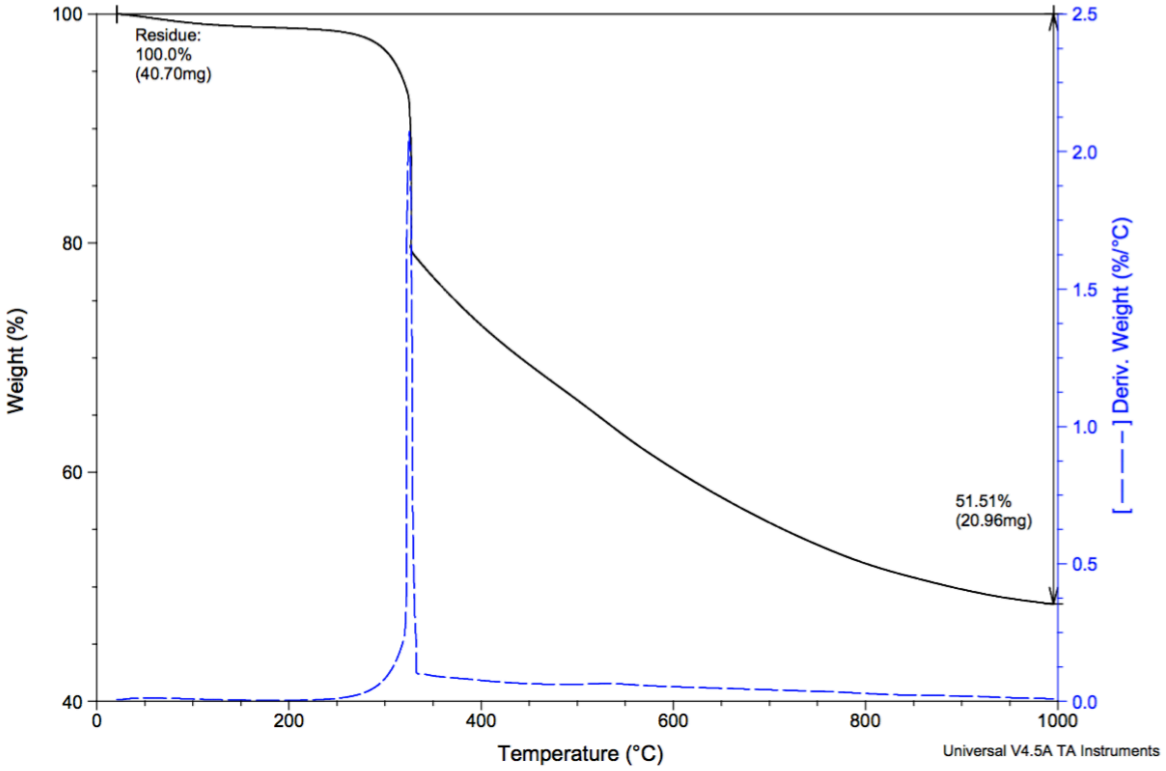

Appendix A2 – TGA for Iodo-functionalized SiO_2 MNPs (**107**)

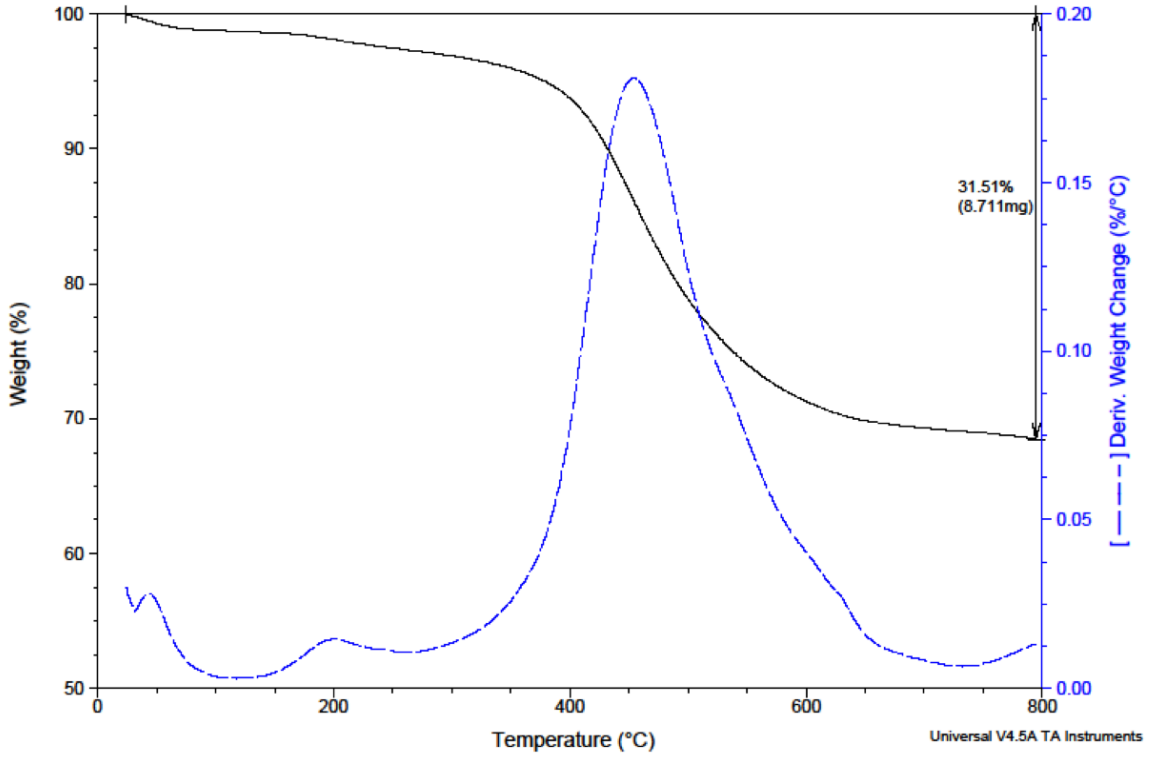

Appendix A2 – TGA for BTPhen-functionalized SiO_2-MNPs (**110**)

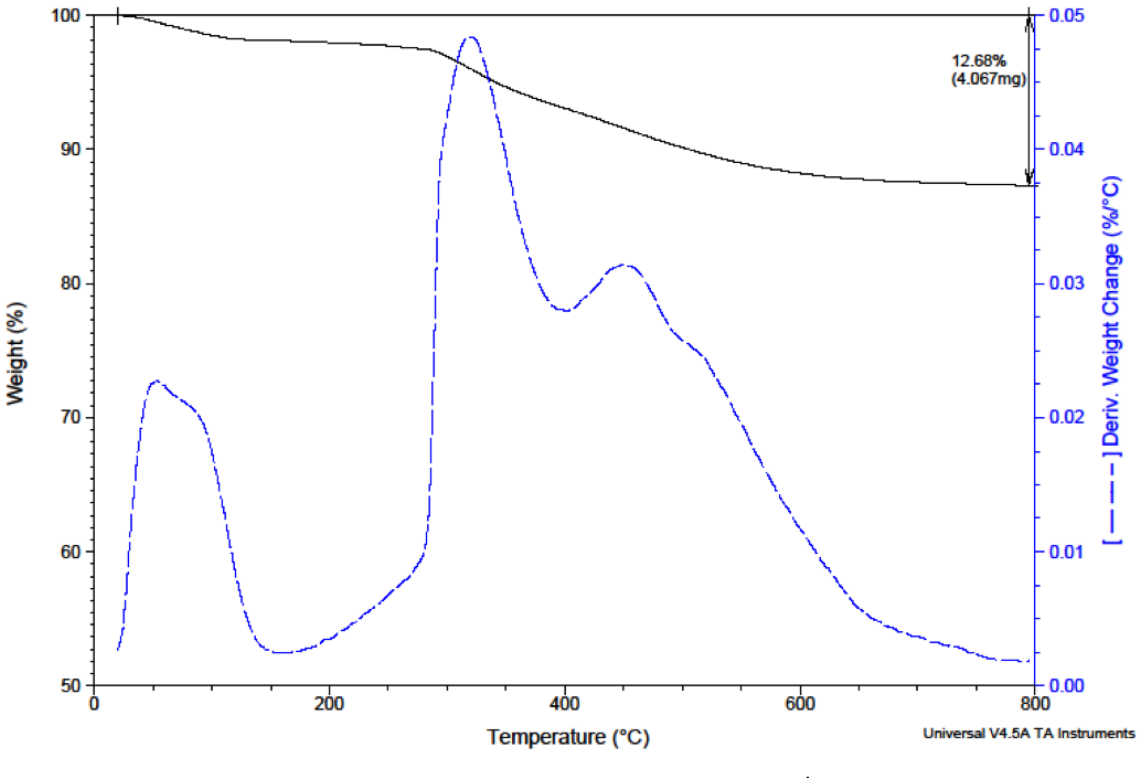

Appendix A3 – TGA for chloro-functionalized SiO_2-gel (**111**)

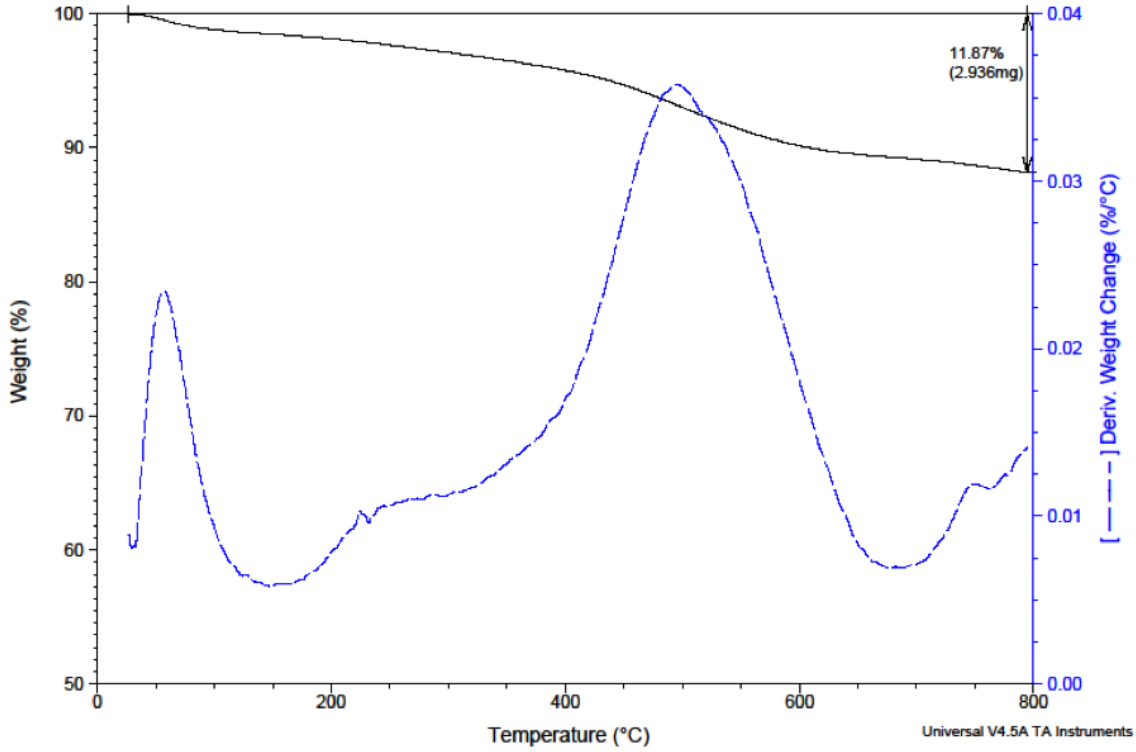

Appendix A3 – TGA for BTPhen-functionalized SiO_2 gel (**112**)

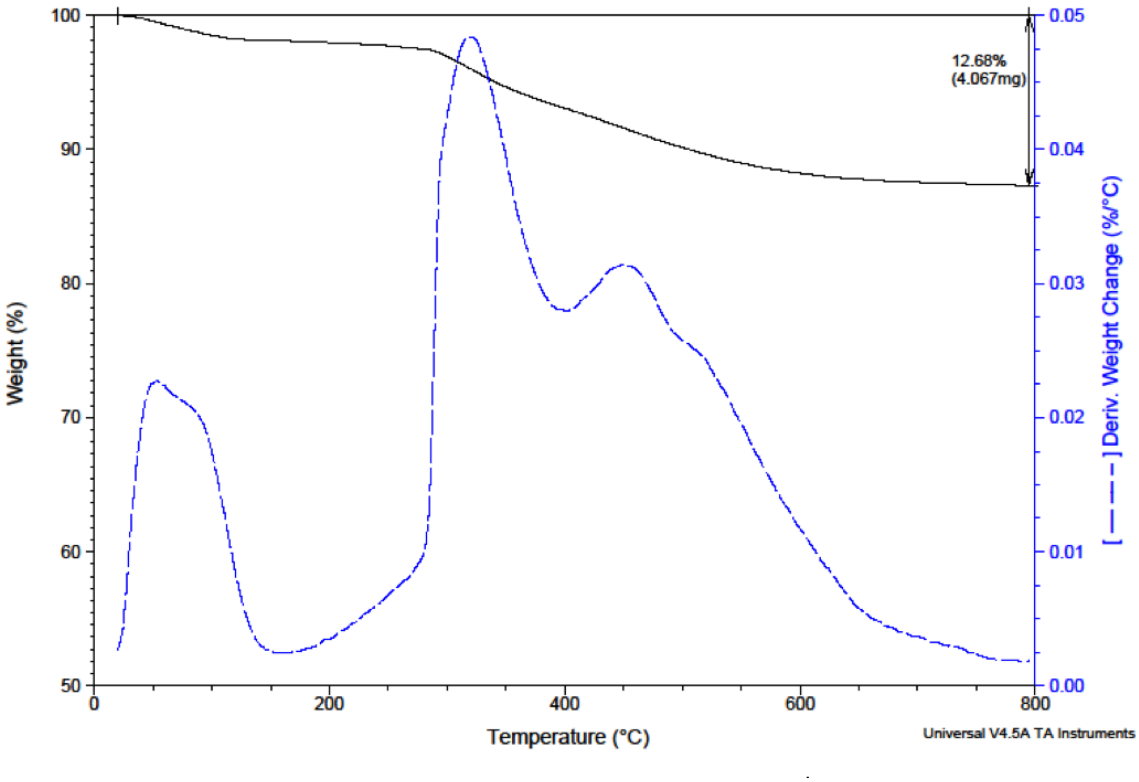

Appendix A4 – TGA for chloro-functionalized SiO_2-gel (**111**)

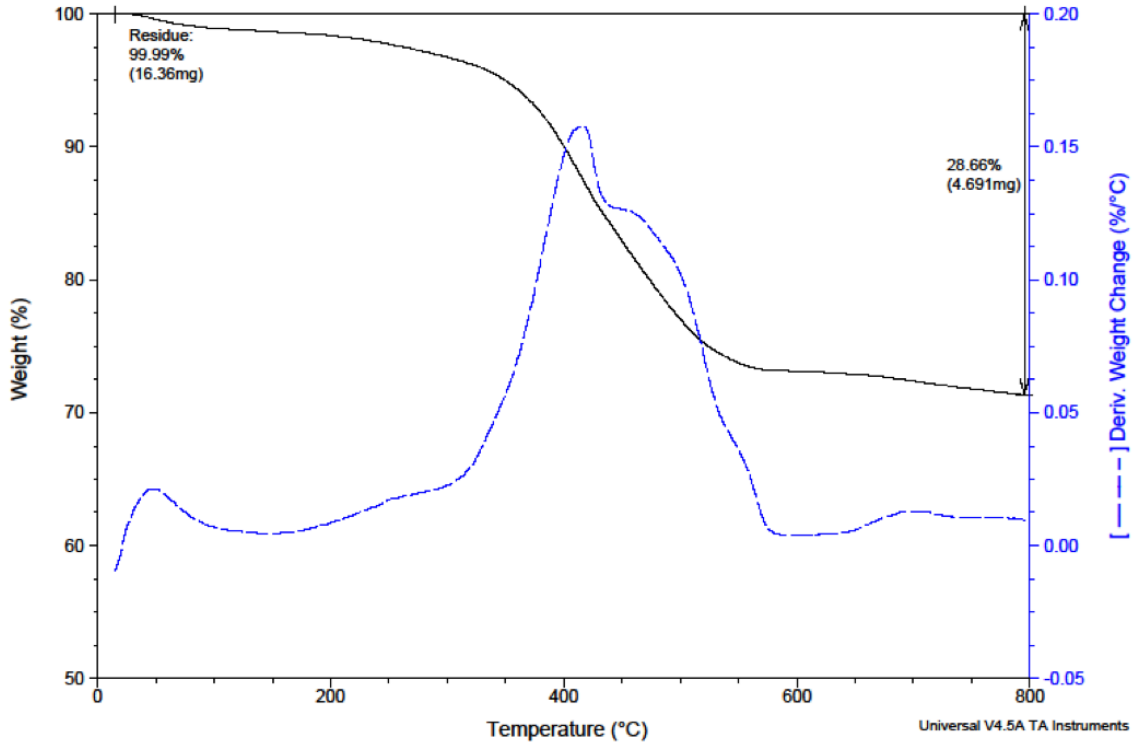

Appendix A4 – TGA for $CyMe_4$-functionalized SiO_2 gel (**118**)

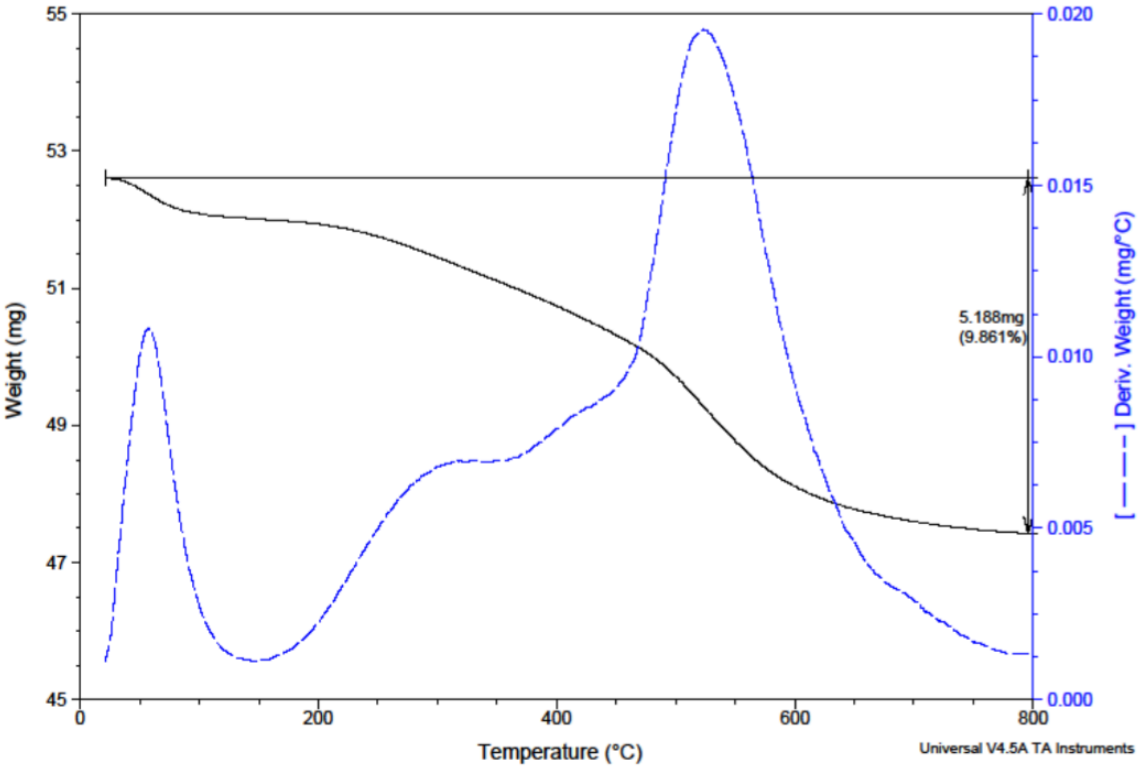

Appendix A5 – TGA for aminopropyl-functionalized SiO_2 gel (**121**)

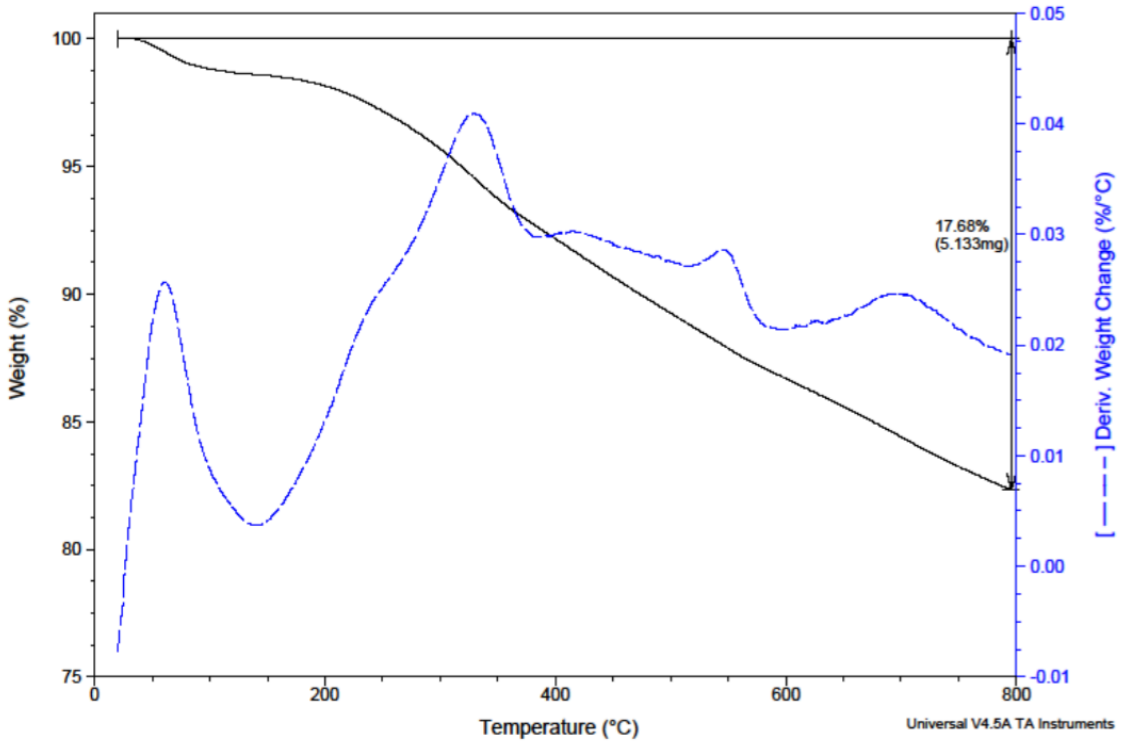

Appendix A5 – TGA for BTBP-functionalized SiO_2 gel (**122**)

References:

1 F. Settle, *J. Chem. Educ.*, 2009, **86**, 316–323.
2 J. Veliscek-Carolan, *J. Hazard. Mater.*, 2016, **318**, 266–281.
3 K. Maher, J. R. Bargar and G. E. Brown, *Inorg. Chem.*, 2013, **52**, 3510–3532.
4 L. Helm, G. M. Nicolle and R. E. Merbach, *Adv. Inorg. Chem.*, 2006, 57, 327–379.
5 J. N. Mathur, M. S. Murali and K. L. Nash, *SolventExtr. Ion Exch.*, 2001, **19**, 357–390.
6 G. R. Choppin and K. L. Nash, *Radiochim. Acta*, 1995, **70**–**71**, 225–236.
7 L. Borges Silverio and W. de Q. Lamas, *Energy Policy*, 2011, **39**, 281–289.
8 F. W. Lewis, M. J. Hudson and L. M. Harwood, *Synlett*, 2011, **18**, 2609–2632.
9 Z. Kolarik, *Chem. Rev.*, 2008, **108**, 4208–4252.
10 N. N. Greenwood and A. Earnshaw, *Chemistry of the elements*, Butterworth-Heinemann, Oxford, 2nd edn., 1997.
11 International Atomic Energy Agency (IAEA), *Nuclear Power and the Paris Agreement*, 2016.
12 International Atomic Energy Agency (IAEA), *2015 Technology Roadmap: Nuclear Energy*, 2015.
13 International Atomic Energy Agency (IAEA), *Key World Energy Statistics*, 2016.
14 International Atomic Energy Agency (IAEA), *Nuclear Technology Review*, 2016.
15 B. Hileman, *Environ. Sci. Technol.*, 1982, **16**, 271A–275A.
16 G. R. Choppin, J. Liljenzin, J. Rydberg and C. Ekberg, *Radiochemistry and Nuclear Chemistry*, Elsevier, 2013.
17 C. A. Sharrad, L. M. Harwood and F. R. Livens, in *Issues in Environmental Science and Technology*, eds. R. E. Hester and R. M. Harrison, 2011, pp. 40–56.
18 S. William and I. Takanobu, *J. Chem. Educ.*, 1991, **68**, 312–314.
19 World Nuclear Association, *Nuclear Fuel Fabrication*, 2017.
20 NFC, https://www.nrc.gov/materials/fuel-cycle-fac/stages-fuel-cycle.html, (accessed 12 January 2018).
21 International Atomic Energy Agency (IAEA), *The Nuclear Fuel Cycle*, 2011.
22 M. J. Hudson, L. M. Harwood, D. M. Laventine and F. W. Lewis, *Inorg. Chem.*, 2013, **52**, 3414–3428.
23 The Royal Society, *Fuel cycle stewardship in a nuclear renaissance*, 2011.
24 *Nuclear Wastes: Technologies for Separation and Transmutation*, National Academies Press, 1996.
25 E. Aneheim, C. Ekberg, A. Fermvik, M. R. S. J. Foreman, T. Retegan and G. Skarnemark, *Solvent Extr. Ion Exch.*, 2010, **28**, 437–458.
26 L. R. Morss, N. M. Edelstein, J. Fuger and J. J. Katz, *The chemistry of the actinide and transactinide elements.*, Springer, 2006.
27 C. E. Housecroft and A. G. Sharpe, *Inorganic chemistry*, Pearson Prentice Hall, 2005.
28 K. Sugasaka, S. Katoh, N. Takai, H. Takahashi and Y. Umezawa, *Sep. Sci. Technol.*, 1981, **16**, 971–985.
29 F. Wu, N. Pu, G. Ye, T. Sun, Z. Wang, Y. Song, W. Wang, X. Huo, Y. Lu and J. Chen, *Environ. Sci. Technol.*, 2017, **51**, 4606–4614.
30 Z. Chen, *J. Rare Earths*, 2011, **29**, 1–6.
31 J. B. Castor, S.B., Hendrick, in *Rare Earth Elements*, 2006, pp. 769–792.
32 S. Cotton, *Lanthanide and Actinide Chemistry*, John Wiley & Sons, Ltd, Chichester,

UK, 2006.
33 J. Lehto and X. Hou, *Chemistry and Analysis of Radionuclides*, Wiley-VCH Verlag GmbH & Co. KGaA, Weinheim, Germany, 2010.
34 M. J. Hudson, F. W. Lewis and L. M. Harwood, in *Strategies and Tactics in Organic Synthesis*, Academic Press, 2013, vol. 9, pp. 177–202.
35 World Nuclear News, Further delay to completion of Rokkasho facilities, http://www.world-nuclear-news.org/WR-Further-delay-to-completion-of-Rokkasho-facilities-2812174.html, (accessed 15 January 2018).
36 C. D. Auwer, M. C. Charbonnel, M. T. Presson, C. Madic and R. Guillaumont, *Polyhedron*, 1998, **17**, 4507–4517.
37 G. Uchiyama, T. Asakura, S. Hotoku and S. Fujine, *Solvent Extr. Ion Exch.*, 1998, **16**, 1191–1213.
38 A. Afsar, *PhD Thesis*, Reading, 2015.
39 M. A. Higginson, P. Thompson, O. J. Marsden, F. R. Livens, L. M. Harwood, F. W. Lewis, M. J. Hudson and S. L. Heath, *Radiochim. Acta*, 2015, **103**, 687–694.
40 D. Serrano-Purroy, P. Baron, B. Christiansen, J. P. Glatz, C. Madic, R. Malmbeck and G. Modolo, *Sep. Purif. Technol.*, 2005, **45**, 157–162.
41 E. Philip Horwitz, D. C. Kalina, H. Diamond, G. F. Vandegrift and W. W. Schulz, *Solvent Extr. Ion Exch.*, 1985, **3**, 75–109.
42 K. L. Nash, J. C. Braley, C. Wai and B. Mincher, *Nucl. Energy Environ.*, 2010, **1046**, 19–38.
43 D. Rosario-Amorin, E. N. Duesler, R. T. Paine, B. P. Hay, L. H. Delmau, S. D. Reilly, A. J. Gaunt and B. L. Scott, *Inorg. Chem.*, 2012, **51**, 6667–6681.
44 O. Courson, M. Lebrun, R. Malmbeck, G. Pagliosa, K. Roemer, B. Saetmark and P. Glatz, *Radiochim. Acta*, 2000, **88**, 857–863.
45 H. Galán, C. A. Zarzana, A. Wilden, A. Núñez, H. Schmidt, R. J. M. Egberink, A. Leoncini, J. Cobos, W. Verboom, G. Modolo, G. S. Groenewold and B. J. Mincher, *Dalton Trans.*, 2015, **44**, 18049–18056.
46 P. Byers, M. G. B. Drew, M. J. Hudson, N. S. Isaacs and C. Madic, *Polyhedron*, 1994, **13**, 349–352.
47 M. Nilsson and K. L. Nash, *Solvent Extr. Ion Exch.*, 2007, **25**, 665–701.
48 B. Weaver and F. A. Kappelmann, *J. Inorg. Nucl. Chem.*, 1968, **30**, 263–272.
49 K. L. Nash, *Solv.Extr. Ion Exch.*, 2015, **33**, 1–55.
50 A. E. V Gorden, M. A. DeVore and B. A. Maynard, *Inorg. Chem.*, 2013, **52**, 3445–3458.
51 A. T. Johnson and K. L. Nash, *Solvent Extr. Ion Exch.*, 2015, **33**, 642–655.
52 N. Kaltsoyannis, *Inorg. Chem.*, 2013, **52**, 3407–3413.
53 Y. Yang, J. Liu, L. Yang, K. Li, H. Zhang, S. Luo and L. Rao, *Dalton Trans.*, 2015, **44**, 8959–8970.
54 T. Vitova, I. Pidchenko, D. Fellhauer, P. S. Bagus, Y. Joly, T. Pruessmann, S. Bahl, E. Gonzalez-Robles, J. Rothe, M. Altmaier, M. A. Denecke and H. Geckeis, *Nat. Commun.*, 2017, **8**, 1–9.
55 I. Kirker and N. Kaltsoyannis, *Dalton Trans.*, 2011, **40**, 124–131.
56 C. Adam, P. Kaden, B. B. Beele, U. Müllich, S. Trumm, A. Geist, P. J. Panak and M. A. Denecke, *Dalton Trans.*, 2013, **42**, 14068-14074
57 H. H. Dam, D. N. Reinhoudt and W. Verboom, *Chem. Soc. Rev.*, 2007, **36**, 367–377.
58 P. J. Panak and A. Geist, *Chem. Rev.*, 2013, **113**, 1199–1236.

59 A. Wilden, G. Modolo, C. Schreinemachers, F. Sadowski, S. Lange, M. Sypula, D. Magnusson, A. Geist, F. W. Lewis, L. M. Harwood and M. J. Hudson, *Solvent Extr. Ion Exch.*, 2013, **31**, 519–537.

60 A. Geist, U. Müllich, D. Magnusson, P. Kaden, G. Modolo, A. Wilden and T. Zevaco, *Solvent Extr. Ion Exch.*, 2012, **30**, 433–444.

61 A. Wilden, G. Modolo, P. Kaufholz, F. Sadowski, S. Lange, M. Sypula, D. Magnusson, U. Müllich, A. Geist and D. Bosbach, *Solvent Extr. Ion Exch.*, 2015, **33**, 91–108.

62 D. M. Whittaker, T. L. Griffiths, M. Helliwell, A. N. Swinburne, L. S. Natrajan, F. W. Lewis, L. M. Harwood, S. A. Parry and C. A. Sharrad, *Inorg. Chem.*, 2013, **52**, 3429–3444.

63 K. N. Tevepaugh, J. Coonce, S. Tai, L. H. Delmau, J. D. Carrick and D. D. Ensor, *J. Radioanal. Nucl. Chem.*, 2017, **314**, 371–376.

64 C. Hill, C. Madic, P. Baron, M. Ozawa and Y. Tanaka, *J. Alloys Compd.*, 1998, **271**–**273**, 159–162.

65 Y. Zhu, *Radiochim. Acta*, 1995, **68**, 95–98.

66 G. Modolo and R. Odoj, *J. Alloys Compd.*, 1998, **271**–**273**, 248–251.

67 C. De Sahb, L. A. Watson, J. Nadas and B. P. Hay, *Inorg. Chem.*, 2013, **52**, 10632–10642.

68 A. Leoncini, J. Huskens and W. Verboom, *Chem. Soc. Rev.*, 2017, **46**, 7229–7273.

69 A. W. Addison and P. J. Burke, *J. Heterocycl. Chem.*, 1981, **18**, 803–805.

70 Z. Kolarik, U. Mullich and F. Gassner, *Solvent Extr. Ion Exch.*, 1999, **17**, 1155–1170.

71 N. S. Isaacs, *Physical Organic Chemistry*, Longman Scientific & Technical, Essex, 2nd edn., 1995.

72 F. H. Case, *J. Heterocycl. Chem.*, 1971, **8**, 1043–1046.

73 M. J. Hudson, C. E. Boucher, D. Braekers, J. F. Desreux, M. G. B. Drew, M. R. S. J. Foreman, L. M. Harwood, C. Hill, C. Madic, F. Marken and T. G. A. Youngs, *New J. Chem.*, 2006, **30**, 1171-1183

74 P. Distler, I. Spendlikova, J. John, L. M. Harwood, M. J. Hudson and F. W. Lewis, *Radiochim. Acta*, 2012, **100**, 747–752.

75 C. Madic, B. Boullis, P. Baron, F. Testard, M. J. Hudson, J. O. Liljenzin, B. Christiansen, M. Ferrando, a. Facchini, a. Geist, G. Modolo, a. G. Espartero and J. De Mendoza, *J. Alloys Compd.*, 2007, **444**–**445**, 23–27.

76 F. W. Lewis, L. M. Harwood, M. J. Hudson, M. G. B. Drew, G. Modolo, M. Sypula, J. F. Desreux, N. Bouslimani and G. Vidick, *Dalton. Trans.*, 2010, **39**, 5172-5182

77 F. W. Lewis, L. M. Harwood, M. J. Hudson, M. G. B. Drew, J. F. Desreux, G. Vidick, N. Bouslimani, G. Modolo, A. Wilden, M. Sypula, T. H. Vu and J. P. Simonin, *J. Am. Chem. Soc.*, 2011, **133**, 13093–13102.

78 M. Nilsson, C. Ekberg, M. Foreman, M. Hudson, J. Liljenzin, G. Modolo and G. Skarnemark, *Solvent Extr. Ion Exch.*, 2006, **24**, 823–843.

79 L. M. Harwood, F. W. Lewis, M. J. Hudson, J. John and P. Distler, *Solvent Extr. Ion Exch.*, 2011, **29**, 551–576.

80 A. Afsar, P. Distler, L. M. Harwood, J. John and J. Westwood, *J. Org. Chem.*, 2016, **81**, 10517–10520.

81 F. W. Lewis, L. M. Harwood, M. J. Hudson, P. Distler, J. John, K. Stamberg, A. Núñez, H. Galán and A. G. Espartero, *European J. Org. Chem.*, 2012, **2012**, 1509–1519.

82 F. W. Lewis, L. M. Harwood, M. J. Hudson, M. G. B. Drew, V. Hubscher-Bruder, V. Videva, F. Arnaud-Neu, K. Stamberg and S. Vyas, *Inorg. Chem.*, 2013, **52**, 4993–

5005.
83 M. Steppert, I. Císařová, T. Fanghänel, A. Geist, P. Lindqvist-Reis, P. Panak, P. Štěpnička, S. Trumm and C. Walther, *Inorg. Chem.*, 2012, **51**, 591–600.
84 J. Narbutt, A. Wodyński and M. Pecul, *Dalton. Trans.*, 2015, **44**, 2657–2666.
85 D. M. Laventine, A. Afsar, M. Hudson and L. M. Harwood, *Heterocycles*, 2012, **86**, 1419–1429.
86 A. C. Edwards, A. Geist, U. Müllich, C. A. Sharrad, R. G. Pritchard, R. C. Whitehead and L. M. Harwood, *Chem. Commun.*, 2017, **53**, 8160–8163.
87 F. W. Lewis, L. M. Harwood, M. J. Hudson, A. Geist, V. N. Kozhevnikov, P. Distler and J. John, *Chem. Sci.*, 2015, **6**, 4812–4821.
88 C. M. Ruff, U. Müllich, A. Geist and P. J. Panak, *Dalton. Trans.*, 2012, **41**, 14594.
89 F. W. Lewis, L. M. Harwood, M. J. Hudson, A. Núñez, H. Galán and A. G. Espartero, *Synlett*, 2016, **27**, 1–5.
90 A. C. Edwards, P. Mocilac, A. Geist, L. M. Harwood, C. A. Sharrad, N. A. Burton, R. C. Whitehead and M. A. Denecke, *Chem. Commun.*, 2017, **53**, 5001–5004.
91 E. Macerata, E. Mossini, S. Scaravaggi, M. Mariani, A. Mele, W. Panzeri, N. Boubals, L. Berthon, M.-C. Charbonnel, F. Sansone, A. Arduini and A. Casnati, *J. Am. Chem. Soc.*, 2016, **138**, 7232–7235.
92 C. Wagner, E. Mossini, E. Macerata, M. Mariani, A. Arduini, A. Casnati, A. Geist and P. J. Panak, *Inorg. Chem.*, 2017, **56**, 2135–2144.
93 A. Afsar, J. Westwood, L. M. Harwood, M. J. Hudson, D. M. Laventine and A. Geist, *Jordan J. Chem.*, 2014, **9**, 50–58.
94 M. A. Higginson, N. D. Kyle, O. J. Marsden, P. Thompson, F. R. Livens and S. L. Heath, *Dalton. Trans.*, 2015, **44**, 16547–16552.
95 A. Afsar, D. M. Laventine, L. M. Harwood, M. J. Hudson and A. Geist, *Chem. Commun.*, 2013, **49**, 8534–8536.
96 J. Mlochowski, *Rocz. Chem.*, 1974, **48**, 2145–2155.
97 A. Afsar, L. M. Harwood, M. J. Hudson, J. Westwood and A. Geist, *Chem. Commun.*, 2015, **51**, 5860–5863.
98 A. C. Edwards, C. Wagner, A. Geist, N. A. Burton, C. A. Sharrad, R. W. Adams, R. G. Pritchard, P. J. Panak, R. C. Whitehead and L. M. Harwood, *Dalton. Trans.*, 2016, **45**, 18102–18112.
99 A. F. Larsen and T. Ulven, *Org. Lett.*, 2011, **13**, 3546–3548.
100 N. J. Williams, J. Dehaudt, V. S. Bryantsev, H. Luo, C. W. Abney and S. Dai, *Chem. Commun.*, 2017, **53**, 2744–2747.
101 L. Nunez, M. D. Kaminski, C. Bradley, B. A. Buchholz, S. Landsberger, S. . Aase, H. . Tuazon and G. F. Vandegrift, *Magnetically assisted chemical separation (MACS) process: preparation and optimization of particles for removal of transuranic elements*, Argonne National Laboratory, Lemont, 1995.
102 M. D. Kaminski and L. Nunez, *Sep. Sci. Technol.*, 2000, **35**, 2003–2018.
103 S. Ojha, S. Chappa, A. M. Mhatre, K. K. Singh, V. Chavan and A. K. Pandey, *J. Radioanal. Nucl. Chem.*, 2017, **312**, 675–683.
104 P. G. Sammes and G. Yahioglu, *Chem. Soc. Rev.*, 1994, **23**, 327-334.
105 A. Afsar, L. M. Harwood, M. J. Hudson, M. E. Hodson and E. J. Shaw, *Chem. Commun.*, 2014, **50**, 7477–7480.
106 A. Afsar, L. M. Harwood, M. J. Hudson, P. Distler and J. John, *Chem. Commun.*, 2014, **50**, 15082–15085.

107 J. H. Jang and H. B. Lim, *Microchem. J.*, 2010, **94**, 148–158.
108 J. Westwood, A. Afsar, L. M. Harwood, M. J. Hudson, J. John and P. Distler, *Heterocycles*, 2016, **93**, 453–464.
109 R. N. Grass, E. K. Athanassiou and W. J. Stark, *Angew. Chem. Int. Ed.*, 2007, **46**, 4909–4912.
110 A. F. Ngomsik, A. Bee, D. Talbot and G. Cote, *Sep. Purif. Technol.*, 2012, **86**, 1–8.
111 Z. Ma, Y. Guan and H. Liu, *J. Magn. Magn. Mater.*, 2006, **301**, 469–477.
112 I. J. Bruce and T. Sen, *Langmuir*, 2005, **21**, 7029–7035.
113 Y. Hu, S. Zhou and L. Wu, *Polymer.*, 2009, **50**, 3609–3616.
114 WO/2011/077081, 2011.
115 J. P. W. Eggert, U. Lüning and C. Näther, *European J. Org. Chem.*, 2005, **2005**, 1107–1112.
116 A.-F. Ngomsik, A. Bee, D. Talbot and G. Cote, *Sep. Purif. Technol.*, 2012, **86**, 1–8.
117 A. L. Morel, S. I. Nikitenko, K. Gionnet, A. Wattiaux, J. Lai-Kee-Him, C. Labrugere, B. Chevalier, G. Deleris, C. Petibois, A. Brisson and M. Simonoff, *ACS Nano*, 2008, **2**, 847–856.
118 A. Afsar, J. Cowell, P. Distler, L. Harwood, J. John and J. Westwood, *Synlett*, 2017, **28**, 2795–2799.
119 P. Secondo and F. Fages, *Org. Lett.*, 2006, **8**, 1311–1314.
120 M. Ghaemy, M. Hassanzadeh, M. Taghavi and S. M. Amini Nasab, *J. Fluor. Chem.*, 2012, **142**, 29–40.
121 A. Afsar, D. L. Laventine, L. M. Harwood, M. J. Hudson and A. Geist, *Heterocycles*, 2014, **88**, 613-620
122 A. Afsar, P. Distler, L. M. Harwood, J. John and J. Westwood, *Chem. Commun.*, 2017, **53**, 4010–4013.
123 M. Kaur, H. Zhang, L. Martin, T. Todd and Y. Qiang, *Environ. Sci. Technol.*, 2013, **47**, 11942–11959.
124 T. Kikuchi, M. Nogami and K. Suzuki, *J. Alloys Compd.*, 2004, **374**, 272–276.
125 M. A. Higginson, O. J. Marsden, P. Thompson, F. R. Livens and S. L. Heath, *React. Funct. Polym.*, 2015, **91**–**92**, 93–99.
126 3-Chloropropyl-functionalized silica gel 230-400 mesh, extent of labeling: ~2.5% loading, matrix active group ~8% functionalized | Sigma-Aldrich, https://www.sigmaaldrich.com/catalog/product/aldrich/364266?lang=en&region=GB, (accessed 21 January 2018).
127 P. N. W. Baxter, J. A. Connor, W. B. Schweizer and J. D. Wallis, *J. Chem. Soc., Dalton Trans.*, 1992, **0**, 3015–3019.
128 3-Aminopropyl-functionalized silica gel 40-63 µm, extent of labeling: ~1 mmol/g NH_2 loading | Sigma-Aldrich, https://www.sigmaaldrich.com/catalog/product/aldrich/364258?lang=en&region=GB, (accessed 20 January 2018).
129 H. K. Kadam and S. G. Tilve, *RSC Adv.*, 2015, **5**, 83391–83407.
130 S. T. Mullins, P. G. Sammes, R. M. West and G. Yahioglu, *J. Chem. Soc. Perkin Trans. 1*, 1996, **0**, 75-81
131 G. F. Smith and F. W. Cagle, Jr., *J. Org. Chem.*, 1947, **12**, 781–784.
132 W. C. Putnam and J. K. Bashkin, *Chem. Commun.*, 2000, **0**, 767–768.
133 C. A. G. N. Montalbetti and V. Falque, *Tetrahedron*, 2005, **61**, 10827–10852.
134 P. Witold and R. Eisenberg, *Inorg. Chem.*, 1997, **36**, 2287–2293.

135 K. Gislason and S. T. Sigurdsson, *Bioorg. Med. Chem. Lett.*, 2013, **23**, 264–267.
136 A. M. S. Garas and R. S. Vagg, *J. Heterocycl. Chem.*, 2000, 37, 151–158.
137 S. E. Pepper, K. R. Whittle, L. M. Harwood, J. Cowell, T. S. Lee and M. D. Ogden, *Sep. Sci. Technol.*, 2017, 1–11.
138 F. W. Lewis, L. M. Harwood, M. J. Hudson, U. Mullich and A. Geist, *Chem. Commun.*, 2015, **51**, 9189–9192.
139 X. G. Liu, J. F. Liang and J. M. Xu, *J. Radioanal. Nucl. Chem.*, 2007, **273**, 49–54.